

Volume 138S2 October 2020

ISSN 0959-8049

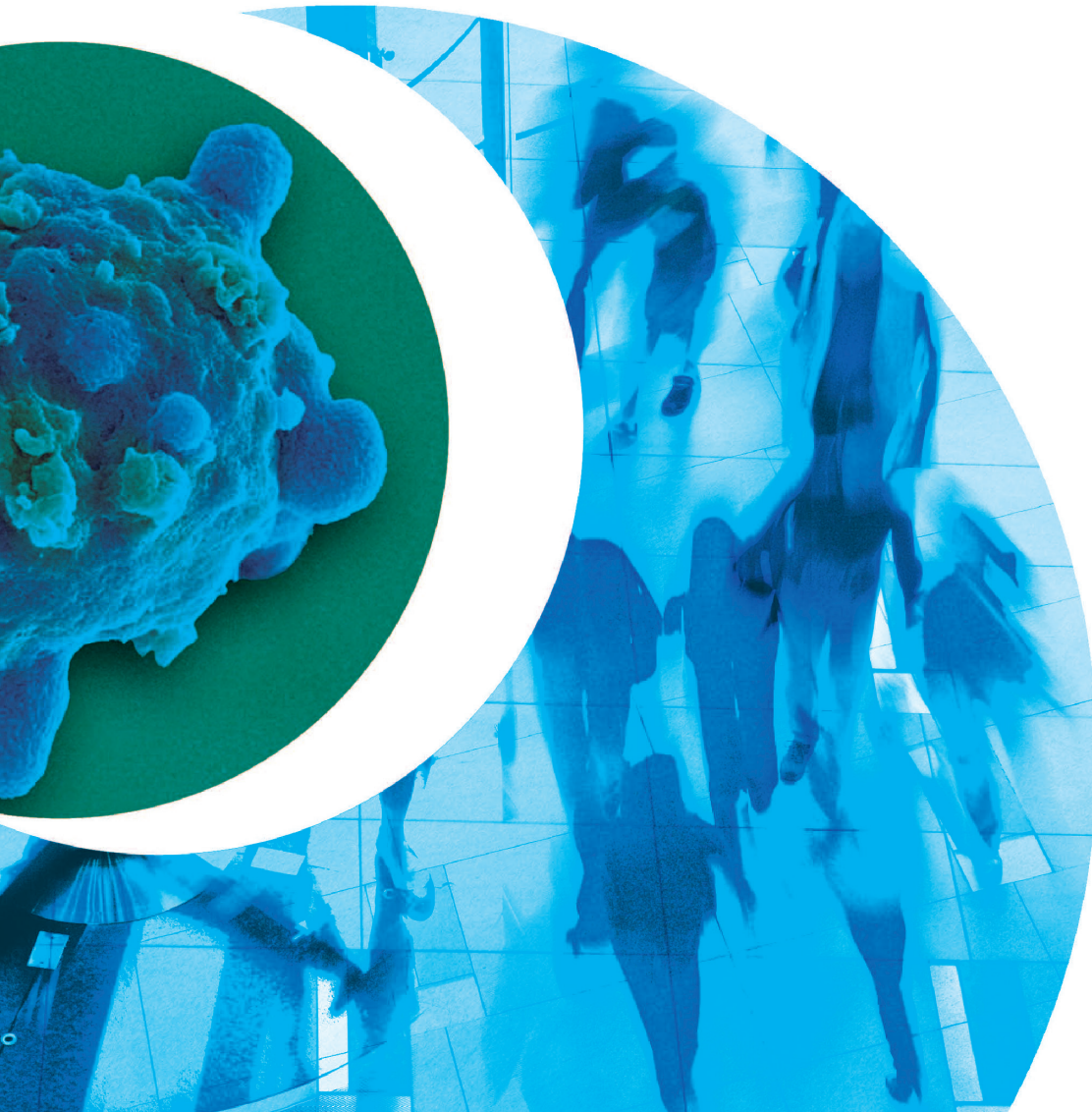
EJC

EUROPEAN JOURNAL OF CANCER

32nd EORTC-NCI-AACR Symposium on Molecular Targets and Cancer Therapeutics

24–25 October 2020
Virtual Conference

ABSTRACT BOOK



THE OFFICIAL JOURNAL OF



The future of cancer therapy



European Journal of Cancer

32nd EORTC-NCI-AACR Symposium on Molecular Targets and Cancer Therapeutics 24–25 October 2020 Virtual Conference

Abstract Book



Publication of this supplement was supported by the EORTC



European Journal of Cancer

Editor-in-Chief:

Alexander M.M. Eggermont
Princess Máxima Center for Pediatric Oncology
Utrecht, Netherlands

Editors:

Preclinical Cancer Research: Ulrich Keilholz, Berlin, Germany
Epidemiology and Prevention: Valery E.P.P. Lemmens, Utrecht, The Netherlands
Tumour Immunotherapy: Aurélien Marabelle, Villejuif, France
Breast Cancer: Giuseppe Curigliano, Milan, Italy
Suzette Delaloge, Villejuif, France
Gastrointestinal Cancers: Volker Heinemann, Munich, Germany
Michel Ducreux, Villejuif, France
Genitourinary Cancers: Karim Fizazi, Villejuif, France
Head and Neck Cancer: J.P. Machiels, Brussels, Belgium
Hemato-Oncology: Roch Houot, Rennes, France
Lung Cancer: Martin Schuler, Essen, Germany
Gynaecological Cancers: Ignace Vergote, Leuven, Belgium
Endocrine, Sarcomas and Other
Rare Tumours: Stefan Sleijfer, Rotterdam, The Netherlands
Melanoma: Dirk Schadendorf, Essen, Germany
Neuro-Oncology: Martin van den Bent, Rotterdam, The Netherlands
Paediatric Oncology: Rob Pieters, Utrecht, The Netherlands

Founding Editor:

Henri Tagnon

Past Editors:

Michael Peckham, London, UK; Hans-Jörg Senn, St Gallen, Switzerland; John Smyth, Edinburgh, UK

Editorial Office:

Elsevier, The Boulevard, Langford Lane, Kidlington, Oxford OX5 1GB, UK
Tel: +44 (0) 1865 843590, Email: ejcancer@elsevier.com

EDITORIAL BOARD

CLINICAL ONCOLOGY

| | | |
|---------------------------------|---------------------------|---------------------------------|
| R. Baird (UK) | J.C. Horiot (Switzerland) | D. Nam (Korea) |
| N. Brünnér (Denmark) | D. Jäger (Germany) | J. Perry (Canada) |
| R. Califano (UK) | A. Katz (Brazil) | J. Ringash (Canada) |
| E. Calvo (Spain) | C. Le Tourneau (France) | A. Rody (Germany) |
| F. Cardoso (Portugal) | Y. Loriot (France) | M. Schmidinger (Austria) |
| E. de Vries (The Netherlands) | C-C. Lin (Taiwan) | S. Sleijfer (The Netherlands) |
| A. Dicker (USA) | P. Lorigan (UK) | S. Stacchiotti (Italy) |
| R. Dummer (Switzerland) | C. Massard (France) | C. Sternberg (Italy) |
| S. Erridge (UK) | K. McDonald (Australia) | A. van Akkooi (The Netherlands) |
| H. Gelderblom (The Netherlands) | F. Meunier (Belgium) | E. Van Cutsem (Belgium) |
| B. Geoerger (France) | A. Miller (Canada) | G. Velikova (UK) |
| B. Hasan (Belgium) | T. Mok (Hong Kong) | E. Winquist (Canada) |
| | | T. Yap (UK) |

BASIC SCIENCE, PRECLINICAL AND TRANSLATIONAL RESEARCH

| | | |
|---------------------------|-----------------------------|----------------------|
| P. Allavena (Italy) | J.M. Irish (USA) | S. Singh (Canada) |
| J. Anderson (UK) | H.E.K. Kohrt (USA) | J. Stagg (Canada) |
| M. Brogginì (Italy) | J. Lunec (UK) | A. Virós (UK) |
| C. Catapano (Switzerland) | A.M. Müller (USA) | B. Weigelt (USA) |
| C. Caux (France) | D. Olive (France) | T. Yap (UK) |
| M. Esteller (Spain) | A.G. Papavassiliou (Greece) | N. Zaffaroni (Italy) |
| E. Garattini (Italy) | V. Rotter (Israel) | |
| R. Giavazzi (Italy) | V. Sanz-Moreno (UK) | |

EPIDEMIOLOGY AND PREVENTION

| | | |
|--------------------------------|--|---|
| B. Armstrong (Australia) | D. Forman (France) | P. Peeters (The Netherlands) |
| P. Autier (France) | A. Green (Australia) | S. Sanjose (Spain) |
| V. Bataille (UK) | K. Hemminki (Germany) | M.K. Schmidt (The Netherlands) |
| J.M. Borrás (Spain) | C. Johansen (Denmark) | I. Soerjomataram (France) |
| C. Bosetti (Italy) | L.A. Kiemeny (The Netherlands) | H. Storm (Denmark) |
| H. Brenner (Germany) | I. Lansdorp-Vogelaar (The Netherlands) | L.V. van de Poll-Franse (The Netherlands) |
| L.E.M. Duijm (The Netherlands) | E. Lynge (Denmark) | H.M. Verkooijen (The Netherlands) |
| J. Faivre (France) | M. Maynadié (France) | E. de Vries (The Netherlands) |
| S. Franceschi (France) | H. Möller (UK) | R. Zanetti (Italy) |

PAEDIATRIC ONCOLOGY

| | | |
|----------------------------|------------------------------------|---|
| C. Bergeron (France) | G. Chantada (Argentina) | L. Sung (Canada) |
| A. Biondi (Italy) | F. Doz (France) | M. van den Heuvel-Eibrink (The Netherlands) |
| E. Bouffet (Canada) | A. Ferrari (Italy) | M. van Noesel (The Netherlands) |
| M. Cairo (USA) | M.A. Grootenhuys (The Netherlands) | |
| H. Caron (The Netherlands) | K. Pritchard-Jones (UK) | |

European Journal of Cancer

Aims and Scope

The *European Journal of Cancer* (EJC) integrates preclinical, translational, and clinical research in cancer, from epidemiology, carcinogenesis and biology through to innovations in cancer treatment and patient care. The journal publishes original research, reviews, previews, editorial comments and correspondence.

The EJC is the official journal of the European Organisation for Research and Treatment of Cancer (EORTC) and the European Society of Breast Cancer Specialists (EUSOMA).

For a full and complete Guide for Authors, please go to <http://www.ejcancer.com>

Advertising information. Advertising orders and inquiries can be sent to: USA, Canada and South America: Bill Hipple Advertising Department, Elsevier Inc., 230 Park Avenue, Suite 800, New York, NY 10169-0901, USA; phone: (+1) 646-671-0385; fax: (+1) (212) 633 3820; e-mail: b.hipple@elsevier.com. Europe and ROW: Advertising Sales: Elsevier Pharma Solutions; 125 London Wall, London, EC2Y 5AS, UK; Tel.: +48 500 259 970; fax: +44 (0) 20 7424 4433; e-mail: k.lach.1@elsevier.com.

Publication information: *European Journal of Cancer* (ISSN 0959-8049). For 2020, volumes 124–141 (18 issues) are scheduled for publication. Subscription prices are available upon request from the Publisher or from the Elsevier Customer Service Department nearest you or from this journal's website (<http://www.elsevier.com/locate/ejca>). Further information is available on this journal and other Elsevier products through Elsevier's website (<http://www.elsevier.com>). Subscriptions are accepted on a prepaid basis only and are entered on a calendar year basis. Issues are sent by standard mail (surface within Europe, air delivery outside Europe). Priority rates are available upon request. Claims for missing issues should be made within six months of the date of despatch.

Orders, claims, and journal inquiries: Please visit our Support Hub page <https://service.elsevier.com> for assistance.

Author inquiries

You can track your submitted article at <http://www.elsevier.com/track-submission>. You can track your accepted article at <http://www.elsevier.com/trackarticle>. You are also welcome to contact Customer Support via <http://support.elsevier.com>.

Language (usage and editing services). Please write your text in good English (American or British usage is accepted, but not a mixture of these). Authors who feel their English language manuscript may require editing to eliminate possible grammatical or spelling errors and to conform to correct scientific English may wish to use the English Language Editing service available from Elsevier's WebShop <http://webshop.elsevier.com/languageediting/> or visit our customer support site <http://support.elsevier.com> for more information.

Illustration services

Elsevier's WebShop (<http://webshop.elsevier.com/illustrationservices>) offers Illustration Services to authors preparing to submit a manuscript but concerned about the quality of the images accompanying their article. Elsevier's expert illustrators can produce scientific, technical and medical-style images, as well as a full range of charts, tables and graphs. Image 'polishing' is also available, where our illustrators take your image(s) and improve them to a professional standard. Please visit the website to find out more.

Funding body agreements and policies. Elsevier has established agreements and developed policies to allow authors whose articles appear in journals published by Elsevier, to comply with potential manuscript archiving requirements as specified as conditions of their grant awards. To learn more about existing agreements and policies please visit <http://www.elsevier.com/fundingbodies>.

© 2020 Elsevier Ltd. All rights reserved

This journal and the individual contributions contained in it are protected under copyright, and the following terms and conditions apply to their use in addition to the terms of any Creative Commons or other user license that has been applied by the publisher to an individual article:

Photocopying. Single photocopies of single articles may be made for personal use as allowed by national copyright laws. Permission is not required for photocopying of articles published under the CC BY license nor for photocopying for non-commercial purposes in accordance with any other user license applied by the publisher. Permission of the publisher and payment of a fee is required for all other photocopying, including multiple or systematic copying, copying for advertising or promotional purposes, resale, and all forms of document delivery. Special rates are available for educational institutions that wish to make photocopies for non-profit educational classroom use.

Derivative Works. Users may reproduce tables of contents or prepare lists of articles including abstracts for internal circulation within their institutions or companies. Other than for articles published under the CC BY license, permission of the publisher is required for resale or distribution outside the subscribing institution or company.

For any subscribed articles or articles published under a CC BY-NC-ND license, permission of the publisher is required for all other derivative works, including compilations and translations.

Storage or Usage. Except as outlined above or as set out in the relevant user license, no part of this publication may be reproduced, stored in a retrieval system or transmitted in any form or by any means, electronic, mechanical, photocopying, recording or otherwise, without prior written permission of the publisher.

Permissions. For information on how to seek permission visit www.elsevier.com/permissions.

Author rights. Author(s) may have additional rights in their articles as set out in their agreement with the publisher (more information at <http://www.elsevier.com/authorsrights>).

Notice. Practitioners and researchers must always rely on their own experience and knowledge in evaluating and using any information, methods, compounds or experiments described herein. Because of rapid advances in the medical sciences, in particular, independent verification of diagnoses and drug dosages should be made. To the fullest extent of the law, no responsibility is assumed by the publisher for any injury and/or damage to persons or property as a matter of products liability, negligence or otherwise, or from any use or operation of any methods, products, instructions or ideas contained in the material herein.

Although all advertising material is expected to conform to ethical (medical) standards, inclusion in this publication does not constitute a guarantee or endorsement of the quality or value of such product or of the claims made of it by its manufacturer.

♻️ The paper used in this publication meets the requirements of ANSI/NISO Z39.48-1992 (Permanence of Paper).

Peer Review Policy for the *European Journal of Cancer (EJC)*

The practice of peer review is to ensure that only good science is published. It is an objective process at the heart of good scholarly publishing and is carried out by all reputable scientific journals. Our reviewers therefore play a vital role in maintaining the high standards of the *European Journal of Cancer (EJC)* and all manuscripts are peer reviewed following the procedure outlined below.

Initial manuscript evaluation

The Editors first evaluate all manuscripts. In some circumstances it is entirely feasible for an exceptional manuscript to be accepted at this stage. Those rejected at this stage are insufficiently original, have serious scientific flaws, have poor grammar or English language, or are outside the aims and scope of the journal. Those that meet the minimum criteria are passed on to experts for review.

Authors of manuscripts rejected at this stage will be informed within 2 weeks of receipt.

Type of Peer Review

The EJC employs single blind review, where the reviewer remains anonymous to the authors throughout the process.

How the reviewer is selected

Reviewers are matched to the paper according to their expertise. Our reviewer database contains reviewer contact details together with their subject areas of interest, and this is constantly being updated.

Reviewer reports

Reviewers are asked to evaluate whether the manuscript:

- Is original
- Is methodologically sound
- Follows appropriate ethical guidelines
- Has results which are clearly presented and support the conclusions
- Correctly references previous relevant work

Reviewers are not expected to correct or copyedit manuscripts. Language correction is not part of the peer review process. Reviewers are requested to refrain from giving their

personal opinion in the “Reviewer blind comments to Author” section of their review on whether or not the paper should be published. Personal opinions can be expressed in the “Reviewer confidential comments to Editor” section.

How long does the peer review process take?

Typically the manuscript will be reviewed within 2-8 weeks. Should the reviewers’ reports contradict one another or a report is unnecessarily delayed a further expert opinion will be sought. Revised manuscripts are usually returned to the Editors within 3 weeks and the Editors may request further advice from the reviewers at this time. The Editors may request more than one revision of a manuscript.

Final report

A final decision to accept or reject the manuscript will be sent to the author along with any recommendations made by the reviewers, and may include verbatim comments by the reviewers.

Editor’s Decision is final

Reviewers advise the Editors, who are responsible for the final decision to accept or reject the article.

Special Issues / Conference Proceedings

Special issues and/or conference proceedings may have different peer review procedures involving, for example, Guest Editors, conference organisers or scientific committees. Authors contributing to these projects may receive full details of the peer review process on request from the editorial office.

Becoming a Reviewer for the EJC

If you are not currently a reviewer for the *EJC* but would like to be considered as a reviewer for this Journal, please contact the editorial office by e-mail at ejcancer@elsevier.com, and provide your contact details. If your request is approved and you are added to the online reviewer database you will receive a confirmatory email, asking you to add details on your field of expertise, in the format of subject classifications.

Contents

Late Breaking Abstracts

Saturday, 24 October 2020

Plenary Session 1

| | |
|---|----|
| Late Breaking and Best Proffered Papers | S1 |
|---|----|

Sunday, 25 October 2020

Plenary Session 2

| | |
|---|----|
| Late Breaking and Best Proffered Papers | S1 |
|---|----|

Sunday, 25 October 2020

Scientific Symposium

| | |
|--|----|
| Targeting Oncogenic RAS signalling: New Approaches To An Old Problem | S2 |
|--|----|

Sunday, 25 October 2020

Closing Session

| | |
|--------------------------|----|
| New Drugs on the Horizon | S2 |
|--------------------------|----|

Poster Session

| | |
|-----------------------|----|
| Late Breaking Posters | S5 |
|-----------------------|----|

Oral Abstracts

Saturday, 24 October 2020

Plenary Session 1

| | |
|---|----|
| Late Breaking and Best Proffered Papers | S7 |
|---|----|

Sunday, 25 October 2020

Plenary Session 2

| | |
|---|----|
| Late Breaking and Best Proffered Papers | S9 |
|---|----|

Poster Abstracts

Saturday, 24 October 2020

Poster Discussion Session

| | |
|--|-----|
| New Therapeutics in Phase I and II studies | S11 |
|--|-----|

| | |
|--|-----|
| Targeting DNA Replication and Repair Systems | S13 |
|--|-----|

| | |
|--------------------------------------|-----|
| Next Generation Targeted Therapies A | S15 |
|--------------------------------------|-----|

| | |
|--|-----|
| Cancer Therapeutics: Preclinical Modeling and Patient Stratification | S18 |
|--|-----|

Sunday, 25 October 2020

Poster Discussion Session

| | |
|--------------------------------|-----|
| New Targets in Immuno-Oncology | S19 |
|--------------------------------|-----|

| | |
|---|-----|
| Approaches to Overcoming Therapeutic Resistance | S21 |
|---|-----|

| | |
|--------------------------------------|-----|
| Next Generation Targeted Therapies B | S23 |
|--------------------------------------|-----|

Poster Session

| | |
|---|-----|
| Angiogenesis and Vascular Disrupting Agents | S25 |
|---|-----|

| | |
|---------------|-----|
| Animal Models | S26 |
|---------------|-----|

| | |
|--|------------|
| Antibody-drug Conjugates | S27 |
| Apoptosis Inducers | S27 |
| Cancer Genomics | S29 |
| Cellular Therapies | S33 |
| Combinatorial Chemistry | S34 |
| Cytotoxics (including Antimetabolites, Anthracyclin, Alkylating agents, Aurora kinases, Polo-like kinase, Topoisomerase inhibitors, Tubulin-binding compounds) | S35 |
| DNA Repair Modulation (including PARP, CHK, ATR, ATM) | S36 |
| Drug Delivery | S37 |
| Drug Design | S38 |
| Drug Resistance and Modifiers | S39 |
| Drug Screening | S42 |
| Epigenetic Modulators (HDAC Bromodomain modulators, EZH2) | S42 |
| Molecular Targeted Agents | S43 |
| New Drugs | S50 |
| New Therapies in Immuno-Oncology | S56 |
| Preclinical Models | S58 |
| Tumour Immunology and Inflammation | S60 |
| Author Index | S63 |

Saturday, 24 October 2020

15:05–16:35

PLENARY SESSION 1

Late Breaking and Best Proffered Papers

1LBA

Late Breaking

First-in-human safety, pharmacokinetics, and preliminary efficacy of TPX-0022, a novel inhibitor of MET/SRC/CSF1R in patients with advanced solid tumors harboring genetic alterations in MET

D. Hong¹, L. Bazhenova², B.C. Cho³, S. Sen⁴, M. Ponz-Sarvisse⁵, R. Heist⁶, Z. Zimmerman⁷, X. Le⁸, D. Xuan⁹, Z. Junming¹⁰, J. Lee¹¹. ¹The University of Texas MD Anderson Cancer Center, Department of Investigational Cancer Therapeutics, Houston, USA; ²UC San Diego Moores Cancer Center, Medical Oncology, San Diego, USA; ³Yonsei Cancer Center- Severance Hospital, Medicine, Seoul, South Korea; ⁴Sarah Cannon Research Institute at HealthONE, Medical Oncology, Denver, USA; ⁵Clinica Universidad de Navarra, Medical Oncology, Pamplona, Spain; ⁶Massachusetts General Hospital, Medicine, Boston, USA; ⁷Turning Point Therapeutics- Inc., Clinical Development, San Diego, USA; ⁸The University of Texas MD Anderson Cancer Center, Department of Thoracic Head and Neck Medical Oncology, Houston, USA; ⁹Turning Point Therapeutics- Inc., Clinical Pharmacology, San Diego, USA; ¹⁰Turning Point Therapeutics- Inc., Biostatistics, San Diego, USA; ¹¹Samsung Medical Center, Hem/Oncology, Seoul, South Korea

Background: Oncogenic alterations in MET, including amplifications, fusions, and activating mutations (kinase domain [KD] or exon 14 [Δ ex14]), occur in many tumor types. TPX-0022 is a novel type I tyrosine kinase inhibitor (TKI) that targets MET, SRC, and CSF1R. SRC family kinases are key downstream nodes for MET signaling that regulate hepatocyte growth factor expression which may contribute to MET inhibitor resistance. Targeting CSF1R modulates tumor associated macrophages which may contribute to TPX-0022 activity. TPX-0022 has shown activity in multiple preclinical xenograft models. This phase I study (NCT03993873) is assessing the maximum tolerated dose (MTD), safety, pharmacokinetics (PK), and clinical activity of TPX-0022 in patients (pts) with advanced solid tumors harboring genetic MET alterations.

Patients and methods: Adults with advanced cancers harboring genetic MET alterations detected by tissue or liquid biopsy were enrolled in a 3+3 dose escalation trial. Expansion was allowed at doses where clinical activity was observed. Treatment with a prior MET inhibitor was allowed. TPX-0022 was given orally in continuous 28-day cycles.

Results: As of 17 September 2020, 18 pts have been enrolled across 4 doses (20–120 mg QD): non-small cell lung cancer (NSCLC; n = 11), colorectal cancer (CRC; n = 4) and gastric (GC; n = 3). MET alterations included amplification (N = 9), Δ ex14 (n = 7) and fusion (n = 2). Median age was 63 (44–84). Median number of prior therapies was 3 (1–6). 7/18 (39%) had received a prior MET inhibitor. The most common adverse events (AEs) were dizziness (61%), amylase increase (33%), lipase increase (33%), fatigue (33%), and nausea (33%). There were no grade \geq 3 treatment-related AEs. No events of interstitial lung disease/pneumonitis, grade 3 edema, or grade 3/4 ALT/AST elevation were reported. MTD was not reached. One dose limiting toxicity of grade 2 dizziness occurred at 120 mg QD. Systemic exposure increased in a dose-dependent manner. The steady state trough concentrations were above the IC₉₅ for inhibition of MET phosphorylation. Efficacy was assessed by RECIST 1.1 and eleven subjects were efficacy evaluable. One subject with Δ ex14 NSCLC achieved a PR. Two subjects with MET amplified GC achieved a PR and one subject with MET amplified CRC achieved a PR (unconfirmed).

Conclusions: TPX-0022 is a novel MET/SRC/CSF1R inhibitor. TPX-0022 was generally well-tolerated. Responses were observed in Δ ex14 NSCLC and MET amplified GC and CRC. TPX-0022 exposure increased in a dose-dependent manner and steady state trough concentrations were above the IC₉₅ for inhibition of MET phosphorylation. Phase 2 studies are planned in pts with cancers harboring MET alterations.

Conflict of interest:

Ownership:

David Hong: Molecular Match (Advisor), OncoResponse (Founder), Presagia Inc (Advisor).

Advisory Board:

Hong: Alpha Insights, Acuta, Amgen, Axio, Adaptimmune, Baxter, Bayer, Boxer Capital, COG, ECOR1, Expert Connect, Genentech, GLG, Group H, Guidepoint, H.C. Wainwright, Infinity, Janssen, Merrimack, Medscape, NTRK Connect, Numab, Pfizer, Prime Oncology, Seattle Genetics, SlingShot, Takeda, Trieza Therapeutics, WebMD.

Board of Directors:

Cho: Gencurix Inc, Interpark Bio Convergence Corp.

Corporate-sponsored Research:

David Hong: AbbVie, Adaptimmune, Aldi-Norte, Amgen, Astra-Zeneca, Bayer, BMS, Daiichi-Sankyo, Eisai, Fate Therapeutics, Genentech, Genmab, Ignyta, Infinity, Kite, Kyowa, Lilly, LOXO, Merck, MedImmune, Mirati, miRNA, Molecular Templates, Mologen, NCI-CTEP, Novartis, Numab, Pfizer, Seattle Genetics, Takeda, Turning Point Therapeutics, Verastem.

Other Substantive Relationships:

Hong: Travel, Accommodations, Expenses: Bayer, LOXO, miRNA, Genmab, AACR, ASCO, SITC.

2LBA

Late Breaking

Discovery of Covalently-bound, First-in-Class Allosteric Inhibitor of PRMT5

D. McKinney¹, M. Ranaghan¹, B. McMillan², M. Brousseau¹, M. O'Keefe¹, J. Moroco¹, R. Singh¹, B. Besnik¹, P. McCarren¹, K. Mulvaney³, W. Sellers³, A. Ianari³. ¹The Broad Institute, CDoT, Cambridge, USA; ²Tango Therapeutics, Biochemistry/Biophysics, Cambridge, USA; ³The Broad Institute, Cancer Program, Cambridge, USA

MTAP-deleted cancer cells are selectively dependent on the expression of both the methyltransferase PRMT5 and its substrate adaptor proteins (SAPs), pICln and Rik1. Inhibition of this interaction represents a possible therapeutic strategy for MTAP-deleted cancers. We recently elucidated the molecular basis for the PRMT5-adaptor interaction, which is mediated by a highly conserved binding motif across SAPs (PRMT5 Binding Motif – or PBM) and a surface exposed pocket on PRMT5 (PBM groove) (Mulvaney et al, 2020 BioRxiv). Based on these observations, we conducted a FP-based HTS against >800 K small molecules to identify compounds that inhibit the interaction between SAPs via the PBM-groove. This screen led to the identification of a class of compounds that target this mechanism with a covalent mode of action. Structure based drug design (x-ray co-crystal and cryo-EM) allowed for improvement in apparent potency with concomitant reduction of chemical reactivity. The resulting exemplar BRD0639 represents a first-in-class PRMT5 covalent allosteric inhibitor that targets this protein-protein interaction.

No conflict of interest.

Sunday, 25 October 2020

15:45–17:15

PLENARY SESSION 2

Late Breaking and Best Proffered Papers

3LBA

Late Breaking

KRYSTAL-1: Activity and Safety of Adagrasib (MRTX849) in Advanced/Metastatic Non–Small-Cell Lung Cancer (NSCLC) Harboring KRAS G12C Mutation

P.A. Jänne¹, I.I. Rybkin², A.I. Spira³, G.J. Riely⁴, K.P. Papadopoulos⁵, J.K. Sabari⁶, M.L. Johnson⁷, R.S. Heist⁸, L. Bazhenova⁹, M. Barve¹⁰, J.M. Pacheco¹¹, T.A. Leal¹², K. Velastegui¹³, C. Cornelius¹³, P. Olson¹³, J.G. Christensen¹³, T. Kheoh¹³, R.C. Chao¹³, S.H.I. Ou¹⁴. ¹Dana Farber Cancer Institute, Thoracic Oncology, Boston, USA; ²Henry Ford Cancer Institute, Medical Oncology, Detroit, USA; ³Virginia Cancer Specialists, US Oncology Research, Fairfax, USA; ⁴Memorial Sloan Kettering Cancer Center, Weill Cornell Medical College, New York, USA; ⁵START Center for Cancer Care, Clinical Research, San Antonio, USA; ⁶Perlmutter Cancer Center, New York University Langone Health, New York, USA; ⁷Sarah Cannon Research Institute, Tennessee Oncology, Nashville, USA; ⁸Massachusetts General Hospital, Cancer Center, Boston, USA; ⁹University of California San Diego, Moores Cancer Center, San Diego, USA; ¹⁰Mary Crowley Cancer Center, Medical Department, Dallas, USA; ¹¹University of Colorado Anschutz Medical Campus, Division of Medical Oncology, Aurora, USA; ¹²University of Wisconsin, Carbone Cancer Center, Madison, USA; ¹³Mirati Therapeutics- Inc., Research & Development, San Diego, USA; ¹⁴University of California- Irvine, Chao Family Comprehensive Cancer Center, Orange, USA

Background: KRAS is a key mediator of a signaling cascade that promotes cellular growth and proliferation and is the most frequently mutated oncogene in cancers, including lung adenocarcinoma. Adagrasib, an investigational

agent, is a potent, covalent inhibitor of KRAS G12C that irreversibly and selectively binds to and locks KRAS G12C in its inactive state. Adagrasib was optimized to exhibit a long half-life in order to achieve durable and continuous KRAS inhibition, which is postulated to prevent feedback loops and lead to deep and durable antitumor activity. Adagrasib has demonstrated objective responses and favorable tolerability in the Phase 1/1b setting.

Methods: Adagrasib is being evaluated in KRYSTAL-1, a multi-cohort Phase 1/2 study in patients with advanced or metastatic solid tumors harboring a KRAS G12C mutation previously treated with chemotherapy and anti-PD-1/PD-L1 therapy. A dose of 600 mg twice daily (BID) was evaluated in dose expansion and established as the recommended Phase 2 dose (RP2D). The study endpoints include safety, pharmacokinetics (PK), and clinical activity and efficacy. Exploratory objectives include evaluation of pharmacodynamic biomarkers and correlation of molecular markers with antitumor activity.

Results: As of 30 August 2020, 79 patients (57% female; median age, 65 years [range 25–85]; 22%/78% ECOG PS 0/1) with pretreated NSCLC were treated with adagrasib 600 mg BID in Phase 1/1b (n = 18) or a Phase 2 (n = 61) cohort. The most commonly reported (>20%) treatment-related adverse events (TRAEs) include: nausea (54%), diarrhea (48%), vomiting (34%), fatigue (28%), and increased ALT (23%). The only commonly reported (>2%) grade 3/4 treatment-related serious adverse event was hyponatremia (3%, 2/79). Among the 51 patients evaluable for clinical activity (14 from Phase 1/1b; 37 from Phase 2), 45% of patients had an objective response (23/51 which includes 5 patients who had an unconfirmed partial response and remain on treatment). Disease control rate was 96% (49/51) of patients. Among the 14 patients evaluable for clinical activity from Phase 1/1b with longer follow-up, the confirmed Objective Response Rate (ORR) was 43% (6/14); and the majority of patients with responses (4/6) have had treatment ongoing >11 months. The median time on treatment was 8.2 months (range: 1.4, 13.1+). Additional data including pharmacodynamic and mechanistic biomarker analyses will be presented.

Conclusions: Adagrasib is tolerable and demonstrates durable clinical activity in patients with previously treated KRAS G12C-mutant NSCLC. Clinical trial information: NCT03785249.

Conflict of interest:

Ownership:
Spira: Stock in Eli Lilly & Co.
Christensen: Owns stock in Mirati Therapeutics and Bluebird Bio.
Chao: Owns stock in Mirati Therapeutics.
Kheoh: Owns stock in Mirati Therapeutics and Tocagen.
Corporate-sponsored Research:
Janne: Has received grants from Transcenta, AstraZeneca, Daiichi Sankyo, PUMA Biotechnology, Astellas Pharmaceuticals, Sanofi.

Sunday, 25 October 2020

19:30–20:45

SCIENTIFIC SYMPOSIUM

Targeting Oncogenic RAS signalling: New Approaches To An Old Problem

4LBA

Late Breaking

KRYSTAL-1: Activity and Safety of Adagrasib (MRTX849) in Patients with Colorectal Cancer (CRC) and Other Solid Tumors Harboring a KRAS G12C Mutation

M.L. Johnson¹, S.H.I. Ou², M. Barve³, I.I. Rybkin⁴, K.P. Papadopoulos⁵, T.A. Lea⁶, K. Velastegui⁷, J.G. Christensen⁷, T. Kheoh⁷, R.C. Chao⁷, J. Weiss⁸. ¹Sarah Cannon Research Institute, Tennessee Oncology, Nashville, USA; ²University of California- Irvine, Chao Family Comprehensive Cancer Center, Orange, USA; ³Mary Crowley Cancer Research, Medical Department, Dallas, USA; ⁴Henry Ford Cancer Institute, Medical Oncology, Detroit, USA; ⁵START Center for Cancer Care, Clinical Research, San Antonio, USA; ⁶University of Wisconsin, Carbone Cancer Center, Madison, USA; ⁷Mirati Therapeutics- Inc., Research & Development, San Diego, USA; ⁸University of North Carolina- Chapel Hill, Lineberger Comprehensive Cancer Center, Chapel Hill, USA

Background: KRAS is a key mediator of a signaling cascade which promotes cellular growth and proliferation across many tumor types. The KRAS G12C mutation occurs in 3–4% of CRC, 2% of pancreatic adenocarcinoma (PDAC), and less commonly in other tumors, including cholangiocarcinoma (CCA). Adagrasib, an investigational agent, is an irreversible covalent inhibitor that selectively binds to KRAS G12C and locks the mutated protein in its inactive state. Adagrasib was optimized for a

long half-life to achieve durable and continuous KRAS inhibition throughout the dosing interval that may prevent feedback loops and hyperactivation of downstream KRAS signaling. Durable inhibition of KRAS G12C may be particularly important in CRC, which may be susceptible to EGFR-mediated feedback signaling loops. Adagrasib also has a high estimated volume of distribution which may facilitate tissue penetration in dense desmoplastic tumor types like PDAC.

Materials and Methods: KRYSTAL-1 is a multi-cohort Phase 1/2 study evaluating adagrasib in patients with advanced solid tumors with a KRAS G12C mutation. A dose of 600 mg BID is being evaluated in Phase 1/1b dose expansion and Phase 2 cohorts. Study endpoints include safety, pharmacokinetics (PK), and clinical activity. Exploratory objectives include evaluation of pharmacodynamic biomarkers and correlation of molecular markers with antitumor activity.

Results: As of 30 August 2020 preliminary safety data are available for 31 patients treated with adagrasib 600 mg BID in Phase 1/1b (CRC, n = 2) and select Phase 2 cohorts (CRC, n = 22; other solid tumors, n = 7). Baseline characteristics for all 31 patients include median age of 63 years (range 25, 80), 45% female, and 29%/71% with ECOG PS of 0/1, respectively. The most commonly reported (>20%) treatment-related adverse events (TRAEs) include: diarrhea (58%), nausea (52%), fatigue (42%), and vomiting (36%). 17% (3/18) of evaluable CRC patients had a confirmed objective response and 2 of these 3 patients remain on treatment. Disease control was observed in 94% (17/18) of patients and 12/18 patients remain on treatment. Six patients in the other solid tumor cohort were evaluable for clinical activity. Confirmed partial responses (PRs) were observed in a patient with endometrial cancer and a patient with pancreatic cancer (n = 1/1 each); unconfirmed PRs were observed in patients with ovarian cancer and CCA (n = 1/1 each). All 6 of these patients remain on treatment.

Conclusions: Adagrasib demonstrates an acceptable safety profile and promising clinical activity in pretreated patients with CRC and other solid tumors with a KRAS G12C mutation. Clinical trial information: NCT03785249.

Conflict of interest:

Ownership:
Christensen: Owns stock in Mirati Therapeutics and Bluebird Bio.
Weiss: Owns stock in Nektar Therapeutics and Vesselon.
Chao: Owns stock in Mirati Therapeutics.
Kheoh: Owns stock in Mirati Therapeutics and Tocagen.

Sunday, 25 October 2020

21:00–22:45

CLOSING SESSION

New Drugs on the Horizon

5LBA

Late Breaking

Interim results from a phase 1/2 precision medicine study of PLX8394- a next generation BRAF inhibitor

F. Janku¹, E.J. Sherman², A.R. Parikh³, L.G. Feun⁴, F. Tsai⁵, E. Allen⁶, C. Zhang⁷, P. Severson⁷, K. Inokuchi⁷, J. Walling⁷, S. Averbuch⁸, G. Tarcic⁸, G. Bollag⁷. ¹The University of Texas MD Anderson Cancer Center, Department of Investigational Cancer Therapeutics, Houston, USA; ²MSKCC, Department of Medical Oncology, New York, USA; ³Massachusetts General Hospital, Department of Medicine, Boston, USA; ⁴Sylvester Comprehensive Cancer Center- University of Miami, Department of Medicine, Miami, USA; ⁵HonorHealth, Department of Medicine, Scottsdale, USA; ⁶Texas Children's Cancer Center- Baylor College of Medicine, Department of Pediatrics, Houston, USA; ⁷Plexxikon, Plexxikon, Berkeley, USA; ⁸Novellus Bio, Novellus, Jerusalem, Israel

Background: BRAF^{V600} inhibition with 1st generation BRAF inhibitors (BRAFi) has provided remarkable clinical benefit in several tumor types; however, paradoxical re-activation of the MAPK pathway contributes to therapeutic resistance. PLX8394 is a next-generation, orally available small-molecule BRAFi that does not induce MAPK paradoxical activation and blocks signaling from both monomeric BRAF^{V600} and dimeric BRAF^{non-V600} mutated protein.

Materials and Methods: This is an ongoing phase 1/2 study of PLX8394 with or without cobicistat (cobi), a CYP3A4 inhibitor to enhance PLX8394 exposure, to determine the safety, PK, tolerability, and efficacy in patients (pts) with refractory solid tumors (NCT02428712). Results are reported as of July 31, 2020.

Results: 75 pts were treated with PLX8394 (450 mg BID, 450 mg TID, and 900 mg BID) with (N = 56) or without cobi (n = 19). Pts had BRAF V600 (n = 49), BRAF non-V600 (n = 17) or non-BRAF mutated (n = 9) tumors. The use of cobi resulted in 2–3-fold increase of PLX8394 exposure, demonstrating a non-saturating dose proportional increase in exposure. Grade 3 (G3) AST elevation and Grade 3 (G3) blood bilirubin increase were the only DLTs and PLX8394 900 mg BID with cobi was declared as RP2D. Other \geq G3 toxicities in \geq 2 pts included increased ALT (4), increased AST (3), blood bilirubin increase (4), and diarrhea (2).

Of 45 evaluable pts with BRAF-mutations, who received a median of 3 prior therapies, including 12 pts (27%) which received prior MAPK pathway targeted therapies, 10 pts (22%) achieved confirmed and mostly durable partial responses (gliomas (3), ovarian (2), and 1 each for papillary thyroid cancer, small bowel, colorectal carcinoma, anaplastic thyroid carcinoma, and melanoma). At time of analysis 10 pts remain on study for \geq 24 months (range, 24–59 months) providing encouraging long-term safety data including lack of secondary skin lesions observed with Class 1 BRAF inhibitors.

Conclusions: PLX8394 + cobi demonstrated favorable safety profile and encouraging activity in refractory solid tumors with BRAF mutations including BRAF fusion. Further studies to refine the RP2D with a modified tablet formulation to reduce dose burden and improve dose linearity are ongoing.

Conflict of interest:

Other Substantive Relationships:

Chao Zhang, Paul Severson, Kerry Inokuchi, Jackie Walling, Gideon Bollag are employees of Plexikon.

Steven Averbuch, Gabi Tarcic are employees of Novellus.

6LBA

Late Breaking

Circulating Tumor DNA Dynamics Predict Outcomes of Systemic Therapy in Patients with Advanced Cancers

M. Gouda¹, H. Huang¹, S. Piha-Paul¹, S.G. Call¹, D. Karp¹, S. Fu¹, A. Naing¹, V. Subbiah¹, S. Pant¹, A.M. Tsimberidou¹, D.S. Hong¹, J. Rodon¹, F. Meric-Bernstam¹. ¹The University of Texas MD Anderson Cancer Center, Investigational Cancer Therapeutics, Houston, USA

Background: Detection of molecular alterations in circulating tumor DNA (ctDNA) has been recently established as a tool to detect molecular targets for cancer therapy. Preliminary data suggest that dynamic changes in ctDNA quantity can be associated with outcomes of cancer therapy.

Material and Methods: We isolated ctDNA from serially collected blood samples from eligible patients with advanced cancers obtained during treatment on early-phase clinical trials with systemic therapies. Blood samples were collected at baseline (BL) (C1D1), mid-cycle (MC) (C1D21), at time of the first restaging (FR), and if feasible throughout the entire course of their therapy. We performed genomically-informed (by the results of molecular testing of tumor tissue) testing of ctDNA using digital droplet PCR (BioRad) and the quantity of ctDNA was measured as mutant variant allele frequency (VAF). Patients were classified based on results of their first restaging imaging as responders (complete [CR] or partial response [PR]) vs. non-responders (stable disease [SD] or progressive disease [PD]), or progressors (PD) vs. non-progressors (CR, PR, SD). Delta value as well as slope value (as a reflection of the trend of ctDNA dynamic) were calculated at MC and at FR and were correlated with clinical outcomes.

Results: A total of 218 patients with advanced cancers (most frequent tumor types: gastrointestinal cancers, n = 101; melanoma, n = 35; and breast cancer, n = 24) treated in early-phase clinical trials (immunotherapy, n = 31; non-immunotherapy, n = 187) were enrolled. Progression in ctDNA quantity preceded or co-occurred with clinical or radiological PD in 65.6% of patients. Detectable ctDNA at BL, MC, or FR was associated with shorter time to treatment failure (10 wks vs. 18 wks; 10 wks vs. 20 wks; 10 wks vs. 24 wks; all $P < 0.001$). Quantity of ctDNA as aggregate VAF was higher in progressors compared to non-progressors (9.7% vs. 4.5%; 8.7% vs. 3.8%; 13.6% vs. 3.5%; all $P < 0.001$) and in non-responders compared to responders (7.4% vs. 3.3%, $P = 0.036$; 6.8% vs. 0.6%, $P < 0.001$; 7.9% vs. 2.7%, $P = 0.002$) at all timepoints. FR delta value was significantly higher in progressors compared to non-progressors (13.6% vs. 3.5%, $P = 0.004$) and in non-responders compared to responders (7.9% vs. 2.7%, $P = 0.026$). Delta value positivity and slope value positivity both correlated with higher likelihood of disease progression, lesser chance of response and shorter time to treatment failure (all $P < 0.05$).

Conclusions: Early dynamic changes in the quantity of ctDNA within the first few weeks of therapy can predict clinical outcomes of systemic therapies in advanced cancers.

No conflict of interest

7LBA

Late Breaking

Milademetan, an oral MDM2 inhibitor, in well-differentiated/dedifferentiated liposarcoma: results from a phase 1 study in patients with solid tumors or lymphomas

M.M. Gounder¹, T.M. Bauer², G.K. Schwartz³, P. LoRusso⁴, P. Kumar⁵, K. Kato⁶, B. Tao⁷, Y. Hong⁸, P. Patel⁹, D. Hong¹⁰. ¹Memorial Sloan Kettering Cancer Center and Weill Cornell Medical Center, Medicine, New York- NY, USA; ²Sarah Cannon Research Institute and Tennessee Oncology- PLLC, Drug Development, Nashville- TN, USA; ³Columbia University Medical Center, Department of Medicine/Division of Hematology Oncology, New York- NY, USA; ⁴Smilow Cancer Hospital at Yale-New Haven, Yale Cancer Center, New Haven- CT, USA; ⁵Daiichi Sankyo- Inc., Oncology Clinical Development, Basking Ridge- NJ, USA; ⁶Daiichi Sankyo- Inc., Oncology Research & Development, Basking Ridge- NJ, USA; ⁷Daiichi Sankyo- Inc., Biostatistics, Basking Ridge- NJ, USA; ⁸Daiichi Sankyo- Inc., Quantitative Clinical Pharmacology, Basking Ridge- NJ, USA; ⁹Daiichi Sankyo- Inc., Clinical Biomarkers- Translational Science, Basking Ridge- NJ, USA; ¹⁰The University of Texas MD Anderson Cancer Center, Medicine, Houston, USA

Background: Patients with well-differentiated and/or dedifferentiated liposarcoma (WD/DD LPS) have few treatment options. The MDM2 gene encodes an E3 ubiquitin ligase that targets the p53 tumor suppressor for degradation; it is amplified in WD/DD LPS and is a diagnostic hallmark. Milademetan (DS-3032b, RAIN-32) is an oral MDM2 inhibitor with demonstrated preclinical antitumor activity.

Materials and Methods: A phase 1, first-in-human study (NCT01877382) of milademetan was conducted in patients with advanced, relapsed or refractory solid tumors or lymphoma, including those with WD/DD LPS. Primary endpoints were safety, tolerability, and maximum tolerated dose (MTD). Secondary endpoints were pharmacokinetics (PK), pharmacodynamics (PD) and preliminary efficacy. Four milademetan dosing schedules (A-D) were evaluated: 2 continuous (A, qd 21/28 days; B, qd 28/28 days) and 2 intermittent (C, qd 7/28 days; D, qd 3/14 days twice in a cycle).

Results: A total of 107 patients were enrolled (WD/DD LPS, 50%; other sarcomas, 9%; melanoma, 21%; other malignancies, 20%). Median age was 61 years, 62% received \geq 3 prior therapies, and 86% had stage III/IV disease. Table 1 lists selected drug-related adverse events (DRAEs). Schedule D was associated with the lowest rate of DRAEs; no dose-limiting toxicities were observed at the MTD of 260 mg. Serum macrophage inhibitory cytokine 1, a PD biomarker, and PK parameters (C_{max} and AUC_{0-24h}) increased in a dose-dependent manner. Of the 107 patients who received \geq 1 dose of milademetan, 5 (4.7%) achieved partial response (PR) and 56 (52.3%) achieved stable disease (SD). Of the 53 patients with WD/DD LPS, 2 (3.8%) achieved PR and 34 (64.2%) achieved SD. Patients on schedules C and D had a longer median progression-free survival (PFS) vs those on schedules A and B (7.4 vs 6.3 months). In patients treated on schedule D at \leq 260 mg, median PFS was 8.0 months; median duration of SD was 59.9 weeks. A notable shift in the tumor growth curves was seen with milademetan, demonstrating its antitumor activity in WD/DD LPS.

Table 1. Milademetan DRAEs and Preliminary Efficacy.

| Selected DRAEs, N (%) | Schedules A, B, and C (n = 78) | | Schedule D (n = 29) | |
|----------------------------|-----------------------------------|------------------------|---------------------------|--|
| | All Grades | Grade \geq 3 | All Grades | Grade \geq 3 |
| All DRAEs | 74 (95) | 43 (55) | 25 (86) | 5 (17) |
| Thrombocytopenia | 56 (72) | 28 (36) | 14 (48) | 4 (14) |
| Anemia | 33 (42) | 14 (18) | 5 (17) | 0 |
| Neutropenia | 24 (31) | 15 (19) | 2 (7) | 1 (3) |
| Nausea | 57 (73) | 2 (3) | 20 (69) | 0 |
| Vomiting | 22 (28) | 2 (3) | 13 (45) | 1 (3) |
| Diarrhea | 26 (33) | 0 | 9 (31) | 0 |
| Fatigue | 36 (46) | 3 (4) | 12 (41) | 0 |
| Efficacy (LPS only) | A, B n = 30 | C, D n = 23 | D (all) n = 18 | D (\leq260 mg, MTD) n = 17 |
| mPFS (95% CI), mo | 6.3 (3.8–10.0) | 7.4 (2.7–14.6) | 7.4 (2.7–28.9) | 8.0 (1.8–28.9) |

Conclusion: Milademetan \leq 260 mg administered on schedule D demonstrated markedly improved tolerability vs schedules A, B, and C and produced objective responses and durable SD in patients with WD/DD LPS, warranting further clinical evaluation.

Conflict of interest**Ownership:**

PK, KK, BT, YH, and PP are employed by Daiichi Sankyo and own stock.
 DH has ownership interest in Molecular Match (Advisor), OncoResponse (Founder), Presagia Inc (Advisor).

Advisory Board.

MG and GS have been on advisory board for Daiichi Sankyo.

PL has been on advisory boards for Abbvie, GenMab, Genentech, CytomX, Takeda, Cybrexa, Agenus, IQVIA, TRIGR, Pfizer, ImmunoMet, Black Diamond, Glaxo-Smith Kline, QED Therapeutics, AstraZeneca, EMD Serono, Shattuck, Astellas, Salarius, Silverback, MacroGenics, Kyowa Kirin, Kineta, Zentalis, Molecular Templates, ABL Bio.

DH has been on advisory boards for Alpha Insights, Acuta, Amgen, Axiom, Adaptimmune, Baxter, Bayer, Boxer Capital, COG, ECOR1, Expert Connect, Genentech, GLG, Group H, Guidepoint, H.C. Wainwright, Infinity, Janssen, Merrimack, Medscape, NTRK Connect, Numab, Pfizer, Prime Oncology, Seattle Genetics, SlingShot, Takeda, Trieza Therapeutics, and WebMD.

Board of Directors.

N/A.

Corporate-sponsored Research.

MG has received research support from Daiichi Sankyo.

TB has received research support from Daiichi Sankyo, Medpacto, Incyte, Mirati Therapeutics, MedImmune, Abbvie, AstraZeneca, MabVax, Stemline Therapeutics, Merck, Lilly, GlaxoSmithKline, Novartis, Genentech, Deciphera, Merrimack, Immunogen, Millennium, Phosphatin Therapeutics, Calithera Biosciences, Kolltan Pharmaceuticals, Principa Biopharma, Peleton, Immunocore, Roche, Aileron Therapeutics, Bristol-Myers Squibb, Amgen, Onyx, Sanofi, Boehringer-Ingelheim, Astellas Pharma, Five Prime Therapeutics, Jacobio, Karyopharm Therapeutics, Foundation Medicine, ARMO Biosciences, Leap Therapeutics, Ignyta, grants, Moderna Therapeutics, Pfizer Loxo, Bayer, Guardant Health, Execlis.

DH has received research/grant funding from AbbVie, Adaptimmune, Aldi-Norte, Amgen, Astra-Zeneca, Bayer, BMS, Daiichi-Sankyo, Eisai, Fate Therapeutics, Genentech, Genmab, Ignyta, Infinity, Kite, Kyowa, Lilly, LOXO, Merck, MedImmune, Mirati, miRNA, Molecular Templates, Mologen, NCI-CTEP, Novartis, Numab, Pfizer, Seattle Genetics, Takeda, Turning Point Therapeutics, and Verstatem.

Other.

PL consulted for SK Life Science and SOTIO and held positions on data safety monitoring committees for Agios, Five Prime, Halozyme, Tyme as well as imCORE Alliance with Roche-Genentech.

DH has received travel, accommodations, expenses from Bayer, LOXO, miRNA, Genmab, AACR, ASCO, and SITC.

POSTER SESSION

Late Breaking Posters

96LBA

Late Breaking

Prevention of Chemotherapy-induced Myelosuppression in SCLC patients treated with the Dual MDMX/MDM2 Inhibitor ALRN-6924

Z. Andric¹, T. Cerić², M. Stanetić³, M. Rancić⁴, M. Jakopović⁵, S. Ponce Aix⁶, R. Ramlau⁷, E. Smit⁸, M. Ułanska⁹, C. Caldwell¹⁰, D. Ferrari¹⁰, A. Annis¹¹, V. Vuković¹⁰, B. Žarić¹². ¹CHC Bežanijska Kosa, Medical Oncology, Belgrade, Serbia; ²University Clinical Center Sarajevo, Medical Oncology, Sarajevo, Bosnia-Herzegovina; ³University Clinical Center Lung Clinic, Medical Oncology, Banja Luka, Bosnia-Herzegovina; ⁴Clinic for Pulmonary Diseases Nis, Medical Oncology, Nis, Serbia; ⁵Clinic for Lung Diseases Jordanovac, Medical Oncology, Zagreb, Croatia; ⁶Hospital Universitario 12 de Octubre, Medical Oncology, Madrid, Spain; ⁷Poznan University of Medical Sciences, Medical Oncology, Poznan, Poland; ⁸Stichting Het Nederlands Kanker Instituut, Medical Oncology, Amsterdam, Netherlands; ⁹Centrum Terapii Współczesnej, Medical Oncology, Lodz, Poland; ¹⁰Aileron Therapeutics Inc, Clinical Development, Watertown, USA; ¹¹Aileron Therapeutics Inc, Translational Research, Watertown, USA; ¹²Institute for Pulmonary Diseases, Medical Oncology, Novi Sad, Serbia

Background: ALRN-6924 is a cell-permeating, stabilized alpha-helical peptide that binds with high affinity to endogenous p53 inhibitors MDM2 and MDMX. Treatment with ALRN-6924 increases intracellular p53 levels and initiates its transcriptional activity, leading to cell cycle arrest. This effect is limited to cells with wild-type, functional p53; therefore, for patients with tumors harboring mutated P53, pre-treatment with ALRN-6924 may selectively induce cell cycle arrest in normal cells allowing chemotherapy to selectively target cancer cells which are actively cycling.

Material and methods: A Phase 1b study in ED SCLC patients with ECOG PS 0–2 receiving topotecan was conducted to evaluate the ability of ALRN-6924 to reduce bone marrow toxicity without impacting the efficacy of topotecan. Inclusion criteria included the presence of p53 mutations in tumor tissue as measured by NGS. Prophylactic use of growth factors was not permitted. ALRN-6924 was given at three dose levels: 0.3, 0.6 and 1.2 mg/kg on days 0–4 of each treatment cycle. Topotecan was administered 24 hrs after ALRN-6924 on days 1–5 at 1.5 mg/m² of each treatment cycle. Hematological laboratory values were coded as AEs based on NCI CTC v5.0. Plasma and serum samples were analyzed for ALRN-6924 pharmacokinetics and pharmacodynamic biomarkers of p53 activation.

Results: 26 patients were enrolled (6 per dose level and 8 additional patients in the expansion cohort); 25/26 patients were evaluable. Baseline characteristics were typical for this patient population (median age 67 years, 80% males, ECOG PS 0 60%, baseline LDH ≥ULN 40%, chemosensitive population 48%). Median number of completed topotecan treatment cycles was 3. 12% of patients required topotecan dose reduction. Disease control rate was 64%. No patients reported Grade ≥3 events of nausea, vomiting, diarrhea, and 1 patient had fatigue Grade 3. Grade 3/4 anemia, thrombocytopenia and neutropenia were reported in 24%, 36% and 88% of patients and compare favorably to recent historical results of Grade 3/4 anemia, thrombocytopenia and neutropenia of 63%, 70% and 86% (Hart et al. ASCO 2019).

The 0.3 mg/kg ALRN 6924 dose level showed the most consistent chemoprotection results, with NCI CTC Grade 3/4 anemia, thrombocytopenia and neutropenia limited to 21%, 37% and 79% of patients, respectively, and a 43% rate of neutropenia Grade 4 in the 1st treatment cycle (historical result: 76%); none of the patients treated at this dose level had hematological SAEs nor did they require RBC/platelet transfusions (historical result: 41% and 36%, respectively).

Conclusions: This is the first clinical study to demonstrate a chemoprotective effect of p53 activation and selective induction of cell cycle arrest in normal cells. This novel strategy has the potential to benefit more than 50% of all cancer patients, with tumors harboring p53 mutations.

Conflict of interest:

Other Substantive Relationships:

Christopher Caldwell, Dora Ferrari, Allen Annis and Vojislav Vukovic are employees of Aileron Therapeutics Inc.

97LBA

Late Breaking

Distinct CDK6 complexes determine tumor cell response to CDK4/6 inhibitors and degraders

P. Poulikakos¹, X. Wu¹, X. Yang², Y. Xiong², T. Ito³, T. Ahmed¹, Z. Karoulia¹, C. Adamopoulos¹, R. Li³, H. Wang⁴, L. Wang⁵, L. Xie⁵, J. Liu⁶,

B. Ueberheide⁷, S. Aaronson¹, X. Chen⁸, S. Buchanan⁴, W. Sellers³, J. Jin². ¹Icahn School of Medicine at Mount Sinai, Oncological Sciences, New York, USA; ²Icahn School of Medicine at Mount Sinai, Pharmacological Sciences, New York, USA; ³Broad Institute, Cancer Program, Boston, USA; ⁴Eli Lilly and Company, Eli Lilly and Company, Indianapolis, USA; ⁵University of North Carolina at Chapel Hill, Biochemistry and Biophysics, Chapel Hill, USA; ⁶Icahn School of Medicine at Mount Sinai, Biochemistry and Molecular Pharmacology, New York, USA; ⁷New York University, Biochemistry and Molecular Pharmacology, New York, USA; ⁸University of North Carolina at Chapel Hill, Biochemistry and Biophysics, New York, USA

CDK4 and CDK6 kinases are master regulators of cell cycle progression, and they have thus been attractive targets for cancer therapy. CDK4/6 inhibitors (CDK4/6i) showed significant clinical effectiveness in ER+ breast cancers, and three CDK4/6i are now FDA-approved for this indication. However, in several tumor types, CDK4/6i have only been modestly effective, but the underlying mechanism(s) accounting for the discrepancy have remained elusive.

To identify the basis of resistance to CDK4/6i, we employed a variety of biochemical, genetic and proteomic approaches, we developed a potent and selective CDK4/6-directed degrader (PROTAC) to investigate in-cell binding of compounds and validated our findings in large tumor and clinical data.

We found that tumor response to CDK4/6i is critically determined by the expression of CDK6. Tumors with low CDK6 expression (CDK6-low) depend on CDK4, and are uniformly sensitive to CDK4/6i. CDK6-low tumors include both entire cancer types (e.g. Ewing Sarcomas, MCL), as well as subgroups of large tumor types, such as 25–30% of non-small cell lung adenocarcinomas (NSCLC). We further validated this finding in NSCLC patients previously treated with CDK4/6i in a clinical trial. In contrast, tumors that express both CDK4 and CDK6 universally depend on CDK6, which is expressed as either CDK4/6i-sensitive CDK6 (CDK6-S) or CDK4/6-resistant CDK6 (CDK6-R) in different cells. Using a CDK4/6 PROTAC, we further found that CDK4/6i binds strongly CDK6-S but weakly CDK6-R, indicating different conformations adopted by CDK6 in the two states. An unbiased proteomic analysis identified binding of components of the HSP90/CDC37 complex associated with the state of CDK6: in tumors in which CDK6 is expressed as a thermo-unstable, strong HSP90/CDC37-client, CDK4/6i (and consequently CDK4/6 PROTACs) bind and potentially inhibit CDK6 and downstream Rb/E2F signaling. In contrast, tumors resistant to CDK4/6i express CDK6 as a thermo-stable, weak HSP90/CDC37-client that binds weakly to CDK4/6i.

Our data uncover the expression state of CDK6 and its dependence on the HSP90/CDC37 complex as a critical determinant of tumor response to CDK4/6i. We further identify low CDK6 expression as a molecular predictor of tumor sensitivity to current CDK4/6i, indicating a potential biomarker for selection of patients that are more likely to benefit from these drugs. Finally, our findings underline the need for novel inhibitors targeting the thermostable CDK6 to be used for the treatment of the large number of patients with of Rb-proficient solid tumors that are resistant to current clinical CDK4/6i. Thus, this unexpected dualism in the dependence of CDK6 kinase on HSP90 explains resistance of a large portion of tumors to current CDK4/6i, and provides a roadmap for developing more effective CDK4/6-directed pharmacologic strategies for cancer therapy.

No conflict of interest.

98LBA

Late Breaking

Results from the primary analysis of a 30 patient extension of the GATTO study, a phase Ib study combining the anti-MUC1 Gatipotuzumab (GAT) with the anti-EGFR Tomuzotumaximab (TO) or Panitumumab in patients with refractory solid tumors

M. Macchini¹, E. Garraida², W. Fiedler³, G. Del Conte¹, C. Rolling³, M. Kebeke³, K.F. Klinghammer⁴, I. Ahrens-fath⁵, B. Habel⁵, H. Baumeister⁵, A. Zurlo⁶, S. Ochsenreiter⁴. ¹Fondazione IRCCS San Raffaele Hospital, Dept. Medical Oncology, Milano, Italy; ²Vall d'Hebron Institute of Oncology, Early Drug Development Unit, Barcelona, Spain; ³Universitätsklinikum Hamburg Eppendorf UKE, Onkologisches Zentrum, Hamburg, Germany; ⁴Charité, Comprehensive Cancer Center, Berlin, Germany; ⁵Glycotope GmbH, Clinical Department, Berlin, Germany

Background: GAT (Gatipotuzumab) is a novel humanized monoclonal antibody, which recognizes the tumor-specific epitope of mucin-1 (TA-MUC1). TO (Tomuzotumaximab) is a second-generation anti-EGFR antibody that specifically binds to EGFR. Both antibodies are glyco-engineered to potentiate antibody-dependent cellular cytotoxicity (ADCC). Preclinical evidence suggests a complex interaction between EGFR and cell surface expressed TA-MUC1 and shows a synergistic antibody dependent cell

cytotoxicity activity with dual targeting of these molecules. The GATTO study initially assessed the tolerability, safety and preliminary activity of anti-TA-MUC1 and anti-EGFR combination in 20 patients with refractory solid tumors (ESMO GI 2019 abstract 848). Afterwards a study extension has been started in which a different anti-EGFR could be optionally used in place of TO.

Methods: In the extension phase, 30 patients with colorectal cancer (CRC), non-small cell lung cancer (NSCLC), head and neck (H&N) cancer and breast cancer (BC) were enrolled to receive TO and GAT administered at 1200 mg and 1400 mg Q2W respectively. Due to the risk of infusion related reactions (IRR), the first dose of TO was reduced to 720 mg split over 2 consecutive days (60 and 660 mg, respectively). Per investigator choice, Panitumumab was used in place of TO in 9 CRC patients. Treatment with GAT started one week after the first dose of anti-EGFR antibody. By the time of the primary analysis in June 2020, 19 CRC (10 received TO, 9 Panitumumab), 5 NSCLC, 4 H&N and 2 BC patients were treated with both antibodies in the study.

Results: Eleven (37%) patients experienced infusion related reactions (IRR) of grade 1–2 CTCAE, often only at the first infusion of TO. Other AE included those commonly observed with anti-EGFR treatment such as skin toxicity in 24 (80%) patients and hypomagnesemia in 7 (23%) patients. Overall, the combined treatment was well tolerated. Four (22%) CRC patients achieved a confirmed RECIST partial response, with 5.8 months median duration of response. The median Progression Free Survival (PFS) of CRC patients who received GAT and Panitumumab was 5.5 months. The median PFS for NSCLC was 5.3 months with 2 patients achieving a prolonged control of disease. Several potential biomarkers were assessed in an extensive translational research program, and promising results were obtained with soluble TA-MUC1 in the serum of the patients; when using the median baseline value as cutoff, higher levels appeared to predict positively the outcome for PFS and Overall Survival (OS).

Conclusion: Results from this study extension confirm the good safety profile of combining TA-MUC1 and EGFR inhibition. Preliminary activity was observed in CRC and NSCLC patients. Levels of serum TA-MUC1 may have predictive value and potentially be used as companion biomarker for further development of the combination.

No conflict of interest.

99LBA

Late Breaking

MDNA55, a Locally Administered IL4 Guided Toxin for Targeted Treatment of Recurrent Glioblastoma Shows Long Term Survival Benefit.

J. Sampson¹, A.S. Achrol², M.K. Aghi³, K. Bankiewicz⁴, M. Bexon⁵, S. Brem⁶, A. Brenner⁷, S. Chowdhary⁸, M. Coello⁵, B.M. Ellingson⁹, J.R. Floyd¹⁰, S. Han¹¹, S. Kesari¹², F. Merchant⁵, N. Merchant⁵, D. Randazzo¹³, M. Vogelbaum¹⁴, F. Vronis¹⁵, M. Zabek¹⁶, N. Butowski¹⁷. ¹Duke University Medical Center, Neurosurgery, Durham- NC, USA; ²Loma Linda University Medical Center, Neurosurgery, Loma Linda- CA, USA; ³University of California San Francisco, Neurosurgery, San Francisco- CA, USA; ⁴Ohio State University College of Medicine, Neurosurgery, Columbus- OH, USA; ⁵Medicenna BioPharma, Clinical, Houston- TX, USA; ⁶Hospital of the University of Pennsylvania, Neurosurgery, Philadelphia- PA, USA; ⁷University of Texas Health Science Center San Antonio, Neuro-oncology, San Antonio- TX, USA; ⁸Boca Raton Regional Hospital, Neuro-oncology,

Boca Raton- FL, USA; ⁹University of California Los Angeles, Brain Tumor Imaging Laboratory, Los Angeles- CA, USA; ¹⁰University of Texas Health Science Center San Antonio, Neurosurgery, San Antonio- TX, USA; ¹¹Oregon Health & Science University, Neurosurgery, Portland- OR, USA; ¹²Pacific Neurosciences Institute, Neuro-oncology, Santa Monica- CA, USA; ¹³Duke University Medical Center, Neuro-oncology, Durham- NC, USA; ¹⁴H. Lee Moffitt Cancer Center & Research Institute, Neurosurgery, Tampa- FL, USA; ¹⁵Boca Raton Regional Hospital, Neurosurgery, Boca Raton- FL, USA; ¹⁶Mazovian Brodowski Hospital, Neurosurgery, Warsaw, Poland; ¹⁷University of California San Francisco, Neuro-oncology, San Francisco- CA, USA

Background: MDNA55 is a novel, first in class, interleukin-4 empowered cytokine fused to Pseudomonas exotoxin being developed for the treatment of GBM, an aggressive disease with uniform fatality. MDNA55 targets the IL-4 receptor (IL-4R) overexpressed by GBM and immunosuppressive cells of the tumor microenvironment, and is designed to simultaneously purge both the tumor and its supportive milieu. A Phase 2b trial of MDNA55 using convection-enhanced delivery to bypass the BBB was completed in subjects with recurrent GBM (rGBM).

Method: MDNA55-05 was an open-label, single-arm study of MDNA55 delivered intratumorally as a single treatment in rGBM patients at 1st or 2nd recurrence with an aggressive form of rGBM (*de novo* GBM, IDH wild-type, not-resectable at recurrence); tumors \leq 4 cm, KPS \geq 70. Primary endpoint was mOS and secondary endpoints included PFS and impact of IL4R status on mOS. Use of low-dose bevacizumab (Avastin[®]), at doses typically used to control radiation induced necrosis (5 mg/kg q2w or 7.5 mg/kg q3w), was allowed for management of symptom control and/or steroid sparing.

Results: Long-term survival data was available as of 15 Sep 2020 (median follow-up time 33.7 months, range 18–42 months). Among all evaluable subjects (n = 44), mOS was 11.9 months with 48% and 20% subjects still alive at 12 and 24 months, respectively. In a sub-population (n = 32) of IL4R High subjects and IL4R Low subjects receiving high dose (median 180mcg), mOS was extended to 14.0 months, with an OS-12 and OS-24 of 56% and 20%, respectively. Among these subjects, 17 had tumors with unmethylated MGMT promoter, a marker associated with resistance to temozolomide. After treatment with MDNA55, this group showed an mOS of 15 months, which is a 55–100% improvement over approved therapies in this difficult to treat population. Survival was also improved with concomitant administration of low dose bevacizumab; mOS was 21.8 months in all evaluable subjects (n = 9) and 18.6 months in the sub-population (n = 8) of IL4R High subjects and IL4R Low subjects receiving high dose MDNA55; OS-24 was 44% and 38%, respectively. PFS rate at 6, 9, and 12 months assessed by mRANO criteria was 33%, 27%, and 27% in all evaluable subjects. MDNA55 showed an acceptable safety profile at doses of up to 240 mcg.

Conclusions: The MDNA55-05 study enrolled rGBM patients with limited treatment options and poor prognostic factors with an expected mOS of only 6–9 months, OS-24 of 0–10% and PFS-12 of 0–17%. Findings from the Phase 2b trial demonstrate that by combining precise drug delivery and targeting the IL4R, a single treatment with MDNA55 has the potential to present a superior treatment option for improved survival and tumor control in rGBM patients who otherwise rapidly succumb to this disease.

No conflict of interest.

Saturday, 24 October 2020

15:05–16:35

PLENARY SESSION 1

Late Breaking and Best Proffered Papers

1

Oral

Genome-scale genetic screening identifies PRMT1 as a critical vulnerability in castration-resistant prostate cancer

S. Tang^{1,2}, N. Metaferia¹, M. Nogueira^{1,2}, M. Gelbard¹, S. Abou Alaiwi¹, J.H. Seo¹, J. Hwang^{1,2}, C. Strathdee², S. Baca^{1,2}, J. Li¹, S. Abuhamad¹, X. Zhang³, J. Doench⁴, W. Hahn^{1,2}, D. Takeda⁵, M. Freedman^{1,2}, P. Choi⁶, S. Viswanathan^{1,2}. ¹Dana-Farber Cancer Institute, Medical Oncology, Boston, USA; ²Broad Institute, Cancer Program, Cambridge, USA; ³Huntsman Cancer Institute- University of Utah, Department of Oncological Sciences, Salt Lake City, USA; ⁴Broad Institute, Genetic Perturbation Platform, Cambridge, USA; ⁵National Cancer Institute- NIH, Laboratory of Genitourinary Cancer Pathogenesis, Bethesda, USA; ⁶Children's Hospital of Philadelphia, Division of Cancer Pathobiology, Philadelphia, USA

Background: Androgen receptor (AR) signaling is the central driver of prostate cancer growth and progression across disease states, including in most cases of castration-resistant prostate cancer (CRPC). While next-generation AR antagonists and androgen synthesis inhibitors are effective for a time in CRPC, tumors invariably develop resistance to these agents, commonly through mechanisms resulting in the overexpression of AR or the production of constitutively active AR splice variants (e.g. AR-V7). Systematic discovery of factors that modulate AR expression and signaling may reveal additional therapeutic intervention points in CRPC.

Material and Methods: We performed genome-scale CRISPR/Cas9 genetic screening to systematically identify regulators of AR/AR-V7 expression in prostate cancer cells. Protein arginine methyltransferase 1 (PRMT1), identified as a top hit in our screen, was validated as a regulator of AR in multiple prostate cancer cell lines. Epigenetic and transcriptome profiling was performed to interrogate the consequence of genetic and pharmacologic inhibition of PRMT1. The ability of PRMT1 inhibition, to impair prostate cancer cell proliferation, alone or in conjunction with inhibition of the AR, was assessed.

Results: We identified protein arginine methyltransferase 1 (PRMT1) as a critical mediator of AR expression and signaling that regulates recruitment of AR to genomic target sites. PRMT1 suppression globally perturbs the expression and splicing of AR target genes and inhibits the proliferation and survival of AR-positive prostate cancer cells. Genetic or pharmacologic inhibition of PRMT1 reduces AR binding at lineage-specific enhancers, which leads to decreased expression of key oncogenes, including AR itself. CRPC cells displaying activated AR signaling due to overexpression of AR or AR-V7 are uniquely susceptible to combined AR and PRMT1 inhibition.

Conclusions: Our findings implicate PRMT1 as a critical regulator of AR output and provide a preclinical framework for co-targeting of AR and PRMT1 as a promising new therapeutic strategy in CRPC.

Conflict of interest:

Other Substantive Relationships: J.G.D. consults for Tango Therapeutics, Maze Therapeutics, Foghorn Therapeutics, and Pfizer. W.C.H. is a consultant for ThermoFisher, Solvasta Ventures, MPM Capital, KSQ Therapeutics, iTeos, Tyra Biosciences, Jubilant Therapeutics, Frontier Medicine and Parexel.

2

Oral

Phase 1 safety, pharmacokinetic and pharmacodynamic study of fadraciclib (CYC065), a cyclin dependent kinase inhibitor, in patients with advanced cancers (NCT02552953)

K.T. Do¹, K. Frej¹, K. Bhushan¹, S. Pruitt-Thompson¹, D. Zheleva², D. Blake², J. Chiao², G.I. Shapiro¹. ¹Dana-Farber Cancer Institute and Brigham and Women's Hospital, Early Drug Development Center, Boston, USA; ²Cyclacel Ltd, Research & Development, Dundee, United Kingdom

Background: Fadraciclib (CYC065) is a potent and selective inhibitor of CDK2 and CDK9. CDK2 drives cell cycle transitions and CDK9 regulates transcription of genes through phosphorylation of the carboxy-terminal domain (CTD) of RNA polymerase II (RNAP II). This ongoing phase 1 study is evaluating a flat fixed dosing schedule of fadraciclib given either by 1-hour infusion or orally on day 1, 2, 8 and 9 every 3 weeks.

Methods: Eligible patients must be at least 18 years of age and have metastatic or unresectable solid tumors for which there is no standard curative or palliative treatment. Recommended phase 2 dose (RP2D) is defined as the highest dose level at which fewer than one-third of at least 6 patients experience cycle 1 dose-limiting toxicity (DLT). Blood samples were taken at pre-dose and up to 24 hours after the first dose of cycle 1 to assess pharmacokinetic (PK) and pharmacodynamic (PD) effects. Biomarkers related to fadraciclib target inhibition, including phosphorylation of RNAP II CTD Ser2, a direct substrate of CDK9, and protein levels of downstream targets, such as MCL1, were determined in PBMCs.

Results: Twenty-one patients were treated with 1-hour infusions and 3 patients were treated with oral fadraciclib. In the 1-hour infusion cohort, dose escalation reached 213 mg where one patient experienced a DLT of grade 2 neutropenia lasting longer than 2 weeks and 2 additional patients required dose reduction for transient elevations in AST (grade 3) and serum creatinine (grade 2). The dose level of 160 mg is being expanded. The most frequent adverse events (all cycles, regardless of causality) included constipation, diarrhea, nausea, vomiting, and hyperglycemia, the majority mild to moderate in intensity. All patients participated in the PK/PD samplings. Exposure to fadraciclib increased with dose. Average half-life ranged from 2.7 h to 3.5 h. The PK of 2 patients treated with oral fadraciclib showed plasma drug concentrations similar to those of comparable IV doses indicating high bioavailability. In the 1-hour IV cohort, one patient with MCL1-amplified endometrial carcinoma achieved partial response that is ongoing at cycle 16, and another patient with CCNE1-amplified ovarian carcinoma had stable disease with 29% shrinkage of target lesions.

Conclusion: Fadraciclib administered by 1-hour infusion is safe and demonstrated anti-tumor activity with radiographic tumor shrinkage. Oral fadraciclib has good bioavailability. The trial is ongoing to define the RP2D of 1-hour infusion and oral dosing.

Conflict of interest:

Ownership: Cyclacel Pharmaceuticals, Inc.: D.Zheleva, D.Blake and J. Chiao.

Advisory Board: G.I.Shapiro: Pfizer, Eli Lilly, G1 Therapeutics, Roche, Merck KGaA/EMD-Serono, Sierra Oncology, Bicycle Therapeutics, Fusion Pharmaceuticals, Cybrexa Therapeutics, Astex, Almac, Ipsen, Bayer, Angiox, Daiichi Sankyo, Seattle Genetics, Boehringer Ingelheim, ImmunoMet, Asana, Artios, Atrin, Syros, Zentalis, Concarlo Holdings.

Corporate-sponsored Research: G.I.Shapiro: Eli Lilly, Merck KGaA/EMD-Serono, Merck, Sierra Oncology.

Other Substantive Relationships: Cyclacel Ltd. Employee: D.Zheleva, D. Blake, J.Chiao.

Cyclacel Ltd. Patents: D.Zheleva, D.Blake, J.Chiao, G.I.Shapiro.

3

Oral

USP1 inhibitors show robust combination activity and a distinct resistance profile from PARP inhibitors

P. Sullivan¹, S. Shenker², M. McGuire¹, P. Grasberger¹, K. Sinkevicius³, E. Tobin¹, E. Chipumuro¹, G. Histen¹, N. Hafeez¹, R. Rahal¹, M. Schlabach⁴, F. Stegmeier⁵, L. Cadzow³, A. Wylie¹. ¹KSQ Therapeutics, Discovery Biology, Cambridge, USA; ²KSQ Therapeutics, Computational Biology, Cambridge, USA; ³KSQ Therapeutics, Pharmacology, Cambridge, USA; ⁴KSQ Therapeutics, Target Discovery, Cambridge, USA; ⁵KSQ Therapeutics, Research, Cambridge, USA

Background: Tumors harboring BRCA1/2 mutations and other homologous repair deficiencies (HRD) are sensitive to agents targeting pathways involved in DNA repair. The most successful class of molecules that have been developed to-date target poly (ADP-ribose) polymerase (PARP). Despite the clinical benefit achieved with these drugs, many patients achieve incomplete disease control and resistance often emerges.

Material and methods: With the goal of addressing this clinical need, we applied our proprietary CRISPRomics[®] technology to identify genetic dependencies that are selectively required in cells with defects in DNA repair pathways. We evaluated the candidate genes for their suitability for drug development with a bias for those involved in DNA repair pathways distinct from those targeted by PARP inhibitors.

Results: One of the top candidates was USP1, a deubiquitinating enzyme involved in regulating both the Fanconi Anemia complex and Translesion Synthesis pathway. Potent, selective inhibitors of USP1 were developed and tested across a broad range of tumor lineages and genetic backgrounds with cell lines harboring mutations in BRCA1/2 representing the best predictor of sensitivity to USP1 inhibitors. Mechanistic studies indicated that the accumulation of ubiquitinated PCNA is the likely cause of synthetic lethality in BRCA/HRD cell lines. To investigate how the distinct mechanisms of action of USP1 and PARP inhibitors would be reflected in their resistance profiles, we used our CRISPRomics[®] technology to perform functional genomic resistance screens. Resistance genes identified in the presence of a PARP

inhibitor included previously reported PARG and 53BP1, thereby validating the approach. Notably, the top scoring resistance genes for the USP1 inhibitor differed from those identified for the PARP inhibitor and were functionally related to its mechanism of action. The complimentary nature of the resistance profiles raises the possibility that combining PARP and USP1 inhibitors may provide more durable disease control by reducing the emergence of resistance. The depth of response to PARP inhibitors may also be enhanced through combination with USP1 inhibitors as a result of their distinct mechanisms of action and the potential for synergistic activity. Indeed, when USP1 and PARP inhibitors were tested in combination across a large panel of cancer cell lines, synergistic activity was frequently observed particularly in lines with BRCA1 and BRCA2 alterations. In addition, in vivo combination studies of USP1 inhibitors and the PARP inhibitor, olaparib, led to strong and durable regressions across multiple models.

Conclusions: This work provides further support for advancing USP1 inhibitors into clinical testing to treat patients with BRCA1/2 mutations or related HRD, both as single agents and in combination with PARP inhibitors.

Conflict of interest:

Ownership: Employee and stockholder of KSQ Therapeutics.

4

Oral

Synthetic lethal interaction between the ESCRT paralogs VPS4A and VPS4B in cancers with chromosome 18q or 16q deletion

J. Neggers¹, B. Paolella², A. Asfaw², M. Rothberg², T. Skipper², R. Kalekar¹, M. Burger², G. Kugener², K. Jérémie², A. Yang¹, D. Nancy², M. Abdusamad², A. Cherniack², A. Tscherniak², A. Hong³, W. Hahn², K. Stegmaier², T. Golub², F. Vazquez², A. Aguirre¹. ¹Dana-Farber Cancer Institute, Medical Oncology, Boston, USA; ²Broad Institute of MIT and Harvard, Cancer Program, Cambridge, USA; ³Dana-Farber Cancer Institute, Pediatric Oncology, Boston, USA

Somatic copy number alterations constitute distinctive driver events of tumorigenesis. Hence, the identification of pharmacologically tractable targets related to somatic copy number alterations represents an opportunity for drug discovery to achieve cancer-selective therapeutics. Here, we examined genome-scale CRISPR-SpCas9 and RNA-interference loss-of-function screens to identify new cancer therapeutic targets associated with genomic loss of common tumor suppressor genes. The ESCRT ATPases VPS4A and VPS4B scored as strong synthetic lethal dependencies, with VPS4A selectively essential in cancers harboring loss of VPS4B adjacent to SMAD4 on chromosome 18q and VPS4B required in tumors with co-deletion of VPS4A and CDH1 (encoding E-cadherin) on chromosome 16q.

VPS4A and B function as paralog AAA ATPases that form hexameric complexes that regulate the endosomal sorting complex required for transport (ESCRT), a multiprotein complex essential for inverse membrane remodeling involved in a wide range of cellular processes, including mitosis, cytokinesis, microvesicle budding, plasma membrane repair, nuclear envelope surveillance, autophagy, endosomal and lysosomal trafficking and viral budding. VPS4A suppression in VPS4B-deficient cells selectively led to ESCRT-III filament accumulation, cytokinesis defects, nuclear deformation, G2/M arrest, apoptosis and potent tumor regression in mouse models of cancer. Genome-scale CRISPR-SpCas9 loss-of-function screening and integrative genomic analysis further revealed that genetic knockout of other ESCRT members and regulators of abscission potentially modify the dependency of VPS4B-deficient cancer cells on VPS4A. Interestingly, VPS4A dependency also correlated with higher baseline expression of interferon type I response and cytokine signaling genes. Furthermore, interferon treatment further sensitized VPS4B-deficient cancer cells to VPS4A depletion, suggesting that expression of inflammatory response genes may regulate cellular sensitivity to VPS4 ablation.

In conclusion, we describe a compendium of synthetic lethal vulnerabilities associated with tumor suppressor gene loss in cancer and credential VPS4A and VPS4B as promising therapeutic targets for cancer.

Conflict of interest:

Corporate-sponsored Research: Some parts of this research were funded by an industry sponsor and the Damon Runyon Cancer Research Foundation. J.N., B.P., F.V., and A.A. are named as co-inventors on a pending patent application related to this work.

5

Oral

Intermittent dosing of RMC-4630, a potent, selective inhibitor of SHP2, combined with the MEK inhibitor cobimetinib, in a phase 1b/2 clinical trial for advanced solid tumors with activating mutations of RAS signaling

J. Bendell¹, S. Ulahannan², M. Koczywas³, J. Brahmer⁴, A. Capasso⁵, S.G. Eckhardt⁵, M. Gordon⁶, C. McCoach⁷, M. Nagasaka⁸, K. Ng⁹, J. Pacheco¹⁰, J. Riess¹¹, A. Spira¹², C. Steuer¹³, R. Dua¹⁴, S. Chittivelu¹⁵, S. Masciarì¹⁶, Z. Wang¹⁷, X. Wang¹⁸, S.H. Ou¹⁹. ¹Sarah Cannon Research Institute/Tennessee Oncology, Drug Development Unit, Nashville, USA; ²Sarah Cannon Research Institute/University of Oklahoma, Oklahoma TSET Phase I Program, Oklahoma City, USA; ³City of Hope Medical Center, Department of Medical Oncology & Therapeutics Research, Duarte, USA; ⁴Johns Hopkins University, Upper Aerodigestive Department, Baltimore, USA; ⁵University of Texas, Department of Oncology, Austin, USA; ⁶Honor Health, Department of Hematology and Oncology, Scottsdale, USA; ⁷University of California, Thoracic Oncology, San Francisco, USA; ⁸Karmanos Cancer Center, Department of Oncology, Detroit, USA; ⁹Dana-Farber Cancer Institute, Department of Medical Oncology, Boston, USA; ¹⁰University of Colorado, Department of Oncology, Denver, USA; ¹¹University of California, Department of Hematology and Oncology, Davis, USA; ¹²US Oncology, Department of Oncology, Fairfax, USA; ¹³Emory University, Department of Hematology and Medical Oncology, Atlanta, USA; ¹⁴Revolution Medicines- Inc., Medical Director, Redwood City, USA; ¹⁵Revolution Medicines- Inc., Oncology, Redwood City, USA; ¹⁶Sanofi, Oncology, Cambridge, USA; ¹⁷Revolution Medicines- Inc., Non-clinical Development and Pharmacology, Redwood City, USA; ¹⁸Revolution Medicines- Inc., Clinical Development, Redwood City, USA; ¹⁹University of California, Department of Hematology and Oncology, Irvine, USA

Background: Single agent MEK inhibition has been disappointing in clinical trials of RAS mutant tumors, probably due to the induction of resistance through upstream activation of receptor tyrosine kinases (RTKs). RMC-4630 is a potent, selective inhibitor of SHP2, a convergent signaling node for many RTKs. RMC-4630 monotherapy has shown anti-tumor activity against RAS-mutant NSCLC in an ongoing phase 1 clinical trial (NCT03634982). RMC-4630 has combinatorial activity with MEK inhibitors in preclinical models of RAS-mutant cancers and tumors harboring loss of neurofibromin 1 (NF1^{LOF}) and BRAF^{class3} mutations. Intermittent dosing of RMC-4630, to provide discontinuous SHP2 inhibition above the EC₅₀ for RAS pathway inhibition, retains anti-tumor activity and is better tolerated than daily continuous dosing.

Methods: In this phase 1b/2 study (NCT03989115), RMC-4630 and cobimetinib were both sequentially dose-escalated in patients with tumors harboring RAS pathway alterations (KRAS^{G12x}, KRAS^{amp}, NF1^{LOF}, BRAF^{class3}). RMC-4630 was administered twice weekly (D1,D4 or D1,D2); cobimetinib was dosed either daily (21 days on, 7 off) or twice weekly on D1,D2.

Results: The study is ongoing and the recommended phase 2 dose and schedule (RP2DS) is currently being refined. As of 18 May 2020, 33 patients have been treated across four different dose cohorts/schedules. The highest dose level of RMC-4630 tested to date is 140 mg (D1,D2 or D1,D4 twice weekly); the highest dose level of cobimetinib tested is 40 mg daily or 60 mg D1,D2. The most common treatment-related adverse events (TRAEs) were diarrhea (63.6%), edema (33.3%), and thrombocytopenia (24.2%). Grade 3–4 TRAEs were diarrhea (9.1%) and thrombocytopenia (6.1%). Blurred vision and retinopathy were reported in 4 patients (1 with Grade 2; 1 with Grade 3 AEs), reversible on holding cobimetinib dosing. The observed safety profile is consistent with an 'on-pathway' effect of the combination and with previous clinical experience of both RMC-4630 and MEK inhibitors. The pharmacokinetic profiles of both RMC-4630 and cobimetinib were generally consistent with monotherapies and no pharmacokinetic interaction has been detected. At all dose levels and schedules tested, exposure was within the range that induced tumor regressions in preclinical models. Preliminary evidence of anti-tumor activity has been observed in KRAS^{mut} colorectal cancer with tumor reduction in 3 of 8 patients including, at data cut-off, 1 unconfirmed PR (range of tumor reduction 10–30%; time on treatment 1.9–5.1 months).

Conclusions: The interim data suggest that the combination of intermittent RMC-4630 plus daily or intermittent cobimetinib has acceptable tolerability at doses that exceed 'target' plasma exposure based on preclinical models of RAS-pathway driven cancers. Further evaluation of anti-tumor activity in RAS-activated tumors will occur at the RP2DS.

Conflict of interest:

Advisory Board: J. Bendell: Consulting /Advisory Role -All to Institution, Gilead, Genentech/Roche, BMS, Five Prime, Lilly, Merck, MedImmune, Celgene, Taiho, MacroGenics, GSK, Novartis, OncoMed, LEAP, TG Therapeutics,

AstraZeneca, BI, Daiichi Sankyo, Bayer, Incyte, Apexigen, Array, Sanofi, ARMO, Ipsen, Merrimack, Oncogenex, FORMA, Arch Oncology, Prelude Therapeutics, Phoenix Bio, Cytel, Molecular Partners, Innate, Torque, Tizona, Janssen, Tolero, TD2 (Translational Drug Development), Amgen, Seattle Genetics, Moderna Therapeutics, Tanabe Research Laboratories, Beigene, Continuum Clinical, Agios, Bicycle Therapeutics, Relay Therapeutics, Evelo, Pfizer, Piper Biotech, Samsung Bioepis.

S. Ulahannan: Array, Incyte, Bayer, Exelixis, Syros.

J. Brahmer: Advisory Boards/Consulting Agreements, Amgen (Advisory Board/Consulting Agreement), BMS (Uncompensated) BMS (Advisory Board/Consulting Agreement), Genentech/Roche (Advisory Board/Honoraria), Eli Lilly (Advisory Board), GlaxoSmithKline (Advisory Board/Consulting Agreement), Merck (Advisory Board/Consulting Agreement), Sanofi (Advisory Board/Consulting Agreement), K. Ng: Advisory Boards: Array Biopharma.

J. Pacheco: Advisory/Consultancy: AstraZeneca, Gerson Lehrman Group, Hengrui Pharmaceuticals, Jazz Pharmaceuticals, Novartis, Pfizer, Takeda. J.W. Riess: Consulting: Novartis, MedTronic.

C. Steuer: Advisory boards, Bergen Bio, Armo, Eli Lilly, ABBVIE.

Corporate-sponsored Research: J. Bendell: Research Funding –All to institution, Gilead, Genentech/Roche, BMS, Five Prime, Lilly, Merck, MedImmune, Celgene, EMD Serono, Taiho, MacroGenics, GSK, Novartis, OncoMed, LEAP, TG Therapeutics, AstraZeneca, BI, Daiichi Sankyo, Bayer, Incyte, Apexigen, Koltan, SynDevRx, Forty Seven, AbbVie, Array, Onyx, Sanofi, Takeda, Eisai, CellDex, Agios, Cytomx, Nektar, ARMO, Boston Biomedical, Ipsen, Merrimack, Tarveda, Tyrogenex, Oncogenex, Marshall Edwards, Pieris, Mersana, Calithera, Blueprint, Evelo, FORMA, Merus, Jacobio, Effector, Novocare, Arrys, Tracoon, Sierra, Innate, Arch Oncology, Prelude Oncology, Unum Therapeutics, Vyriad, Harpoon, ADC, Amgen, Pfizer, Millennium, Imclone, Acerta Pharma, Rgenix, Bellicum, Gossamer Bio, Arcus Bio, Seattle Genetics, TempestTx, Shattuck Labs, Synthorx, Inc., Revolution Medicines, Inc., Bicycle Therapeutics, Zymeworks, Relay Therapeutics, Scholar Rock, NGM Biopharma, Stemcentrx, Beigene, CALGB, Cytel Therapeutics, Foundation Bio, Innate Pharma, Morphotex, Oncologie, NuMab.

S. Ulahannan: Institutional support for research, all funds to institution, AbbVie, Inc, ArQule, Inc, AstraZeneca, Boehringer Ingelheim, Bristol-Myers Squibb, Celgene Corporation, Ciclomel LLC, Evelo Biosciences, Inc., G1 Therapeutics, Inc., GlaxoSmithKline GSK, Incyte, Isofol, Klus Pharma, Inc., MacroGenics, Merck Co. Inc., Mersana Therapeutics, OncoMed Pharmaceuticals, Inc., Pfizer, Regeneron, Inc., Revolution Medicines, Inc., Takeda, Tarveda Therapeutics, Tesaro, Tempest, Vigeo Therapeutics Inc. J. Brahmer: Grant Research Funding, AstraZeneca, BMS, Genentech/Roche, Merck, RAPT Therapeutics, Inc., Revolution Medicines, Data and Safety Monitoring Board/Committees, GlaxoSmithKline, Sanofi.

S.G. Eckhardt: Research Grant: Revolution Medicine

M. Gordon: Institutional Research Support: MedImmune, Merck, BMS, Amgen, Tesaro, Beigene, ABBVIE, Aeglea, Agenus, Arcus, Astex, BluePrint, Calithera, CellDex, Corcept, Clovis, Eli Lilly, Endocyte, Five Prime, Genosca, Neon, Plexxicon, Imaging Endpoints, Revolution Medicine, Seattle Genetics, Serono, SynDevRx, Tolero, Tracoon, Deciphera, Salarius.

C. McCoach: Research Funding: Novartis, Revolution Medicines.

M. Nagasaka: Grant, Tempus.

K. Ng: Research funding: Revolution Medicines, Pharmavite, Evergrande Group.

J. Pacheco: Research Grant (Institution): Pfizer.

J.W. Riess: Research Grants (to Institution): Revolution Medicines, Merck, Novartis, Spectrum, AstraZeneca.

A. Spira: Research Funding, Revolution Medicines.

Other Substantive Relationships: J. Bendell: Food/Beverage/Travel, Gilead, Genentech/Roche, BMS, Lilly, Merck, MedImmune, Celgene, Taiho, Novartis, OncoMed, BI, ARMO, Ipsen, Oncogenex, FORMA.

M. Gordon: Personal Fees, Agenus, Imaging Endpoints, Tracoon, Deciphera, Salarius.

C. McCoach: Honoraria: Genentech, Novartis, Guardant Health.

M. Nagasaka: Personal Fees: AstraZeneca, Caris Life Sciences, Daiichi Sankyo, Takeda, Novartis.

Non-Financial Support: An Heart Therapeutics.

J. Pacheco: Honoraria (self): Takeda, Genentech.

Travel/Accommodation/Expenses: AstraZeneca, Novartis, Pfizer, Takeda.

R. Dua: I am an employee of Revolution Medicines, the trial sponsor, and own stocks and stock options of Revolution Medicines.

S. Chittivelu: I am an employee of Revolution Medicines, the trial sponsor. I also own stock options of Revolution Medicines.

S. Masciari: I am an employee of Sanofi, the Revolution Medicine partner company, and I own Sanofi shares. The SHP2 inhibitor program, including RMC-4630, is the focus of an exclusive global research, development and commercialization agreement between Revolution Medicine and Sanofi. I declare that I have no conflict of interest.

Z. Wang: I am an employee of Revolution Medicines, the trial sponsor, and own stocks and stock options of Revolution Medicines.

X. Wang: I am an employee of Revolution Medicines, the trial sponsor, and own stocks and stock options of Revolution Medicines.

S.I. Ou: Personal Fees: Pfizer, AstraZeneca, Takeda/ARIAD, Roche/Genentech, Daiichi Sankyo.

Stock Ownership: Turning Point Therapeutics.

Sunday, 25 October 2020

15:45–17:15

PLENARY SESSION 2

Late Breaking and Best Proffered Papers

6

Oral

Bevacizumab-induced hypertension and proteinuria: A genome-wide analysis of more than 1,000 patients

F. Innocenti¹, J. Wang², A. Sibley³, C. Jiang³, A. Etheridge¹, F. Shen⁴, J. Patel⁵, H. Daniel⁶, E. Dees⁷, M. Howard⁸, M. Bertagnoli⁹, H. Rugo¹⁰, H. Kindler¹¹, W. Kelly¹², M. Ratain¹¹, D. Kroetz¹³, K. Owzar¹⁴, B. Schneider⁴, D. Lin², J. Quintanilha¹. ¹University of North Carolina at Chapel Hill, Eshelman School of Pharmacy, Chapel Hill, USA; ²University of North Carolina at Chapel Hill, Department of Biostatistics, Chapel Hill, USA; ³Duke University Medical Center, Duke Cancer Institute, Durham, USA; ⁴Indiana University School of Medicine, Department of Medicine, Indianapolis, USA; ⁵Levine Cancer Institute, Levine Cancer Institute, Charlotte, USA; ⁶University of Michigan, College of Pharmacy, Ann Arbor, USA; ⁷University of North Carolina at Chapel Hill, Lineberger Comprehensive Cancer Center, Chapel Hill, USA; ⁸Department of Cancer Epidemiology, Moffitt Cancer Center, Tampa, USA; ⁹Dana Farber Cancer Institute, Dana Farber Cancer Institute, Boston, USA; ¹⁰University of California at San Francisco, Department of Medicine-Hematology/Oncology, San Francisco, USA; ¹¹University of Chicago Comprehensive Cancer Center, University of Chicago Comprehensive Cancer Center, Chicago, USA; ¹²Yale School of Medicine, Department of Medical Oncology, New Haven, USA; ¹³University of California at San Francisco, Department of Bioengineering and Therapeutic Sciences, San Francisco, USA; ¹⁴Duke University Medical Center, Department of Biostatistics and Bioinformatics, Durham, USA

Background: Hypertension and proteinuria are the most common toxicities induced by bevacizumab. No validated biomarkers are available to identify patients at risk for these toxicities. This study aimed to discover and validate genetic predictors of bevacizumab-induced hypertension and proteinuria.

Material and methods: Genome-wide association studies (GWAS) were conducted in 1,041 patients treated with bevacizumab in clinical trials from Cancer and Leukemia Group B (now Alliance, CALGB 40502, 40503, 80303, 90401). Grade ≥ 2 hypertension and proteinuria were recorded (CTCAE v.3.0). Associations between single-nucleotide polymorphisms (SNPs) and toxicity were performed by a cause-specific Cox model. Top hits for hypertension were selected for validation in another GWAS of 582 cancer patients treated with bevacizumab (ECOG-ACRIN E5103).

Results: For hypertension, the most statistically significant SNPs associated with hypertension were rs2350620 ($p = 1.44 \times 10^{-6}$) and rs6770663 ($p = 4.79 \times 10^{-6}$). They were selected for validation in 582 patients treated with bevacizumab in ECOG-ACRIN E5103. rs2350620 (minor allele frequency, MAF = 0.32) was not validated in ECOG-ACRIN E5103 ($p = 0.235$). rs6770663 (A > G, MAF 0.09) was validated in ECOG-ACRIN E5103, as it was associated with an increased risk of systolic blood pressure ≥ 160 mm Hg ($p = 0.005$). rs6770663 (A > G) is intronic in *KCNAB1*, which encodes a K^+ voltage activated channel. The serum-response factor (SRF), a cardiac-enriched transcription factor, is more likely to bind the A allele than the G allele of rs6770663, activating *KCNAB1*. In patients with the G allele of rs6770663, lower activation of *KCNAB1*, impaired activation of the K^+ voltage activated channel, and increased vasoconstriction results in an increased risk of bevacizumab-induced hypertension. For proteinuria, the most statistically significant SNP associated with proteinuria was rs339947 (C > A, $p = 7.66 \times 10^{-8}$) located between *DNAH5* and *TRIO*. The A allele of rs339947 (MAF 0.14) increased the risk of proteinuria and has been associated with increased *TRIO* expression in the glomerulus ($p = 0.005$). *TRIO* induces Rac1 activity, contributing to podocyte injury. In patients with the A allele of rs339947, increased expression of *TRIO* in the glomerulus and increased podocyte injury would result in an increased risk of bevacizumab-induced proteinuria.

Conclusions: In the largest GWAS of bevacizumab-induced toxicity from randomized trials, we have identified new common variants associated with bevacizumab-induced hypertension and proteinuria. Among them, rs6770663 in *KCNAB1* can be regarded to as a new validated biomarker

to predict the risk of bevacizumab-induced hypertension and can be used to inform decisions of treating patients with bevacizumab. rs339947 as a biomarker of bevacizumab-induced proteinuria requires further validation.

Conflict of interest:

Other Substantive Relationships: JCFQ, JW, DL, and FI are coinventors of a provisional patent application (serial number 62/903,442). FI is an advisor for Emerald Lake Safety.

7

Oral

Impact of angiotensin II pathway inhibition on tumor response to anti PD(L)1 based therapy

J. Strauss¹, A. Rajan¹, A. Apolo¹, J.M. Lee¹, A. Thomas¹, A. Chen¹, G. O'Sullivan Coyne¹, R. Madan¹, M. Bilusic¹, F. Karzai¹, H. Abdul Sater¹, J. Redman¹, M. Gatti-Mays¹, C. Floudas¹, J. Marte¹, L. Cordes¹, J. Schlom¹, J. Gulley¹. ¹National Institutes of Health, National Cancer Institute, Bethesda, USA

Background: Angiotensin II (Ang II) has been shown in preclinical work to increase TGF- β production through AT1 receptor signaling and to decrease TGF- β through AT2 receptor signaling. Thus, the ang II pathway through overlap with the TGF- β pathway may have a critical role in carcinogenesis as well as immune evasion and inhibiting AT1 may enhance clinical responses in combination with PD(L)1 blockade. Here we report efficacy of anti PD(L)1 based therapy in pts with advanced solid tumors concomitantly taking angiotensin receptor blockers (ARBs).

Methods: We pooled and analyzed data on 599 pts with advanced solid tumors enrolled on 20 prospective anti PD(L)1 based trials using the National Institutes of Health's Biomedical Translational Research Information System. Descriptive statistics and chi-squared tests were used to compare pts who were concomitantly receiving an ARB to pts who were not. The same analysis was done comparing pts who were concomitantly receiving an ACE inhibitor (ACEi) to pts who were not.

Results: In total, 599 pts with more than three dozen different tumor types were included. All protocols included treatment with a PD(L)1 inhibitor plus or minus additional agent(s) (e.g. vaccine, cytokine, chemotherapy, CTLA4 inhibitor, multikinase VEGF inhibitor, anti TGF beta, PARP inhibitor). Of the 599 evaluated patients, 71 pts were concomitantly taking ARBs and 82 were taking ACEi. ARB use was associated with a statistically significant increase in ORR (33.8% vs 17.4%; $p = 0.001$) as well as complete response (CR) rate (11.3% vs 3.2%; $p = 0.001$) compared with pts not taking ARBs. Notably ACEi use was not statistically associated with any improvement in ORR (19.5% vs 19.3%; $p = 0.97$) nor CR rate (3.7% vs 4.3%; $p = 0.80$) compared with pts not taking ACEi.

Conclusions: Concomitant ARB use was associated with a statistically significant near doubling in ORR and more than tripling in CR with anti PD(L)1 based therapy. This same benefit was not seen with ACEi. This discrepancy may be due to selective blockade of AT1 by ARBs versus dual blockade of AT1/AT2 by ACEi. These preliminary findings are hypothesis generating and further study is needed to determine if selective AT1 inhibition can improve outcomes when combined with anti PD(L)1 based therapy.

No conflict of interest.

8

Oral

HER2-XPAT, a novel protease-activatable pro-drug T cell engager (TCE), with potent T-cell activation and efficacy in solid tumors and large predicted safety margins in non-human primate (NHP)

F. Cattaruzza¹, C. Koski¹, Å. Nazeer¹, Z. Lange¹, A. Henkensiefken¹, M. Hammond¹, M. Derynck¹, V. Schellenberger¹, B. Irving¹. ¹Amunix Pharmaceuticals, Research and Development, Mountain View, USA

Background: TCEs are effective at inducing remissions in hematologic cancers but have been challenging in solid tumors due to on-target, off-tumor toxicity. Attempts to circumvent CRS include fractionated or step-up dosing, complex molecular designs, but these have been unsuccessful due to toxicity and/or enhanced immunogenicity. Amunix has developed a conditionally active TCE, XPAT or XTENylated Protease-Activated bispecific T Cell Engager, that exploits the protease activity present in tumors vs. healthy tissue to expand the therapeutic index (TI). The core of the HER2-XPAT (PAT) consists of 2 tandem scFVs targeting CD3 and HER2. Two unstructured polypeptide masks (XTEN) are attached to the core that sterically reduce target engagement and extend T1/2. Protease cleavage sites at the base of the XTEN masks enable proteolytic activation of XPATs in the tumor microenvironment, unleashing a highly potent TCE with a short T1/2, and further improving the TI.

Methods: Preclinical studies were conducted to characterize the activity of HER2-XPAT, HER2-PAT (cleaved XPAT) and HER2-NonClv (a non-cleavable XPAT) for cytolytic activity in vitro, anti-tumor efficacy in xenograft models, and for stability and safety in NHPs.

Results: HER2-PAT demonstrated potent *in vitro* tumor-directed T cell cytotoxicity (EC50 1-2pM) and target-dependent T-cell activation and production of cytokines by PBMCs. XPAT provided up to 14,000-fold protection against killing of HER2 tumor cells and exhibited no cytotoxicity against cardiomyocytes at concentrations up to 1uM. In vivo, XPAT induced complete tumor regressions in both BT-474 and SK-OV-3 tumor models with equimolar dosing to PAT. In NHP, HER2-XPAT has been dose-escalated safely up to 42mpk (MTD), but was not tolerated at 50mpk. XPAT demonstrated early T-cell margination at 2 mg/kg but largely spared CRS and tissue toxicity at doses up to 42 mg/kg. PK profiles of HER2-XPAT and non-cleavable HER2-NonClvXTEN were comparable in NHP, indicating minimal systemic cleavage of XPAT, consistent with its *ex vivo* stability when incubated in the plasma of cancer pts for 7 days at 37°Cdegrees. Given by continuous infusion, PAT induced lethal CRS at 0.3 mg/kg/d, but was tolerated at 0.1 mg/kg/d, providing XPAT with >3000-fold protection in tolerated Cmax vs. PAT and a 20-fold margin of safety over the dose required for pharmacodynamic activity.

Conclusions: HER2-XPAT is a potent pro-drug T cell engager with promising evidence of activity at low doses while exhibiting minimal CRS and a potential wide TI in NHP at doses up to 42 mg/kg. With XTEN's prior clinical data of low immunogenicity, the XPAT TCEs provide a promising solution and will enter phase I in 2021. Additional PK, PD, cytokines, safety, and efficacy data will be presented.

Conflict of interest:

Ownership: Amunix Pharmaceuticals, Genentech/Roche, Pliant, Regeneron, Amarin, Moderna.

9

Oral

Targeting a KRAS neoantigen peptide vaccine to DNGR-1+ dendritic cells

R. Ambler¹, S. Von Karstedt², J. Downward¹. ¹The Francis Crick Institute, Oncogene biology lab, London, United Kingdom; ²University of Cologne, Cologne Excellence Cluster on Cellular Stress Response in Aging-Associated Diseases CECAD, Cologne, Germany

Background: Oncogenic point mutations in KRAS drive some of the most aggressive forms of human cancer, including approximately 32% of lung adenocarcinomas, 50% of colorectal cancers and 88% of pancreatic cancers. Despite a pressing clinical need and decades of research there are currently no licensed selective inhibitors of KRAS oncoproteins, although recent development of several KRAS^{G12C} selective inhibitors appear highly promising. As an alternative approach, we are pursuing research into the immune response to KRAS mutant proteins. We propose that expansion of a mutant-KRAS specific T cell response using vaccination strategies could provide the specificity and efficacy which pharmacological approaches have so far failed to achieve.

Materials and methods: We have designed a panel of anti-DNGR-1 antibody conjugated peptides covering three of the most common KRAS point mutations, KRAS^{G12V}, KRAS^{G12C} and KRAS^{G12D}. Conjugation to anti-DNGR-1 antibodies results in vaccine delivery to cross presentation competent DNGR-1⁺ CD8⁺ dendritic cells, thus strengthening the adaptive immune response. Vaccines were tested using both therapeutic and prophylactic experimental designs in mouse models of KRAS driven lung adenocarcinoma.

Results: The prophylactic application of an anti-DNGR-1-KRAS^{G12V} vaccine significantly impaired tumour growth following challenge, with 40% of vaccinated mice displaying zero tumour burden. The remaining mice experienced a prolonged tumour free period followed by rapid tumour growth, indicating escape. A therapeutic vaccination strategy showed reduced tumour growth in mice with advanced tumour burden using a subcutaneous KRAS^{G12V} lung cancer model. Tumour TILs were dominated by CD8⁺ T cell populations, which possessed KRAS^{G12V} specificity and cancer cell killing potential *ex vivo*. Therapeutic vaccination against KRAS^{G12D} significantly slowed the growth of tumours in an autochthonous KRAS^{G12D} mouse lung cancer model.

Conclusions: Targeting KRAS^{G12V} and KRAS^{G12D} peptide vaccines to DNGR-1⁺ dendritic cell populations resulted in a detectable and protective T cell response in both prophylactic and therapeutic vaccination strategies.

No conflict of interest.

Saturday, 24 October 2020

20:45–21:35

POSTER DISCUSSION SESSION

New Therapeutics in Phase I and II studies

20

Poster Discussion

Preliminary results from an open-label, multicenter phase 1/2 dose escalation and expansion study of THOR-707, a novel not-Alpha IL-2, as a single agent in adult subjects with advanced or metastatic solid tumors

F. Janku¹, R. Abdul-Karim², A. Azad³, J. Bendell⁴, H. Gan⁵, S. Sen⁶, T. Tan⁷, J. Wang⁸, N. Marina⁹, L. Baker⁹, L. Ma⁹, J. Mooney⁹, D. Luo⁹, J. Leveque⁹, M. Milla⁹, T. Meniawy¹⁰. ¹The University of Texas MD Anderson Cancer Center, Investigational Cancer Therapeutics, Houston, USA; ²NEXT Oncology, Texas Oncology, San Antonio, USA; ³Peter MacCallum Cancer Centre, Clinical and Translational Research, Melbourne, Australia; ⁴Sarah Cannon Research Institute, Tennessee Oncology, Nashville, USA; ⁵Olivia Newton-John Cancer Research Institute, Austin Health, Melbourne, Australia; ⁶Sarah Cannon Research Institute, HealthONE, Denver, USA; ⁷National Cancer Centre Singapore, Division of Medical Oncology, Singapore, Singapore; ⁸Sarah Cannon Research Institute, Florida Cancer Specialists, Sarasota, USA; ⁹Synthorx, a Sanofi Company, La Jolla, USA; ¹⁰Linear Clinical Research, Early Phase Clinical Research, Nedlands, Australia

Background: THOR-707 is a recombinant human IL-2 variant, site-specifically pegylated for treatment of cancer, providing a not α pharmacologic profile designed to prevent engagement of the IL-2 receptor α chain. Generated using Synthorx's Expanded Genetic Alphabet technology, it has been shown to have key advantages over current IL-2 therapies: improved selectivity, increased therapeutic index, ease of use and reduced risk for anti-drug antibodies.

Here we report preliminary findings from an ongoing 3-part open-label, phase 1/2 study of THOR-707, designed to evaluate PK/PD, safety, tolerability and preliminary anti-tumor activity.

Methods: In Part 1, dose escalation of single agent THOR-707 was administered via IV infusion Q2W (Cohort A) or Q3W (Cohort B) using a conventional 3+3 dose escalation design (DED) to identify the maximum tolerated dose (MTD) and/or recommended Phase 2 dose (RP2D). Part 2 patients (pts) received escalating doses of THOR-707 with pembrolizumab 200 mg IV (Cohort C) following a 3+3 DED to identify the MTD and/or RP2D of the combination.

Results: As of 11 March 2020, 22 pts in 8 tumor types were enrolled—4 (Cohort A) at 8 μ g/kg; 14 (Cohort B): 4 at 8 μ g/kg (starting dose), 6 at 16 μ g/kg, 4 at 24 μ g/kg; 4 (Cohort C) at 8 μ g/kg + 200 mg pembrolizumab.

An increase in CD8 counts was seen post-treatment across doses in all pts in Cohort B (fold increase 1.5–5.2). All had post-dose peripheral expansion of NK cells exceeding 4-fold above baseline and an increase in lymphocyte counts of at least 2-fold. CD4 counts increased across doses with a minimum increase of 1-fold per pt. Eosinophil counts, a surrogate marker of potential Vascular Leak Syndrome (VLS) ranged from 100 to 400 count/ μ L in all 14 pts with IL-2 induced eosinophilia.

Mean fold expansion of CD4+ Tregs post first dose in 6 pts enrolled at 16 μ g/kg was 1.9. No ADAs (IL-2 or PEG) were observed, no meaningful elevations in IL-5 and only 1 pt with IL-6 elevation at 24 hrs to 1,000 pg/mL. All pts at 8 and 16 μ g/kg doses had post-dose CD8+ Ki67 expression levels exceeding 60%, with peripheral expansion of CD8+ Teff cells and post-dose NK cell Ki67 expression levels of nearly 100%.

Safety data across cohorts includes several pts who received up through 5 cycles of treatment, with 1 pt on treatment for 6 months. No DLTs were observed across doses, no reports of VLS and 1 TRAE leading to discontinuation. TRAEs resolved with accepted SOC. Most pts experienced flu-like symptoms, nausea, or vomiting during the first 16 hrs post dose which was managed with supportive care. No cumulative toxicity or end organ toxicity was observed, no QTc prolongation or other cardiac toxicity.

Conclusions: THOR-707 demonstrated encouraging biomarker data analogous to the not- α IL-2 effect observed in preclinical models with no indicators of VLS in this ongoing trial. Clinical trial information: NCT04009681.

Conflict of interest:

Corporate-sponsored Research: Clinical trial sponsored by Synthorx, a Sanofi Company, Other Substantive Relationships: Employees of Synthorx, a Sanofi company.

21

Poster Discussion

Phase 1/2 study of the safety and efficacy of APL-101, a specific c-MET inhibitor

S.H. Kizilbash¹, A. El-Khoueiry², R.E. Lerner³, P.C. Ma⁴, M. Almubarak⁵, K. Mody⁶, M.E. Burkard⁷, M. Guarino⁸, J. Jenab-Wolcott⁸, N. Sanka⁹, G. Choy⁹, L. Espiritu⁹, X. Zhang⁹, A. Luria⁹, F. Benedetti⁹, E.C. Dees¹⁰. ¹Mayo Clinic, Medical Oncology, Rochester, USA; ²University of Southern California- Norris Comprehensive Cancer Center, Medical Oncology, Los Angeles, USA; ³Park Nicollet Clinic, Hematology and Oncology, Saint Louis Park, USA; ⁴Penn State Cancer Institute – Penn State Health Milton S. Hershey Medical Center, Medical Oncology, Hershey, USA; ⁵West Virginia University – West Virginia Cancer Institute, Medical Oncology, Morgantown, USA; ⁶Mayo Clinic, Hematology and Oncology, Jacksonville, USA; ⁷University of Wisconsin – Carbone Cancer Center, Hematology and Oncology, Madison, USA; ⁸Helen F. Graham Cancer Center at Christiana Care Health System, Medical Oncology, Wilmington, USA; ⁹Apollomics Inc., Clinical Development, Foster City, USA; ¹⁰University of North Carolina-Lineberger Comprehensive Cancer Center, Medical Oncology, Chapel Hill, USA

Background: APL-101 is an oral, ATP-competitive, selective type 1b c-MET inhibitor. Herein, we report results of a Phase 1 dose-escalation study in subjects with advanced c-MET-dysregulated solid tumors. This study assessed the safety and tolerability of APL-101 and determined the maximum tolerated dose (MTD) and recommended Phase 2 dose (RP2D).

Methods: Subjects with locally advanced or metastatic incurable refractory solid tumors with c-MET dysregulation were enrolled (NCT03175224). c-MET dysregulation was quantified by fluorescence in situ hybridization or next generation sequencing (NGS) for c-MET amplification (c-Met/Cep 7 \geq 2.2; GCN \geq 6 copy), NGS for c-MET EXON 14 skipping, and immunohistochemistry for c-MET overexpression (\geq 50% tumor cells). Subjects were enrolled in a standard 3 + 3 dose escalation based on a modified Fibonacci sequence. APL-101 was orally administered at daily doses of 100 to 400 mg in two divided doses. Toxicities were graded according to the CTCAE 4.03, and preliminary efficacy was based on RECIST 1.1.

Results: A total of 17 subjects were enrolled and treated in 4 dose cohorts. The mean age was 60.9 years (SD, 14.3) and 76.5% of subjects (n = 13) had an Eastern Cooperative Oncology Group performance status of 1. The median number of prior lines of therapy was 3.5 (range, 1–10). Median time since diagnosis was 34.9 months (range, 4.0–168.6). Eight subjects had c-MET amplification, 7 had c-MET overexpression, 1 had non-lung cancer c-MET EXON 14 skipping mutation and one had a c-MET kinase domain mutation (H1094Y). APL-101 demonstrated linear pharmacokinetics. Following single oral administration of enteric-coated capsules of APL-101 at 50, 100, 150, and 200 mg, the average $T_{1/2}$ ranged from 16 to 38 hours. No DLTs were observed. The most common (>10%) treatment-related adverse events (AEs) included, fatigue (35.3%), hypoalbuminemia (29.4%), diarrhea (23.5%), peripheral edema (23.5%), hypocalcemia (17.6%), anemia (11.8%), dyspnea (11.8%), hyponatremia (11.8%), nausea (11.8%), and rash (11.8%). No Grade 3 or above related Serious AEs were observed in any dose cohort. Among the 15 subjects in the efficacy-evaluable population, 1 subject with Schwannoma had a partial response and 9 had best response as stable disease (60%). The clinical benefit rate (SD \geq 4 cycles) was 20.0%. Median progression-free survival (PFS) was 84 days (95% CL: 57, 224). The median duration of exposure was 58 days (range 13–443 days). The RP2D is 400 mg total daily dose.

Conclusions: APL-101 was generally well tolerated in advanced solid tumors with c-MET dysregulations. No DLTs were observed and the RP2D was determined to be 400 mg. Enrollment in the global Phase 2 basket-type trial focusing on lung cancer with Exon 14 skipping and solid tumors with c-MET gene amplification or fusions is underway.

Conflict of interest:

Ownership: Apollomics Inc Stock Ownership: G. Choy, L. Espiritu, X. Zhang, A. Luria, F. Benedetti.

Advisory Board: P. Ma - Apollomics Advisory Board.

M. Burkard - Medical Advisory Board of Strata Oncology.

Other Substantive Relationships: S.H. Kizilbash - No personal funds received from any entity.

Grants paid directly to institution for clinical trial execution from: (1) Orbus Therapeutics, Inc., (2) Apollomics, Inc., (3) Celgene, (4) Wayshine Biopharma, (5) Delmar Therapeutics, Inc.

P. Ma - Speakers Bureau - Merck, AstraZeneca, Bayer, Takeda.

K. Mody - NIH Grant # P50 CA21064, Consulting with Astra Zeneca Pharmaceuticals, Agios, Senwha Biosciences, Basilea Pharmaceuticals, Genentech, Incyte, Puma Biotechnology, Eisai, Exelixis, Ipsen.

M. Burkard - Research funding from Abbvie, Genentech, Puma, Arcus, Apollomics, and Loxo Oncology.
N. Sankar - Consultant for Apollomics Inc.

22

Poster Discussion

A phase II study of Guadecitabine (G) with Irinotecan (IRI) vs regorafenib or TAS-102 in metastatic colorectal cancer (mCRC) patients (pts)

V. Lee¹, M. Zahurak², A. Cercek³, H. Verheul⁴, H. Lenz⁵, P. Jones⁶, S. Baylin¹, R. Parkinson¹, V. Rami¹, E. Lilly¹, T. Miles¹, T. Brown¹, N. Ahuja⁷, A. El Khoeiry⁵, N. Azad¹. ¹Johns Hopkins University, Medical Oncology, Baltimore, USA; ²Johns Hopkins University, Statistics, Baltimore, USA; ³Memorial Sloan Kettering Cancer Center, Medical Oncology, New York, USA; ⁴Vu University, Medical Oncology, Amsterdam, Netherlands; ⁵University of Southern California, Medical Oncology, Los Angeles, USA; ⁶Van Andel Institute, Epigenetics, Grand Rapids, USA; ⁷Johns Hopkins University, Surgery, Baltimore, USA

Background: Treatment of IRI-resistant CRC lines with a DNA methyltransferase inhibitor (DNMTi) reverses IRI resistance. A phase I trial demonstrated safety of the combination G + IRI in treatment of mCRC pts. We completed a large randomized phase II trial of G+IRI compared to regorafenib or TAS-102 in pts with advanced mCRC refractory to irinotecan.

Materials and Methods: Pts with mCRC refractory to IRI were randomized to G + Iri (Arm A) versus standard of care regorafenib or TAS-102 (Arm B) (2:1 ratio) on a 28-day cycle. Arm A pts received G 45 mg/m² SC on days 1–5 and IRI 125 mg/m² on days 8 and 15 with growth factor support for cycle 1. Arm B pts received regorafenib 160 mg daily on days 1–21 or TAS-102 35 mg/m² BID on days 1–5 and 8–12. Target sample sizes of 64 and 32 for Arms A and B provided 83% power to detect an improvement of the expected median PFS from 1.9 months to 3.6 months.

Results: Between Jan 15, 2016–Oct 24, 2018, with preliminary data lock on November 14, 2019. 103 pts were randomized at four international sites (Johns Hopkins, Memorial Sloan Kettering, University of Southern California, and VU University Amsterdam), with 96 pts undergoing treatment, 62 in Arm A and 34 in Arm B. 33.9% of pts in Arm A were female, while 55.9% in arm B. Median age was 55.5 [29–80] years in Arm A and 63 [31–78] years in Arm B, with Arm A receiving median 2.5 prior lines of therapy compared to 2 prior lines of therapy in Arm B. Common ≥ Grade 3 treatment related AEs in Arm A were neutropenia (40%), anemia (17%), diarrhea (11%), compared to Arm B pts with neutropenia (12%), anemia (12%). Median PFS was 2.37 months and 2.15 months in Arm A and B, respectively [HR 0.79, 95% CI: 0.51–1.22, p = 0.29]. Median OS was 7.15 months for Arm A and 7.66 months for Arm B [HR 0.93, 95% CI 0.58–1.49, p = 0.75]. The Kaplan-Meier rates of PFS at 4 months were 32% in Arm A and 26% in Arm B.

Conclusions: G+IRI did not meet our pre-specified PFS goal of improving median PFS to > 3.6 months in the experimental arm. G+IRI was not superior or inferior to standard of care. A comprehensive panel of biomarkers is currently under evaluation and will be presented in the future. Clinical trial information: NCT01896856. Supported by Astex Pharmaceuticals, Inc. and AACR-VARI SU2C Epigenetics Dream Team.

Conflict of interest:

Advisory Board: Andrea Cercek - Array Biopharma, Bayer.
Corporate-sponsored Research: Andrea Cercek - Seattle Genetics, Tesaro/GSK, RGenix.
Nilofer Azad – Astex.

23

Poster Discussion

Initial results from a phase 1 trial of OKI-179, an oral Class 1-selective depsipeptide HDAC inhibitor, in patients with advanced solid tumors

J. Diamond¹, G. Gordon², J. Kagihara¹, B. Corr¹, C. Lieu¹, J. Pacheco¹, A. Heim², J. DeMattei³, S.G. Eckhardt⁴, J. Winkler³, A. Piscopio⁵. ¹University of Colorado, Anschutz Medical Campus, Aurora, USA; ²OnKure, Clinical, Boulder, USA; ³OnKure, Translational, Boulder, USA; ⁴University of Texas, Dell Medical School, Austin, USA; ⁵OnKure, Management, Boulder, USA

Background: Epigenetic escape is a major mechanism for cancer progression during treatment with targeted therapies. While HDAC inhibitors are approved as single agents in hematological cancers, activity in solid tumors has been limited. This is possibly due to the promiscuous inhibitory properties of unselective inhibitors, toxicity profiles that limit combination strategies, and, in some cases, inferior pharmacokinetic profiles. OKI-179 is a novel, oral pro-drug analog of largazole, a compound in the romidepsin-depsipeptide class of natural products. OKI-179 potently inhibits HDAC 1,2,3

(IC₅₀ = 1.2, 2.4, 2.0 nM, respectively), with no significant inhibition of Class IIa HDACs. Here we present the initial data for OKI-179 in a phase I dose-escalation trial (NCT03931681).

Materials and Methods: Patients with advanced solid tumors were enrolled into cohorts of escalating doses of OKI-179 (30 mg to 350 mg) administered oral, once daily 4 days on/3 days off for 3 consecutive weeks in each cycle. The objectives of this study are to establish the maximum tolerated dose (MTD) and characterize dose-limiting toxicity (DLTs), adverse events (AEs), and the pharmacokinetic (PK) and pharmacodynamic (PD) profiles.

Results: As of June 1, 2020, 14 patients (median age 60) were treated with OKI-179 in single patient cohorts from 30 mg–210 mg and 3 patient cohorts at 270 mg and 350 mg. Intra-patient dose escalation occurred in 3 patients. No DLTs were observed. The most common treatment-related AEs (TRAEs) were grade 1 nausea (N = 5, 36%), grade 1 vomiting (N = 3, 21%) and grade 1 anorexia (N = 3, 21%). One grade 2 TRAE (hypokalemia) and no grade 3/4 TRAEs occurred. OKI-179 achieved good exposure following oral administration, with C_{max} > 2,000 ng/ml and AUC > 8,000 hr*ng/ml; exposures that are above the efficacious target exposure based on pre-clinical studies. T_{max} occurred by 2 hours and the half-life was approximately 6–8 hours. The PK profile was reproducible at day 15 compared to day 1 and dose-proportional. OKI-179 treatment resulted in > 3X increased T cell histone acetylation at multiple doses. The best response was stable disease (SD) in 4 patients and progressive disease in 10. A patient with platinum-resistant ovarian cancer remains on study after 1 year with SD and a patient with adenoid cystic nasopharyngeal carcinoma remains on study with SD after 8 months.

Conclusions: OKI-179 is well-tolerated and has a favorable PK profile with expected target modulation. Promising stabilization of disease was observed, and dose escalation continues to identify the MTD. An update on clinical and translational data will be presented.

Conflict of interest:

Ownership: John DeMattei, S. Gail Eckhardt, James Winkler, Anthony Piscopio.
Board of Directors: Anthony Piscopio.
Corporate-sponsored Research: Jennifer Diamond.

24

Poster Discussion

Continuous vs intermittent adenosine 2A receptor (A2AR) inhibition in preclinical colon cancer (CC) models and in a Phase (Ph) II study of taminadenant (NIR178) + spartalizumab (PDR001) in patients (pts) with non-small cell lung cancer (NSCLC)

C.C. Lin¹, M. Joerger², P. Grell³, A.A. Chiapponi⁴, T.A. Leal⁵, S. Kasper⁶, G. Jerusalem⁷, A. Gonçalves⁸, J. Wolf⁹, F. De Braud¹⁰, M.J.A. de Jonge¹¹, J. Otero¹², S. Chhagan¹², D. Cipolletta¹³, E. Morris¹⁴, N.R. Chowdhury¹⁵, F.K. Hurtado¹⁶, D.S. Tan¹⁷. ¹National Taiwan University Hospital, Department of Oncology, Taipei, Taiwan; ²Cantonal Hospital, Division of Medical Oncology, St. Gallen, Switzerland; ³Masaryk Memorial Cancer Institute, Clinic of Comprehensive Oncology Care, Brno, Czech Republic; ⁴Moffitt Cancer Center, Oncology and Medicine for the Thoracic Oncology Program, Tampa-FL, USA; ⁵University of Wisconsin, Carbone Cancer Center, Madison- WI, USA; ⁶West German Cancer Center, University Hospital Essen, Essen, Germany; ⁷Centre Hospitalier Universitaire de Liège, University of Liège, Liège, Belgium; ⁸Institut Paoli-Calmettes, Aix-Marseille University, Marseille, France; ⁹University Hospital Cologne, Center for Integrated Oncology, Cologne, Germany; ¹⁰Fondazione IRCCS Istituto Nazionale dei Tumori, University of Milan, Milan, Italy; ¹¹Erasmus MC Cancer Institute, Department of Medical Oncology, Rotterdam, Netherlands; ¹²Novartis Institutes for BioMedical Research, Translational Clinical Oncology, East Hanover- NJ, USA; ¹³Novartis Institutes for BioMedical Research, Exploratory Immuno-Oncology, Cambridge- MA, USA; ¹⁴Novartis Institutes for BioMedical Research, Oncology Translational Research, Cambridge- MA, USA; ¹⁵Novartis Pharmaceuticals Corporation, Novartis Pharmaceuticals Corporation, East Hanover- NJ, USA; ¹⁶Novartis Institutes for BioMedical Research, Clinical Pharmacology, East Hanover- NJ, USA; ¹⁷National Cancer Centre Singapore, Division of Medical Oncology, Singapore, Singapore

Background: Taminadenant (A_{2A}R antagonist) +/- spartalizumab (anti-programmed death-1 [PD-1] antibody [Ab]) has preliminary efficacy in NSCLC (Ph I/II). A_{2A}R blockade can enhance innate and adaptive immune responses but A_{2A}R deletion in murine models did not inhibit growth of all tumor types, increasing growth of ectopic melanoma and bladder tumors. This may be due to impaired T-cell maintenance and effector-memory differentiation in A_{2A}R-deficient mice. Dose optimization may maximize A_{2A}R

antagonist efficacy. We present results of continuous vs intermittent taminadenant + mouse-specific anti-PD-1 Ab in a preclinical CC model and + spartalizumab in a Ph II study in pts with NSCLC (NCT03207867).

Material and methods: Preclinical: C57B1/6 mice with implanted MC38 CC cells received continuous or intermittent (4-days-on/3-days-off) 50 mg/kg twice-daily (BID) taminadenant +/- a mouse-specific anti-PD-1 Ab.

Clinical: Adult pts with immunotherapy-naïve advanced NSCLC and 1–3 prior therapies were randomized 1:1:1 to 160 mg BID oral taminadenant on continuous (C), 2-weeks (wks)-on/2-wks-off (Int2), or 1-wk-on/1-wk-off (Int1) schedules + 400 mg spartalizumab every 4 wks. The primary endpoint was overall response rate (ORR; local review). Pre- and post-treatment tumor biopsies were collected for RNAseq and CD8, PD-L1, and CD73 immunohistochemistry and blood samples for pharmacokinetics (PK), RNAseq, and circulating free DNA sequencing.

Results: Preclinical: Intermittent vs continuous taminadenant led to better tumor growth control and significantly decreased intratumoral T-reg and Helios-positive CD8 T cells. Continuous taminadenant phenocopied A_{2A}R-deficient models with a lack of efficacy and significantly decreased B cells and memory T cells.

Clinical: Across 3 schedules, 62 pts were enrolled (C: n = 22; Int2: n = 20; Int1: n = 20). Of 62 pts, 4 (6%) had a partial response (confirmed at ≥4 wks; C: n = 2; Int1: n = 2), 17 (27%) stable disease (C: n = 5; Int2: n = 7; Int1: n = 5), 29 (47%) progressive disease (C: n = 11; Int2: n = 9; Int1: n = 9), and 12 response unknown (19%; 4 per schedule); ORRs were 9% (C), 0% (Int2), and 10% (Int1). Common all-grade (G) treatment-related adverse events (AEs; ≥15% pts per schedule) were fatigue and pruritus (C), and fatigue and aspartate/alanine aminotransferase increase (Int2); G3/4 AEs were uncommon (1 pt each per schedule) but more G3/4 AEs were reported in schedule C. Taminadenant PK did not meaningfully differ between schedules. Progression-free survival, biomarker, and subgroup analyses for the 3 schedules will be presented.

Conclusions: In contrast to the preclinical data presented, clinical efficacy results do not support the hypothesis that intermittent dosing improves taminadenant + spartalizumab antitumor activity. Intermittent and continuous taminadenant dosing + spartalizumab was well tolerated in pts with NSCLC.

Conflict of interest:

Ownership: Dr Otero, Dr Chowdhury, and Dr Hurtado are all stockholders of Novartis Pharmaceuticals Corp.

Advisory Board: Dr Lin reports Advisory roles for Blueprint Medicines, Boehringer-Ingelheim, Daiichi Sankyo, Novartis, Takeda.

Dr Leal reports Advisory Board/Consulting for BeyondSpring, AstraZeneca, BMS, Merck, Takeda, Genentech, InvisionFirst Lung, PharmaMar.

Dr Wolf reports Advisory boards and lecture fees from Amgen, AstraZeneca, Bayer, Blueprint, BMS, Boehringer-Ingelheim, Chugai, Daiichi Sankyo, Ignyta, Janssen, Lilly, Loxo, MSD, Novartis, Pfizer, Roche, Seattle Genetics, Takeda.

Dr Tan reports Advisory Role and Consultant to Novartis, Bayer, Boehringer Ingelheim, Celgene, Astra Zeneca, Eli-lilly, Loxo, Takeda, Amgen, Pfizer.

Corporate-sponsored Research: Dr Wolf reports research support (Institution) from BMS, Janssen Pharmaceutica, Novartis, Pfizer.

Dr Tan reports Research Funding (Institution) from Novartis, GSK, Bayer, AstraZeneca, Pfizer.

Dr Kasper reports study fees from Novartis, during the conduct of the study grants from BMS, grants from Roche, grants from Lilly, grants from Servier, outside the submitted work.

Dr Jerusalem reports grants from Novartis, grants from Roche, grants from Pfizer, outside the submitted work.

Other Substantive Relationships: Dr Lin reports personal fees from Blueprint Medicines, personal fees from Boehringer-Ingelheim, personal fees from Daiichi Sankyo, personal fees from Novartis, personal fees from Takeda, personal fees from Bristol Myers Squibb, personal fees from Roche, personal fees from BeiGene, personal fees from Eli Lilly, outside the submitted work. Dr Joergers has nothing to disclose.

Dr Grell reports personal fees and non-financial support from Novartis.

Dr Chiappori reports grants and personal fees from Novartis, grants and personal fees from Astra Zeneca, personal fees from Merck, grants from BMS, personal fees from Takeda, personal fees from Celgene, personal fees from Pfizer, personal fees from Genentech, personal fees from Amgen, personal fees from AbbVie, personal fees from Jazz, outside the submitted work.

Dr Kasper reports personal fees from BMS, personal fees from AstraZeneca, personal fees from Roche, personal fees from Lilly, personal fees from Merck, personal fees from MSD, personal fees from Servier, outside the submitted work.

Dr Jerusalem reports non-financial support from Novartis, during the conduct of the study personal fees and non-financial support from Novartis, personal

fees and non-financial support from Roche, personal fees and non-financial support from Pfizer, personal fees and non-financial support from Lilly, personal fees and non-financial support from Amgen, personal fees and non-financial support from BMS, personal fees and non-financial support from Astra-Zeneca, personal fees from Daiichi Sankyo, personal fees from Abbvie, non-financial support from Medimmune, non-financial support from MerckKGaA, outside the submitted work.

Dr Gonçalves reports non-financial support from Roche, non-financial support from Novartis, non-financial support from Astra Zeneca, non-financial support from Pfizer, outside the submitted work.

Dr De Braud reports personal fees from Tiziana Life Sciences, personal fees from BMS, personal fees from Celgene, personal fees from Servier, personal fees from Pharma Research, personal fees from Daiichi Sankyo, personal fees from Ignyta, personal fees from Novartis, personal fees from Amgen, personal fees from Pfizer, personal fees from Octimet Oncology, personal fees from Incyte, personal fees from PIERRE FABRE, personal fees from Eli Lilly, personal fees from Roche, personal fees from Astra Zeneca, personal fees from Gentili, personal fees from Dephaforum, personal fees from Novartis, personal fees from MSD, personal fees from Bayer, personal fees from Fondazione Menarini, outside the submitted work.

Dr de Jonge reports personal fees and non-financial support from Faron Pharmaceutical, outside the submitted work.

Dr Otero, Dr Chowdhury, Dr Hurtado, Dr Cipolletta, Dr Morris and Dr Chhagan, are full-time employees of Novartis Pharmaceuticals Corp.

Dr Tan reports Travel and Honorarium from Merck, Pfizer, Novartis, Boehringer Ingelheim, AstraZeneca, BMS.

Saturday, 24 October 2020

20:45–21:25

POSTER DISCUSSION SESSION

Targeting DNA Replication and Repair Systems

25

Poster Discussion

Hypoxia-activated prodrugs of DNA-dependent protein kinase as radiosensitisers

M. Hay¹, L. Liew¹, W. Wong¹, B. Dickson¹, G. Cheng¹, C.R. Hong¹, W. Wilson¹, S. Jamieson¹. ¹University of Auckland, Auckland Cancer Society Research Centre, Auckland, New Zealand

Background: Inhibition of the repair of radiation-induced DNA double strand breaks offers the potential to sensitise tumours to radiation therapy. DNA-dependent protein kinase (DNA-PK) is a well validated target, but inhibition also has the potential to radiosensitise normal tissues within the radiation field, and to target normal tissue functions outside of DNA-PK's canonical role in DNA repair. Early DNA-PK inhibitors (DNA-PKi) displayed cross-reactivity against other PIKK and PI3K enzymes resulting in efficacy-limiting toxicity. Exploiting hypoxia to selectively trigger hypoxia-activated prodrugs of DNA-PKi in tumours can enhance tumour selectivity, with the advantage of sensitising the most radioresistant (hypoxic) subpopulation, as well as sensitising adjacent oxic cells through a bystander effect.

Methods: We used molecular modelling of the multi-kinase inhibitor dactolisib (IC50 for kinase inhibition: DNA-PK, 0.8 nM; PI3Kα, 1.4 nM; mTOR, 4.3 nM) in the mTOR crystal structure 4JSX and identified three binding domains. We synthesised a library of 150 analogues, systematically varying the substituents in each domain of the core structure. We identified compounds with a wide range of potency and selectivity against three signal targets: DNA-PK, PI3Kα and mTOR, and screened them as radiosensitisers with a growth inhibition endpoint. This set of structure-activity relationships underpinned a pharmacophore model for DNA-PKi. We have identified a lead DNA-PKi, SN39536, and a corresponding prodrug, SN39884.

Results: SN39536 is an effective inhibitor of DNA-PK activity, both biochemically and in cells, with substantial selectivity compared to other PIKK and PI3K enzymes. SN39536 provided radiosensitisation of DNA-PK proficient HAP1 cells, but was inactive against isogenic (CRISPR) DNA-PKcs knockout (HAP1/PRKDC^{-/-}) cells, demonstrating on-mechanism activity. SN39536 also provided robust radiosensitisation of oxic UT-SCC-54C HNSCC cells using a clonogenic endpoint: Sensitiser Enhancement Ratio (SER) = 1.7 at 1 μM. Prodrug SN39884 was deactivated as a DNA-PKi and released SN39536 under reductive conditions. Incubation of the prodrug with HCT116 cells overexpressing cytochrome P450

oxidoreductase (POR) or UT-SCC-54C cells led to hypoxia-dependent metabolism of the prodrug and efficient release of SN39536. SN39536 is an effective radiosensitizer in UT-SCC-54C cells under either aerobic or hypoxic conditions, while prodrug SN39884 only sensitised cells under anoxia. SN39536 and its prodrug demonstrated radiosensitisation of hypoxic cells in UT-SCC-54C tumour xenografts using an *ex vivo* clonogenic survival endpoint.

Conclusions: We have identified a new class of potent and selective DNA-PK inhibitors and demonstrated the ability of a hypoxia-activated prodrug to selectively release the inhibitor under hypoxia *in vitro* and *in vivo*.

No conflict of interest.

26

Poster Discussion

Poly(ADP-ribose) glycohydrolase inhibition sequesters NAD⁺ to potentiate the metabolic lethality of alkylating chemotherapy in IDH mutant tumor cells

H. Nagashima¹, C. Lee¹, K. Tateishi², F. Higuchi³, M. Subramanian¹, S. Rafferty¹, L. Melamed¹, J. Miller⁴, H. Wakimoto¹, D. Cahill¹.
¹Massachusetts General Hospital- Harvard medical School, Neurosurgery, Boston, USA; ²Yokohama City University Graduate School of Medicine, Neurosurgery, Yokohama, Japan; ³Dokkyo Medical University, Neurosurgery, Mibu, Japan; ⁴Massachusetts General Hospital- Harvard medical School, Neurology, Boston, USA

Background: Mutations in IDH1 or IDH2 characterize the most prevalent diffuse glioma of younger adulthood. DNA alkylator chemotherapy is an effective treatment for IDH mutant glioma, yet recurrences remain common and improved treatments are needed. Nicotinamide adenine dinucleotide (NAD⁺) is an essential cofactor metabolite, serving as the currency of metabolic transactions critical for cell survival. IDH mutant cancer cells have unique dependencies on NAD⁺-dependent metabolic pathways, which include poly(ADP-ribose) polymerases (PARPs). PARPs catalyze oligomerization of NAD⁺ monomers into poly(ADP-ribose) (PAR) chains during cellular response to alkylating chemotherapeutics such as temozolomide (TMZ). We hypothesized that we could exploit the intrinsic metabolic vulnerability of IDH mutant cancer cells with combined treatment: TMZ would promote PARP activation and outflow consumption of cellular NAD⁺ pools, while concomitant inactivation of the PAR breakdown enzyme poly(ADP-ribose) glycohydrolase (PARG) would then sequester NAD⁺ as polymerized PAR, by blocking subsequent breakdown.

Material and methods: We tested the combination efficacy of TMZ with the selective small molecule PARG inhibitor (PARGi) in 5 IDH mutant cancer cells and 7 IDH wild-type cell lines. To test the cytotoxic mechanism of the combination, we used NAD⁺ assays and western blot analyses, with and without NAD⁺ precursors for rescue. In addition, we engineered PARG knock-out (KO) cells using two independent CRISPR guide RNAs and tested the efficacy of TMZ in these lines. The *in vivo* efficacy of combination of PARG inactivation and TMZ was tested in IDH mutant xenograft mouse models.

Results: We find that, in endogenous IDH1 mutant tumor models, alkylator-induced cytotoxicity is markedly augmented by pharmacologic inhibition or genetic knockout of the PAR breakdown enzyme PARG. Both *in vitro* and *in vivo*, we observe that concurrent alkylator and PARG inhibition results in sequestration of free NAD⁺ by preventing PAR breakdown, which depletes available NAD⁺ and causes a collapse of metabolic homeostasis. This effect reversed with NAD⁺ rescue supplementation, confirming the mechanistic basis of cytotoxicity. PARG inactivation potentiates the efficacy of TMZ in an IDH mutant xenograft model *in vivo*.

Conclusions: The combination of TMZ and PARG inhibitors is highly effective against IDH mutant tumor cells. Alkylating chemotherapy exposes a genotype-selective metabolic weakness in tumor cells that can be selectively exploited by PARG inactivation.

No conflict of interest.

27

Poster Discussion

Mechanism based signatures of TGFβ competency and DNA repair predict response to genotoxic therapies across cancer types

M. Barcellos-Hoff¹, I. Guix Sauquet¹, J. Moore¹, M.A. Pujana².
¹UCSF, Radiation Oncology, San Francisco, USA; ²Bellvitge Institute for Biomedical Research, Catalan Institute of Oncology, Barcelona, Spain

Background: Transforming growth factor β (TGFβ) has a poorly understood in genomic stability. Here we show that the association of TGFβ signaling on genomic changes in human cancer and therapeutic vulnerability. In prior work, we have shown that inhibition or loss of TGFβ signaling decreases

homologous recombination and increases use of alternative end-joining (alt-EJ), an error-prone DNA repair process (Liu et al. Clin. Ca. Res. 2018). Because many cancers lose the ability to respond to TGFβ, we postulated that this mechanistic relationship may be associated with response to therapies that cause DNA damage.

Materials and Methods: The mechanistic relationship between TGFβ and the DNA damage response (DDR) was used to identify gene expression signatures. We validated the relevance of the signatures to their biological functions in primary tumor explants treated with TGFβ to measure pSMAD or irradiated and assayed 5 hr later for 53BP1 foci, a marker of residual or mis-repaired damage. A custom NanoString™ panel was used to examine the relative expression of the two signatures. The Cancer Genome Atlas (TCGA) was probed to evaluate association of the signatures with outcomes.

Results: The TGFβ signature was significantly correlated with pSMAD2 ($p < 0.001$), and the DDR signature was significantly correlated with residual 53BP1 foci ($p < 0.02$), confirming their biological relevance. TGFβ competency was anti-correlated with unrepaired DNA damage ($PCC = 0.52$; $p < 0.001$). The analysis of TGFβ and alt-EJ signatures in TCGA revealed significant anti-correlation in 16 of 17 solid cancer types (Pearson's correlation coefficient = -0.37 ; $p < 0.0001$). Moreover, those patients characterized by high TGFβ fare significantly worse ($p = 0.006$; Hazard Ratio = 1.694; 95% CI: 1.161–2.473). Consistent with error-prone repair, more of the genome was altered in glioblastoma, lung squamous cell cancer, and serous ovarian cancer classified as low TGFβ and high alt-EJ and the corresponding patients had better outcomes in response to genotoxic therapy.

Conclusions: These data from experimental studies and analysis of human cancer database reveal that loss of TGFβ signaling compromises the DNA damage response and results in ineffective repair. Prospective identification of this anti-correlation used to predict response to genotoxic therapies could expand the potential therapeutic scope of TGFβ inhibitors in cancer therapy.

No conflict of interest.

28

Poster Discussion

DS-7300a, a novel B7-H3-targeting antibody-drug conjugate with a novel DNA topoisomerase I inhibitor DXd, exhibits potent anti-tumor effects in nonclinical models

M. Yamato¹, J. Hasegawa², C. Hattori², T. Maejima³, T. Shibutani⁴, T. Deguchi⁵, N. Izumi⁶, A. Watanabe⁵, Y. Nishiyama⁷, T. Nakada², Y. Abe⁷, T. Agatsuma².
¹Daiichi Sankyo Co.- Ltd., Early Clinical Development Department, Tokyo, Japan; ²Daiichi Sankyo Co.- Ltd., Oncology Research Laboratories I, Tokyo, Japan; ³Daiichi Sankyo Co.- Ltd., Biomarker & Translational Research Department, Tokyo, Japan; ⁴Daiichi Sankyo RD Novare Co.- Ltd., Translational Research Department, Tokyo, Japan; ⁵Daiichi Sankyo Co.- Ltd., Quantitative Clinical Pharmacology Department, Tokyo, Japan; ⁶Daiichi Sankyo Co.- Ltd., Drug Metabolism & Pharmacokinetics Research Laboratories, Tokyo, Japan; ⁷Daiichi Sankyo Co.- Ltd., Oncology Research Laboratories II, Tokyo, Japan

Background: B7-H3 (CD276) is a type I transmembrane protein belonging to the B7 family which includes immune checkpoint molecules such as CTLA-4 ligands and PD-L1. B7-H3 is highly expressed in various types of solid tumors with low expression in normal tissues. Several studies have reported that B7-H3 overexpression is associated with poor prognosis in several types of cancers. These findings support B7-H3 as an attractive molecular target for anti-cancer therapies. We generated DS-7300a, a B7-H3-targeting antibody-drug conjugate (ADC), which is composed of a humanized anti-B7-H3 monoclonal antibody, an enzymatically cleavable peptide-based linker, and a novel exatecan derivative (DXd) that is a potent DNA topoisomerase I inhibitor. In this study, we evaluated the pharmacological activities of DS-7300a in nonclinical models.

Material and methods: Human cancer cells were cultured with DS-7300a and cell viability was examined to evaluate *in vitro* cell growth inhibitory effects of DS-7300a. DNA damage and apoptosis induced by DS-7300a were assessed by western blotting. To evaluate *in vivo* anti-tumor effects of DS-7300a, human tumor xenograft mice were treated with DS-7300a intravenously and tumor growth was assessed. B7-H3 expression in tumors was analyzed by immunohistochemistry and tumor concentrations of a free payload, DXd, were also measured in xenograft mouse models.

Results: DS-7300a inhibited the growth of B7-H3-expressing cancer cells *in vitro*, but not of B7-H3-negative cancer cells. Neither a parental anti-B7-H3 antibody nor isotype control ADC inhibited the growth of these cells. In addition, treatment with DS-7300a and DXd alone induced DNA damage and apoptosis in cancer cells. These results demonstrated that DS-7300a inhibited target-dependent cell growth through ADC-mediated cytotoxic

effects. Moreover, DS-7300a exhibited a strong *in vivo* anti-tumor effect in a high-B7-H3 tumor xenograft model compared with in a low-B7-H3 tumor xenograft model. In these models, higher tumor concentrations of DXd were observed in the high-B7-H3 model than in the low-B7-H3 model. Furthermore, DS-7300a showed potent anti-tumor effects in various tumor types of high-B7-H3 patient-derived xenograft (PDX) models.

Conclusion: DS-7300a demonstrated potent anti-tumor activity in high-B7-H3 tumors in nonclinical models including PDX models used in this study. Therefore, DS-7300a could provide a new therapeutic opportunity for patients with B7-H3-expressing solid tumors at clinical setting. Recently, a first in human, phase I/II, study of DS-7300a in patients with various advanced solid tumors has been initiated to investigate its potential safety and preliminary efficacy (NCT04145622).

Conflict of interest:

Other Substantive Relationships: T. Shibutani is an employee of Daiichi Sankyo RD Novare Co., Ltd., The other co-authors and I (M. Yamato) are employees of Daiichi Sankyo Co., Ltd.

Saturday, 24 October 2020

22:00–23:20

POSTER DISCUSSION SESSION

Next Generation Targeted Therapies A

29

Poster Discussion

GITR agonist sensitizes MC38/OVA tumor to CTLA4 treatment by attenuating Tregs in GITR HuGEMM

D.X. He¹, C. Nie¹, L. Zheng¹, A.X. An¹, H.Q.X. Li¹, D. Ouyang¹. ¹Crown Bioscience Inc., Scientific Research & Innovation, San Diego, USA

Background: GITR (glucocorticoid-induced TNFR-related protein), a member of the TNF receptor superfamily, is highly expressed on the activated T cells, including CD4⁺ T cells, CD8⁺ T cells and Tregs. Upon binding to its ligand, GITR serves as a co-stimulating molecule, playing a vital role in T cell proliferation and anti-tumor activity by converting immune-suppressive Tregs into antitumor effector T cells. Activating GITR by agonistic antibodies, in combination of immune checkpoint inhibitors (ICIs), has been thought to be a highly plausible combo strategy which is now being tested in a few clinical studies. However, we are lacking preclinical models to evaluate efficacy of therapeutic GITR agonistic antibodies, which usually don't cross-bind to mouse targets. To fill this gap, we developed a human GITR knock-in model (GITR HuGEMM).

Methods: The GITR HuGEMM was developed via CRISPR/Cas9 engineering, in which the mouse GITR extracellular domain corresponding to exons 1–4 of mouse *Tnfrsf18* gene was replaced by human counterparts, resulting in expression of chimeric GITR receptors with human extracellular domain & mouse trans-membrane and intracellular domains.

Results: We have characterized the surface expression of human/mouse chimeric GITR on CD4⁺ & CD8⁺ T cells as well as on FOXP3⁺ Treg cells after mCD3/mCD28 activation *in vitro* by FACS analysis. The expression pattern of humanized GITR in splenocytes-derived T cells of GITR HuGEMM mice can recapitulate the endogenous mGITR expression in wild-type mice and hGITR expression in human PBMC with high levels of GITR detectable on activated Tregs. We then inoculated MC38-OVA syngeneic tumors into the GITR HuGEMM mice and treated the mice with 30 mpk of anti-human GITR (MK4166) and 5 mpk of anti-mouse CTLA-4 (9D9) 3 days post tumor engraftment (Day 4). Both MK4166 and 9D9 alone led to ~80% tumor growth inhibition (TGI), however, the combination of MK4166 and 9D9 led to >100% tumor growth inhibition significantly, and 7 out of 8 mice were completely cured. Intriguingly, we observed a reversal of an exhaustion phenotype that could not be reproduced with either Treg depletion or agonistic GITR signaling alone.

Conclusions: Our GITR HuGEMM provides ideal and powerful preclinical animal models to evaluate the efficacy of the human GITR antibodies or its combination with CTLA-4 or other immune modulators.

Conflict of interest:

Corporate-sponsored Research: Crown Bioscience Inc.

30

Poster Discussion

CX-2043, an EpCAM-targeting probody drug conjugate, demonstrates anti-tumor activity with a favorable safety profile in preclinical models

B. Liu¹, J. Shen¹, W. Yu¹, C. Jing², S. Saha³, V. Rangan², J. Richardson³, Y. Liu⁴, S. Boule⁴, J. Lucas⁴, O. Ab⁴, S. Hicks⁴, M. Belvin¹, M. Kavanaugh¹, S. Schleyer¹. ¹CytomX Inc., Cancer Biology, South San Francisco, USA;

²CytomX Inc., Protein Science, South San Francisco, USA; ³CytomX Inc., Toxicology, South San Francisco, USA; ⁴Immunogen Inc., Cancer Biology, Waltham, USA

Background: Ideal targets for antibody drug conjugates (ADCs) are efficiently internalized and are highly and homogeneously expressed on tumor cells in large proportion of patients across wide variety of tumor types. EpCAM represents an example of a such a target that is highly expressed in the majority of epithelial cancers. However, past efforts to target EpCAM with antibody-based therapeutics have failed in large part due to toxicity in normal tissues with high expression (e.g. gastro-intestinal tract and pancreas).

Probody™ drug conjugates (PDCs) are masked, protease-activatable antibody prodrugs designed to localize drug activity to the tumor microenvironment and to minimize interaction with healthy tissues. In this way, PDCs have the potential to deliver potent toxin payloads more precisely to the tumors, and to mitigate on-target/off-tumor toxicity. Our data demonstrate effective targeting of EpCAM by a PDC with a favorable tolerability profile, which would not be possible with a traditional ADC approach.

Materials and methods: CX-2043 consists of an EpCAM-targeting Probody conjugated to a novel maytansinoid payload optimized for bystander activity. Conjugation is via lysine residues on the Probody, using a peptide linker selected for enhanced stability in circulation (DM21L). CX-2043 was evaluated for cytotoxicity and binding *in vitro* to tumor cells, for efficacy *in vivo* with tumor models, and for tolerability in Cynomolgus monkeys.

Results: *In vitro* cytotoxicity of activated CX-2043 or unmasked EpCAM-DM21L ADC across cancer lines was mostly in the sub-nanomolar range and correlated with target expression. Consistent with *in vitro* activity, CX-2043 exhibited potent single dose efficacy in cell line-derived xenograft tumor models. Importantly, CX-2043 showed a favorable safety profile in a repeat-dosing toxicology study in monkeys relative to the unmasked EpCAM-DM21L ADC.

Conclusions: Preclinical data suggest that CX-2043 represents a novel and promising therapeutic directed against EpCAM, a compelling but historically “difficult-to-drug” target.

PROBODY is a trademark of CytomX Therapeutics, Inc.

No conflict of interest.

31

Poster Discussion

The anti-HER3 monoclonal antibody seribantumab effectively inhibits growth of patient-derived and isogenic cell line and xenograft models with NRG1 rearrangements

I. Odintsov¹, E. Gladstone¹, W.J. Sisso¹, L. Delasos¹, A.J.W. Lui¹, E.M. Sisso¹, M. Vojnic¹, I. Khodos², M.S. Mattar², E. de Stanchina², D. Plessinger³, S.M. Leland³, M. Ladanyi¹, R. Somwar¹. ¹Memorial Sloan Kettering Cancer Center, Pathology Department, New York, USA; ²Memorial Sloan Kettering Cancer Center, Antitumor Core Facility, New York, USA; ³Elevation Oncology- Inc., Drug Development, New York, USA

Background: Chromosomal translocations involving the neuregulin 1 gene (*NRG1*) generate chimeric ligands that predominantly bind HER3/ERBB3, leading to dimerization with other ERBB family members and activation of growth and survival pathways. Oncogenic *NRG1* fusions have been detected in 0.2% of malignancies across multiple histologies, but to date no targeted therapy has been approved. Preventing NRG1 from binding ERBB3 represents a promising approach to target NRG1-induced oncogenesis. Our goal in this study was to generate new patient-derived and isogenic cancer models harboring *NRG1* fusions and evaluate in these systems the effect of the anti-HER3 monoclonal antibody seribantumab on growth and signaling *in vitro* and *in vivo*.

Materials and methods: We generated isogenic human bronchial epithelial cells expressing NRG1 fusions by cDNA overexpression and generated lung cancer patient-derived xenograft (PDX) and cell line models from patient samples. Activation state and expression of signaling proteins were determined using proteomic arrays and Western blotting. The efficacy of seribantumab was determined in cell line (lung and breast cancer cells) and PDX models (lung and ovarian). The effect of NRG1 expression on ERBB levels and stability was also examined.

Results: We generated bronchiolar epithelial cell line models expressing *CD74/NRG1*, *VAMP2/NRG1* or *SLC3A2/NRG1* fusions by cDNA overexpression. In addition, we generated 2 lung cancer PDX models with matching cell lines, harboring *CD74/NRG1* (LUAD-0007C) or *SLC3A2/NRG1* fusions (LUAD-0061AS3, afatinib-resistant patient). To our knowledge, this represents the most comprehensive collection of NRG1 fusion-driven disease models. Expression of NRG1 fusions resulted in increased phosphorylation of ERBB proteins, AKT, ERK1/2 and STAT3, as well as increased stability of ERBB2 and ERBB3. Treatment of LUAD-0061AS3 and

MDA-MB-175-VII (DOC4/NRG1 fusion, breast cancer) cells with seribantumab reduced growth, induced apoptosis, blocked the formation of ERBB3-ERBB2 dimers, reduced phosphorylation of EGFR, ERBB2, ERBB3 and ERBB4, and known downstream signaling molecules such as AKT and ERK1/2. Administration of seribantumab (0.6–10 mg, BIW) to mice bearing LUAD-0061AS3 or OV-10-0050 (ovarian cancer PDX, *CLU/INRG1* fusion) PDX tumors significantly reduced tumor growth, leading to approximately 60% and 100% regression in tumor size, respectively. Notably, afatinib was much less effective at the clinically relevant therapeutic dose in both models.

Conclusions: Our data show that the anti-ERBB3 antibody seribantumab is effective *in vitro* and *in vivo* at blocking NRG1-dependent tumorigenesis, lung, breast and ovarian cancer models. These findings support clinical efforts for the development of a tumor agnostic therapeutic approach for NRG1-driven malignancies.

Conflict of interest:

Ownership: Shawn Leland owns shares of Elevation Oncology, Doug Plessinger owns shares of Elevation Oncology.

Advisory Board: Marc Ladanyi has received advisory board compensation from Boehringer Ingelheim, AstraZeneca, Bristol-Myers Squibb, Takeda, and Bayer.

Board of Directors: Shawn Leland is on the board of directors of Elevation Oncology.

Corporate-sponsored Research: Romel Somwar received grants from Elevation Oncology, LOXO Oncology, MERUS and Helsinn healthcare.

Marc Ladanyi received grants from Elevation Oncology, MERUS, LOXO Oncology, and Helsinn Healthcare.

32

Poster Discussion

Discovery and characterization of novel, potent, and selective hypoxia-inducible factor (HIF)-2 α inhibitors

K. Lawson¹, K. Sivick Gauthier², D. Piovesan², J. Fournier¹, B. Rosen¹, A. Maliyan¹, J. Beatty¹, L. Jin³, M. Leleti¹, E. Ginn³, A. Udyavar⁴, C. Ada⁵, J. Au⁵, C. Meleza⁵, S. Zhao⁵, S. Young⁵, M. Walters², J. Powers¹. ¹Arcus Biosciences, Chemistry, Hayward, USA; ²Arcus Biosciences, Biology, Hayward, USA; ³Arcus Biosciences, Drug Metabolism and Pharmacokinetics, Hayward, USA; ⁴Arcus Biosciences, Bioinformatics, Hayward, USA; ⁵Arcus Biosciences, Quantitative Biology, Hayward, USA

The microenvironment of solid tumors is known to be hypoxic and requires induction of genes associated with metabolism, growth, proliferation, angiogenesis, and erythropoiesis for tumor cells to survive and metastasize. Hypoxia-inducible factors (HIFs) are the master driving force for the cellular response to hypoxia. HIFs are heterodimers composed of an oxygen-sensitive HIF- α subunit (HIF-1 α , HIF-2 α , and HIF-3 α) and a constitutively expressed HIF-1 β subunit. Under normoxic conditions, proline residues present in the oxygen-dependent degradation domain of the HIF- α subunits are hydroxylated and subject to recognition and proteasomal degradation via the von Hippel-Lindau (pVHL) E3-ubiquitin ligase complex. When exposed to low oxygen conditions or loss of pVHL function, via mutation or silencing, this process is inhibited, allowing HIF-2 α translocation to the nucleus where, in complex with HIF-1 β , it promotes transcription of various pro-tumorigenic gene sets. In patients, overexpression of HIF-2 α is associated with poor prognosis, and both preclinical and clinical evidence is mounting that suggests inhibiting HIF-2 α is an effective strategy to mitigate tumor growth, particularly in clear cell renal cell carcinoma, warranting further development of HIF-2 α inhibitors.

Applying a pharmacophore mapping and structure-based design approach, we have discovered multiple novel series of HIF-2 α inhibitors which were characterized in various *in vitro* and *in vivo* assays designed to evaluate HIF-2 α -specific effects. Highly optimized compounds exhibit low-nanomolar inhibition of HIF-2 α -dependent transcription in a human renal cell adenocarcinoma hypoxia-responsive element reporter assay. Inhibitors did not affect expression of HIF-1 α target genes in a hepatocellular carcinoma cell line confirming high selectivity for HIF-2 α . Additionally, multiple analogs exhibit a favorable pharmacokinetic profile with minimal potential for drug-drug interactions, as negligible inhibition was observed against a panel of CYP isoforms and absence of time-dependent CYP inhibition. Our presentation will describe the preclinical characterization of several potential development candidates from this program. These data provide further support for using HIF-2 α inhibitors for the treatment cancer, particularly indications which feature pVHL loss-of-function or our internally established HIF-2 α -driven hypoxia signature.

Conflict of interest:

Ownership: Authors are shareholders in Arcus Biosciences, Inc.

33

Poster Discussion

XL092, a multi-targeted inhibitor of MET, VEGFR2, AXL and MER with an optimized pharmacokinetic profile

J. Hsu¹, C. Chong¹, L. Goon¹, J. Balayan¹, S. Wu¹, E. Johnson¹, G. Lorenzana¹, L. Bannen², L. Nguyen³, C. Scheffold⁴, P. Lamb¹, W. Xu², P. Yu¹. ¹Exelixis- Inc., Discovery, Alameda, USA; ²Exelixis- Inc., Discovery Medicinal Chemistry, Alameda, USA; ³Exelixis- Inc., Non Clinical Development, Alameda, USA; ⁴Exelixis- Inc., Clinical Development, Alameda, USA

Background: Receptor tyrosine kinases (RTKs) MET, VEGFR2, AXL and MER are believed to play important roles in tumor growth, vascularization, resistance to therapy and in modulating the tumor immune microenvironment. Consistent with this the multi-targeted RTK inhibitor cabozantinib, a potent inhibitor of these RTKs as well as others, has shown significant clinical activity in a variety of solid tumors, and shows promising activity in combination with checkpoint inhibitors. Cabozantinib has an extended plasma half-life which results in drug accumulation during initial dosing. We sought to develop a novel RTK inhibitor that retains the target profile of cabozantinib but with a significantly shorter clinical half-life. The profile of XL092, a compound meeting these criteria, will be presented.

Methods: XL092 inhibition of MET, VEGFR2, AXL and MER was evaluated using biochemical and cellular assays, and *in vivo* inhibition of p-MET and p-VEGFR2 was assessed in tumor (MET) or lung (VEGFR2) tissue following oral dosing of XL092. *In vivo* efficacy was evaluated in xenograft or syngeneic tumor models following dosing of XL092 alone or in combination with a PD1 antibody. Preclinical pharmacokinetic (PK) studies following oral or intravenous dosing were conducted in mice, rats and dogs. Clinical PK data was derived from multiple cohorts of an ongoing Phase 1 clinical trial of XL092 dosed daily to patients with advanced solid tumors (NCT03845166).

Results: XL092 is an ATP-competitive inhibitor of multiple RTKs including MET, VEGFR2, AXL and MER, with IC₅₀ values in cell-based assays of 15, 1.6, 3.4, and 7.2 nM respectively. In xenograft studies, XL092 caused substantial tumor growth inhibition following 10 mg/kg daily oral dosing for 14 days. Assessment of p-MET and p-VEGFR2 from a xenograft study showed 82% and 96% inhibition, respectively. When XL092 was combined with anti-PD1 antibody in a syngeneic tumor model, the combination was significantly more efficacious than either XL092 or anti-PD1 alone. PK studies in preclinical species showed that XL092 has good oral bioavailability and a significantly shorter half-life than cabozantinib. PK data from the ongoing Phase 1 clinical trial assessing daily dosing of XL092 in patients with advanced solid tumors shows a terminal half-life of 24 hr versus a 99 hr terminal half-life for cabozantinib.

Conclusions: XL092 retains the target inhibition profile of the clinically active drug cabozantinib, simultaneously targeting MET, VEGFR2, AXL and MER. In preclinical studies XL092 showed potent pharmacodynamic inhibition of MET and VEGFR2 phosphorylation, which was associated with significant anti-tumor activity. PK data from the Phase 1 trial of XL092 shows a significantly shorter terminal half-life compared to cabozantinib, consistent with the desired profile.

Conflict of interest:

Ownership: Exelixis, Inc: CS, LG, LB, PY, PL, RSU/ESPP stock ownership: CC, Other Substantive Relationships: Exelixis, Inc (employment): All authors Exelixis, Inc (patent, copyright, or licensing): CS, LB.

34

Poster Discussion

TPX-0005 (Repotrectinib), a next-generation ALK/ROS1/NTRK1-3 inhibitor, has potent antiproliferative and anti-tumor activity as monotherapy and in combination with chemotherapy in neuroblastoma cell lines and pediatric patient derived xenograft models

T. O'donohue¹, G. Ibáñez¹, A. Mauguen², A. Siddiquee¹, N. Rosales¹, P. Calder¹, A. Ndengu¹, S. Roberts¹, F. Dela Cruz¹, A. Kung¹. ¹Memorial Sloan Kettering Cancer Center, Pediatrics, New York, USA; ²Memorial Sloan Kettering Cancer Center, Biostatistics, New York, USA

Background: Abnormal activation of the ALK tyrosine kinase receptor drives the malignant behavior of many pediatric cancer subtypes, including neuroblastoma. Somatic *ALK* mutations have been reported in 6–10% of patients with neuroblastoma. Patients with relapsed and refractory disease have poor outcomes despite multimodal treatment with chemotherapy, immunotherapy, radiation, and surgery; thus, this population is in dire need of novel and less toxic therapies. TPX-0005 (Repotrectinib) is a novel multi-tyrosine kinase inhibitor that selectively targets ALK, ROS1, and NTRK1-3 (including solvent-front and gatekeeper mutations) as well as accessory pathways including JAK/STAT and SRC/FAK, that are implicated in

oncogenesis. Therefore, TPX-0005 could be a promising novel therapeutic option for patients with *ALK*-mutant neuroblastoma.

Methods: *In vitro* sensitivity to *ALK* inhibitors (TPX-0005 and ensartinib) and cytotoxic chemotherapy, singly or in combination, were evaluated in neuroblastoma cell lines harboring *ALK* mutations and with variable *MYCN* status. *In vivo* anti-tumor effect of TPX-0005 monotherapy, and in combination with chemotherapy, was evaluated using pediatric patient derived xenograft (PDX) models of neuroblastoma and an *NTRK*-fusion positive solid tumor model.

Results: Treatment of three neuroblastoma cell lines demonstrates that TPX-0005 has cytotoxic activity across *ALK*-mutant and *ALK*-WT cell lines (with IC₅₀ 2–3X lower in *ALK*-mutant lines). Combination of *ALK* inhibition (TPX-0005 or ensartinib) with irinotecan and temozolomide demonstrated synergistic antiproliferative activity across cell lines. *In vivo* therapeutic studies evaluated anti-tumor effect and event-free survival of models treated with TPX-0005 compared to a comparator drug (ensartinib for neuroblastoma models and entrectinib for the *NTRK*-fusion solid tumor). TPX-0005 monotherapy treatment prolongs event-free survival ($p < 0.05$, log-rank test) and has notable anti-tumor effect ($p = 0.006$ versus vehicle and $p = 0.05$ versus comparator drug). Furthermore, TPX-0005 plus chemotherapy *in vivo* is superior to chemotherapy alone when comparing tumor growth curves in an *ALK*-mutant neuroblastoma model ($p = 0.025$, Vardi's test). TPX-0005 also induced a near complete response (>80% tumor volume reduction) after four weeks of treatment in a PDX model characterized by *ETV6-NTRK3* fusion harboring a known solvent front mutation.

Conclusions: TPX-0005 demonstrates anti-tumor activity in *ALK*-mutant tumor models singly and in combination with chemotherapy *in vivo*. A significant improvement in event-free survival across all models, and particularly when combined with chemotherapy in an *ALK*-mutant PDX model, provides preclinical rationale for further exploration of TPX-0005 in *ALK*-mutant pediatric tumors.

No conflict of interest.

35

Poster Discussion

High-throughput small molecule screens reveal therapeutic opportunities against TFE3-fusion renal cell carcinoma

M. Lang¹, C. Sourbier¹, L.S. Schmidt¹, D. Wei¹, B.K. Gibbs¹, C.J. Ricketts¹, C. Vocke¹, K. Wilson², C.J. Thomas², W.M. Linehan¹. ¹Urologic Oncology Branch, National Cancer Institute/NIH, Bethesda, USA; ²Division of Preclinical Innovation, National Center for Advancing Translational Sciences/NIH, Bethesda, USA

Background: Accounting for 1–5% of all renal cell carcinoma (RCC) cases, TFE3-fusion RCC comprise an aggressive subset of neoplasms typically diagnosed in early and middle adulthood, for which treatment options are currently scarce. We sought to describe the distinctive TFE3-fusion RCC transcriptomic landscape, to perform high-throughput drug screening and to validate potential therapeutic targets using a combination of *in vitro* and *in vivo* experimental approaches.

Material and methods: Seven TFE3-fusion RCC tissue samples were subjected to RNA sequencing and pathway analysis was performed on differentially expressed genes. High-throughput drug screening with 1912 clinically relevant compounds was carried out on 3 patient-derived TFE3-fusion RCC cell lines harboring different TFE3-fusion genes. Cell viability results were validated in 2D and 3D spheroid models of 5 TFE3-fusion RCC cell lines. Drug mechanism was assessed by evaluating cell cycle and apoptosis, transcriptional activity assays and mTOR pathway inhibition assays. Subcutaneous nude mice xenograft studies were carried out using 2 TFE3-fusion RCC cell lines. Combination drug studies were performed *in vitro* and *in vivo*.

Results: Transcriptomics analyses of human TFE3-fusion tumor tissues showed high expression of lysosomal-related genes and upregulation of transcriptional profiles driving cell cycle and chromosome segregation. These data were integrated into the drug prioritization process of the quantitative high-throughput small molecule screen. After *in vitro* validation of candidate small molecules, the *in vivo* efficacy of 5 compound classes, namely proteasome inhibitors, PI3K/mTOR inhibitors, SRC inhibitors, RNA synthesis and microtubule inhibitors was validated in xenograft studies. The SRC inhibitor Dasatinib, the RNA synthesis inhibitor Mithramycin and the PI3K/mTOR inhibitor NVP-BGT226 presented significant antitumor activities *in vivo* as single agents. Molecular analyses of the mechanism of action of

each compound identified the importance of the activation the SRC pathway, SP1 transcription factor activation and the expression of survivin in the cell cycle progression and survival of TFE3-fusion RCC cell lines, and confirmed the role of the Akt/mTOR pathway in the growth of TFE3-fusion RCC cells. Combination drug studies of these compounds, together with a previously discovered drug target, the GPNMB-targeting antibody-drug-conjugate CDX-011, showed significant tumor inhibitory activities *in vitro* and *in vivo*.

Conclusions: PI3K/mTOR pathway inhibitors (NVP-BGT226), transcription inhibitors (Mithramycin), and combinations among each other and with the antibody-drug conjugate CDX-011, show promising preclinical efficacy against TFE3-fusion RCC. This preclinical study provides an unbiased foundation to identify potential therapeutic approaches against TFE3-fusion RCC patients.

No conflict of interest.

36

Poster Discussion

Screening of fractions from marine sponges and other invertebrates to identify new lead compounds with anti-tumor activity in lymphoma models

E. Spriano¹, M. Barreca², M. Miguel-Gordo³, S. O'Brien³, A.J. Arribas¹, L. Jennings³, O. Thomas³, F. Berton¹. ¹Institute of Oncology Research, Faculty of Biomedical Sciences, Bellinzona, Switzerland; ²Università degli Studi di Palermo, Scienze e Tecnologie Biologiche Chimiche e Farmaceutiche, Palermo, Italy; ³National University of Ireland Galway, Marine Biodiscovery- School of Chemistry and Ryan Institute, Galway, Ireland

Background: Diffuse large B-cell lymphoma (DLBCL) is the commonest type of lymphomas, accounting for 30%–40% of new cases each year. Despite the big improvements achieved in the treatment, still 25–40% of patients still succumb due to refractory or relapsed disease. This highlights the need of new drugs for this cancer. The marine environment has recently been recognized as a source of anti-cancer compounds, as demonstrated by different marine drugs approved by different regulatory agencies (trabectedin, cytarabine, eribulin, plitidepsin) or as components of antibody drug conjugates for lymphoma patients (monomethyl auristatin E in polatuzumab vedotin and brentuximab vedotin). Here, we present a large screening of fractions obtained from different marine invertebrates collected in Ireland and in the Pacific Ocean on DLBCL cell lines.

Material and methods: Marine invertebrate fractions were prepared by C18 Solid Phase extraction using solvents of different polarities and they were stored in DMSO at 10 mg/mL; Cells were seeded in 96 well plate with the semi-automatic dispenser INTEGRA VIAFLO at the density of 10000 cells for each well. Cell lines were exposed to fractions for 72 hours at the concentration of 100 or 10 or 1 mg/ml followed by MTT assay, as previously performed (Spriano et al, CCR 2018).

Results: 583 fractions were tested in 2 DLBCL cell lines (TMD8 and OCI-LY10) and 1 non neoplastic lymphoblastoid B cell line (CB33), used as DLBCL normal counterpart. At the concentration of 100 mg/ml the majority of the fractions showed an anti-proliferative activity in both lymphoma cell lines, while at 10 mg/ml only around half of the fractions still showed such biologic activity. Conversely, only 20 fractions determined over 30% reduction of cell proliferation in both lymphoma cell lines when given at 1 mg/ml concentration. Moreover, among these 20 with antitumor activity, 5 showed no activity at all in the lymphoblastoid cell line; 4 fractions caused the same effect as in the lymphoma cell lines and 11 cause some reduction in proliferation but not as much as in the neoplastic models. Among the most promising fractions we identified those coming from the Irish ascidian *Diplosoma listerianum* and the nudibranch *Janolus cristatus* but also the Pacific sponge *Stylissa cf. carteri*. Work is ongoing to identify the compounds responsible for the remarkable bioactivities.

Conclusions: In this first screening, we identified fractions derived from marine invertebrates with anti-tumor activity in lymphoma cell lines, including some without any effect on the proliferation of a non-tumoral B-cell model. These fractions provide the material to potentially identify novel anti-cancer compounds of marine origin. OT and FB are members of the COST Action CA18238 Ocean4Biotech.

No conflict of interest.

Saturday, 24 October 2020

22:00–22:50

POSTER DISCUSSION SESSION

Cancer Therapeutics: Preclinical Modeling and Patient Stratification

37

Poster Discussion

Prospective validation of single mouse testing (SMT) by the pediatric preclinical testing consortium (PPTC)

P.J. Houghton¹, R.T. Kurmasheva¹, S. Erickson², M.A. Smith³, R.B. Lock⁴, K. Evans⁴, C. Toscan⁴. ¹Greehey Children's Cancer Research Institute, Oncology, San Antonio, USA; ²RTI International, BioStats, Research Triangle Park, USA; ³NIH, National Cancer Institute, Bethesda, USA; ⁴Children's Cancer Institute- Lowy Cancer Research Centre, Oncology, Sydney, Australia

Background: The Research to Accelerate Cures and Equity for Children Act (RACE for Children Act) requires the FDA to develop a list of molecular targets of new drugs and biologics in development that are determined to be substantially relevant to the growth and progression of pediatric cancer, and that may trigger the requirement for pediatric investigations. This will require approaches to preclinical testing that incorporate models that accurately represent the genetic/epigenetic heterogeneity of pediatric cancers.

Materials and Methods: Patient-derived xenografts (PDXs) from 90 pediatric acute lymphoblastic leukemia (ALL) and 50 solid tumor models were used to evaluate small molecule drugs and antibody drug conjugates (ADCs) using Conventional Testing (CT; n = 8 mice/group for ALL; n = 10 for solid tumors) or using a SMT design (n = 1) to determine the accuracy of SMT and the feasibility of evaluating drugs in a wide panel of models.

Results: For the ALL models, the topoisomerase I inhibitor topotecan, the SMAC mimetic birinapant and the Selective Inhibitor of Nuclear Export (SINE) eltanexor were evaluated against 71, 72 and 90 PDXs, respectively, in the SMT format of which 7, 17 and 12 PDXs, respectively, had previously been evaluated using CT. Using stringent objective response criteria modeled after the clinical setting in which the response of the single mouse in the SMT was compared with the group median of the CT, both methods exhibited a high degree of concordance for all 3 drugs (topotecan r = 0.90, p = 0.014; birinapant r = 0.80, p < 0.0001; eltanexor r = 0.94, p < 0.0001).

For solid tumor models, SMT and CT results for the ADCs trastuzumab-deruxtecan (DS-8201a; CT = 5; SMT = 31), and mCD276-PBD (CT = 8; SMT = 51) were compared. For DS-8201a, results from SMT and CT were identical. Of note, DS-8201a induced regression in 5 of 5 rhabdoid tumor models. For mCD276-PBD, an ADC that recognizes the cell surface protein B7H3, resulted in objective regressions in 7 of 7 models common to both CT and SMT experiments. Of note CD276-PBD had broad-spectrum antitumor activity causing maintained complete response (MCR) in 30 models, CR/PR in 14 models with only 4 models showing Progressive Disease (PD). Two models were excluded due to death (cause unknown).

Conclusions: SMT accurately recapitulates CT, for both leukemia and solid tumor models, allows more clinically representative genetic/epigenetic models to be included, and yields more information than traditional experimental approaches. SMT may be particularly valuable for identifying responsive tumor types, and biomarkers that associate with tumor response. Thus, SMT potentially allows incorporation of disease heterogeneity that may be required for evaluating new agents under the RACE for Children Act.

Support: NO1-CM42216, UO1CA199297, CA165995, CA199000, CPRIT-RP160716.

No conflict of interest.

40

Poster Discussion

MatchMiner: Computational matching of cancer patients to precision medicine clinical trials

T. Mazar¹, P. Kumari¹, J. Lindsay¹, A. Ovalle¹, E. Siegel¹, J. Yu¹, M. Hassett², E. Cerami¹. ¹Dana-Farber Cancer Institute, Data Science, Boston, USA; ²Dana-Farber Cancer Institute, Medical Oncology, Boston, USA

To facilitate interpretation of complex tumor sequencing data and clinical trial genomic eligibility criteria, we developed MatchMiner, an open-source platform to computationally match cancer patients to precision medicine clinical trials based on clinical and genomic features. MatchMiner enables

physicians to identify clinical trial options for individual patients and enables clinical trial investigators to identify patients eligible for genomically-driven trials. MatchMiner can also be used to display profiling reports, independent of trial matching.

MatchMiner has been operational at Dana-Farber Cancer Institute (DFCI) since 2017 and currently holds 315+ trials and data from 37,000+ patients. Over 80% of living patients match to 1+ open clinical trials (average: 6 trials per patient). 118+ patients have enrolled in clinical trials due to MatchMiner.

To enable computational matching to clinical trials, we developed Clinical Trial Markup Language (CTML), a flexible and structured format to encode detailed trial information. Clinical (e.g. cancer type), demographic (e.g. age) and genomic (e.g. specific mutations, copy number alterations, structural variants or mutational signatures) eligibility is encoded as boolean logic. Eligibility can be applied at the arm or dose level to support any trial design.

MatchMiner supports multiple assays and data sources. MatchMiner initially presented sequencing results and trial matches based on OncoPanel, a targeted gene panel used at DFCI for solid tumors. Recently, we added support for the Rapid Heme Panel, a smaller panel used for hematologic malignancies, as well as ImmunoProfile, a novel multiplex immunofluorescence assay. Currently ImmunoProfile data is view-only, but we plan to utilize this non-genomic data for trial matching. Support for additional assays will be added in the future.

MatchMiner is an open-source software; code is freely available through GitHub (<https://github.com/dfci/matchminer>). We are committed to supporting MatchMiner as an open-source software; to our knowledge, at least five cancer centers are implementing MatchMiner locally. MatchMiner is HIPAA-compliant and can connect to existing clinical systems, including clinical trial management systems or electronic health record systems.

In summary, we have defined a standard for encoding clinical trial information in a computable form and developed an open-source computational trial matching platform to support patient-specific trial identification as well as trial-specific patient recruitment. The system is flexible and easily extensible to support new data types or assays. We are actively collaborating with clinical groups to understand the role of MatchMiner in clinical workflows and are committed to continuing to evolve MatchMiner to meet clinical needs.

No conflict of interest.

41

Poster Discussion

Stratification method based on RAS pathway oncogenic activity predicts outcome in lung adenocarcinoma

P. East¹, G. Kelly¹, D. Biswas², D. Hancock³, C. Swanton², S. de Carne³, J. Downward³. ¹The Francis Crick Institute, Bioinformatics & Biostatistics, London, United Kingdom; ²The Francis Crick Institute, Cancer Evolution and Genome Instability Laboratories, London, United Kingdom; ³The Francis Crick Institute, Oncogene Biology, London, United Kingdom

Activating mutations in the *KRAS* oncogene occur in some 30% of lung adenocarcinomas, where it acts as a driver of tumour formation. However, the association between *KRAS* mutational status and patient outcome or response to treatment remains largely obscure in lung cancer. Other events in addition to *KRAS* mutation can activate RAS signalling pathways, including not only mutations in other RAS pathway genes but also alterations in gene expression that promote signalling through the RAS network. To obtain a broader measure of RAS pathway activation beyond just *KRAS* mutation we have used, as a surrogate for oncogenic RAS signalling, a signature of RAS-induced transcriptional activity selected to separate *KRAS* mutant lung cancer cell lines from RAS-pathway wild type lines. We then validated the use of this signature to measure oncogenic RAS signalling using several independent lung adenocarcinoma clinical cohorts containing both *KRAS* mutant and wild type tumours. More than 80% of lung adenocarcinomas showed clear transcriptional evidence of RAS pathway activation, falling into four main groupings. These are characterised by coincident mutation of *STK11/LKB1* (KL), *TP53* (KP), *CDKN2A* (KC), or no obvious co-mutation (K). Given that 65% of these RAS pathway active tumours do not have *KRAS* mutations, we find that the classifications developed when considering only *KRAS* mutant tumours have significance in a much broader cohort of patients. The highest RAS activity signature groupings showed adverse clinical outcome in both univariate and multivariate Cox proportional hazards analysis. The stratification of patients using gene expression patterns linked to oncogenic RAS signalling activity instead of genetic alterations in proto-oncogenes provides improved ability to study the functional effect of RAS on cancer progression and resistance to treatment, and could ultimately help clinical decision making.

No conflict of interest.

42

Poster Discussion

Tumor drug exposure is positively correlated with an improved outcome, in patients with advanced solid tumors, upon treatment with a high dose intermittent sunitinib regimen

S. Gerritse¹, R. ter Heine², M. Labots³, E. van den Hombergh², H. Dekker³, D. Lehutová³, M. Rudek⁴, N. van Erp², H. Verheul¹. ¹Radboud University Medical Center, Department of Medical Oncology- Radboud Institute for Health Sciences, Nijmegen, Netherlands; ²Radboud University Medical Center, Department of Pharmacy- Radboud Institute for Health Sciences, Nijmegen, Netherlands; ³Amsterdam UMC- Vrije Universiteit Amsterdam, Department of Medical Oncology- Cancer Center Amsterdam, Amsterdam, Netherlands; ⁴The Johns Hopkins University- The Sidney Kimmel Comprehensive Cancer Center, Department of Oncology and Clinical Pharmacology, Baltimore, USA

Background: Innovative strategies for the clinical use of multitargeting tyrosine kinase inhibitors (TKIs), like sunitinib, are needed to fully exploit their antitumor activity. The inhibitory activity of these drugs depends on the tumor drug concentration, its affinity for kinases and kinase activity in tumor cells. Their broader inhibitory capacity at high concentrations might be essential for optimal suppression of tumor growth and induction of apoptosis. In a recent phase I trial NCT02058901, we administered high dose intermittent sunitinib 300 mg once a week and 700 mg once every two weeks, to patients with advanced tumors. This strategy resulted in higher peak plasma concentrations compared to regular dosing of sunitinib, without drug accumulation and with promising clinical benefit. We hypothesized that these plasma concentrations subsequently lead to higher tumor drug concentrations. Here, we determined tumor- and skin tissue drug concentrations of patients participating in this trial and related them to the plasma concentrations and clinical outcome.

Methods: Plasma samples were collected predose and at multiple timepoints postdose. Tumor and skin biopsies were collected on day 17 (2 days after the 2nd or 3th dose). Sunitinib and N-desethyl sunitinib were analyzed by liquid chromatography–tandem mass spectrometry. Nonlinear mixed-effect modeling was used to describe the plasma pharmacokinetic (PK) data. Individual C_{max} , $C_{average}$ and C_{trough} were estimated. Potential relationships were tested with linear regression. Pearson's correlation coefficients (PCC) were computed and tested for significance.

Results: Plasma samples of 82 patients, skin biopsies of 36 patients and tumor biopsies of 22 patients were collected. The PK results are presented in the table. No significant relationship of the sunitinib concentration in tumor, skin and plasma ($C_{average}$, C_{max}) could be identified. The sum concentration of sunitinib in tumor biopsies significantly correlates with progression free survival (PCC 0.50; p-value 0.018) and overall survival (PCC 0.59; p-value 0.006), in contrast to plasma and skin concentrations. The geometric mean (GM) tumor drug concentration of responders was 31.6 μ M compared to 10 μ M in non-responders.

| | Sunitinib + N-desethyl sunitinib concentration μ M | | |
|-------|--|----------------------------|------------|
| | Plasma | | Tumor |
| | C_{max} | $C_{average}$ (0-day17) | |
| Mean | 0,91 | 0,35 | 45,98 |
| Range | 0,2–2,20 | 0,15–0,92 | 1,4–78,79 |
| GM | 0,79 | 0,33 | 19,69 |
| | | | Skin |
| Mean | | | 8,86 |
| Range | | | 0,69–48,18 |
| GM | | | 4,82 |

Conclusion: With this feasible strategy, we are the first to demonstrate that a higher tumor drug concentration, in contrast to the plasma concentration, is predictive for an improved clinical outcome, in a phase I study population treated with high dose intermittent sunitinib. These findings have the potential to change the dose and schedule of multitargeting TKIs, like sunitinib and thereby enhance their clinical efficacy.

Conflict of interest:

Advisory Board: Glycostem (Inst), Bristol-Myers Squibb (Inst). Other Substantive Relationships: Receive grants from: Novartis, Astellas, AstraZeneca, Bristol-Meyers Squibb, Gilead, Ipsen, Janssen, Pfizer, and Roche.

43

Poster Discussion

Circulating tumour DNA analysis using three next generation sequencing approaches in a phase 1b trial of ER positive metastatic breast cancer

R. Masina¹, M. Gao¹, R. Baird², M. Callari¹, C. Caldas¹. ¹University of Cambridge, Cancer Research UK - Cambridge Institute, Cambridge, United Kingdom; ²on behalf of the POSEIDON investigators, Cancer Research UK - Cambridge Institute, Cambridge, United Kingdom

Background: Circulating tumour DNA (ctDNA) has shown promise in cancer detection, prognostication and monitoring. Clinical trials offer unique opportunities to explore the potential of ctDNA in a well-defined and homogeneous clinical context.

Methods: The POSEIDON phase 1b trial recruited 30 patients with ER-positive, metastatic breast cancer who had failed prior endocrine therapy. Patients were treated with escalating doses of taselisib combined with tamoxifen. Taselisib is a potent, selective, beta-isoform-sparing PI3 kinase inhibitor. The trial has been reported, and the randomised phase 2 is currently recruiting. Serial plasma samples have been collected at predefined time points from screening to disease progression. In these samples we performed extensive next generation sequencing-based ctDNA analysis: whole exome sequencing (WES, n = 83), shallow whole genome sequencing (sWGS, n = 290) and next-generation tagged-amplicon sequencing (NGTAS, n = 299). In addition, matched tumour biopsies were profiled (12 by WES, 41 by sWGS, 23 by NGTAS). A number of metrics were derived from sequencing data and associated with time to progression (TTP) and clinical benefit (CB) using Cox Proportional-Hazards Models and Logistic regression.

Results: ctDNA was detected in at least one sample in 22/22 patients by WES, 30/30 patients by sWGS and 25/30 patients by NGTAS. Good agreement was observed between tissue and liquid biopsies. We compared the prognostic and predictive potential of the three sequencing approaches. Overall, copy number profiles showed the highest performance in predicting prognosis and provided an early indication of treatment response. Multiple sequencing-based metrics were able to estimate tumour burden as quantified by gold standard imaging. Gene- and pathway-level comparison of ctDNA profiles before and after treatment shed light on potential mechanisms of acquired drug resistance to PI3K inhibition.

Conclusions: We show that ctDNA monitoring in early-phase clinical trials has value for the assessment of biomarkers which can predict response to therapy. Circulating tumour DNA conveys information about the tumour that holds potential i) to inform the oncologist during clinical decision-making ii) to generate hypothesis on therapeutic strategies able to overcome resistance.

Conflict of interest:

Advisory Board: R.D. Baird reports receiving speakers bureau honoraria from Novartis and Roche/Genentech.

C. Caldas reports receiving speakers bureau honoraria from Illumina, is a consultant/advisory board member for AstraZeneca.

Corporate-sponsored Research: R.D. Baird reports receiving commercial research grants from Genentech, AstraZeneca, and Boehringer-Ingelheim and commercial research support from AstraZeneca.

C. Caldas reports receiving commercial research grants from AstraZeneca, Servier, Genentech, and Roche.

Sunday, 25 October 2020

14:30–15:20

POSTER DISCUSSION SESSION

New Targets in Immuno-Oncology

44

Poster Discussion

Inhibition of 4NQO-induced oral squamous cell carcinoma progression by novel TGF- β inhibitors and PD-L1 antibodies

N. Ludwig¹, S.S. Yerneni², J.H. Azambuja³, Ł. Wieteska⁴, C.S. Hinck⁴, R.J. Bauer¹, T.E. Reichert¹, A.P. Hinck⁴, T.L. Whiteside³. ¹University Hospital Regensburg, Department of Oral and Maxillofacial Surgery, Regensburg, Germany; ²Carnegie Mellon University, Department of Biomedical Engineering, Pittsburgh, USA; ³University of Pittsburgh School of Medicine, Department of Pathology, Pittsburgh, USA; ⁴University of Pittsburgh School of Medicine, Department of Structural Biology, Pittsburgh, USA

Background: TGF- β is a key regulator of oral squamous cell carcinoma (OSCC) progression and its potential role as a therapeutic target has been

investigated with a limited success. This study evaluates two novel TGF- β inhibitors as mono or combinatorial therapy with PD-L1 antibodies (Abs) in a murine OSCC model. The inhibitors were developed in Dr. Andrew Hinck's laboratory and have been previously described.

Material and methods: Immunocompetent C57BL/6 mice bearing malignant oral lesions induced by the carcinogen, 4-nitroquinoline 1-oxide (4-NQO), were treated for 4 weeks with TGF- β trap mRER (intraperitoneal injections, 50 μ g/d) or the engineered TGF- β monomer mmTGF- β 2-7M (10 μ g/d delivered by osmotic pumps) alone or in combination with PD-L1 antibodies (7 intraperitoneal injections of 100 μ g/72 h). Tumor progression was monitored by gross observation, calipers and determination of body weight. Levels of bioactive TGF- β in serum were quantified using the MFB-F11 reporter cell line. Tumors were analyzed by immunohistology and splenocytes were analyzed by flow cytometry.

Results: Therapy with mRER or mmTGF- β 2-7M reduced numbers and size of tumors ($p < 0.05$) and decreased the loss of body weight compared to control mice. In the inhibitor-treated mice, levels of TGF- β in tumor tissue and serum were reduced ($p < 0.05$), while they increased with tumor progression in plasma of controls. Both inhibitors stimulated CD8⁺ T cell infiltration into tumors and reduced levels of myeloid-derived suppressor cells ($p < 0.001$). In combination with PD-L1 Abs, the TGF- β inhibitors further ameliorated the weight loss of mice ($p < 0.05$) and the number of tumors per mice ($p < 0.05$). The collagen-rich stroma was reduced by using combinatorial TGF- β /PD-L1 therapies ($p < 0.05$), enabling an accelerated immune cell infiltration into the tumor tissue.

Conclusion: The data show that the blockade of TGF- β signaling by the novel inhibitors, mRER and mmTGF- β 2-7M, is a promising approach for treatment of OSCC. The inhibitors alone promoted anti-tumor immune responses and in combination with immune checkpoint inhibitory Abs, in particular PD-L1, were especially effective in inhibiting tumor progression.

Conflict of interest:

Other Substantive Relationships: A. Hinck is the Co-Inventor of RER, which is covered by U.S. patent 9,611,306, and holds royalty rights for clinical deployment of RER, which is currently being pursued. A. Hinck is also the Co-Inventor of a provisional patent (United States Patent Application 62/423,920) that covers mmTGF- β 2-7M.

45

Poster Discussion

Targeting immune tolerance and stromal fibrosis with an LXR agonist in a conditional transgenic model of mammary fibrosis

R. Glazer¹, S. Gao², H. Yuan³, S. Ranjit⁴, J. Lu³, H. Xiang⁵, A. Bhattacharya⁵, P. Brandish⁵, M. Levi⁴. ¹Georgetown University, Oncology, Washington, USA; ²Nanjing University of Chinese Medicine, Medicine, Nanjing, China; ³Georgetown University, Oncology, Washington-DC, USA; ⁴Georgetown University, Biochemistry & Molecular Biology, Washington-DC, USA; ⁵Merck & Co. Inc., Discovery Therapeutics, Boston, USA

Background: One of the central challenges for cancer therapy is the identification of factors in the tumor microenvironment that increase tumor progression and immune tolerance. One such factor associated with breast cancer is fibrosis, a histopathologic criterion for invasive cancer and poor survival. Fibrosis results from inflammatory factors and remodeling of the extracellular matrix that produces excessive collagen deposition and an immune tolerant environment.

Materials and Methods: We developed a conditional ErbB2-dependent breast cancer model of mammary fibrosis named NeuT/ATTAC. Induction of fibrosis results from partial ablation of mammary fat by transgene activation and its replacement with fibrotic tissue. Mice were administered either a murine anti-PD-1 mAb (DX400, Merck) or a diet containing 0.05% of the LXR agonist, N, N-Dimethyl-3- β -Hydroxy-Cholenamide (DMHCA). Fibrosis was monitored by changes in collagen composition using fluorescence lifetime imaging microscopy (FLIM) and second harmonic generation (SHG) microscopy. Tumor immune cell infiltrates were characterized by FACS, and transcriptional changes were assessed by RNAseq.

Results: Induction of fibrosis in NeuT/ATTAC mice resulted in resistance to weekly treatment with DX400 over five months. In contrast, treatment with DMHCA over a similar time interval reduced tumorigenesis and suppressed fibrosis as shown by loss of collagen structure by FLIM and SHG microscopy. This resulted in a marked reduction of Treg cell and MDSC infiltration, and an increase in CD8⁺ effector T cells, and downregulation of an LXR-dependent gene network targeting CCL5, PTGS2 and SPP1.

Conclusions: DMHCA therapy reduced fibrosis and immune tolerance in an anti-PD-1 resistant mouse model. These results suggest that DMHCA may be useful for enhancing immunotherapies that target immune suppressor cells as well as for other anticancer therapies. Unlike many LXR agonists, DMHCA does not increase serum triglycerides or produce hepatic steatosis, and may therefore be a good candidate for clinical studies.

Supported by a Sher Award, 1P30CA051008 from the NCI, NIH, to the Lombardi Comprehensive Cancer Center, and R01 HL133545 and R01 DK116567 from the NIH to M.L.

No conflict of interest.

46

Poster Discussion

A highly selective and potent HPK1 inhibitor enhances immune cell activation and induces robust tumor growth inhibition in a murine syngeneic tumor model

D. Ciccone¹, V. Lazari², I. Linney², M. Briggs², S. Carreiro¹, I. Waddell², C. Hill², C. Loh¹, P. Tummino¹, A. Collis¹, N. Kaila¹. ¹Nimbus Therapeutics, Research and Development, Cambridge, USA; ²Charles River Laboratories, Research, Chesterford Park, United Kingdom

Background: HPK1, a member of the MAP4 K family of protein serine/threonine kinases, is involved in regulating signal transduction cascades in cells of hematopoietic origin. Recent data from HPK1 knockout animals and kinase-inactive knock-in animals underscores the role of HPK1 in negatively regulating lymphocyte activation. This negative-feedback role of HPK1 downstream of lymphocyte activation and function, combined with its restricted expression in cells of hematopoietic origin, make it a compelling drug target for enhancing anti-tumor immunity.

Methods: A structure-based drug design approach was used to identify potent and selective inhibitors of HPK1. Biochemical assays, as well as primary human and mouse immune cell-based activation assays, were utilized for multiple iterations of structure-activity relationship (SAR) studies. *In vivo* efficacy, target engagement and pharmacodynamic data were generated using murine syngeneic tumor models.

Results: A highly potent, HPK1 inhibitor was identified, that showed high selectivity against T cell-specific kinases and kinases in the MAP4 K family. *In vitro*, HPK1 small molecule inhibition resulted in enhanced IL-2 production in primary mouse and human T cells, as well as enhanced IL-6 and IgG production in primary human B cells. Furthermore, HPK1 inhibition alleviated the immuno-suppressive effects of PGE2 on naive human T cells and restored the proliferative capacity of exhausted human T cells. HPK1 inhibition completely abrogated T cell receptor-stimulated phospho-SLP-76, enhanced cytokine production, and demonstrated robust tumor growth inhibition in a murine syngeneic tumor model.

Conclusion: Pharmacological blockade of HPK1 kinase activity represents a novel and potentially valuable immunomodulatory approach for anti-tumor immunity.

No conflict of interest.

47

Poster Discussion

RAS orchestrates an increase of interstitial adenosine in lung adenocarcinoma to promote immune evasion

S. de Carné Trécesson¹, J. Boumhela¹, C. Moore¹, D. Caswell², E. Mugarza-Strobl¹, M. Molina-Arcas¹, P. Smith³, K. Sachsenmeier⁴, P. East³, J. Downward¹. ¹Francis Crick Institute, Oncogene Biology Laboratory, London, United Kingdom; ²Francis Crick Institute, Cancer Evolution and Genome Instability Laboratory, London, United Kingdom; ³AstraZeneca, Oncology R&D, Cambridge, United Kingdom; ⁴AstraZeneca, Translational Science, Waltham, USA; ⁵Francis Crick Institute, Bioinformatics and Biostatistics, London, United Kingdom

The RAS pathway is frequently activated in human cancers, including lung adenocarcinoma, leading to poor prognosis and resistance to therapy. Despite huge efforts, it is still not possible to target this pathway directly. In contrast, immune checkpoint blockade has shown remarkable yet varied efficacy in lung cancer. To find a vulnerable point in these aggressive tumours, we ask here whether oncogenic RAS shapes the immune landscape of lung adenocarcinoma.

We classified human lung adenocarcinoma (LUAD) samples from the publicly available dataset from TCGA according to their RAS activity using a RAS transcriptional signature (RAS84) we previously developed. We correlated the immune infiltrate with RAS activity using CIBERSORT and the Danaher method. We also identified the expression of immune-related genes that were associated with RAS activity. Using MEK or RASG12C inhibitors, we then validated the regulation of immune-related genes by RAS-MAPK in KRAS-mutant human lung cell lines and several Kras-driven mouse models of lung adenocarcinoma. Finally, we established the KPAR1.3 (*Kras*^{G12D/wt}; *Trp53*^{fl/fl}; *APOBEC3B*) orthotopic model to test combinations of treatments targeting the RAS-dependent immunomodulators we discovered.

RAS84 classified human lung adenocarcinoma tumours in five groups (RAG-0 to RAG-4), independently of the mutational status of KRAS. Each

group was associated with concomitant genomic alterations and increased level of oncogenic RAS activity. Despite having the worse prognostic and the highest expression of RAS84, RAG-3 and RAG-4 were highly infiltrated with leucocytes and strongly expressed IFN-stimulated genes (ISGs), necessary to achieve an anti-tumoural immune response. RAG-3 and RAG-4 also expressed high levels of several immune checkpoint genes (e.g. CD274 (PD-L1), PDCDL2 (PD-L2), PVR, TIGIT) and deregulated genes related to adenosine metabolism or function (e.g. NT5E (CD73), ADORA2B, SLC29A4 (ENT4)). The latter suggests an increase in interstitial adenosine, known to dampen the immune system. We validated the RAS-MAPK-dependent regulation of adenosine genes and showed that a combination of anti-PD-1, anti-CD73 and anti-TIGIT improved survival of KPAR1.3 tumour-bearing mice.

Altogether, these data suggest that oncogenic RAS activity induces immune evasion by increasing adenosine level in the tumour microenvironment, notably through the expression of CD73, the enzyme that converts extracellular AMP to adenosine. Patients with highly aggressive and resistant RAS-driven lung cancers could benefit from targeting adenosine metabolism (anti-CD73) or activity (A2AR inhibitors) in combination with other immunotherapies targeting PD-1/PD-L1 and TIGIT.

Conflict of interest:

Other Substantive Relationships Paul Smith and Kris Sachsenmeier are employees of AstraZeneca.

48

Poster Discussion

Molecular profiling of post-pembrolizumab muscle-invasive bladder cancer reveals unique features that may inspire new sequential therapies in nonresponders

L. Marandino¹, J.J. de Jong², D. Raggi¹, A. Gallina³, M. Bandini⁴, P. Giannatempo¹, M. Colechia⁵, A. Briganti⁴, F. Montorsi⁴, E. Davicioni⁶, R. Seiler⁷, P. Black⁸, E.A. Gibb⁶, A. Necchi¹. ¹Fondazione IRCCS Istituto Nazionale dei Tumori di Milano, Medical Oncology, Milan, Italy; ²Erasmus MC- University Medical Center Rotterdam, Department of Urology, Rotterdam- Netherlands; ³Urological Research Institute URI- IRCCS Ospedale San Raffaele, Unit of Urology- Division of Experimental Oncology, Milan, Italy; ⁴Urological Research Institute- IRCCS Ospedale San Raffaele- Vita-Salute San Raffaele University- IRCCS Ospedale San Raffaele- Milan- Italy- Vita-Salute San Raffaele University, Unit of Urology, Milan, Italy; ⁵Fondazione IRCCS Istituto Nazionale dei Tumori di Milano, Uropathology Unit, Milan, Italy; ⁶Decipher Biosciences Inc., Decipher Biosciences Inc., Vancouver- British Columbia, Canada; ⁷Bern University Hospital, Department of Urology, Bern, Switzerland; ⁸University of British Columbia, Department of Urologic Sciences, Vancouver- British Columbia, Canada

Background: The pembro-induced alterations in immunotherapy-resistant tumors remain largely unstudied. In the PURE-01 study (NCT02736266), a proportion of patients (pts) with muscle-invasive bladder cancer (MIBC) had residual invasive disease at radical cystectomy (RC) after neoadjuvant pembrolizumab (pembro). The primary objective of this analysis was to investigate the biological characteristics of pembro-resistant tumors in comparison to neoadjuvant chemotherapy (NAC)-resistant tumors. In addition, we investigated post therapy changes of Nectin-4 and Trop-2 expression.

Material and methods: Gene expression profiling was performed on 26 RC samples from pts with ypT2-4 disease post-pembro, of which 22 had matched pre-pembro transurethral resection of the bladder tumor (TURBT) samples. Matched cases were analyzed by differential gene expression, hallmark signatures, and molecular subtyping (Decipher Bladder, TCGA, Consensus and Lund classifiers). Unsupervised consensus clustering (CC) was used to compare the 26 post-pembro samples with 133 post-NAC samples and to 21 samples collected from the former tumor bed of NAC-treated patients (scar tissue), all derived from RC specimens. For the secondary aim of this study, Nectin-4 and Trop-2 expression according to molecular subtyping (Decipher Bladder, TCGA, Consensus) on TURBT samples, and post therapy changes on unmatched RC samples from pts enrolled in the PURE-01 were evaluated.

Results: Molecular subtyping of the pre- and post-pembro samples showed significant "subtype switching" with only 41% of samples having concordant subtypes using the Decipher Bladder classifier. The post-pembro samples did not cluster with scar tissues on clustering but were highly associated with immune-infiltrated cases from the post-NAC cohort. Two major groups of post-pembro tumors were identified, the first defined by higher immune, stromal, angiogenesis and epithelial-to-mesenchymal signature scores and the second by higher tumor purity, KRAS and reactive oxygen species signature scores.

For all three subtyping models, the expression of Nectin-4 and Trop-2 was higher in tumors with luminal subtypes versus basal and NE-like.

A significant lower expression of Nectin-4 and Trop-2 expression was found in post-therapy residual tumors compared to pre-therapy lesions ($p = 0.0038$ for Nectin-4; $p < 0.001$ for Trop-2).

Conclusions: This study expands our knowledge of pembro-resistant tumors finding the molecular characteristics of these tumors is strikingly different from NAC-resistant tumors. Two distinct clusters of tumors were identified post-pembro, neither of which were characterized as having a scar-like character. Both Nectin-4 and Trop-2 correlated with luminal subtype, and a lower expression was found in residual tumors post-pembro. A larger cohort will be required to further understand the clinical implications of these findings.

Conflict of interest:

Other Substantive Relationships: E. Davicioni, E.A. Gibb: employees of Decipher Biosciences Peter C. Black has a patent on genomic markers in bladder cancer with Decipher Biosciences, Vancouver, BC, Canada. This work was supported by Merck & Co., Inc., Kenilworth, NJ, USA Associazione Italiana per la Ricerca sul Cancro (AIRC) ClinicalTrials.gov (number NCT02736266) and Decipher Biosciences.

Sunday, 25 October 2020

14:30–15:20

POSTER DISCUSSION SESSION

Approaches to Overcoming Therapeutic Resistance

49

Poster Discussion

Acquired resistance to selective FGFR inhibitors in FGFR-altered cholangiocarcinoma

L. Goyal¹, I. Baiev¹, K. Zhang², S. Dalgai³, R.T. Shroff⁴, R.K. Kelley², N. Uboha⁵. ¹Massachusetts General Hospital, Gastrointestinal Oncology, Boston, USA; ²University of California- San Francisco Helen Diller Family Comprehensive Cancer Center, Gastrointestinal Oncology, San Francisco, USA; ³University of Arizona College of Medicine, Department of Medicine, Tucson, USA; ⁴University of Arizona College of Medicine, Division of Hematology and Oncology, Tucson, USA; ⁵University of Wisconsin Carbone Cancer Center, Division of Hematology and Oncology, Madison, USA

Background: Acquired resistance to selective FGFR inhibitors (FGFRi) in FGFR2 fusion positive intrahepatic cholangiocarcinoma (ICC) has been shown to be polyclonal and limit the efficacy of this class of drugs. FGFRi's achieve a 25–37% objective response rate (ORR) and 7.5–8.3 month median duration of response in this population, and defining mechanisms of resistance is essential for future drug development. We present the largest multi-institutional study of clinically acquired resistance to FGFRi's in CCA.

Methods: Patients (pts) with advanced FGFR-altered CCA who were treated with an FGFRi and had at least one post-progression tumor biopsy or circulating tumor DNA (ctDNA) analysis were included. Tissue genotyping was performed using institutional or commercial assays, and ctDNA analysis was performed on Guardant360.

Results: Among 42 pts (median age 55 years, 52% female, 98% ICC), 36 (86%) harbored an FGFR2 fusion and 6 (14%) an FGFR mutation. Pts received an ATP-competitive, reversible FGFRi including infigratinib (19%), pemigatinib (5%), Debio1347 (2%), ponatinib (2%), or AZD4547 (2%), or the covalently-binding, irreversible inhibitor futibatinib (69%) as their first FGFRi. In the FGFR2 fusion+ cohort, the ORR was 39%, and an additional 25% had stable disease for >6 months, with an overall clinical benefit rate of 64%. Pts with clinical benefit were more likely to develop FGFR2 kinase domain mutations (KDMuts) upon progression compared to patients with primary resistance (65% vs 15%, $p = .004$). Pts who progressed on a reversible vs irreversible FGFRi developed KDMuts at progression at a rate of 58% vs 42%, respectively ($p = 0.35$). The most common mutations among pts treated with a reversible inhibitor involved the gatekeeper V565 residue (57%) and/or the molecular brake N550 residue (43%), and 57% of patients developed >1 KDMut. In futibatinib-treated pts, the most common mutations involved N550 (70%), V565 (50%), and/or E565A (20%), and 60% developed >1 KDMut. Only 1 patient (4%) treated with futibatinib developed a mutation in FGFR2 C492. Among pts who had both tumor biopsy and ctDNA analysis post-progression, 64% had mutations identified in plasma only and 36% in both.

Conclusions: On-target resistance with acquired mutations in the FGFR2 kinase domain emerges over time in pts experiencing clinical benefit from FGFRi, suggesting FGFR pathway dependence in these patients. Only ~40% of pts on futibatinib developed FGFR2 KDMuts, suggesting that most may have off-target mechanisms of resistance. Mutation of the cysteine residue to which futibatinib binds was not a common mechanism of

resistance in this small series. ctDNA analysis enables serial, non-invasive monitoring and can detect polyclonal secondary FGFR2 mutations. Further study of acquired resistance patterns to FGFRi's are needed to inform the development of the next generation of inhibitors.

Conflict of interest:

Advisory Board: Nataliya Ubaha: Taiho, Incyte, AZ.
Lipika Goyal: Debiopharm, H3 Biomedicine, Agios Pharmaceuticals, Taiho Pharmaceuticals, Klus Pharmaceuticals, QED, Pieris Pharmaceuticals, Alentis Pharmaceuticals, and Incyte.
Robin Katie Kelley: Genentech/Roche, Gilead.
Corporate-sponsored Research: Nataliya Ubaha: Taiho, EMD Serono, Eli Lilly, Ipsen.
Rachna Shroff: Celgene, Halozyme Therapeutics, Agios Pharmaceuticals, Eli Lilly.
Robin Katie Kelley: Agios, Astra Zeneca, Bayer, BMS, Eli Lilly, EMD Serono, Exelixis, Merck, Novartis, Partner Therapeutics, QED, Taiho.
Other Substantive Relationships: Nataliya Ubaha: Consulting for Ipsen, Eli Lilly.
Rachna Shroff: Received personal fees from Seattle Genetics, Exelixis, Merck & Co, and Codiak Biosciences.
Robin Katie Kelley: Travel support from Ipsen for satellite symposium.

50

Poster Discussion

ORIC-101 overcomes GR-driven resistance to AR degradation in castration-resistant prostate cancer models

H. Zhou¹, S. Barkund¹, L.S. Friedman², A. Daemen¹. ¹ORIC Pharmaceuticals, Translational Medicine, South San Francisco, USA; ²ORIC Pharmaceuticals, ORIC Pharmaceuticals, South San Francisco, USA

Prostate cancer is the second leading cause of cancer-related death in men. Androgen deprivation and blockade are commonly used to treat prostate cancer. However, relapse occurs with subsequent progression to metastatic castration-resistant prostate cancer (mCRPC). New therapeutic strategies are needed for patients who relapse with mCRPC. Previously we have shown that the glucocorticoid receptor (GR) is a potential bypass mechanism to antiandrogen therapy in preclinical CRPC models, and ORIC-101, a potent and selective, orally bioavailable small molecule GR antagonist, reverses GR-mediated resistance to enzalutamide in these models.

In this study we hypothesized that GR may be a mechanism of resistance to androgen receptor (AR) degraders, and ORIC-101 may reverse GR-mediated resistance to AR degradation in mCRPC. We used two AR Degradator (ARD) compounds (exemplary compounds 7 and 13, US 2018/0099940 A1) and confirmed that both ARD compounds degraded AR protein, inhibited AR target gene expression, and blunted cell growth in CRPC cell lines. We observed that upon chronic ARD treatment, GR mRNA and protein levels were significantly upregulated in a time-dependent manner, similar to GR upregulation seen after dosing with enzalutamide. Concordant with enhanced GR expression, glucocorticoids promoted tumor cell growth, stimulated androgen-regulated gene expression, and drove resistance to ARD treatment. Importantly, these effects were completely reversed by ORIC-101. We also noted that secreted PSA was induced by glucocorticoids and this induction was fully inhibited by ORIC-101. These data demonstrate that GR may be a mechanism of resistance to AR degraders in response to glucocorticoids and that ORIC-101 overcomes GR-driven resistance to AR degradation.

Currently, a phase 1b study of ORIC-101 in combination with enzalutamide in patients with metastatic prostate cancer is ongoing (NCT04033328). Our data indicate that targeting GR may help overcome resistance to many methods of antiandrogen therapy.

Conflict of interest:

Corporate-sponsored Research: All authors are current employees of ORIC Pharmaceuticals.

51

Poster Discussion

Vertical pathway inhibition with a SOS1::KRAS inhibitor enhances the efficacy of KRAS G12C inhibitors, delays feedback resistance and demonstrates durable response

F. Savarese¹, M. Gmachl¹, L. Federico², F. Trapani¹, D. Gerlach¹, J. Daniele², N. Feng², C.A. Bristow², A. Machado², J. Huang², D. Rudolph¹, I. Waizenegger¹, J. Ramharther¹, C.P. Vellano², M. Petronczki¹, J.R. Marszalek², T.P. Heffernan², D.B. McConnell¹, N. Kraut¹, M. Hofmann¹. ¹Boehringer Ingelheim RCV GmbH & Co KG, Cancer Pharmacology and Disease Positioning, Vienna, Austria; ²The University of Texas MD Anderson Cancer Center, TRACTION Platform- Therapeutics Discovery Division, Houston, USA

BI 1701963 is the first SOS1::KRAS inhibitor, which has entered Phase I clinical trials both as a mono-therapy as well as in combination with MEK inhibitors in patients with KRAS mutated advanced solid tumors. Both, BI 1701963 as well as the previously reported probe compound BI-3406 are orally bioavailable small molecules, designed to bind to the catalytic domain of SOS1, thereby preventing the interaction with GDP-loaded KRAS. In KRAS-dependent cancers, both SOS1::KRAS inhibitors potentially reduce the formation of GTP-loaded KRAS and inhibit MAPK pathway signaling. SOS1::KRAS inhibitors exhibit activity on a broad spectrum of KRAS alleles, including all major G12D/V/C and G13D oncoproteins, while sparing the interaction of KRAS with SOS2. This increases the targetable patient population beyond tumors with a KRAS G12C mutation and suggests a favorable therapeutic window to enable rational combinations. We previously showed that combining the SOS1::KRAS inhibitor BI-3406 with a MEK inhibitor blocks the negative feedback relief induced by MAPK inhibition. Combining SOS1::KRAS inhibition with MEK inhibitor treatment enhances pathway blockade leading to stronger anti-tumor efficacy in xenograft models driven by mutant KRAS such as G12D/V/C, G13D as well as Q61 K.

Here, we present data for the combination of a SOS1::KRAS inhibitor with covalent KRAS G12C inhibitors. Several covalent KRASG12Ci are currently in clinical development. Data from KRASG12Ci clinical trials have shown so far the highest response rate for patients with NSCLC, whereas patients with CRC demonstrated a lower response rate. Preclinically, CDX and PDX models initially often respond to KRASG12Ci monotherapy treatment followed by relapse and outgrowth of tumors. Combination therapy of a KRASG12Ci may therefore lead to enhanced anti-tumor efficacy and may address adaptive resistance mechanisms. Treatment with SOS1::KRAS inhibitors represses KRAS activation and shifts the equilibrium from the active KRAS-GTP form towards the inactive KRAS-GDP form. Consequently, SOS1::KRAS inhibitors have the potential to sensitize KRAS G12C mutant tumors to covalent KRASG12Ci that are only binding to the GDP-KRAS form. Indeed, combination treatment of SOS1::KRASi+KRASG12Ci led to a synergistic anti-proliferative effect in vitro, enhanced MAPK pathway modulation and apoptosis induction as well as blockade of adaptive feedback relief. Testing the SOS1::KRASi+KRASG12Ci combination in CDX and PDX models demonstrated enhanced efficacy in combination compared to both mono-therapies and the observed response was more durable and well tolerated.

Our results highlight SOS1::KRAS inhibitors as a combination backbone that has the potential to augment the anti-tumor effect of KRASG12C inhibitors by vertical pathway inhibition.

Conflict of interest:

Corporate-sponsored Research: MDAnderson is in a collaboration agreement with Boehringer Ingelheim.
Other Substantive Relationships: Employees of Boehringer Ingelheim: Fabio Savarese, Michael Gmachl, Francesca Trapani, Daniel Gerlach, Dorothea Rudolph, Irene Waizenegger, Jürgen Ramharther, Mark Petronczki, Darryl McConnell, Norbert Kraut, Marco H. Hofmann.
Co-inventors on patents for SOS1 inhibitors: Fabio Savarese, Michael Gmachl, Dorothea Rudolph, Jürgen Ramharther and Marco H. Hofmann.

52

Poster Discussion

CHD-loss promotes tumor heterogeneity, lineage plasticity and resistance to AR targeted therapy resistance

P. Mu¹. ¹UT Southwestern Medical Center, Molecular Biology, Dallas, USA

Background: Pharmacological targeting of driver alterations in cancer has resulted in many clinical successes but is limited by concurrent or novel genomic alterations. One potential explanation for this heterogeneity is the presence of additional genomic alterations which modify the degree of dependence on the targeted driver mutation. Metastatic prostate cancer (mPCa) serves as a relevant example, where the molecular target is the androgen receptor (AR) which functions as a lineage survival factor of luminal prostate epithelial cells. Next generation AR therapies such as abiraterone, enzalutamide and apalutamide have significantly improved survival of men with mPCa, but resistance remains an issue.

Methods: To gain functional insight into the genes impacted by the copy number alterations in mPCa, we screened 4234 short hairpin RNAs (shRNAs) targeting 730 genes often deleted in human prostate cancer (the prostate cancer deletome) for hairpins that confer *in vivo* resistance to the antiandrogen enzalutamide.

Results: The chromodomain helicase DNA-binding protein 1 (*CHD1*) emerged as a top candidate, a finding supported by patient data showing that *CHD1* expression is inversely correlated with clinical benefit from next generation antiandrogen therapy. *CHD1* loss led to global changes in open and closed chromatin, indicative of an altered chromatin state, with associated changes in gene expression. Integrative analysis of ATAC- and RNA-seq changes identified 22 transcription factors as candidate drivers of enzalutamide resistance. CRISPR deletion of four of these (*NR3C1*, *BRN2*,

NR2F1, *TBX2*) restored in vitro enzalutamide sensitivity in *CHD1* deleted cells. Independently derived, enzalutamide-resistant, *CHD1*-deleted subclones expressed elevated levels of 1 or more of these 4 transcription factors. This pattern suggests a state of chromatin plasticity and enhanced heterogeneity, initiated by *CHD1* loss, which enables upregulation of distinct sets of genes in response to selective pressure. This concept is further supported by RNA-seq data from a mCRPC patients cohort, in which we examined the co-association of *CHD1* levels with each of these four TFs across 212 tumors. Furthermore, we observed increased lineage plasticity in most of the resistant tumors driven by heterogeneous resistant driver genes, including the downregulation of luminal lineage transcriptional program and upregulation of genes specify epithelial to mesenchymal transition (EMT).

Conclusions: We demonstrated that loss of the chromodomain gene *CHD1*, a commonly deleted prostate cancer gene, through global effects on chromatin, establishes a state of plasticity that accelerates the development of hormone therapy resistance through heterogeneous activation of downstream effectors.

No conflict of interest.

53

Poster Discussion

Metabolic modulation combined with mTOR pathway inhibition may overcome cutaneous melanoma resistance to MAPK inhibitors treatment

C. Sampaio¹, B. Domingues¹, P. Soares^{1,2}, J. M. Lopes^{1,2,3}, H. Pópulo^{1,2}.
¹IPATIMUP/3S, Cancer signalling and metabolism group, Porto, Portugal;
²Medical Faculty- University of Porto, Department of Pathology and Oncology, Porto, Portugal; ³Hospital São João, Department of Pathology, Porto, Portugal

Background: Cutaneous melanoma is a very aggressive malignancy, and despite being the least common type of skin cancer, it is responsible for most skin cancer-related deaths. Several therapies have been approved by Food and Drug Administration (FDA), namely selective inhibitors of the MAPK pathway and immunotherapy. However, available therapies still have limitations, due to rapidly acquirement of resistance to the first and the adverse effects associated with the latter, resulting in a high mortality rate from metastatic disease. Recently, FDA also approved the combination of two MAPK inhibitors, BRAF and MEK inhibitors, for the treatment of melanomas harbouring *BRAF* mutations, which cannot be surgically removed or display metastization, however acquirement of resistance continues to occur. Therefore, there is a need to develop therapeutic modalities to achieve more efficient melanoma therapies that improve survival of melanoma patients.

As the mechanisms of resistance to MAPK pathway inhibitors, which occur frequently in *BRAF*^{V600E} melanoma patients, may be related with the deregulation of PI3K/AKT/mTOR pathway and the presence of the Warburg effect in melanoma cells, we hypothesize that the metabolic modulator DCA and mTOR inhibition, can be promising new therapies for melanoma patients.

Material and methods: We assessed the expression of DCA targets and mTOR pathway effectors in cutaneous melanoma samples. We evaluated the effect of DCA treatment and mTOR inhibition, alone or in combination, in vemurafenib sensitive and resistant melanoma cell lines viability, proliferation and apoptosis, comparing with the effect of approved therapeutics.

Results: We detected DCA targets expression in cutaneous melanoma samples, associated with the expression of the mTOR pathway effectors. Melanoma cell lines treated with DCA or everolimus showed a down-regulation of proliferation and an increase of apoptosis. The mTOR pathway inhibitor seems to have effects on melanoma cell dynamics that were potentiated when combined with DCA treatment. The *BRAF*^{V600E} -vemurafenib resistant melanoma cell line showed to retain sensitive to both DCA and everolimus.

Conclusions: Our results suggest that combined metabolism modulation with inhibition of mTOR pathway may constitute possible strategies in order to overcome resistance to MAPK inhibition.

Funding was obtained from the project "Advancing cancer research: from basic knowledge to the project "NORTE-01-0145-FEDER-000029; "Projetos Estruturados de I&D+i," funded by Norte 2020 – Programa Operacional Regional do Norte.

No conflict of interest.

Sunday, 25 October 2020

14:30–15:30

POSTER DISCUSSION SESSION

Next Generation Targeted Therapies B

54

Poster Discussion

The integrated stress response exposes a therapeutic vulnerability in KRAS driven lung cancer

N. Ghaddar¹, S. Wang², B. Woodvine³, J. Krishnamoorthy², C. Darini², V. Van Hoef⁴, H. Popper⁵, I. Topisirovic⁶, O. Larsson⁴, J. Le Quesne³, A. Koromilas⁶.
¹McGill University, Experimental Medicine, Montreal, Canada; ²Lady Davis Institute, Oncology, Montreal, Canada; ³University of Leicester, Leicester Cancer Research Centre, Leicester, United Kingdom; ⁴Karolinska Institute, Department of Oncology-Pathology- Science for Life Laboratory, Stockholm, Sweden; ⁵Medical University of Graz, Diagnostik and Research Institute of Pathology, Graz, Austria; ⁶McGill University, Oncology, Montreal, Canada

Background: Mutations in *KRAS* account for ~25% of lung cancer cases and are refractory to therapy. Tumors with *KRAS* mutations encounter increased levels of genotoxic, proteotoxic and metabolic stress, which disrupt proliferation and homeostasis. The Integrated Stress Response (ISR) plays a key role in adaptation to stress via phosphorylation of eukaryotic initiation factor 2 (p-eIF2). When ISR is activated, p-eIF2 mediates translational and transcriptional reprogramming of genes with roles in survival and adaptation. Here we demonstrate the importance of ISR in the development of *KRAS* lung adenocarcinoma (LUAD), the most common histological type of lung cancer and a leading cause of cancer death worldwide.

Materials and Methods: We analyzed tissue microarrays (TMAs) of 928 patients with lung adenocarcinoma to investigate a prognostic value of p-eIF2 in lung adenocarcinoma. To verify our findings, we induced the formation of lung tumors in *KRAS* G12D (flx/flx) mice that were either wild-type or have a conditional knock-in mutation of p-eIF2α. We monitored lung tumor formation by ultrasound imaging and dissected the underlying molecular mechanisms by immunohistochemical analysis of lung sections from these mice. Primary cell lines were also established for the analysis of the signaling properties of activated *KRAS* and the translational effects of p-eIF2. In addition, we used a pre-clinical model to determine the effects of pharmacological disruption of ISR in *KRAS* lung tumor growth.

Results: Analysis of 928 lung adenocarcinoma patients showed that increased p-eIF2 associates with a significant decrease in overall survival by ~12 months. These findings underscore the prognostic significance of ISR in the development and treatment of human lung adenocarcinoma. In mouse models of *KRAS*-driven lung cancer, we demonstrate the pro-tumorigenic function of ISR via its ability to stimulate phosphorylation of mitogen activated kinase ERK. Mechanistically, we show that increased p-eIF2 translationally represses dual specificity phosphatase DUSP6, which antagonizes ERK phosphorylation. In addition to discovering an important mechanism of *KRAS*-driven lung cancer, our work demonstrates that pharmacological ISR inactivation is highly effective for treatment of *KRAS* lung cancer in mice. That is, ISR disruption by inactivating the translational effects of p-eIF2 by the ISR inhibitor (ISRIB) substantially reduces lung tumor growth in mice and prolong their survival. ISR inhibition is equally effective to inhibition of lung tumors by AMG-510, a potent and specific inhibitor of *KRAS* G12C.

Conclusion: The significance of our data is highlighted by the ability of ISR inhibitors to impair lung tumor growth with different *KRAS* mutations. Our findings provide a novel rationale for implementing ISR-based regimens in lung adenocarcinoma treatment.

No conflict of interest.

55

Poster Discussion

An allosteric modulator of PRC2 methyltransferase activity inhibits renal cancer cell proliferation

G. Gerona-Navarro¹, G. Zhang¹, F. Barragan¹, B. Elie¹, K. Wilson¹, A. Herskovits¹, Y. Rodriguez², M. Cornejo¹.
¹Brooklyn College of CUNY, Chemistry, New York, USA; ²Hostos Community College, Natural Sciences, New York, USA

Cancer is a genetic disease, but its development also involves multiple epigenetic alterations. Epigenetics regulates transcription by modulating chromatin architecture through different mechanisms. Hence, dysregulation of such mechanisms can result in aberrant gene expression or silencing,

which in turn can lead to carcinogenesis. One of the most relevant epigenetic modifications is the methylation of lysine 27 at histone 3 (H3K27), a broadly known repressive histone mark. H3K27 methylation is incorporated by the polycomb repressive complex 2 (PRC2), a multimeric protein complex formed by four core components: EZH2, EED, SUZ12 and RbAp46/48, all of which are essential for its catalytic activity. Overexpression of PRC2 proteins, particularly of EZH2, results in hyperactivation of the complex and high levels of H3K27me3, which are associated to a myriad of human cancers. Hence, the discovery of PRC2 inhibitors is an area of active research for both the pharmaceutical industry and academic laboratories. The relevance of such compounds is highlighted by the recent accelerated approval of the first in class EZH2 inhibitor (tazemetostat, Epizyme), for the treatment of metastatic or locally advanced epithelioid sarcoma. Here, we describe the design, synthesis and biological evaluation of a new family of stapled peptides as inhibitors of PRC2 methyltransferase activity, designed to target the intramolecular SANT1L-SBD interaction in EZH2. Our lead cyclopeptide showed potent inhibition of H3K27 trimethylation in both *in vitro* and cellular assays, demonstrating that it is cell permeable and active in physiological conditions. Its inhibition of PRC2 catalytic activity produced a marked dose-dependent antiproliferative effect in metastatic Caki-1 cells. Notably, in these experiments our compound was almost as effective as GSK126, a well-known orthosteric EZH2 inhibitor. We further present compelling evidences suggesting that our stapled peptide targets selectively PRC2, and more specifically, its catalytic subunit EZH2 in an allosteric fashion. To our knowledge, this bithioether stapled peptide may well be the first example of such allosteric EZH2 inhibitors described to date. This class of compounds could be extremely valuable in addressing the resistance profiles recently reported in clinical trials with EZH2-SET domain inhibitors, in which extended dosing of these drugs have led to secondary EZH2 mutants resistant to treatment. Our compound's unique mechanism of PRC2 inhibition, together with its potency, remarkable H3K27me3 inhibition selectivity, and low cytotoxicity to non-cancerous cells demonstrate this stapled peptide's potential for future development of novel epigenetic cancer therapies.

Table 1. Structure and Biological Activity of Lead Cyclopeptide.

| Sequence. | Linker. | Helicity (%) | IC ₅₀ (mM). |
|--|---|--------------|------------------------|
| Ac-TVD[CIASC] LSVLAEVPPQN- CONH ₂ . | CH ₂ CH ₂ CH ₂ . | 23. | 0.17 ± 0.02. |

No conflict of interest.

56

Poster Discussion

Theranostic ⁶⁴Cu-DOTHA₂-PSMA for metastatic prostate cancer treatment, a preclinical study

M.C. Milot¹, O. Béliassant Benesty¹, V. Dumulon-Perreault², S. Ait-Mohand¹, É. Rousseau¹, P. Richard³, B. Guérin¹. ¹Université de Sherbrooke, Nuclear Medicine and Radiobiology, Sherbrooke, Canada; ²CRCHUS, Centre d'imagerie moléculaire de Sherbrooke, Sherbrooke, Canada; ³Université de Sherbrooke, Surgery, Sherbrooke, Canada

Background: Metastatic prostate cancer (PC)'s treatment by ¹⁷⁷Lu-PSMA-617 targeting prostate specific membrane antigen (PSMA) is currently showing interesting potential in clinical research. We developed a new PSMA radioligand, ⁶⁴Cu-DOTHA₂-PSMA that is stable *in vivo*, uses a locally produced radioisotope (in opposition to ¹⁷⁷Lu), and shows an advantageous biodistribution with an especially low uptake in kidneys 1 h post-injection (p.i.). Based on the unique decay characteristics of ⁶⁴Cu (T_{1/2} 12.7 h; β⁺ 0.65 MeV [17.8%]; β⁻ 0.58 MeV [38.4%]; Auger electrons [40%]), our hypothesis is that our radioligand will be more cytotoxic than ¹⁷⁷Lu-PSMA-617 for PC. The aim of this preclinical study is to evaluate ⁶⁴Cu-DOTHA₂-PSMA's potential for PC treatment.

Methods: Optimal injected activity (IA) for animals was assessed by comparing a single injection of ⁶⁴Cu-DOTHA₂-PSMA (70, 120 or 150 MBq IV) based on a 21-days follow-up of NRG mice (n = 6). Survival experiments on NRG LNCaP tumor-bearing mice injected with a single dose of the determined optimal IA of ⁶⁴Cu-DOTHA₂-PSMA, the same molar amount of the non-radioactive control (^{nat}Cu-DOTHA₂-PSMA), or 120 MBq of ¹⁷⁷Lu-PSMA-617 (optimal IA according to literature) were performed. The animals were followed up to 62-days post-injection. Overall survival of PC-bearing animals were estimated by the Kaplan-Meier method and compared with log-rank test (Mantel-Cox). Animals that had reached endpoints (1 cm tumor diameter, tumor ulceration, 20% weight loss or pain) were euthanized and organs and fluid were collected for future toxicity studies.

Results: The optimal IA was 150 MBq. Mice treated with 150 MBq of ⁶⁴Cu-DOTHA₂-PSMA presented a significantly longer survival (p < 0.0001) than

controls. Although their survival was also longer than ¹⁷⁷Lu-PSMA-617 treated mice the difference was non statistically significant (p = 0.09). All ⁶⁴Cu-DOTHA₂-PSMA treated mice (n = 8) experienced transient weight loss. Six of them were euthanized after reaching tumor size endpoint and 1 for pain behaviour at 60 days p.i. and the remaining one survived up to 62 days p.i.

Conclusions: ⁶⁴Cu-DOTHA₂-PSMA offers therapeutic potential for PC lesions. Its therapeutic capacity is comparable to the clinically studied ¹⁷⁷Lu-PSMA-617, thus it encourages future translation towards clinic to improve patient survival. Our next steps will be toxicity and dosimetry assays.

No conflict of interest.

57

Poster Discussion

Identification of physiologically relevant EWS-FLI1 target genes in Ewing sarcoma via CRISPRa screening

V. Saratov¹, Q. Ngo¹, G. Pedot¹, B. Schäfer¹. ¹University Children's Hospital of Zurich, Oncology, Zurich, Switzerland

Background: Ewing sarcoma is an aggressive pediatric bone and soft tissue cancer with a pathognomonic chromosomal translocation t(11;22) resulting in expression of EWS-FLI1, an "undruggable" fusion protein acting as a transcriptional modulator. Identification and ranking of repressed EWS-FLI1 target genes essential for cancer cell survival will potentially provide much-needed insights to develop novel therapeutic strategies.

Materials and methods: We performed a CRISPR activation (CRISPRa) dropout screen in Ewing cells. We generated a clonal SKNMC cell line homogeneously expressing the synergistic activation mediator (SAM) CRISPRa system to functionally interrogate repressed EWS-FLI1 target genes. The systems functionality was tested using CD44, a surface marker absent on the surface of Ewing cells. We found robust and stable expression of CD44 after introduction of promoter targeting gRNAs.

The library of repressed EWS-FLI1 target genes, named LIBerty, was constructed to target 872 genes bioinformatically selected from publicly available silenced EWS-FLI1 RNA-Seq datasets as well as genes identified as repressed signature genes in Ewing's sarcoma via meta-analysis with 3777 unique gRNAs. LIBerty was lentivirally delivered into SAM SKNMC cells and data from four biological replicates was gathered at three time points: three, ten and 21 days after infection. Cells were harvested and samples were prepared for next generation sequencing (NGS) via PCR. The NGS data was evaluated with the analysis tool PinAPL-Py.

Results: Preliminary analysis of the screen revealed efficient selection of the positive control genes BAD and BBC3. In addition, high-ranking hits included CDKN1A and CDKN1C, both cell cycle regulators and known tumor suppressor genes. Furthermore, we identified PCDH7 and TGFBR2, two genes already known from the literature to play a role in Ewing's sarcoma. The presence of validated genes amid highest-ranking candidates confirms robustness of the conducted CRISPRa screen. Further analysis and validation of previously unexplored targets and pathways is currently ongoing.

Conclusions: Our CRISPRa screen revealed both known as well as previously unknown EWS-FLI1 repressed genes whose absence of function is essential for tumor cell survival.

No conflict of interest.

58

Poster Discussion

Combined SHP2 and MEK inhibition is effective in models of NF1-deficient malignant peripheral nerve sheath tumors

J. Wang¹, K. Pollard¹, A. Allen¹, T. Tomar², D. Pijnenburg², Z. Yao³, F. Rodriguez⁴, C. Pratilas¹. ¹Johns Hopkins University School of Medicine, Oncology, Baltimore, USA; ²PamGene International BV, PamGene International BV, 's-Hertogenbosch, Netherlands; ³Memorial Sloan Kettering Cancer Center, Program in Molecular Pharmacology, New York, USA; ⁴Johns Hopkins University School of Medicine, Pathology, Baltimore, USA

Background: Loss of the RAS GTPase-activating protein (RAS-GAP) NF1 drives aberrant activation of RAS/MEK/ERK signaling in the majority of malignant peripheral nerve sheath tumors (MPNST). These dysregulated pathways represent potential targets for therapeutic intervention. Studies of novel single agents, including MEK inhibitors (MEKi), however, have demonstrated limited efficacy both preclinically and clinically, with little advancement in overall patient survival. Novel therapeutic approaches are an urgent need.

Material and methods: We identified the mechanisms underlying adaptive resistance to MEKi through unbiased kinase activity profiling, and evaluated signaling and biological responses to MEK inhibition, SHP2

inhibition and their combination *in vitro* and *in vivo* using biochemical and functional assays.

Results: We have identified global activation of upstream receptor tyrosine kinases (RTK) that converges on activation of RAS, as a mechanism limiting the sensitivity to MEK inhibition. The combination of MEKi plus SHP099, an inhibitor of the protein tyrosine phosphatase SHP2 that is a critical mediator of signal transduction downstream of multiple RTK, was superior to MEKi alone in models of NF1-deficient MPNST, including those with acquired resistance to MEKi.

Conclusions: Our findings demonstrate that combined SHP2 and MEK inhibition is effective in models of NF1-deficient MPNST, both those naïve to and those resistant to MEKi, as well as in the MPNST precursor lesion – plexiform neurofibroma. This work has immediate translational implications and may inform future clinical trials for patients with MPNST harboring *NF1* alterations.

Conflict of interest:

Other Substantive Relationships: T.T. and D.P. are employed by PamGene International B.V. C.A.P. is a paid consultant for Genentech/ Roche. The remaining authors have declared that no conflicts of interests exist.

59

Poster Discussion

NLS designed algorithm to develop peptides with a net-neutral charge as potential next-generation vectors for drug delivery to the nucleus

A. Rioux-Chevalier¹, V.J. Leyton². ¹Sherbrooke University- Medecine and Health Sciences Faculty, Nuclear Medecine and Radiobiology Department, Sherbrooke, Canada; ²Centre d'imagerie moléculaire de Sherbrooke and Sherbrooke University- Medecine and Health Sciences Faculty, Nuclear Medecine and Radiobiology Department, Sherbrooke, Canada

Background: Active import of proteins in the nucleus is primarily determined by the recognition and binding of nuclear localization signals (NLSs) contained in cargo proteins with specific NLS receptors known as importins. Typically, cargo proteins are bound by the adaptor protein importin- α . Importin- β then binds importin- α and the complex is transported and docks at the nuclear pore complex where the cargo is released into the nucleus. As a result, there is great effort to develop NLS-tagged vectors for numerous therapeutic applications that involve maximizing effectiveness via localization inside the nucleus. Despite these efforts, efficient nuclear localization has been difficult.

In our previous work, we developed a peptide containing the classical NLS from SV40 large T-antigen linked to cholic acid. When the peptide was attached to antibody-drug conjugates (ADCs), cholic acid mediated endosome escape via activation of the sphingomyelin-ceramide pathway. This resulted in efficient nuclear localization and enhanced cytotoxicity *in vitro*. However, NLS peptides are highly positively charged and resulted in non-specific sequestration of modified ADCs in healthy organs, rapid elimination from the blood, and reduced their tumor uptake and killing.

Material and methods: We developed a novel and robust NLS design algorithm to identify peptides with a net-neutral charge but that retained high binding affinity for importin- α . PDB files were selected as templates that contained structures of human importin- α 1 or its mouse homolog (99.4% identical sequence) bound to various protein cargoes. The algorithm performed alanine scanning with Molecular Operating Environment (MOE) software to identify essential residues in the NLS that could not be mutated. A subsequent residue scan was performed on all non-essential residues. The inventory of all generated peptides were then evaluated by MOE docking studies to generate a predictive binding score distribution. Finally, a thorough statistical analysis was performed to assess if the binding behavior of a given mutant was significantly different from its corresponding wild type. The peptides were then modeled in MOE to identify interactions with amino acid side chains in the NLS binding pockets.

Results: Several similar affinity-predicted mutant peptides were generated for each PDB file indicating our NLS design algorithm was highly robust. The major characteristics of the generated peptides when focused on net-neutral charge were that i) rotamer flexibility of mutated amino acids allowed for large number of generated peptides and ii) it is possible to mutate some of the residues from consensus NLS basic clusters.

Conclusions: We were able to establish an *in silico* methodological route for the development of strong candidate NLS peptides for the future modification and testing of therapeutic agents active in the nucleus.

No conflict of interest.

POSTER SESSION

Angiogenesis and Vascular Disrupting Agents

100

Poster

Evaluation of surufatinib, an orally available VEGFR, FGFR1 and CSF-1R inhibitor, in combination with immune checkpoint blockade or chemotherapy in preclinical tumor models

M. Cheng¹, S. Fan¹, R. Tang¹, W. Zhang¹, J. Hu¹, J. Yu¹, D. Shi¹, C. Wang¹, L. Wang¹, W. Qing¹, Y. Ren¹, W. Su¹. ¹Hutchison MediPharma Ltd., Translational Medicine, Shanghai, China

Background: Surufatinib (sulfatinib, HMPL-012) is a small molecule inhibitor targeting VEGFR 1/2/3, FGFR1 and CSF-1R tyrosine kinases. In two randomized, double-blind phase III studies (NCT02589821 and NCT02588170), surufatinib showed a significant PFS benefit in patients with advanced neuroendocrine tumors originating from pancreas or extra-pancreas. Given tumor heterogeneity and complexity, monotherapies or single signaling pathway inhibition often fails to induce durable clinical benefit or prevent development of drug resistance, so that exploration of combinations of multiple mechanisms emerges as the trend of cancer treatment. Here, we reported preclinical anti-tumor effect of surufatinib in combination with clinical standard therapies in varied indications.

Material and methods: The combination of surufatinib with PD-1 blockade in murine syngeneic breast cancer and colon cancer models, and with chemotherapy in multiple human tumor xenograft models including sarcoma, lung and colon cancer were explored. Tumor volume was measured to calculate tumor growth inhibition and animal survival extension. Tumor microenvironments were analyzed with flowcytometry and histopathology technology.

Results: In MC-38 murine syngeneic colon cancer, combination of surufatinib and anti-PD-1 antibody yielded a higher tumor growth inhibition with statistical significance compared with either of single-agent treatment. The analysis of tumor microenvironments demonstrated combination treatment increased tumor infiltration of CD8⁺ T cells, markedly decreased TAMs as well as suppressed angiogenesis marker CD31 expression, suggesting that the improved anti-tumor effect might be ascribed to inhibition of multiple cell types or multiple pathways. The combinational effect of surufatinib and PD-1 blockade was also observed in murine breast cancer EMT-6 model. Furthermore, surufatinib enhanced anti-tumor activities of chemo-drugs in multiple human xenograft models including in combination with paclitaxel in lung cancer, with 5-FU or CPT-11 in colon cancer, with gemcitabine in sarcoma as well. The research of the underlying mechanisms of action is ongoing.

Conclusions: Surufatinib improved anti-tumor activities of PD-1 blockade or chemotherapy in preclinical tumor models. Further investigation of combination therapies in clinical trials was warranted.

No conflict of interest.

101

Poster

Derazantinib, an oral fibroblast growth factor receptor inhibitor, in phase-2 clinical development, shows anti-angiogenic activity in pre-clinical models

P. Mcsheehy¹, J. Boulton², S. Robinson², F. Bachmann¹, M. El Shemery¹, L. Kellenberger¹, H. Lane¹. ¹Basilea Pharmaceutica International Ltd, Cancer Biology, Basel, Switzerland; ²The Institute of Cancer Research-London- UK, Division of Radiotherapy & Imaging, London, United Kingdom

Background: Derazantinib (DZB) is a fibroblast growth factor receptor inhibitor (FGFRi) with clinical activity in FGFR2-fusion intrahepatic cholangiocarcinoma. Biochemical kinase assays indicate potential activity against other important targets in oncology, including CSF1R and VEGFR2. We have recently shown that DZB can inhibit phosphorylation of CSF1R upon ligand stimulation in mouse macrophages *ex vivo* (GI50 = 100 nM); a concentration readily achievable in mouse tissues (<500 nM) at tolerable doses. To explore the potential of VEGFR2 as a target, a range of *in vitro* and *in vivo* assays were utilized.

Materials and Methods: Human umbilical vein endothelial cells (HUVECs) were cultured to 50% confluence and incubated with DZB for 72 h to determine the GI50, and for 2 h to assess effects on cell-signaling by Westernblot. A Miles assay was performed in normal mice by measuring leakage of Evans Blue (EB) into skin, 3 h after *i.v.* injection of EB (40 mg/kg) and 0.5 h after *i.d.* injection of VEGF (20 ng/0.1 mL). The effect of different

doses of DZB, and a positive-control (vatalanib, 50 mg/kg, bid) were assessed after 24–72 h of treatment. Susceptibility-contrast magnetic resonance imaging (SC-MRI), using an intravascular USPIO contrast agent was used to non-invasively quantify R_2^* (sensitive to hemodynamic vasculature) and fractional blood volume (fBV) in SW620 colon cancer xenografts grown subcutaneously in athymic mice. SC-MRI was performed prior to and 48 h after treatment with DZB (75 mg/kg, qd) or vatalanib (50 mg/kg, bid), following which the perfusion marker Hoechst 33342 was injected i.v., and histological analysis of tumor vasculature, blood vessel density (BVD) and necrosis subsequently performed.

Results: DZB inhibited HUVEC proliferation ($GI_{50} = 400$ nM) and at similar concentrations reduced MEK and VEGFR phosphorylation. In the Miles assay, time-dependent studies showed that a 24 h period was more sensitive to the effects of DZB and vatalanib than 48/72 h. At 24 h, DZB dose-dependently (25–100 mg/kg, qd) decreased EB permeability with the standard efficacious dose of 75 mg/kg causing a mean reduction of 58%; in comparison, vatalanib caused an 88% reduction (both $p < 0.001$ versus vehicle; one-way ANOVA). SC-MRI revealed no change in R_2^* or fBV of tumors in vehicle-treated mice over 48 h, but was reduced 36–40% by DZB and vatalanib ($p < 0.01$ and $p = 0.05$ respectively, 2-way repeated-measures ANOVA).

Conclusions: The effects of DZB on HUVEC proliferation, EB permeability, R_2^* and fBV are consistent with an anti-angiogenic component to the compound's mechanism of action that may facilitate clinical activity against some solid tumors.

Conflict of interest:

Ownership: Employee of Basilea and share-holder.

102

Poster

The antiangiogenic effect of the metronomic combination of 5-Fluorouracil plus vinorelbine is mediated by FAK/AKT pathway downregulation and apoptosis activation

A. Scagliotti¹, E. Grassilli¹, M.E. Cazzaniga², L. Capizzi¹, M. Lavitrano¹, M.G. Cerrito¹. ¹University of Milano-Bicocca, School of Medicine and Surgery, Monza, Italy; ²Phase 1 Research Centre, University of Milano-Bicocca, Monza, Italy

Background: Angiogenesis is a crucial step for tumor growth and metastasis propagation. Many antiangiogenic drugs have been developed but have shown limited efficacy in the clinical setting, due to the restoration of damaged tumor vasculature during the rest periods imposed by the standard-of-care schedule of chemotherapy (STD). The administration of continuous low doses of chemotherapeutic drugs without drug-free breaks, defined as metronomic treatment (MET), revealed an antiangiogenic effect of some antitumoral agents. In this study, we investigated the antiangiogenic properties of the metronomic combination of 5-Fluorouracil (5-FU) + Vinorelbine (VNR) in comparison to the STD administration.

Materials and methods: We investigated the effect of STD and MET administration of 5-FU+VNR on HUVECs viability by MTT. Then, we evaluated cell migration and tube formation to explore the neoangiogenic capacity of HUVECs after STD and MET treatment. Molecular mechanisms involved in response to the two different modalities of treatments were analyzed by Western blot.

Results: MET 5-FU+VNR affects HUVECs viability at doses significantly lower compared to the STD ones, with an IC_{50} of $4.5 \mu M + 0.5 nM$ vs. $80 \mu M + 30 nM$ of the STD treatment. STD and overall MET administration of 5-FU+VNR strongly reduce HUVECs migration, but only the MET schedule impairs HUVECs tube formation capacity, which is halved compared to the untreated control. Both STD and MET administration of 5-FU+VNR inhibit the FAK/AKT pathway resulting in the downregulation of VEGF and VEGFR2 expression, while only the MET treatment induces caspase-3 cleavage, indicating the occurrence apoptotic cell death.

Conclusions: Metronomic administration of 5-FU+VNR inhibits neoangiogenesis by blocking the FAK/AKT proangiogenic signaling pathway and activating apoptosis. Our results confirm the multitarget action of the metronomic schedule and indicate that administering the combination of 5-FU+VNR metronomically can target not only tumor cells but also tumor neoangiogenesis.

No conflict of interest.

POSTER SESSION

Animal Models

103

Poster

Annona senegalensis extract demonstrates anticancer properties in N-diethylnitrosamine induced hepatocellular carcinoma in male wistar rats

O. Yakubu¹, O. Metibemu², I. Adelani¹, G. Adesina¹, C. Edokwe¹, O. Oseha¹, A. Adebayo¹. ¹Covenant University, Biochemistry Department, Ota, Nigeria; ²Adekunle Ajasin University- Akungba-Akoko, Ondo State-Nigeria, Biochemistry, Akungba-Akoko, Nigeria

Background: Hepatocellular carcinoma (HCC) is a common and leading cancer around the globe. This study investigated the anticancer properties of the extract of *Annona senegalensis* in N-diethylnitrosamine (DEN) - induced hepatocarcinoma in male Wistar rats.

Methods: Rats were simultaneously induced with a combination of 100 mg/kg b.wt of DEN and 0.5 mL/kg of carbon tetrachloride (CCl_4) intraperitoneally, once a week for three weeks in a row. Animals were thereafter treated with 100 mg/kg and 200 mg/kg b.wt of *A. senegalensis* extract daily for 21 days. Analysis using gas chromatography-mass spectrometry (GC-MS) was carried out to discover the phytoconstituents contained in the n-hexane extract of *A. senegalensis*. The levels of liver function parameters and antioxidant enzyme activities were determined via spectrophotometric analysis. Reverse transcriptase-polymerase chain reaction technique was used to assess the gene expression patterns of BCL-2, P53, P21, IL-6, FNTA, VEGF, HIF, AFP, XIAP, and EGFR mRNAs.

Results: Treatment of DEN-induced hepatocellular carcinoma Wistar rats with the extract caused significant ($p < 0.05$) decrease in the activities of ALT and AST. It also resulted in a decrease in the concentration of MDA and a significant increase in SOD and GSH activities. IL-6, BCL-2, VEGF, EGFR, XIAP, FNTA, and P21 mRNAs expressions were significantly ($P < 0.05$) downregulated after treatment. Histopathological analysis revealed that the extract improved the liver architecture.

Conclusion: *A. senegalensis* n-hexane extract demonstrates its anticancer properties by improving the liver architecture, increasing the antioxidant defense systems, downregulating the pro-inflammatory, anti-apoptotic, angiogenic, alpha-fetoprotein and farnesyl transferase mRNAs expression and hitherto up-regulate the expression of tumor suppressor (P21 and P53) mRNAs.

No conflict of interest.

104

Poster

Genetically characterizing spontaneously-occurring cancer in canines to serve as a model for human studies

B. Lewis¹. ¹One Health Company, Research, Palo Alto, USA

Background: One of the root-causes of late-stage clinical failures is non-predictive animal models, which inadequately identify shortcomings in safety and efficacy. While induced-disease models are necessary for research and discovery it is hubris to believe that our understanding of cancer is comprehensive enough to accurately and precisely induce disease in otherwise healthy animals. The next logical fallacy, demonstrated by decades of data, is that artificial ailments in animals are predictive of actual disease in humans. Conversely, naturally-sick animals in the pet population provide a fascinating opportunity to investigate cancer therapies. Specifically, pet dogs share many of the cancer histologies and underlying mutations as their owners and present an interesting opportunity to evaluate novel therapies and combinations of therapies. Outcomes assessed can include safety and tolerability as well as efficacy. The spontaneously sick dog presents a unique learning space for the biopharma space.

Materials and Methods: Canine cancer patients were recruited from 287 veterinary hospitals nationwide. Over 200 veterinary oncologists enrolled patients in the FidoCure Precision Medicine Platform. Each patient was identically characterized: histopathology by a Board-certified veterinary pathologist and genomically using an NGS panel run in a CAP/CLIA lab. Beneficially, all the veterinary specialists keep electronic medical records and veterinary medicine is not encumbered by HIPAA regulations, so access to clinical outcomes and adverse events reporting was straightforward. Each

veterinarian electronically consented to share patient data. Drug recommendations were based on biomarker data from DNA sequencing.

Results: Our study accrued over 700 patients in 1.5 years. Each patient was confirmed to have cancer and molecularly characterized. As of this writing, we have 455 patients on targeted therapies (the APIs of FDA-approved human drugs) and follow up on 390 of those patients. The remaining 250 patients opted solely for traditional standards of care treatment.

The 5 most common tumor types evaluated were hemangiosarcoma (human angiosarcoma), bladder cancer, Mast Cell Tumor (similar mutational profile to GIST), osteosarcoma, and melanoma. The 5 most common mutations seen in the dogs were KMT2C, ROS1, p53, BRCA1, and BRCA2.

Conclusion: Dogs and Humans share similar cancer types and underlying mutations. Only the naturally sick canine has all the qualities of a good animal model, including relevant tumor histologies, intact immune system (particularly for IO), intact tumor microenvironment, large numbers (6 million dogs diagnosed with cancer each year), existing network of veterinary oncologists to treat and assess outcomes. This abstract should serve as the basis for additional studies.

Conflict of interest:

Ownership: One Health Company.

Board of Directors: One Health Company.

POSTER SESSION

Antibody-drug Conjugates

105

Poster

An advanced in silico drug discovery platform, 4HF Data Miner for identifying novel targets for tumors and tumor-stroma

S. Das¹, V. Vuaroqueaux¹, H. Al-Hasani¹, A.L. Peille¹, A. Musch¹, R. Dixit², H.H. Fiebig³. ¹4HF Biotech GmbH, Research & Development, Freiburg im Breisgau, Germany; ²Bionavigen, CEO & Founder, 24211 Primula Ct.-Gaithersburg-Maryland 20882., USA; ³4HF Biotech GmbH, CEO & Founder, Freiburg im Breisgau, Germany

Background: For treatment of cancer patients, the emergence of the Antibody-Drug Conjugates (ADCs) has offered a novel approach of combining the oncolytic activity of highly potent chemotherapy agents with the target specificity of an antibody. Over the past three decades, profound advancements have been made in the development of the next generation of ADCs. The latest generation ADCs consist of non-immunogenic mAbs, linkers with enhanced stability, and diverse cytotoxic agents display enhanced compatibility for clinical use. A number of clinical trials have already demonstrated promising results with the latest generation ADCs. Concomitantly, the number of registered compounds is growing with 8 ADCs that have been approved by the FDA.

Materials & Method: 4HF Biotech has established a unified *in silico* platform integrating large OMICS and drug sensitivity datasets for cancer data mining. Data are continuously collected from diverse sources and connected with their in-house proprietary data. 4HF has developed a specific software that enables simultaneous visualization of target gene expression in a wide range of tumors and normal tissues comprising 40000 samples. The tumor models enable us to visualize the tumor-specific targets while patient tumors display the integrative expression contributed by both the tumor and tumor-stroma. Data-driven approaches and knowledge-based approaches are implemented in combination to determine potential targets.

Results: To this end, as a *proof-of-concept*, we investigated several ADC targets that are present either in the tumor or in the tumor stroma. The following examples are presented for the tumor cell targets (approved: CD79b, CD33, Phase II/III: CD19, gpNMB) and stromal cells targets (LRRC15, TEM-8, FAP- α) being in preclinical development.

Conclusion: In parallel, by the data-driven screening approaches, we have developed an innovative methodology to prioritize novel targets that paves the way for the development of new ADCs with an enhanced therapeutic index. At this juncture, it is noteworthy to mention that many novel targets have been identified by the 4HF cancer Data Miner across a wide range of tumor types including several solid cancers for the development of novel ADCs.

No conflict of interest.

106

Poster

Analysis of the cystine/glutamate antiporter xCT (SLC7A11) as a biomarker in several tumor types using immunohistochemistry

A. Rojas¹, A. Salameh¹, P. Blezinger¹, J. Caldeira², M. Perrine², J. Patti². ¹AgilVax- Inc, Research & Development, Houston- TX, USA; ²AgilVax- Inc, Research & Development, Albuquerque-NM, USA

xCT (SLC7A11), uptakes cystine for the synthesis of glutathione (GSH) and the maintenance of intracellular redox levels. It has been reported that cancer cells have adopted xCT as a means of protection from chemotherapeutics and to meet increased biosynthetic and bioenergetic needs. Due to xCT's role in tumor development, xCT has become a potential biomarker for early detection of cancer and as a target for new therapeutics. AgilVax has conducted extensive studies to demonstrate the importance of xCT in tumor progression in different types of cancer (breast, lung and colon). Here, we show through the use of immunohistochemistry (IHC) and immunofluorescence that high xCT levels appear to be linked to positive results for biomarkers used in cancer detection and planification of treatment.

Methods: A multiplex IHC assay was developed and optimized to establish changes in the expression levels of xCT in several types of cancer. In summary, human samples from breast (n = 110), colon (n = 110), lung (n = 120) and liver (n = 90) (TMAs obtained from Biomax) were stained using several anti-xCT mAbs developed at AgilVax. The xCT recognition was done using DAB staining and hematoxylin. Pathologist annotations provided by Biomax were used to establish stage and grade of the tumor as well as presence or absence of biomarkers. An algorithm for Inform software (Vectra Polaris) developed at the lab was used to perform a complete quantification of xCT (H score) for each cancer and posterior statistical analysis was performed to find significant changes in the xCT expression and its relation with tumor progression (stage and grade) as well as its association with other biomarkers in the context of cancer diagnosis.

Results: AgilVax has developed anti-xCT mAbs and we are utilizing these mAbs to generate antibody drug conjugates (ADC) to target xCT expressing cancer cells. A significant reduction in tumor size in mice treated (IV) with our ADC candidates in multiple models of cancer CT-26 (colorectal), HCT-116 (colorectal) and 4T1 (TNBC) was observed. In the present study, we have used our mAbs in human specimens from several cancer types and we have found significant upregulation of xCT in cancer cells. Conversely, IHC assays performed in non-cancer tissues from mouse, rat, monkey and human, had lower levels of xCT expression.

Our IHC staining for xCT shows that specimens with high levels of xCT are also positive for the canonical biomarkers for breast cancer such as progesterone (83.3%) or estrogen receptor (83%). We observed that late stages of breast cancer, III A/B show high levels of xCT expression (indicated by the H-score values) indicating that xCT may play a key role in tumor progression and the metastatic process. Together, these observations, suggest xCT, is a potential novel biomarker for targeting-therapy of patients at the late stages of breast cancer.

No conflict of interest.

POSTER SESSION

Apoptosis Inducers

107

Poster

Molecular and genetic determinants of dysfunctional wild type TP53 in glioblastoma

Y. Zhao¹. ¹Mayo Clinic, Radiation Oncology, Rochester, USA

Background: Glioblastoma (GBM) is an aggressive and fatal disease. p53 is a nuclear transcription factor and tumor suppressor involved in the induction of cell cycle arrest and apoptosis. To date, almost all known functions of p53 rely on its tumor suppressor activity, and targeting the interaction of MDM2 and p53 is currently the central focus of developing MDM2/p53-oriented cancer drugs.

Material and methods: We analyzed the p53 status using RNA-seq and exome-seq in 35 GBM PDX lines. The improved bioinformatics analysis is used for the p53 status based on the known p53 target genes and pathway. In vivo brain in situ injection is used to test MDM2 inhibitors efficacy. In vitro CellTiter-Glo is used for cell viability measurement. Loss of function experiment is exhibited to detect the biological roles of p53 in PDX cell phenotypes in vitro.

Results: Here, we found that some GBM lines have resistant capability to MDM2 inhibitors, even though the p53 is wild type (WT) in these lines. Using the improved bioinformatics analysis (RNA-seq and exome-seq in GBM PDX lines), we defined the WT p53 into two subgroups (normal functional and dysfunctional p53). Further *in vitro* and *in vivo* data demonstrated that p53 was functional tumor suppressor in PDXs: GBM14 and GBM108 (with normal functional WT p53), but no tumor suppressor functional in GBM10 and GBM148 (with dysfunctional WT p53). Even though targeting MDM2 to reactivate p53 function is a hopeful strategy to treat cancers, this paradigm is challenged by our finding that elevated p53 expression by MDM2 inhibitor had drug resistance because of dysfunctional WT p53. Thus, we find that the elevated p53 expression is no effect on suppressing tumor in some cancer types.

Conclusions: Cancers with sequence WT *TP53* may have unknown subgroups and should be treated by distinct therapy strategies. Based on these novel findings, we conclude that dysfunctional WT p53 is the loss of function type to define a new subgroup of dysfunctional p53 and may provide therapeutic window to treat MDM2 inhibitor resistant GBMs with new strategy.

No conflict of interest.

108

Poster

Multiple myeloma cells inhibit adipogenesis, increase senescence-related and inflammatory gene transcript expression, and alter metabolism in preadipocytes

M. Reagan¹, H. Fairfield¹, S. Costa¹, C. Falank¹, M. Farrell¹, C. Murphy¹, A. D'Amico¹, H. Driscoll². ¹Maine Medical Center Research Institute, Center for Molecular Medicine, Scarborough, USA; ²Norwich University, Biology, Northfield, USA

Background: Bone marrow adipocytes can support tumor cell proliferation and progression to drug resistance, and since multiple myeloma (MM) cells have been shown to hijack their local bone marrow (BM) microenvironment, we investigated the modulation of the adipocyte population by MM cells. MM-associated mesenchymal stromal cells (MSCs) are distinct from healthy MSCs, and their gene expression profiles may be predictive of myeloma patient outcomes, however the link between these MM-induced changes and adipogenic capacity is not well understood. Here we directly investigated how MM cells affect the differentiation capacity and gene expression profiles of preadipocytes and BM-MSCs.

Materials and methods: We examined changes in the transcriptional profiles of MM patient-derived MSCs (MM-MSCs) compared to normal donor MSCs with a specific emphasis on metabolic and adipogenic-related gene expression. To directly test if altered gene expression in adipocyte lineage cells could be induced by MM cells, we performed co-culture experiments with MM cell lines and preadipocytes (3T3-L1 cells and mouse BM-MSCs). Following co-culture, adipogenesis was induced and changes were detected by microarray, qRT-PCR, and oil red o staining in adipocytes.

Results: MM-MSCs exhibited changes in key metabolic genes including upregulation of a number of enzymes involved in fatty acid oxidation (*ACAA1*, *ACOX1*, *ACOX2*, *ACADL*). *In vitro*, MM-MSCs exhibited diminished adipogenic differentiation capacity, which was mirrored in 3T3-L1 cells exposed to MM cells. MM cells and MM-conditioned media altered gene expression profiles of both 3T3-L1 and mouse BM-MSCs. 3T3-L1 cells exposed to MM cells before adipogenic differentiation displayed gene expression changes leading to significantly altered pathways. KEGG Pathways involved in proliferation were downregulated (eg. Cell cycle, $p = 1.67E-12$, FC = -1.09; and DNA replication, $p = 1.23E-07$, FC = -1.14), while Oxidative phosphorylation, ($p = 1.46E-06$, FC = 1.04) and inflammatory pathways were increased (eg. Rheumatoid arthritis, $p = 4.03E-07$, FC = 1.08). MM cells induced a marked increase in 3T3-L1 cell expression of known MM-supportive genes including *Il-6* and *Cxcl12* (SDF1), which was confirmed in MSCs by qRT-PCR, suggesting a forward-feedback mechanism. *In vitro* experiments revealed that MM exposure prior to differentiation drives a senescent-like phenotype in differentiating MSCs, and this trend was confirmed in MM-associated MSCs compared to normal donor MSCs.

Conclusions: Combined, our results suggest that MM cells inhibit adipogenic differentiation while stimulating expression of the senescence associated secretory phenotype (SASP) and other pro-myeloma molecules. This study provides insight into how MM cells manipulate their microenvironment by altering the expression of supportive cytokines and skewing the cellular diversity of the marrow.

No conflict of interest.

109

Poster

The non-peptidomimetic cIAP1/2 and XIAP antagonist ASTX660 promotes an anti-tumour immune response in T-cell lymphoma

N. Ferrari¹, G. Ward¹, C. Gewinner¹, S. Jueliger¹, T. Smyth², J. Munck¹, M. Davis³, R. Ferraldeschi¹, J. Lyons¹, M. Sims¹. ¹Astex Pharmaceuticals, Translational Biology, Cambridge, United Kingdom; ²Astex Pharmaceuticals, Biology, Cambridge, United Kingdom; ³Astex Pharmaceuticals, Molecular Sciences, Cambridge, United Kingdom

Background: ASTX660 is a potent, non-peptidomimetic antagonist of the cellular and X-linked inhibitors of apoptosis proteins (cIAP1/2 and XIAP), which is currently being tested in a first in human phase I-II study in patients with advanced solid tumours and lymphomas (NCT02503423). IAP antagonists have been reported to exhibit broad immuno-modulatory effects on both the innate and adaptive immune systems. We have investigated the profile of ASTX660 in preclinical T cell lymphoma models and evaluated ASTX660's ability to enhance immune mediated killing of T cell lymphoma cells, both *in vitro* and *in vivo*.

Materials and Methods: The anti-proliferative ability of ASTX660 was tested in a panel of human and mouse T-cell lymphoma tumour cell lines. To assess ASTX660 effects on immune-mediated cell killing we used a novel suspension co-culture system of human lymphoma cell lines with anti-CD3 activated human peripheral blood mononuclear cells (PBMC) or the human NK92 cell line. Target engagement along with cell death markers were analysed by Western blotting and flow cytometry. Murine tumour models were utilised to evaluate the anti-tumour effects of ASTX660 in the presence or absence of an effective immune response.

Results: ASTX660 antagonised IAP proteins, as demonstrated by a decrease in cIAP1 protein levels and a disruption of the XIAP:SMAC protein complex. In co-culture models ASTX660 demonstrated enhanced killing of a human lymphoma cell line by anti-CD3 antibody-stimulated PBMCs or the IL-15-stimulated NK92 cells line. Further, ASTX660-dependent lymphoma cell killing was partially dependent on secreted TNF- α . In immunocompetent mice, administration of ASTX660 resulted in a complete regression of BW5147 tumour, which was not seen in mice deficient in T and B cells. These mice remained refractory to subsequent tumour re-challenge several months after initial complete regression. Mechanistically, biomarker evaluation from this model indicated necroptotic response after ASTX660 dosing and upregulation of immune effector cells within the tumour microenvironment.

Conclusions: In addition to its known role as an IAP antagonist in inducing apoptosis in cancer cells, we describe a novel role for ASTX660 as an immunomodulatory molecule capable of boosting an anti-tumour immune response as demonstrated in *in vitro* and *in vivo* pre-clinical models of T-cell lymphoma. These data add to our understanding of ASTX660's mode of action behind the clinical activity that has been reported.

No conflict of interest.

110

Poster

Proteomics reveal extensive translational reprogramming and biomarkers of rocaglate toxicity and resistance in cancer

J.J.D. Ho¹, T.A. Cunningham¹, C.A. Coughlin¹, S. Lee¹, J.R. Krieger², J.H. Schatz¹. ¹University of Miami, Sylvester Comprehensive Cancer Center, Miami, USA; ²Bioinformatics Solutions Inc., Applications, Waterloo, Canada

Translational activation is a major convergence point for oncogenic signals, and its direct targeted inhibition is an attractive cancer treatment strategy that bypasses signaling redundancies limiting the efficacy of many cancer drugs. Rocaglates are potent anti-cancer compounds historically identified as translation/elf4A inhibitors. Prior studies focused exclusively on proteins whose expression is inhibited by rocaglates. However, this singular perspective alone cannot fully explain the potent toxicity of rocaglates across cancer types. The first rocaglate zotatifin recently entered phase I clinical evaluation for advanced solid tumor malignancies, and is receiving much attention as a potent inhibitor of SARS-CoV-2 replication and infectivity. The rapid push to develop rocaglates as cancer therapeutics and our ongoing efforts against the COVID-19 pandemic inject immense urgency for a more comprehensive understanding of rocaglate mechanisms.

Here, we present evidence that rocaglates lead to complex global translational reprogramming, including the induction of an extensive population of unique proteins that mediate cellular rocaglate responses. This conceptually transforms their current one-dimensional definition as translation inhibitors. Using dedicated proteomic technologies including TMT-pSILAC to interrogate system-wide translational reprogramming, and

our recently developed MATRIX platform to capture blueprints of translation machinery adaptations, we discovered previously unrecognized biomarkers that mediate both rocaglate toxicity and resistance. As proof-of-concept, rocaglate-specific induction of GEF-H1 activates RHOA/JNK-dependent apoptosis across solid and blood cancer cells, whereas rocaglate-induced CD98hc up-regulation suppresses JNK signaling to exert pro-survival effects. Induction of these proteins depends on rocaglate-dependent augmentation of eEF1 ϵ 1 translational activity. These results represent the first characterization of rocaglate-inducible proteins with direct relevance to their potent *in vivo* toxicity. Overall, these findings transform our understanding of rocaglates, from pure translation inhibitors to comprehensive remodelers of the cellular protein synthesis landscape.

No conflict of interest.

111

Poster

Small molecule compound induces cell cycle arrest and subsequent apoptosis in an in-vitro model of triple negative breast cancer

S. Okpechi^{1,2}, S. Dong^{1,2}, H. Yousefi^{1,2}, J. Harman¹, T. Nguyen¹, J. Guidry^{1,3}, S. Alahari^{1,2}. ¹Louisiana State University Health Sciences Center, Biochemistry and Molecular Biology, New Orleans, USA; ²Louisiana Cancer Research Center, Louisiana State University Health Sciences Center, New Orleans, USA; ³Proteomics Core Facility, Louisiana State University Health Sciences Center, New Orleans, USA

Background: Triple negative breast cancer (TNBC) accounts for approximately 20% among clinical breast cancer subtypes found in patients. TNBC is very aggressive and has been associated with early and advanced-stages of the disease. TNBC patients harbor tumors that lack estrogen receptor (ER), progesterone receptor (PR), and human epidermal growth factor receptor 2 (HER2) expression; therefore, these patients cannot undergo hormonal therapy. The lack of targeted therapies for TNBC patients has intensified the need for more diagnostic modalities and treatment options.

Material and methods: We screened 1360 compounds from the National Cancer Institute (NCI) Diversity and Mechanistic Set library and identified ten compounds with less than 20% cell viability in a 24-hour timepoint. One compound was selected based on literature review, then, we used proteomic approach to investigate, globally, top protein regulators and associated canonical pathways. Subsequently, we validated the proteomic analysis using apoptosis, cell cycle, and western blot assays. Furthermore, we tested the efficacy of the NCI small molecule in a 3D tissue culture platform which is the closest representation of the physiological environment. Data sets were graphed using GraphPad Prism Software 5.0. and analysis was done using one-way ANOVA with unpaired two-tailed Student's t-test.

Results: Proteomic analysis implicated a myriad of canonical signaling pathways including G2/M DNA damage checkpoint regulation, mitotic roles of polo-like kinase, cyclins and cyclin dependent kinase regulation. We validated these findings using molecular techniques and confirmed a significant dose-dependent increase in apoptosis when TNBC cells (MDA-MB-231 and MDA-MB-468) were stained with Annexin V and propidium iodide. In agreement with our proteomics data, at low dose, a significant cell cycle arrest was observed in the G2/M phase in our flow cytometry data. Furthermore, using 2D and 3D cell culture systems, this antitumor drug reduces the cell viability of TNBC cells in a dose-dependent manner.

Conclusion: Overall, our results suggest that this NCI small molecule drug may be clinically relevant for use in TNBC patients due its therapeutic potential. Next, we plan to investigate the efficacy of this drug compound using *in vivo* mice model of TNBC.

No conflict of interest.

112

Poster

The marine natural product HB-395 selectively induces apoptosis in MDA-MB-231 triple negative breast cancer cell spheroids

E. Guzman¹, T. Pitts¹, A. Wright¹. ¹Florida Atlantic University, Harbor Branch Oceanographic Institute, Fort Pierce, USA

The uniqueness, chemical diversity and structural complexity of marine natural products represent an unexploited supply of potential new drugs, lead compounds for medicinal chemistry or biological probes to allow for better understanding of diseases. A multiparametric high content imaging assay was set up to measure cell death on MDA-MB-231 triple negative breast cancer (TNBC) cells grown as spheroids. A discrete screening of genetically diverse marine samples from the Harbor Branch Oceanographic Institute library led to the identification of a novel activity for the previously reported compound HB-395. This compound induces apoptosis on triple negative

breast cancer cells when grown as spheroids but not when grown in traditional two-dimensional adherent cultures. Protein from cells treated with HB-395 or solvent control was subjected to a reverse phase protein array containing 450 antibodies. The results confirmed that there are few effects of HB-395 on cells grown traditionally, but treatment of spheroids changed important proteins associated with increased TNBC patients' survival. The results from the array were queried in the Broad Institute Connectivity Map which suggested the hypothesis that the compound works as a MEK inhibitor. The activity of HB-395 in this spheroid model of triple negative breast cancer makes it an interesting compound with strong therapeutic potential that merits further study.

No conflict of interest.

POSTER SESSION

Cancer Genomics

113

Poster

Inhibiting eIF4A in liposarcoma to identify key regulators using ribosome profiling

P. Mohan¹, Y.M. Kim². ¹Memorial Sloan Kettering Cancer Center, Cancer Biology and Genetics, New York, USA; ²Memorial Sloan Kettering Cancer Center, Department of Surgery, New York, USA

Well-differentiated/dedifferentiated liposarcomas (WD/DD-LPS) are the most common soft tissue sarcoma and account for approximately 20% of all mesenchymal malignancies. In recent years, although there have been several genomics and epigenomics studies that led to identifying several drivers of LPS such as cyclin-dependent kinase 4 (CDK4) and murine double minute 2 (MDM2), not much is known regarding the mechanisms of mRNA translational control in LPS. To gain a better understanding of aberrant translation promoting LPS and to identify opportunities for detection and therapy, we performed ribosome profiling. This is a technique that produces a 'global snapshot' of all active ribosomes translating in a cell at a particular time point. We focused specifically on the activity of eIF4A RNA helicase, a key translational factor in the eIF4F complex of the cap-dependent translation. Our previous studies in other cancer types such as T-cell acute lymphoblastic leukemia and pancreatic cancer have shown that inhibition of eIF4A activity leads to translational inhibition of genes with G-quadruplex (GQ) structure in their 5' UTR. Interestingly, several oncogenes in the translationally down regulated list of sarcoma, have GQ elements enriched in their 5' UTR. Here, we tested eIF4A inhibitor called Silvestrol and its synthetic analogue CR31B as a possible therapeutic agent in LPS. Significant antiproliferative activity was observed *in vitro* in WD/DDLS cells with CR31B and synergistic effect leading to apoptosis was observed with a combination of CR31B and an MDM2 inhibitor. CR31B treatment of DDLS8817 Xenograft mouse model *in vivo* also showed significant impairment in tumor growth. In addition, down regulation of several key oncogenes in LPS was observed after treatment with CR31B.

No conflict of interest.

114

Poster

Identification of novel tumor suppressors for pancreatic cancer initiation and progression from normal human pancreatic acinar cells

Y. Xu¹, L. Jun¹, N. Michael¹, X. Han², W. Pei¹. ¹The University of Texas Health San Antonio, Cell System and Anatomy, San Antonio, USA; ²MD Anderson Cancer Center, Epigenetics and Molecular Carcinogenesis, Smithville, USA

Background: Pancreatic ductal adenocarcinoma (PDAC) is commonly associated with aberrant genetic status. Although the most frequently mutated cancer drivers were previously identified, including KRAS, p16, p53 and SMAD4, none of them are good therapeutic targets. Recently, thousands of somatic mutations in PDAC have been identified, some of them are potential driver genes that may provide selective growth advantages to initiate and promote PDAC development. In this work, we aim to employ CRISPR library screen to identify new tumor suppressor genes in PDAC and evaluate their contributions to PDAC development, which will offer us the opportunity to develop targeted treatments.

Materials and Methods: Normal human pancreatic tissues from organ donors are sorted by flow cytometry to isolate acinar cells for 3D culture. The cells were lentivirally introduced with oncogenic KRAS, and inactivation of p16, p53, and SMAD4, which served as a platform for our further study. From published whole exome sequencing data, we compiled a list of 199 candidate

PDAC tumor suppressor drivers. A CRISPR library was created to target these genes with 4 sgRNA per gene. The pooled sgRNA library was packaged into lentivirus to transduce primary acinar cells, which were then implanted into immune-deficient mice to assess tumorigenesis. The enrichment of specific sgRNA were identified by next generation sequencing. The functions of identified genes were individually investigated.

Results: Introduction of all four common driver mutations including KRAS, p16, p53 and SMAD4 was able to transform normal human acinar cells to PDAC in our mouse xenograft model. However, combinations of fewer mutations failed to transform acinar cells, suggesting additional mutations are required for PDAC initiation. We introduced the CRISPR library in acinar cells with oncogenic KRAS together with inactivation of p16 and p53, which resulted in 82% tumor transformation in mice model ($n = 22$), whereas the control cells without CRISPR library developed to tumor with a much lower rate 25% ($n = 12$). Next generation sequencing revealed significant enrichment of sgRNAs targeting a set of specific genes, including NF2, FBXW7, ZAN, TGFBR1, and AXIN1, etc. Among these genes, FBXW7 and TGFBR1 have been reported to play roles in PDAC development, confirming the effectiveness of our working platform. The roles of other candidate genes in PDAC progression are poorly understood. Our ongoing study is to create individual CRISPR knockout of these genes in acinar cells to verify their functions in PDAC development.

Conclusion: Our unique system combining 3D organoid culture of primary healthy human pancreatic cells along with CRISPR screening technique serves as an innovative platform to identify additional genes important to PDAC progression, which help to reveal the molecular mechanisms underlying human PDAC development.

No conflict of interest.

115

Poster

Functional genomics screens to identify genes involved in tolerance of tumour microenvironment stress

T.W. Lee^{1,2}, H. Yong¹, S. Bhatta¹, D. Singleton^{1,2}, B. Lipert^{1,2}, P. Tsai³, S. Bohlander^{2,3,5}, C. Print^{2,3}, F. Hunter^{1,2,6}, W. Wilson^{1,2}, S. Jamieson^{1,2,4}.
¹University of Auckland, Auckland Cancer Society Research Centre, Auckland, New Zealand; ²University of Auckland, Maurice Wilkins Centre for Molecular Biodiscovery, Auckland, New Zealand; ³University of Auckland, Department of Molecular Medicine and Pathology, Auckland, New Zealand; ⁴University of Auckland, Department of Pharmacology and Clinical Pharmacology, Auckland, New Zealand; ⁵University of Auckland, Leukaemia and Blood Cancer Research Unit, Department of Molecular Medicine and Pathology, Auckland, New Zealand; ⁶Janssen Research and Development, Spring House, PA, USA

Due to a network of dysfunctional blood vessels, many parts of tumours have poor delivery of oxygen and nutrients, leading to a tumour microenvironment (TME) that is hypoxic, low in glucose and acidic. These tumour-specific conditions have been targeted by various therapeutic agents in development, such as hypoxia-activated pro-drugs and proton pump inhibitors. Although a number of genes are known to play a role in tolerance to these TME stressors, the relative importance of these is unknown, while there could be additional genes that contribute that have yet to be identified.

To identify genes involved in tolerance of TME stress tolerance, we performed functional genomic screens with the full-genome Brunello knockout library in UT-SCC-54C, a head and neck squamous cell carcinoma cell line. Cell populations transduced with the library were subjected to chronic hypoxia (28 days at 0.2% oxygen), glucose deprivation (grown in no glucose medium for 21 days) or acidosis (pH 6.5 for 31 days). To account for differential cell growth between control and experimental conditions, we analysed our data with a novel method called growth-corrected voom-limma (GCVL) analysis to correct for confounding effects of cell growth. Our results revealed selection of gene knockouts involved in glucose metabolism, HIF signalling and oxidative respiration under hypoxia and glucose deprivation, although not always in the expected direction, suggesting the involvement of these pathways to cell survival may depend on the exact nature of the stress (e.g. acute vs chronic hypoxia). Under acidosis, there were surprisingly few proton transporters among our hit list, which we attribute to functional redundancy among these transporters.

In conclusion, our functional genomic screens have provided an intriguing snapshot into the relative importance of various genes involved in tolerance to TME stressors. Among these are cellular signalling pathways that could be targeted by novel therapeutic or repurposed drugs as a means of improving cancer therapy.

No conflict of interest.

116

Poster

Global chromatin landscape identifies bladder cancer metastatic progression

L. Varticovski¹, S. Kim¹, S. Baek¹, L. Prokunina², G. Hager¹. ¹National Cancer Institute, Laboratory of Receptor Biology and Gene Expression, Bethesda, USA; ²National Cancer Institute, Division of Cancer Epidemiology and Genetics, Rockville, USA

Metastatic bladder cancer carries a poor prognosis which cannot be predicted based on available genetic or epigenetic markers. We investigated changes in genome-wide chromatin landscape during metastatic evolution of bladder cancer by surveying DNase hypersensitivity sites (DHS) in 8 non-metastatic and 8 cell lines, most of these acquired spontaneous metastatic potential during *in vivo* passaging. DHS profiles identified massive chromatin alterations corresponding to specific enhancer signatures. Metastatic progression was associated with loss in DHS common to normal bladder cells and enrichment in DHS shared with embryonic stem cells. A large homozygous deletion within *SMARCA4* and alterations in other remodeling complex SWI/SNF components were found only in metastatic cells. These alterations were significantly associated with advanced tumor stage and decreased survival in bladder cancer patients. Our study suggests that alterations in genes controlling chromatin remodeling affect global chromatin landscape associated with metastatic evolution, which can be monitored by genomic tools.

No conflict of interest.

117

Poster

Long noncoding RNA functions as a direct transcriptional target of p73 and plays a critical role in suppression of cancer cell migration, invasion and metastasis via sponging of miR-1273g-3p

A. Uboveja¹, Y.K. Satija¹, F. Siraj², D. Saluja¹. ¹Dr.B.R.Ambedkar Centre for Biomedical Research, University of Delhi, Delhi, India; ²National Institute of Pathology ICMR, Safdarjung Hospital Campus, Delhi, India

Background: Recent evidences suggest that p73 exerts its tumor suppressor functions by suppressing metastasis, but the exact mechanism remains unknown. The present study is aimed to identify novel lncRNAs that play a role in p73-mediated suppression of metastasis in colorectal cancer cells.

Materials and Methods: RNA sequencing was carried out to identify novel lncRNAs differentially expressed in presence and absence of p73 under genotoxic stress and further confirmed by real-time PCR. p73 binding to FER1L4 promoter was confirmed through luciferase, ChIP and site-directed mutagenesis assays. Annexin-V/PI, TUNEL and cell cycle assays were employed to determine the functional aspect of lncRNA FER1L4. The invasion and migration rate of FER1L4kd and p73kd colorectal cancer cells was compared by cell invasion and migration assays. RNA-In situ Hybridization (RNA-ISH) was employed to examine the expression of p73 and FER1L4 in metastatic and non-metastatic colon cancer tissues.

Results: RNA sequencing revealed FER1L4 lncRNA to be significantly up-regulated in the presence of p73, which was further confirmed by qRT-PCR. Through bioinformatics analysis, we identified two p73-binding sites in FER1L4 promoter. Luciferase and ChIP assays confirmed p73 binding onto FER1L4 promoter. Site-directed mutagenesis of both the binding sites totally abrogated p73 responsiveness, indicating that both the sites are equally responsible and essential for p73 binding. qRT-PCR demonstrated a rapid increase in endogenous FER1L4 mRNA upon induction of p73. Knockdown of FER1L4 and p73 significantly increased the invasion and migration rate of colorectal cancer cells as confirmed by wound-healing assay. Knockdown of FER1L4 decreased the expression of E-cadherin and increased the expression of other EMT markers such as N-cadherin, Snail, Vimentin and Fibronectin. Additionally, FER1L4 causes a G2/M cell cycle arrest in a p73-dependent manner in HCT116p53^{-/-}p73^{+/-} colon cancer cells and upon FER1L4kd, normal cell cycle progression was observed. Also, FER1L4 induced apoptosis in HCT116p53^{-/-}p73^{+/-} colon cancer cells with increase in time-dependent treatment of etoposide and FER1L4kd inhibited apoptosis even in the presence of p73. The protein expression level of several pro-apoptotic genes such as Bad, Bax, Bik, Bim, BID, Bak and PUMA decreased upon FER1L4kd and p73kd. FER1L4 also sponges the expression of miR-1273g-3p, thus inhibiting its oncogenic role. RNA-ISH confirmed the decreased expression of p73 and FER1L4 mRNA in 30 human metastatic CRC tissues as compared to 30 human non-metastatic CRC tissues.

Conclusion: Our study provides conclusive evidence that p73 acts as a positive transcriptional regulator that directly regulates the expression of lncRNA FER1L4 and FER1L4 is indispensable for p73-mediated inhibition of colorectal cancer cell invasion, migration and metastasis.

No conflict of interest.

118

Poster

Clinical usefulness of tumor mutational burden (TMB) assessed by NGS in solid tumors

H. Kim¹, S.T. Kim¹. ¹Samsung Medical Center- Sungkyunkwan University School of Medicine- Seoul- Korea, Hematology-Oncology, Seoul, South Korea.

Background: Immune checkpoint blockade (ICB) has become established as an anti-cancer treatment for multiple solid cancers. However clinical responses vary and some groups of patients do not respond to ICB. We tried to validate effectiveness of tumor mutational burden (TMB) as an immunotherapy biomarker in solid tumors.

Material and methods: We analyzed 501 patients and 14 types of tumors who had TMB results. The NGS test by Illumina's TruSight™ Oncology 500 assay was used to confirm TMB, microsatellite instability (MSI). Disease responses were evaluated by RECIST 1.1 criteria and logistic regression analyses were used to figure out the factors associated to immunotherapy responses.

Results: TMB-high was identified in 38 (11.6%) and MSI-High was confirmed in 7 out of 501 cases (1.4%). High TMB rate above 10% was confirmed in bladder cancer, cervical cancer, colorectal cancer, duodenal cancer, gallbladder cancer, melanoma, and urothelial cancer. TMB-low and microsatellite stable (MSS) was 443 cases and TMB-high and MSS was 51 cases. All 7 MSI-high cases were identified to be TMB-high. Patients with TMB-high had better durable response to ICB than TMB-low patients ($p = 0.004$). Objective response rate was 75% (9 out of 12) in TMB-high on the other hand 25% (10 out of 40) in TMB-low group. MSI-high cases were confirmed only 3 cases in this study, so it did not show a significant result. Programmed cell death receptor-1 (PD-L1) was a statistically significant variable in univariate logistic analysis ($p = 0.015$) but removed in multivariate logistic regression model ($p = 0.071$) and TMB was the only factor that explain the regression model ($p = 0.036$).

Conclusions: We confirmed the usefulness of TMB as an immunotherapy biomarker in solid tumors. We recommend TMB analysis by NGS as a useful biomarker add on PD-L1 in clinical setting.

No conflict of interest.

119

Poster

Transcriptome comparison among patients, PDX, PDO, PDXO, PDXC and cell lines

B. Mao¹, X. Xu², G. Sheng¹, W. Qian¹, H.Q. Li³. ¹CrownBio Inc., Systems Biology, Suzhou, China; ²CrownBio Inc., Cancer Biology & Immunology, Beijing, China; ³CrownBio Inc., Chief Scientific Officer, San Diego, USA

Background: Patient-derived tumor models, e.g. patient derived xenograft (PDX), have been increasingly viewed as predictive preclinical cancer models for recapitulating features of patient tumors in molecular/histopathology and pharmacology. Patient derived organoids (PDO), a 3-D culture of human tumor, have also been shown to maintain relevant structure and functions, as well as pharmacology. Both PDO and PDX are hence considered clinically relevant in vitro and in vivo models respectively. However, a systematic and comprehensive cross-examination of these two patient-derived models (including PDX-derived organoid, or PDXO), along with the traditional cell lines (including PDX-derived cells or PDXC) has yet to be undertaken. The present study sets out to systematically investigate the molecular pathology of the aforementioned cancer model libraries, along with cancer patient populations, using the available large datasets and statistical methodology.

Material and methods: We collected RNAseq data of cancer patients (TCGA), PDO, PDX, PDXO, PDXC, and other cell lines (CCLE) across three solid tumor types, including CRC, NSCLC, and pancreatic cancer. We performed correlation analysis to evaluate transcriptome similarity between TCGA (standard) and the other five non-TCGA platforms. We also conducted principal component analysis (PCA) to measure the transcriptome similarity among different platforms, as well as the number of differentially expressed genes (DEGs) between TCGA and non-TCGA platforms for each tumor type.

Results: We found that when the number of top varied genes was small, the Pearson correlation coefficient (PCC) with TCGA had the following order: PDO>PDX/PDXO>PDXC>CCLE, which indicates for the expression level of those top varied genes, PDO models are most similar with patients (TCGA) while cell lines (CCLE) were most divergent from patients. In addition, we selected the top 5000 most varied genes for Principle component (PCA) analysis, and Principle component 1 (PC1) contributed a large portion of variance (35.8%). Judged by the distance at the PC1 axis, transcriptome similarity with TCGA has the following order: PDO>PDXO/PDX>PDXC>CCLE, which is consistent with the results from the correlation analysis. Finally, for all three individual cancer types comparison, the number of DEGs

between TCGA and non-TCGA models has the following order: PDO<PDX<PDXO<PDXC<CCLE.

Conclusions: Our study is the first large-scale comparative study to quantify transcriptome similarity between TCGA and PDO, PDX, PDXO, PDXC, and CCLE. We found that at the transcriptome level, PDO models are most similar to patients and cell line models are least similar to patients, while PDX and PDX derived models sit in the middle.

No conflict of interest.

120

Poster

Multi-omics approaches to clarify adaptive mechanisms of cancer cells to antiproliferative effects by chromosomal instability

T. Y. Morita¹, H. Haeno², H. Makinoshima³, A. Suzuki², S. S. Kobayashi^{1,4}, A. Ohashi¹. ¹National Cancer Center, Exploratory Oncology Research & Clinical Trial Center, Kashiwa, Japan; ²Graduate School of Frontier Sciences- The University of Tokyo, Department of Computational Biology and Medical Sciences, Kashiwa, Japan; ³National Cancer Center, Tsuruoka Metabolomics Laboratory, Tsuruoka, Japan; ⁴Beth Israel Deaconess Medical Center- Harvard Medical School, Division of Hematology/Oncology, Boston, USA

Background: Chromosomal instability (CIN), which includes polyploidy and aneuploidy, is characterized as the pillar of cancer hallmarks. CIN is observed in >90% solid tumors, and correlated with malignancy grades, poor prognosis, and drug resistance. On the contrary, CIN also has been reported to elicit a potent antiproliferative stress, termed a CIN-mediated stress, by drastically changing the signaling networks such as metabolism and gene expression. In this study, establishing our original cell line model for CIN, we aimed to understand how cancer cells could be adapted to the CIN-mediated stress, overcoming its antiproliferative pressure.

Method: A colorectal cancer cells, HCT116, were treated with an Aurora-B kinase inhibitor AZD-1152 for 24 hours to transiently induce CIN in these cells, and then cultured in a drug-free medium for >10 days to establish "CIN-adapted cells." Cell growth was evaluated by intracellular ATP concentrations. RNAs and DNAs extracted from the cells were subjected to RNA-seq, Exome-seq, and ATAC-seq by the NovaSeq sequencing systems. The cell lysates were subjected to metabolomics analyses by GC-MS system. Bioinformatics analyses were performed using these multiple-omics data.

Results: Although >90% AZD-1152-treated cells were dropped out during a long-period culture, a small population of the CIN-adapted cells were successfully established, which kept a high proliferation rate equivalently to the parental euploid cells to overcome the CIN-mediated antiproliferative pressure. The CIN-adapted cells, however, exhibited vulnerability under nutrient deprivation conditions, such as low-glucose and hypoxic condition, compared to the euploid parental cells. In addition, transcriptome and metabolome analyses also revealed the "CIN-specific" metabolic pathways, which were significantly modulated in the CIN-adapted cells. These findings suggest that the CIN-adapted cells may restructure their signaling networks, especially metabolic pathways, to survive under the selection pressures by the CIN-mediated stress.

Conclusions: We comprehensively characterized the CIN-adapted cancer cell model by the multi-omics approaches. These findings would provide further insights into not only the biological significance of CIN in cancer cells, but also novel cancer therapeutics against the CIN cancer cells.

No conflict of interest.

121

Poster

Amplification of SNRPE promotes tumor proliferation and invasion in triple-negative breast cancer by activating mTOR signaling

G. Xie¹, X. Xu¹. ¹Fudan University Shanghai Cancer Center, Breast Surgery, Shanghai, China

Background: The small nuclear ribonucleoprotein E gene (SNRPE) is notably amplified in triple-negative breast cancer (TNBC) and associated with poor diagnosis in our multi-omics database and METABRIC database. However, the function and the mechanism of SNRPE is poorly understood.

Material and methods: Here, we profiled the copy number variations of SNRPE in 400 TNBCs and found that SNRPE was amplified or gained in 250 (62.5%) patients. We further demonstrated SNRPE promoted tumor proliferation and invasion of TNBC cells both in vitro and in mouse models. Using stable-isotope labelling by amino acids in cell culture (SILAC) technology, we analyzed the interacting proteins of SNRPE to explore the its biological role in TNBC.

Results: The protein interaction experiments showed that SNRPE interacted with the co-transcriptional factor DP103, which could activate

mTOR signaling pathway by previous studies. Furthermore, the knockdown of SNRPE re-sensitized tumor cells to the mTOR inhibitor everolimus which was proved invalid in TNBCs.

Conclusions: Our study reveals that SNRPE was highly amplified in TNBCs and promoted the progression of tumor cells via DP103-mediated mTOR signaling activation. Thus, our study provides a promising therapeutic target for TNBC.

No conflict of interest.

122

Poster

Targeting BRAF WT metastatic melanomas: Identifying ERBB4 mutant alleles as biomarkers for novel combinatorial treatment strategies

L. Lucas¹, R. Cullum², V. Dwivedi¹, D. Waits³, T. Ghosh¹, D. Kaufmann¹, E. Knerr⁴, J. Markham³, E. Williams¹, J. Woods¹, K. Halanych³, A. David², D. Riese¹. ¹Auburn University, Drug Discovery and Development, Auburn, USA; ²Auburn University, Chemical Engineering, Auburn, USA; ³Auburn University, Biological Sciences, Auburn, USA; ⁴Auburn University, Chemistry and Biochemistry, Auburn, USA

Background: The treatment of metastatic melanoma (MM) has been dramatically improved through the use of BRAF and MEK inhibitors in patients whose tumors harbor activating mutations in BRAF. However, these mutations occur in only ~50% of MMs and a targeted therapy(ies) has yet to be identified for those MMs that contain wild-type (WT) BRAF. Using The Cancer Genome Atlas melanoma (TCGA-SKCM) dataset, we discovered that 20% of BRAF WT melanomas harbor a missense mutation in ERBB4, which encodes a member of the epidermal growth factor receptor (EGFR/ ErbB1) family of receptor tyrosine kinases. Hence, our goal is to evaluate whether ERBB4 mutant alleles function as biomarkers and targets for therapeutic intervention in BRAF WT MMs.

Materials, Methods, and Results: Of the 469 genomes in the TCGA-SKCM dataset, 70 harbor at least one missense mutation in ERBB4, resulting in a total of 76 unique ERBB4 missense mutations. These mutations do not appear to be random occurrences, but instead appear to be the result of selection. For example, the incidence of ERBB4 mutant alleles is greatly reduced in melanomas that possess BRAF driver mutations and/or driver events in PI3K pathway genes. In contrast, the incidence of ERBB4 mutant alleles is markedly elevated in melanomas that possess genetic alterations that result in elevated RAS signaling. Indeed, melanomas that possess an ERBB4 mutant allele AND a genetic alteration that results in elevated RAS signaling are associated with a marked decrease in survival. Taken together, these data indicate that ERBB4 mutant alleles cause elevated PI3K signaling, which cooperates with elevated RAS signaling to drive the genesis and/or progression of BRAF WT MMs.

The existence of 76 unique ERBB4 mutations in the TCGA-SKCM dataset highlights one of the challenges in identifying the ERBB4 mutant alleles that function as *bona fide* BRAF WT MM drivers. The other challenge is that ERBB4 functions as a context-dependent oncogene and tumor suppressor gene. Hence, we will describe the ongoing development and validation of innovative, positive-selection screens for gain-of-function ERBB4 mutant alleles and for loss-of-function ERBB4 mutant alleles from the library of ERBB4 mutant alleles found in the TCGA-SKCM dataset. The gain-of-function ERBB4 mutant alleles would enhance ERBB4 signaling in contexts in which ERBB4 functions as an MM oncogene, whereas the loss-of-function ERBB4 mutant alleles would disrupt ERBB4 signaling in contexts in which ERBB4 functions as an MM tumor suppressor gene.

Conclusions: *In silico* analyses of the TCGA-SKCM dataset indicate that ERBB4 mutant alleles function as drivers of BRAF WT MM. We will present our progress in developing and validating *in vitro* positive selection strategies to identify which of the 76 ERBB4 mutant alleles found in the TCGA-SKCM dataset function as *bona fide* drivers of BRAF WT MMs.

No conflict of interest.

123

Poster

Arcagen: Molecular profiling of rare cancer patients – analysis of the pilot study (87 patients)

M. Morfouace¹, I. Ray-Coquard², N. Girard³, A. Stevovic¹, I. Treilleux², P. Meeus², S. Aust², A. Floquet⁴, S. Croce⁴, M. Seckl⁵, J. Gietema⁶, M. Caplin⁷, C. delaFouchardiere², L. Licitra⁸, H. Kapiteijn⁹, S. Piperno Neumann³, A. Idhah¹⁰, J.Y. Blay², On behalf of EURACAN. ¹EORTC, TRU, Brussel, Belgium; ²Centre Léon Bérard, Lyon, France; ³Institut Curie, Paris, France; ⁴Institut Bergonié, Bordeaux, France; ⁵Imperial College, London, United Kingdom; ⁶University Medical Centre, Groningen, Netherlands; ⁷Royal Free London NHS Trust, London, United Kingdom;

⁸Fondazione IRCCS Istituto Nazionale dei Tumori, Milan, Italy; ⁹Leiden University Medical Centre, Leiden, Netherlands; ¹⁰Sorbonne Université and AP-HP, Paris, France

Rare cancers, defined as histological diagnoses with an incidence of <6/100,000/year, include more than 300 histological subtypes and may affect all organs. Even though they represent 20% of all adult cancers, they account for more than 30% of cancer mortality. They are clearly under-represented in clinical research programs, especially in research programs exploring genomic alterations of cancer. In order to fill this gap, the EORTC-EURACAN developed a collaborative clinical research project called "Arcagen." This project aims to recruit 1,000 patients with rare cancer and perform a molecular profiling, using the Foundation Medicine tests.

Here, we present the results of the pilot study (feasibility) including 87 patients from three French sites. In total, 98 samples were analysed (55 using the FoundationOne and 43 using the FoundationOne Heme test). We had a global failure rate of 14.3% (only 4.6% for FoundationOne Heme), mainly due to sample quality issues or limited tumor tissue.

Seventy-seven patients (85 samples) had available molecular and clinical data and were included in the analysis. Forty-one patients (53.2%) were diagnosed with sarcoma, 9 (11.6%) with ovarian Yolk Sac Tumor (YST), 14 (18.2%) with rare head and neck cancers and 13 (17%) with thymic cancer. Male to female ratio was almost 1:1 (38 male and 35 female) and the median age at diagnosis was 48 years (range 28–85).

Most patients had reportable genomic alterations (89%). The most common alterations were linked to the cell cycle regulation, in particular in sarcoma and rare head and neck tumors (TP53, RB1 as well as CDKN2A/B deletions or MDM2 amplification). Multiple single-nucleotide variants (SNVs) were detected in the RAS/RAF family, and could be of notable interest in the YST and thymic tumors. The TMB status was globally low across all samples with a median of 3 Muts/MB (range). Only 5.1% of tumors had mutations that were directly targetable with approved agents: NTRK fusion (n = 1; sarcoma), EGFR 20 insertion (n = 1; head and neck tumor) and FGFR fusion/amplification (n = 2; sarcoma). However, regarding global actionability (independently of disease type), we could recommend a targeted treatment for 39% of the patient population (n = 30). The respective targeted therapies comprised CDK4/6 inhibitors, RTKI, PARPi, mTOR inhibitors, and immune checkpoint inhibitors.

Prospective recruitment is ongoing for this project. Liquid biopsy possibility was added in case of screening failure on FFPE material, to optimize the success rate for molecular analysis for all patients. The pilot study highlights a need for specific research on rare cancers to find driver alterations and develop adequate therapies.

Conflict of interest:

Corporate-sponsored Research: This research is done with a grant from Roche.

124

Poster

Mutations and copy number alterations in diffuse gliomas are shaped by different mechanisms

K. Ozduman¹, E. Ulgen², S. Karacan², U. Gerlevik², O. Can³, K. Bilguvar⁴, C.B. Akyerli⁵, S.K. Yuksel⁵, A. Ersen-Danyeli⁵, T. Tihan⁷, C. Yakicier⁸, O.U. Sezerman², M.N. Pamir¹. ¹Acibadem MAA University- School of Medicine, Department of Neurosurgery, Istanbul, Turkey; ²Acibadem MAA University- School of Medicine, Department of Biostatistics and Medical Informatics, Istanbul, Turkey; ³Acibadem MAA University- School of Engineering, Medical Engineering, Istanbul, Turkey; ⁴Yale University, Genetics, New Haven, USA; ⁵Acibadem MAA University- School of Medicine, Department of Medical Biology, Istanbul, Turkey; ⁶Acibadem MAA University- School of Medicine, Department of Pathology, Istanbul, Turkey; ⁷University of California San Francisco UCSF- School of Medicine, Department of Pathology- Division of Neuropathology, San Francisco, USA; ⁸Acibadem MAA University- School of Arts and Sciences, Department of Molecular Biology, Istanbul, Turkey

Background: Mutational mechanisms that shape the genome in gliomas remain largely unknown. Uncovering these mechanisms can help improve current treatments and guide further treatments, which are desperately needed for gliomas. Various mutational processes leave their individual marks in the form of single nucleotide variations (SNV), indels, copy number variations (CNV) or their combinations. We hypothesized that different molecular subsets of gliomas may be caused by different mechanisms, which would be reflected by differences in the burden of different forms of these genetic alterations. In this work we quantified the burden of SNV, indels and CNV using exome sequencing and compared them in diffuse gliomas.

Materials and methods: Whole exome sequencing was performed in 37 primary diffuse glioma patients (tumor and matched blood). 8 further exomes

of recurrences were used for comparison. Findings were validated using the TCGA pan-glioma cohort. Only (IDH- wild type and H3.3-K27 wild type) diffuse gliomas were included as (IDH-mutant astrocytomas & oligodendrogliomas) and (H3.3-K27M mutant diffuse midline gliomas are proven to be different pathological entities. The final cohort included (molecularly defined glioblastoma) (n = 31) and ("others" which are gliomas without TERTp-mutations, EGFR amplification or 7/10 pattern) (n = 6). SNV, indels and CNV were quantified using 5 different parameters (SNV-burden, indel-burden, weighted genome instability index, chromosomal arm event ratio, copy number amplitude). Correlations were made to known mutational mechanisms using analyses for mutational signatures, chromothripsis, double minutes, microsatellite instability.

Results: There was no correlation between parameters of SNV and parameters of CNV. (Molecularly defined glioblastomas) and (others) exhibited significantly different SNV and CNV parameters but were comparable for the indel-burden. Age at diagnosis correlated only with SNV-burden but not with indel- or CNV-parameters. Chromothripsis correlated significantly with a higher frequency of CNV; while double minutes correlated significantly with higher number of chromosomal arm events and higher copy number amplitude. Recurrences after radiochemotherapy displayed significantly higher SNV-burden and a significant association with mismatch repair deficiency; but had comparable CNV-parameters. None of the 5 parameters tested was associated with survival in cox regression.

Conclusions: Molecular subsets of glioma differ in their burden for mutations and copy number alterations. Mismatch repair deficiency is an important driver of single nucleotide variations, it increases over time and at recurrences after radiochemotherapy. Chromothripsis is one, but not the only, mechanism that drives copy number variations.

No conflict of interest.

POSTER SESSION

Cellular Therapies

125

Poster

The functional anatomy of chimeric antigen receptors in acute T cell responses to antigen

H. Xu¹, A. Hamburger¹, J.Y. Mock¹, X. Wang¹, A. Martin¹, T. Tokatlian¹, J. Oh¹, M. Daris¹, K. Negri¹, G. Gabrelow¹, D. Nampe¹, G. Asuelime¹, M. McElvain¹, M. Sandberg¹, A. Kamb¹. ¹A2 Biotherapeutics, Discovery Research, Agoura Hills, USA

Background: Despite their central role in many T-cell therapeutics, the functional anatomy of chimeric antigen receptors (CARs) is not well understood. We have compiled by far the largest structure-activity dataset for CARs that has been reported to our knowledge (10 peptide-major-histocompatibility complex (pMHC) targets, 1254 constructs). As practiced in the T cell receptor (TCR) field for years, pMHC targets enable highly quantitative readouts of sensitivity, by facilitating dose-response measurements where exogenous peptides are loaded onto target cells to control precisely the pMHC epitope number.

Materials and methods: We describe the assessment of the structural components of CARs with regard to acute T cell response in both Jurkat and primary T cell assays. For this purpose we use a pMHC-directed binders in a variety of constructs, including TCRs as comparators.

Results: We present evidence that:

(i) Of the basic CAR structural components (ligand-binding domain (LBD), hinge, transmembrane domain, and canonical intracellular signaling domains), the LBD dominates structure-function relationships for acute response to pMHCs; CARs are remarkably tolerant to the other elements.

(ii) CAR binding avidity is weakly correlated with T cell acute response.

(iii) The workhorse Jurkat/T2 cell model is a reliable surrogate for human primary T cell acute response to antigen *in vitro*.

Conclusions: The conclusions are strengthened not only by the depth and breadth of the study but also by the use of pMHC targets. We believe this work helps solidify a foundation for CAR structure-function in this emerging field in biomedical science.

No conflict of interest.

126

Poster

miR-149-3p inhibits the GSC phenotype cells and re-sensitizes therapy-resistant GBM cells

H. Lopez-Bertoni¹. ¹Johns Hopkins School of Medicine, Neurology, Baltimore, USA

Background: Intra-tumor heterogeneity presents one of the biggest challenges in the development of solid cancer therapeutics. Cells within the same tumor display distinct phenotypes that affect their growth rate, survival, migration, therapy-response, and tumor-propagating capacity. We now understand cancer stem cells (CSCs) play critical roles in driving intra-tumor cellular heterogeneity by establishing dynamic cellular transitions within tumors. GBM are highly aggressive tumors that display a poorly differentiated cell phenotype. Lineage-tracing experiments show that stem-like cells are responsible for GBM re-growth after therapy and this process is in part mediated by known drivers of stemness (e.g. Sox2).

Purpose: Understand the contribution of stem-cell driving mechanisms to the therapy-resistant phenotype of GBM.

Methods: We used human GBM-derived neurosphere lines as cell models. miRNA expression was performed using commercially available mimics. Change in self-renewal capacity were measured via neurosphere formation assays, and levels of miRNA and stem cell markers were quantified by qRT-PCR.

Results: We show that GBM cells expressing transgenic Oct4 and Sox2 are more resistant to ionizing radiation (IR) treatment and exposing GBM neurospheres to temozolomide (TMZ) and IR gives rise to a cell sub-set with higher gene expression levels of Oct4 and Sox2 compared to untreated cells. The clinical relevance of this phenotype is supported by multi-dimensional transcriptome analyses that identifies a group of genes induced by Oct4 and Sox2 enriched in recurrent GBM. We identified miR-149-3p as a high-priority candidate capable of simultaneously inhibiting several transcripts induced by Oct4/Sox2 in recurrent GBM. Transient expression of miR-149-3p decreases the capacity of GSCs to self-renew as spheres and re-sensitized therapy-resistant GSCs to TMZ treatment.

Conclusion: These results show that GSC-driving mechanisms induce a subset of genes that give rise to therapy-resistant GBM cells and suggests that miR-149-3p can be developed as a therapeutic for recurrent GBM.

No conflict of interest.

127

Poster

SOX2-mediated 5hmC dysregulation in GBM Stem Cells

H. Lopez-Bertoni¹. ¹Johns Hopkins School of Medicine, Neurology, Baltimore, USA

Background: Primary brain tumors are among the most devastating forms of cancer and glioblastoma (GBM) represents the most aggressive and lethal form of the disease. We now know that GBM contain small subsets of cells that display tumor-propagating stem-like phenotypes (*i.e.* glioma stem cells or GSCs) that act as critical determinants of GBM resistance to current treatments and tumor recurrence for which there is no proven therapy. Altered patterns of DNA methylation are widely reported in human GBM.

DNA methylation generally occurs in cytosine-guanine (CpG) sequences and is established by DNMTs, which catalyze the conversion of cytosine to 5-methylcytosine (5mC). DNA methylation is a reversible process and is partially mediated by the ten-eleven translocation (TET) family of enzymes which function as deoxygenases to catalyze the conversion of 5mC to 5-hydroxymethylcytosine (5hmC). Multiple studies found negative correlations between 5hmC levels and glioma grade and loss of 5hmC correlates with poor prognosis of GBM patients, strongly suggesting that these enzymes activate tumor suppressing mechanisms. Understanding and ultimately targeting the epigenetic mechanisms that induce and maintain these tumor-propagating cell subsets is critical to improving GBM therapy and patient outcomes.

Methods: For *in vitro* studies, we used human GBM-derived neurosphere lines GBM1A and 612 low-passage primary isolates. shRNA knock-downs and miRNA inhibition were performed using commercially available lentiviral vectors. Change in self-renewal capacity were measured via neurosphere formation assays, and levels of miRNA and stem cell markers were quantified by qRT-PCR. GBM1A or 612 cells were injected stereotactically into the striatum of nude athymic mice to form tumors. Animals were sacrificed and their brains sectioned and stained with H&E for histopathological analysis.

Results: Our preliminary data shows that exogenous SOX2 represses the TET2 demethylase and decreases 5hmC, the enzymatic product catalyzed by TET proteins, in GSCs. TET2 repression using 2 independent shRNA hairpins efficiently decreases 5hmC levels and significantly enhanced self-renewal capacity and tumor growth capacity of low-passage GSC isolates. We also show that SOX2 induces expression of miR-10b-5p, a known onco-

miR predicted to target TET2, and inhibiting this miRNA partially rescues the reduction in 5hmC expression observed in GSCs expressing transgenic SOX2, thus implicating miR-10b-5p as a critical mediator of SOX2-induced onco-methylation, GSC induction and glioma malignancy.

Conclusion: Our preliminary results support a mechanism in which SOX2 represses TET2 leading to 5hmC loss by directly activating miR-10b-5p transcription and predicts that targeting this novel mechanism of epigenetic dysregulation by inhibiting miR-10b-5p *in vivo* can lead to pre-clinical GBM therapeutics.

No conflict of interest.

128

Poster

Gemcitabine stimulates HLA class I expression in pancreatic cancer cells

A. Larson¹, S. Knoche¹, J. Solheim¹. ¹University of Nebraska Medical Center, Eppley Institute for Research in Cancer & Allied Diseases and Fred & Pamela Buffett Cancer Center, Omaha, USA

Background: In the United States, pancreatic cancer represents the fourth leading cause of cancer-related deaths. The dismal survival rate associated with this disease perpetuates a need to not only enhance performance of chemotherapeutics that are currently offered to patients, but also to increase the number of treatment options available. One possibility to achieve this goal is through amplification of the immune response to enhance therapeutic effectiveness. Gemcitabine, a nucleoside analog, is a primary standard of care in pancreatic cancer. In addition to its normative cytotoxic function, evidence suggests that this chemotherapy drug also harnesses immunomodulatory capabilities in the form of increasing human leukocyte antigen (HLA) class I expression in lung, breast, colon, and cholangiocarcinoma cells. Because many malignant cells employ downregulation of HLA class I as a means of evasion, upregulation of this molecule can overcome the immune escape employed by tumor cells and instigate their T cell-mediated death.

Methods: To investigate the effect of gemcitabine treatment on HLA class I expression in pancreatic cancer, alterations in HLA class I protein levels were monitored via western blot analysis and flow cytometry in a pancreatic cancer cell line (S2-013). In western blot analysis, HLA class I expression was measured in both a time (24, 48, 72, and 96 hours) and concentration-dependent manner (0, 6.25, 12.5, 25, 50, and 100 nM). The time points and dosages which solicited the largest increase in HLA class I expression were subsequently examined by flow cytometry.

Results: Administration of gemcitabine to a pancreatic cancer cell line (S2-013) increased total protein levels of both HLA class I constituents (α heavy chain and beta 2-microglobulin light chain [β_2m]), with maximal increases of 141% (HLA-A), 323% (HLA-B/C), and 321% (β_2m) respectively. Flow cytometry revealed a 3-fold increase in HLA-A2 surface expression post-gemcitabine treatment and a maximal 2-fold increase in HLA-B/C expression at the corresponding gemcitabine concentration, but differing time points. Both western blot and flow cytometry analyses indicate HLA-B/C generally has its largest increase in expression at an earlier time point than its HLA-A counterpart.

Conclusion: In summary, gemcitabine demonstrates an immunomodulatory ability to stimulate expression of HLA class I in pancreatic cancer cells, without allele specificity. Further exploration will ensue to discover the mechanism behind this phenomenon, as well as the impact of gemcitabine-enhanced HLA class I expression on the cytotoxic T cell-mediated defense. These results suggest the potential for gemcitabine treatment as a priming mechanism to enhance immunotherapy efficacy in pancreatic cancer.

No conflict of interest.

129

Poster

Devimistat induces reprogramming of glycolytic metabolism to augment its anticancer potency in head and neck cancer

L. He¹, F. Wang¹, C. Shay², Y. Teng¹. ¹Augusta University, Department of Oral Biology and Dx Sciences, Augusta, USA; ²Emory University, Department of Pediatrics, Atlanta, USA

Lipoic acids are mostly synthesized within the mitochondria as a cofactor necessary during mitochondrial energy metabolism, which have been shown to decrease cell viability and proliferation in head and neck cancer. Devimistat, a novel derivative of lipoate inhibiting the energy metabolism in mitochondria shows the new hope for cancer treatment as an efficient and well-tolerated therapeutic option treated alone or in combination with chemotherapy. We report here that devimistat exhibits radical oxygen species (ROS)-associated apoptosis in head and neck cancer HN6 and

HN31, which is concomitant with repressed glycolytic metabolism and mitochondrial fusion. Mechanistic analysis further shows that devimistat inhibits the specific enzymes of central carbon metabolism, including phosphofructokinase platelet (PFKP) and pyruvate dehydrogenase (PDH). Overexpression of either PFKP or PDH significantly attenuates the anticancer efficacy of devimistat by preventing head and neck cancer cells from apoptosis, suggesting that the drug effect relies heavily on PFKP/PDH-mediated glycolysis. In line with the *in vitro* data, devimistat treatment results in robust tumor growth inhibition coupled with reduced levels of PFKP and PDH in orthotopic mice of oral cancer, with no significant systemic toxicity, suggesting devimistat-mediated glycolytic reprogramming contributes to its cytotoxicity. Our study explores the critical role of glycolytic metabolism in apoptosis, providing new insights into the PFKP-PDH signaling axis in crosstalk between glycolysis and apoptosis in devimistat-mediated anti-mitochondrial treatment.

No conflict of interest.

POSTER SESSION

Combinatorial Chemistry

130

Poster

The synergistic action of isolated sesquiterpene with cisplatin against non-small cell lung cancer cells

A. Ahmed¹, B. Zehra¹. ¹International Center for Chemical and Biological Sciences- University of Karachi, Dr. Panjwani Center for Molecular Medicine and Drug Research, Karachi, Pakistan

Non-small cell lung carcinoma (NSCLC) is the most frequently diagnosed and heterogeneous subtype of lung cancer, contributing to 85% of new lung cancer cases worldwide. The prevalence of lung cancer especially NSCLC in Pakistan is also on the rise due to tobacco smoking and chewing as well as air pollution. The asymptomatic and poor prognostic nature of the disease usually results in advanced stage metastatic lung cancer and development of resistance against available treatment modalities. This obviates the extensive need for significant improvements in disease management strategies and its therapeutics. This study was designed to evaluate the synergistic properties of isolated natural sesquiterpene i.e. **Compound 3** isolated from the aerial parts of *Polygonum barbatum*, with cisplatin an FDA approved anticancer drugs against NSCLC NCI-H460 cells. The combinatorial efficacy of **compound 3** and cisplatin was evaluated for anti proliferation, apoptosis induction and anti metastatic potential by using MTT, wound healing, invasion assays, zymography, FACS analysis, gene and protein expression assays. The results showed that a strong synergistic interaction between **Cisplatin** and **Compound 3**, leading to anti-cancer effects at much lower doses than the individual drugs alone. Furthermore, combined drug dose also triggered apoptosis as demonstrated through Yo-Pro-1 assay and deregulated metastasis in H460 cells, as found by transwell invasion and cell migration assays. The drug combination significantly downregulated inhibitory apoptotic markers, i.e. BCL-2L1 and p53 and upregulated apoptogenic BAK, BAX and caspases family proteins. On the other hand, the metastatic markers: MMP-2/-9, VEGF, and COX-2 were also downregulated with the subsequent treatment of combined dose of **Cisplatin/Compound 3**. The common regulator of apoptosis and metastasis, osteopontin, was also subjected to analysis and found to be regulated suppressively to manage the tumor progression and spread. These results suggest that compound 3 being anticancer itself also has capabilities to sense and synergize cisplatin which can be helpful to minimize cisplatin related toxicity and resistance development.

No conflict of interest.

131

Poster

Development of metastatic tumor-targeting NIR persistent luminescence nanomaterials to treatment for lung cancer

M.H. Chan¹, M. Hsiao². ¹Academia Sinica, Genomics Research Center, Taipei, Taiwan; ²Department of Chemistry, National Taiwan University, Taipei 106, Taiwan

Background: Lung cancer is the major cause of cancer-related deaths in the world; the treatment options for non-small cell lung cancer (NSCLC) are based mainly on the stage of cancer. Developing multi-functional nanoplatforms for, sensing cancer, and gene delivery systems is important for biological application. For example, fluorescent nanomaterials have high

resolution and can track specific cells during blood circulation to facilitate diagnosis.

Material and methods: Near-infrared persistent luminescence nanoparticles (NIR PLNs) reveal a special nonlinear radiation process, involving the absorption and retention of photons for several hours, followed by, the emission of long-term luminescence lasting for, one to two hours. Persistent luminescence is an optical phenomenon whereby luminescence lasts for an appreciable time after the ceasing of excitation. In the past few decades, persistent phosphors have been used in important resources for our daily life.

Results: For the biological applications, NIR persistent luminescence materials have recently attracted increasing academic attention because of their potential as novel optical contrast agents for *in vivo* bioimaging within the NIR biological window. NIR persistent luminescence within the tissue transparency window (650 – 1350 nm) will be seen for hours after the termination of excitation.

Conclusions: It is expected that sample injections will be performed using intratracheal, subcutaneous, and intravenous injections to evaluate the response of mice to different conditions of drug administration.

No conflict of interest.

POSTER SESSION

Cytotoxics (including Antimetabolites, Anthracyclin, Alkylating agents, Aurora kinases, Polo-like kinase, Topoisomerase inhibitors, Tubulin-binding compounds)

132

Poster

Phase IIa/IIb clinical trial of NC-6004 (Nanoparticle Cisplatin) plus Pembrolizumab in patients with head and neck cancer (HNSCC) who have failed platinum or a platinum-containing regimen

A. Osada¹, L. Mangel², J. Fijuth³, B. Żurawski⁴, T. Ursulovic⁵, B. Nikolin⁶, I. Djan⁷, J. Grilley Olson⁸. ¹NanoCarrier Co.- Ltd., Clinical Development Div, Tokyo, Japan; ²University of Pécs, Department of Oncotherapy, Pécs, Hungary; ³Wojewódzkie Wielospecjalistyczne Centrum Onkologii i Traumatologii im. M. Kopernika, Department of Radiation Oncology, Łódź, Poland; ⁴Centrum Onkologii im. Prof. Franciszka Łukaszczyka, Chemotherapy Dispensary in The Franciszek Łukaszczyk Oncology Centre, Bydgoszcz, Poland; ⁵Oncology and Radiology of Serbia, Department of Medical Oncology- Head and Neck Cancer, Belgrade, Serbia; ⁶Institute of Oncology Vojvodina, Clinic for Internal Oncology, Sremska Kamenica, Serbia; ⁷Clinic for Neurosurgery- Clinical center Serbia, Center for Stereotactic Surgery, Belgrade, Serbia; ⁸UNC Lineberger Comprehensive Cancer Center, Division of Hematology and Oncology, Chapel Hill, USA

Background: Immune checkpoint inhibitors (ICI) have revolutionized advanced cancer treatment. Nevertheless, less than 20% of cancer patients currently benefit. In order to enhance antitumor activity of ICI, combination trials are under investigation and chemotherapy combination is the most popular. It is known that cisplatin (CDDP), one of most widely used chemotherapeutic agent, induces immunogenic cell death resulting in boosting ICI activity. In fact, ICI in combination with platinum agents have been approved in several cancers. NC-6004 is a polymeric micelle exhibiting sustained release of CDDP and selective distribution to tumors due to the enhanced permeability and retention (EPR) effect. Previous data showed (1) NC-6004 could overcome multiple drug resistance and (2) NC-6004 has equivalent activity to conventional CDDP and better safety profile. Accrual of the Phase IIa portion has been completed but the study is ongoing. Phase IIb will be initiated later in 2020.

Material and methods: In the Phase IIa portion, patients were enrolled at 5 sites in Europe. NC-6004 at 90, 105, 120 or 135 mg/m² IV was given over 1 hr on day 1 with Pembrolizumab at 200 mg IV over 30 mins on day 1 every 3 wks. Patient enrollment was done by traditional 3+3 design. Primary endpoint was to determine MTD and Recommended Phase 2 Dose (RP2D). Safety, antitumor activity as well as pharmacokinetics were evaluated as secondary endpoints.

Results: Overall 16 pts (14 M, 2 F) with HNSCC enrolled. All subjects were ICI naïve and CDDP pre-treated. 7 patients (44%) had prior cetuximab treatment. Two patients (13%) had high PD-L1 expression (TPS≥50%). No DLT was observed, therefore MTD was not identified. RP2D was determined to be 135 mg/m². Neither Grade 3/4 toxicity nor serious adverse event was

observed in Cycle 1 at each dose level. The most common AE was hypomagnesaemia (31%). No Grade 3 or greater eGFR reduction was observed. All AEs were manageable and no unexpected AE was identified. Activity was observed: tumor shrinkage in 8/14 (57%), PR in 3/14 (21%, 1 confirmed, 2 unconfirmed).

Conclusions: Although MTD and RP2D of 135 mg/m² are higher than conventional CDDP doses usually used in HNSCC treatment, no clinically significant neuro- oto- or nephrotoxicity was observed owing to the nanoparticle formulation. Thus, unlike the toxicity of CDDP, NC-6004 combination didn't jeopardize the ability to deliver ICI, resulting in a combination regimen with a good safety profile. Overall, this data demonstrates promising activity and excellent tolerability of NC-6004 in conjunction with pembrolizumab in a platinum pre-treated population.

Conflict of interest:

Ownership: N/A.

Advisory Board: N/A.

Board of Directors: N/A.

Corporate-sponsored Research: Atsushi Osada is a full-time employee of NanoCarrier.

Other Substantive Relationships: N/A.

133

Poster

Evaluation of [1,2]oxazolo[5,4-e]isoindoles in lymphoma cells

M. Barreca¹, V. Spanò¹, M.V. Raimondi¹, A. Montalbano¹, R. Bai², E. Gaudio³, S. Alcaro⁴, E. Hamel², F. Berton³, P. Baraja¹. ¹University of Palermo, Department of Biological- Chemical and Pharmaceutical Sciences and Technologies, Palermo, Italy; ²Frederick National Laboratory for Cancer Research- National Cancer Institute, Screening Technologies Branch- Developmental Therapeutics Program, Frederick, USA; ³Università della Svizzera italiana- Institute of Oncology Research, Faculty of Biomedical Sciences, Bellinzona, Switzerland; ⁴University Magna Græcia of Catanzaro, Department of Health Sciences, Catanzaro, Italy

Background: Anti-tubulin agents are important chemotherapeutics. Combretastatin A-4 (CA-4) emerged as lead compound for the design of new tubulin-binding agents. Its analogues 4,5-diarylisoxazoles, containing the [1,2]oxazole ring as linker of two aryl moieties, displayed higher anti-tubulin activity than CA-4. [1,2]oxazolo[5,4-e]isoindoles also gave excellent results reducing cell growth of NCI-60 tumor cell lines and diffuse malignant peritoneal mesothelioma (DMPM) cells. Selected derivatives showed *in vivo* antitumor activity at well-tolerated doses in a DMPM xenograft model.

[1,2]oxazolo[5,4-e]isoindoles were screened in four lymphoma histotypes: germinal center B-cell and activated diffuse large B cell lymphoma, marginal zone lymphoma and mantle cell lymphoma.

Material and methods: Cell proliferation was measured with the MTT test after 72 h treatment. Compounds were pre-screened at the dose of 1 µM in SU-DHL-10, HBL1, VL51 and MINO cell lines. Those with percentage of proliferating cells down to 60% proceeded to screenings with a wider range of concentrations.

Results: At 1 µM, 6 out of 13 derivatives determined a reduction in the proliferation rate down to 7–61%. Hence, they were tested at concentrations range of 0.15–10 µM and showed anti-proliferative activity with IC₅₀ values between the low micromolar and the nanomolar range. The most potent derivative, SIX2-G, reached nanomolar activity in the majority of cell lines. Furthermore, the compounds inhibited tubulin assembly and colchicine binding.

Structure-activity relationship suggest that a methoxybenzyl substitution at the pyrrole nitrogen is crucial. In particular, methoxy groups in position 3,4 and/or 5 are relevant.

| CPD | VL51 | MINO | HBL1 | SU-DHL-10 | Inhibition of tubulin assembly (IC ₅₀) | % inhibition of colchicine binding |
|---------|-------------|-------------|-------------|-------------|--|------------------------------------|
| SIX13 | 0.27 | 0.23 | 0.25 | 0.28 | 2.1 ± 0.2 | 77 ± 0.5 |
| SIX2-A | 1 | 0.75 | 0.73 | 0.83 | 5.2 ± 0.7 | 69 ± 1 |
| SIX2-G | 0.12 | 0.07 | 0.08 | 0.07 | 2.3 ± 0.3 | 80 ± 0.6 |
| SIX13-O | 0.25 | 0.23 | 0.27 | 0.26 | 1.7 ± 0.2 | 72 ± 2 |
| SIX13-S | 0.27 | 0.37 | 0.47 | 0.5 | 3.2 ± 0.1 | 34 ± 4 |
| SIX13-U | 0.1 | 0.07 | 0.09 | 0.1 | 1.7 ± 0.06 | 57 ± 2 |

IC₅₀ values are expressed in µM.

Conclusions: [1,2]oxazolo[5,4-e]isoindoles are promising anti-tubulin agents with anti-tumor activity in different lymphoma histotypes.

No conflict of interest.

POSTER SESSION

DNA Repair Modulation (including PARP, CHK, ATR, ATM)

134

Poster

Role of AKT3 in the intrinsic radioresistance of lung adenocarcinoma

A. Chauhan¹, A.N. Bhatt¹. ¹Institute of Nuclear Medicine and Allied Sciences, Division of Radiation Biosciences, Delhi, India

Background: Radioresistance poses a critical challenge to effective radiotherapy in the management of lung adenocarcinomas (LUAD). The hyperactivated PI3K-AKT pathway is one of the molecular events by which tumors become radioresistant. The AKT kinase, the downstream effector of PI3K kinase, comprised of three highly homologous isoforms, AKT1, AKT2, and AKT3. Despite several studies on AKT isoforms, the exact role of AKT3 in conferring radioresistance remains elusive.

Methods: To investigate the correlation between AKT3 and lung adenocarcinoma, we analyzed a dataset of LUAD patients from the Cancer Genome Atlas (n = 706), quantified mRNA and protein levels of AKT isoforms in a panel of seven non-small cell lung carcinoma (NSCLC) cell lines. To explore the function of AKT3 in the radioresistance of LUAD, we generated AKT3 shRNA expressing NCI-H1299 and A549 stable LUAD cell lines. We investigated the consequences of AKT3 depletion on the response of these cells to ionizing radiation (IR). Cell proliferation index, clonogenic survival, γ -H2AX foci formation, levels of DNA repair proteins, radiation-induced apoptosis, and spheroid growth kinetics were studied as indices of radiation response of AKT3 knockdown cell lines and to establish the role of AKT3 in radioresistance of LUAD.

Results: Analysis of copy number variation and gene expression levels of AKT isoforms in the TCGA dataset revealed that AKT3 comprises the most frequently amplified and expressed AKT isoform in LUAD patients. The analysis of mRNA and protein levels of all three AKT isoforms in a panel of NSCLC cell lines revealed that AKT3 was expressed in all the NSCLC cell lines we tested in our study, with relatively high levels in LUAD cell lines. The knockdown of AKT3 resulted in a significant reduction in the proliferation index of NCI-H1299 and A549 cells at 2 Gy and 4 Gy dose of IR. Correspondingly, in comparison to scrambled shRNA expressing cells, a loss of clonogenicity to IR was observed in both the cells expressing AKT3 shRNA. Further, AKT3 knockdown significantly increased the residual double-stranded breaks (DSB) after IR as assessed from γ -H2AX foci formation and protein levels of DNA repair pathway proteins. AKT3 knockdown also resulted in a significant increase in radiation-induced cell death, leading to radiosensitization. In addition to that, AKT3 depletion resulted in a significant reduction in 3-dimensional multicellular spheroids volume. Upon irradiation, a significant decrease in the spheroid growth was also observed in NCI-H1299 and A549 cells expressing AKT3 shRNA. Taken together, these findings demonstrate the role of AKT3 in the intrinsic radioresistance of LUAD and highlight the rationale for the development of AKT isoform-selective small molecule inhibitors.

No conflict of interest.

135

Poster

A CDC7-selective Inhibitor, TAK-931, suppresses homologous recombination repair activity to enhance antiproliferative activity of a PARP inhibitor

J. Yu¹, Y. Kashima², S.I. Kageyama², H. Niu¹, K. Kannan¹, A. Ohashi². ¹Millennium Pharmaceuticals- Inc., Oncology Drug Discovery Unit, Cambridge, USA; ²National Cancer Center Japan, Exploratory Oncology Research & Clinical Trial Center, Kashiwa, Japan

Background: Cell division cycle 7 (CDC7) is a serine/threonine kinase, which plays important roles in initiation of DNA replication. We developed a CDC7-selective inhibitor, TAK-931, as a clinical candidate compound. We previously demonstrated that TAK-931 enhances the biological activity of the DNA damaging agents for antiproliferation in cancer cells. In this study, we aimed to identify novel molecular mechanisms of TAK-931

focusing on homologous recombination repair (HRR) pathways, which would be involved in enhanced antiproliferative effects in combination with TAK-931.

Methods: Stable isotope labeling using amino acids in cell culture (SILAC)-labeled H460 cells in combination treatment with IR and TAK-931 were subjected to quantitative mass spectrometry. For HRR assay, DR-GFP and Sce-I plasmids were co-transfected into 293 T cells in presence or absence of TAK-931. In vivo combination studies of TAK-931 with a PARP inhibitor were conducted in multiple human xenograft models including patient-derived xenograft models (PDXs).

Results: In the phosphoproteomics analysis, informatics analysis revealed that double-strand break (DSB) repair ($p < 0.01$) pathway was significantly enriched in the combination-treated cells with irradiation and TAK-931 (IR+TAK-931) compared with the untreated cells after 24 hours. In the DSB repair pathway, phosphorylations of homologous recombination repair (HRR)-associated proteins, such as BRCA2, ATM, and Rad50, were particularly elevated. The DR-GFP-based HRR reporter assay also revealed that TAK-931 intensively suppresses HRR activity. These findings suggest that TAK-931-mediated insufficient HRR, which appears to exhibit a chemically-induced BRCA defectiveness (termed "BRCAness"), would accumulate more DSBs by the combination treatment, and accordingly prolong the activation of HRR-associated proteins in these cells. We also conducted in vivo combination studies with a PARP inhibitor, which is expected to be more effective for BRCAness tumors. Consistent with our hypothesis, in vivo combination treatments of TAK-931 with PARP inhibitor, also enhanced antitumor activities in multiple human xenograft models, including breast and ovarian PDXs.

Conclusions: Our findings suggest that TAK-931 could chemically induce BRCAness in cancer cells to enhance antiproliferative activity of the PARP inhibitor.

Conflict of interest:

Corporate-sponsored Research: This research was supported by Takeda Pharmaceutical Company, Ltd. Other Substantive Relationships: YJ, HN, KK, and AO are/were employees of Takeda Pharmaceutical Company.

136

Poster

Investigating synergy between WEE1 and PARP inhibitors in BRCA2 mutant and corrected cells

H. Smith¹, L. Prendergast¹, N. Curtin¹. ¹Newcastle Centre for Cancer, Faculty of Medical Sciences, Newcastle upon Tyne, United Kingdom

Background: The PARP inhibitor (PARPi) rucaparib exploits defective homologous recombination repair (HRR) in BRCA mutated cancer cells via synthetic lethality. PARPi causes stalled replication forks resulting in an increase in replication stress (RS). RS activates ATR, which signals to HRR and cell cycle checkpoints via CHK1 and WEE1. Here we investigated the synergy between rucaparib and the WEE1i MK-1775 (AZD1775) and the mechanism underpinning this.

Materials and Methods: The effects of rucaparib and MK-1775 were examined in V-C8 (BRCA2 mutant Chinese hamster fibroblasts) and V-C8.B2 (BRCA2corrected) cell lines. Cytotoxicity was determined using colony formation assays. Endogenous PAR levels and PARP activity was determined by measuring the PAR product by immunoblotting with the 10H Ab. WEE1 activity was measured by CDK1y15phosphorylation, and upstream CHK1 and ATR activity were measured by, CHK1s296 and CHK1s345phosphorylation, respectively, by Western blot. DNA damage and repair by HRR was determined by gammaH2AX and RAD51 foci formation, respectively, by immunofluorescence microscopy. Cell cycle analysis was investigated using flow cytometry.

Results: HRR defective V-C8 cells were significantly more sensitive to rucaparib cytotoxicity than HRR competent V-C8.B2 cells (LC50s: $<0.01 \mu\text{M}$ vs. $>10 \mu\text{M}$, $p < 0.001$). There was no significant difference in sensitivity to MK-1775 cytotoxicity (LC50s: 454.5 nM vs 372.1 nM). MK-1775 (100 nM) sensitised V-C8.B2 cells to rucaparib 7.2-fold ± 1.4 . No sensitisation was observed in V-C8 cells. PARP activity was similar in both cell lines but V-C8 cells had 2.3-fold higher endogenous PAR levels than V-C8.B2 cells, indicating a higher level of endogenous DNA breakage. Rucaparib inhibited PARP activity similarly in both cell lines (IC50: 59 nM and 53 nM). Rucaparib ($10 \mu\text{M}$) increased CDK1y15phosphorylation in both V-C8 and V-C8.B2 cells (1.8 and 1.5-fold, respectively). Upstream ATR and CHK1 were also activated by rucaparib in both cell lines to a similar extent. MK-1775 (100 nM) completely inhibited the increased CDK1y15phosphorylation as well as activating CHK1 and ATR upstream (1.3 to 1.4-fold and 3.1 to 5.0-fold, respectively). Rucaparib ($10 \mu\text{M}$) caused a 4.8-fold increase in RAD51 foci in γ H2AX positive V-C8.B2 cells. Addition of MK-1775 (100 nM) inhibited this

RAD51 foci formation completely, indicating inhibition of HRR. No RAD51 foci were formed in γ H2AX positive V-C8 cells.

Conclusions: WEE1 MK-1775 sensitised HRR competent V-C8.B2 cells to rucaparib, but not V-C8 cells, suggesting that the mechanism underpinning this synergy was inhibition of HRR by MK-1775. Cell cycle analysis is ongoing to assess the contribution of inhibition of S and G2/M checkpoint control.

No conflict of interest.

137

Poster

Potential use of the PARP inhibitor rucaparib to enhance cervical cancer treatment

S. Saha¹, R. Howarth², I. Pappworth³, K. Marchbank³, N. Curtin¹.

¹Newcastle University, Translational and Clinical Research Institute- Newcastle University Centre for Cancer-DNA damage response group, Newcastle upon Tyne, United Kingdom; ²Newcastle University, Translational and Clinical Research Institute- Newcastle University Centre for Cancer-Pathology, Newcastle upon Tyne, United Kingdom; ³Newcastle University, Translational and Clinical Research Institute-Complement biology and kidney research group, Newcastle upon Tyne, United Kingdom

Background: Cervical cancer (CC) is the fourth most common cancer in women worldwide. In the UK, peak age of CC is 30–35 years and 10-years survival is ~63%. Standard treatment for locally advanced CC is chemoradiotherapy (CRT) with cisplatin (weekly 40 mg/m² × 5). However, cisplatin-induced kidney toxicity results in discontinuation of the treatment. The poly(ADP-ribose) polymerase inhibitors (PARPi) targeting homologous recombination repair deficient breast and ovarian cancers are clinically used although, chemo-radio sensitising property of PARPi has widened their therapeutic application. Here we investigate the potential of the PARPi rucaparib to increase the therapeutic index of CRT by reducing kidney toxicity and increasing cisplatin and radiation cytotoxicity.

Methods: 1) Cytotoxicity of cisplatin (0.1 μ M) and radiation/IR and in combination with rucaparib (1 μ M) was assessed in HeLa cells by clonogenic assay. 2) The maximum tolerated dose (MTD) of cisplatin 10–20 mg/kg i.p. (day 1 X1) causing acute kidney toxicity (AKT) in 5 days was determined in wild type CD1 female mice. 3) Low dose of rucaparib (1 mg/kg i.p. days 1–5) was given with the MTD of cisplatin (10 mg/kg i.p. day 1) to test any reduction of cisplatin-induced AKT. For toxicity study, mice were monitored for piloerection, hunching and body weight loss. Pathological examination was done with FFPE kidney tissues for H&E, PAS staining and AKT biomarker Lipocalin-2 by IHC. Mechanism of cisplatin-induced PARP activation (PAR levels) by oxidative stress (4HNE) was studied by IHC. Regions of kidney sections from IHC data was quantified by Leica Aperio ImageScope™.

Results: 1) The effect of CRT at 2 Gy IR in HeLa cell was potentiated ~1.3-fold by rucaparib. 2) The MTD of cisplatin causing AKT was 10 mg/kg (human equivalent dose 30 mg/m²). Compared to saline, cisplatin increased Lipocalin-2 expression at the kidney's cortex regions (cortex: ~19 fold vs. medulla: ~2 fold), PAR level was also found significantly elevated at the cortex (cortex: ~9 fold vs. medulla: ~1.5 fold). Whereas, 4-HNE was higher at kidney's medulla regions (medulla: ~2 fold vs. cortex: ~1.25 fold). Compared to cisplatin treatment, rucaparib 1 mg/kg reduced PAR levels (cortex: ~5.5 fold, medulla: ~1.7 fold) and cisplatin-induced AKT measured with the reduction in Lipocalin-2 (cortex: ~6 fold, medulla: ~4 fold). Rucaparib did not affect cisplatin-induced oxidative stress and 4-HNE levels were not significantly altered.

Conclusion: Rucaparib showed chemo-radio sensitisation in CC cell line HeLa. In mice treated with cisplatin there was an increase in oxidative stress throughout the kidney but PARP hyperactivation and toxicity was observed primarily in the kidney cortex. Rucaparib protected from cisplatin induced AKT. Combination of rucaparib with conventional CRT can contribute new therapeutic strategies in CC treatment.

Conflict of interest:

Other Substantive Relationships: Nicola Curtin has served on the scientific advisory boards of various companies making PARP inhibitors (Abbvie, BioMarin, Eisai, Tesaro). She has received royalty payments from the commercial development of rucaparib (Rubraca®), which have been used to fund her group's research and to establish the charity Curtin PARP (Passionate About Realising your Potential) Fund at the Community Foundation (UK). Her PARP related work has been supported by funding from Agouron Pharmaceuticals, Pfizer, Clovis, BioMarin and BiPar Sciences.

138

Poster

Dysregulated binding of Sp1 at double strand breaks increases cell sensitivity to PARP inhibition

M. Swift¹, J. Azizkhan-Clifford¹. ¹Drexel University College of Medicine, Biochemistry and Molecular Biology, Philadelphia, USA

The exploitation of the addiction of cancer cells to a DNA repair pathway is the basis of synthetic lethality and has wide applicability to the treatment of many types of malignancies. We have demonstrated that the transcription factor Sp1 is rapidly recruited to DSBs and is necessary for repair. Here we demonstrate that Sp1 is recruited to DSBs in G1 but not in S, and is necessary for recruitment of 53BP1 and repair via NHEJ. Sp1 is phosphorylated by cyclin A/CDK2 upon entry into S phase, evicting both Sp1 and 53BP1 from the break site and thereby permitting BRCA1 binding. Mutation of this phosphorylation site (Sp1-S59A) results in persistent presence of Sp1 and 53BP1 at DSBs in S phase cells, precluding BRCA1 binding and HR. Similar to BRCA1 deficiency, expression of Sp1-S59A also increases cell sensitivity to PARP inhibition in BRCA1^{+/+} cells. These data demonstrate how mutations in DNA repair factor proteins can be therapeutically exploited to preferentially kill cancer cells.

No conflict of interest.

POSTER SESSION

Drug Delivery

139

Poster

Tumor cell membrane-based peptide delivery system targeting to tumor microenvironment for cancer immunotherapy and diagnosis

Y. Zhu¹, J. Wang¹, X. Meng¹. ¹Suzhou Institute of Nano-tech and Nanobionics- CAS, Nanobiomedicine, Suzhou, China

Background: The development of effective delivery system for peptides targeting to tumor microenvironment is the hot point of research for cancer diagnosis and therapy.

Material and Methods: A multifunctional delivery system by encapsulating superparamagnetic iron oxide nanoparticles (SPIO NPs) with tumor cell membrane to effectively deliver therapeutic peptides was constructed. SPIO nanoparticles were encapsulated with H460 lung cancer cell membranes (SPIO NP@M) and peptides consisted of PD-L1 inhibitory peptide (TPP-1) and MMP2 substrate peptide (PLGLLG) was conjugated to H460 membrane.

Results: TPP-1peptide was delivered to and released to the tumor microenvironment through the homotypic effect of tumor cell membrane and specific digestion by the tumor specific enzyme, MMP2. The newly developed delivery system (SPIO NP@M-P) for PD-L1 inhibitory peptide could effectively extend the half-life of the peptides (60 times longer) and meanwhile maintain the ability to re-activate T cell and inhibit the tumor growth in vitro and in vivo. Furthermore, SPIO in the system could mark the tumor loci and indicate the effect of peptide treatment.

Conclusion: The SPIO NP@M might provide a promising theranostic platform for therapeutic peptide application in cancer therapy.

No conflict of interest.

140

Poster

Tinagl1 gene therapy for tumor-wide remodeling of triple negative breast cancer

S. Musetti¹, H. Leaf¹. ¹UNC Chapel Hill, Pharmaceutical Sciences, Chapel Hill, USA

Purpose: Triple-negative breast cancer (TNBC) is one of the deadliest forms of cancer, tending to strike earlier and metastasize faster than other breast cancers. Unfortunately, due to its lack of progesterone, estrogen, or HER2 receptors, there are no targeted therapies available to patients with TNBC. However, in 2019 Shen *et al* found that TNBC tumors with higher levels of tubulointerstitial nephritis antigen-like 1 (Tinagl1) had better prognoses, and that treating tumors with free Tinagl1 protein can suppress TNBC tumor growth by interrupting EGFR and integrin signaling.¹ We sought to expand upon this work in two ways. First, we sought to improve the delivery of Tinagl1 by transitioning from the recombinant protein used in Shen (2019) to lipid-nanoparticle based gene therapy. Second, we sought to characterize the changes to the tumor microenvironment that Tinagl1 treatment induces.

Methods: Using our lipid-protamine-DNA nanoparticles (LPDs), we encapsulated Tinagl1-expressing plasmid DNA (Tinagl1 pDNA) and targeted them to tumors through sigma-receptor targeting moiety aminoethyl anisamide (AEAA).² Briefly, Tinagl1 pDNA is condensed into a solid core with protamine. This protamine-pDNA core is encapsulated into liposomes decorated with DSPE-PEG(2000) and DPSE-PEG-AEAA (10:1). Tinagl1 LPDs can be injected intravenously into Balb/C mice bearing 4T1 tumors in the mammary fat pad. Tumor growth is measured with calipers three times a week, with tumor volume calculated as length x width x width/2. AKT phosphorylation was measured by Western blotting; angiogenesis, measured by CD31 and VEGF, as well as Hif1a expression, were measured using immunofluorescence staining.

Results: Tinagl1 LPDs injected intravenously suppress tumor growth in a transient, controllable fashion. Confirming the results shown in Shen (2019), Tinagl1 reduces the phosphorylation of AKT. Shen (2019) showed that this is a combined result of interfering with integrin binding and EGFR dimerization on the surface of TNBC cells, resulting in poor activation of the MAPK and FAK pathways. However, our second goal for this study was to further analyze the effects of Tinagl1 expression on the tumor microenvironment. In addition to suppressing tumor cell proliferation, Tinagl1 significantly promotes angiogenesis in the tumor. The increase in blood flow appears to reduce the expression of Hif1a in the tumor, indicating less hypoxia and potentially improving the susceptibility of tumors to treatment.

Conclusion: In addition to halting the growth of TNBC tumor cells, Tinagl1 is able to remodel the tumor microenvironment by increasing angiogenesis. Because Tinagl1 suppresses tumor proliferation and metastasis simultaneously, angiogenesis results in reduced Hif1a and hypoxia without the typical detrimental effects.

No conflict of interest.

141

Poster

A comprehensive analysis of cetuximab combinatorial polymeric nanocomplexes with potent radionuclide uptake to combat metastatic liver cancer

R. Poojari¹, B. Mohanty², V. Kadwad³, D. Suryawanshi⁴, P. Chaudhari⁵, B. Khade⁶, R. Srivastava¹, S. Gupta⁶, D. Panda¹. ¹Indian Institute of Technology Bombay, Department of Biosciences and Bioengineering, Mumbai, India; ²Advanced Centre for Treatment- Research and Education in Cancer ACTREC- Tata Memorial Centre TMC, Comparative Oncology and Small Animal Imaging Facility, Navi Mumbai, India; ³Board of Radiation and Isotope Technology BRIT, Radiopharmaceuticals Production, Navi Mumbai, India; ⁴Omega Laboratories, Department of Pathology, Pune, India; ⁵Advanced Centre for Treatment- Research and Education in Cancer ACTREC- Tata Memorial Centre TMC, Comparative Oncology and Small Animal Imaging Facility- Navi Mumbai, India; ⁶Advanced Centre for Treatment- Research and Education in Cancer ACTREC- Tata Memorial Centre TMC, Epigenetics and Chromatin Biology Group, Navi Mumbai, India

Background: Herein, we have determined the anticancer effects of Cetuximab targeted combinatorial polymeric nanocomplexes comprising either combretastatin A4 or methoxyestradiol in ectopic and orthotopic metastatic liver cancer SCID mice models.

Material and methods: The efficacy and mechanistic interactions of synthesized targeted and non-targeted polymeric nanocomplexes encapsulated microtubule inhibitors was investigated as a combinatorial therapy against liver cancer ectopic and orthotopic metastatic models and orthotopic metastatic in SCID mice. The radionuclide (¹²⁵I and ¹⁸F-FDG) uptake efficiency in the nanocomplexes treated mice was studied.

Results: Systemic delivery of Cetuximab combinatorial polymeric nanocomplexes based microtubule inhibitors resulted in potent tumor growth inhibition (85%, P < 0.0001), tumor cell death and less toxic effects. The uptake of ¹²⁵I targeted polymeric nanocomplexes and ¹⁸F-FDG in tumor revealed accumulation and long-term retention of the nanocomplexes, and reduction in tumor metabolism upon treatment with Cetuximab targeted combinatorial polymeric nanocomplexes. Histopathological, ultrastructural, immunohistochemical and immunoblotting studies of Cetuximab combinatorial polymeric nanocomplexes treatment depicted significant amelioration in the pathological features, and key protein biomarkers.

Conclusion: The findings support the development of Cetuximab targeted combinatorial polymeric nanocomplexes approach for liver cancer therapy.

No conflict of interest.

POSTER SESSION

Drug Design

142

Poster

Disrupting cancer dynamics by a novel pleiotropic benzopyrane derivative

T. Altel¹, R. El-Awady¹, H. Omar¹, W. Ramadan¹, D. Zaher¹, Drug Design and Discovery Group. ¹University of Sharjah, Sharjah Institute for Medical Research, Sharjah, U.A.E.

Introduction: Multitarget drug discovery became an important tool to overcome the limited efficacy, resistance and adverse side effects encountered by many single-target or combination-based anticancer therapies.

Results: In this context, dual inhibition of GSHR and TrxR systems represents an attract strategy that is recognized to synergistically kills neoplastic cells, decreases anticancer drug resistance, and enhances the immune system. To this end, we demonstrate the discovery of SIMR1281, a novel benzopyrane derivative, that strongly inhibits GSHR (IC₅₀ = 590 nM) while moderately inhibits TrxR (IC₅₀ = 2.4 μM). This dual inhibition was found to correlate with an elevated level of reactive oxygen species, a decrease in ATP content, and an increase in mitochondrial membrane potential. SIMR1281 potently inhibits cell proliferation of various cancers, including multi-drug resistant cancer cells with IC₅₀ values range between 0.60 to 5.5 μM. In addition, SIMR1281 induces DNA damage, stimulation of DNA damage response machinery, perturbations in the cell cycle, and inactivation of Ras/ERK and PI3K/Akt pathways. Furthermore, SIMR1281 upregulates the pro-apoptotic proteins p53, p21, and Bax, and cleavage of caspase-9 and caspase-3. Besides, SIMR1281 strongly attenuated cell survival machinery via strong inhibition of the oncogene c-MYC and inhibition of mitotic spindle formation. The compound showed a high safety profile when tested in vivo. The multitarget antitumor activity of SIMR1281 was consistent with a significant reduction of tumor volume in a xenograft mice model.

Conclusion: These findings places SIMR1281 in a privileged position as a novel anticancer modality and forms the foundation for further studies in clinical trials.

Methods: SIMR1281 was developed and screened against a panel of cancer cell lines. The mechanism of action was explored and validated using various *in vitro* molecular biology techniques such as cell viability analysis, Western blotting, cell cycle analysis DARTS assay, and various enzymatic assays. Besides, the safety and efficacy *in vivo* were confirmed using a mouse xenograft model.

Conflict of interest:

Ownership: The authors declare competing financial interests since part of this article is in the patent application (T. H. Al-Tel, Raafat A. El-Awady, Srinivasulu Vunnam, Cijo G. Vazhapilly, Hany A. Omar, Novel heterocyclic systems and pharmaceutical compositions thereof. US Patent No US20190292204A1).

143

Poster

Discovery and characterization of potent and selective AXL receptor tyrosine kinase inhibitors for cancer therapy

D. Miles¹, Y. Chen², S.L. Paprcka³, C.N. Foley¹, R. Grange¹, M.R. Leleti¹, X. Zhao², L. Jin⁴, S.W. Young², M.J. Walters³, J.P. Powers¹. ¹Arcus Biosciences, Chemistry, Hayward CA, USA; ²Arcus Biosciences, Quantitative Biology, Hayward CA, USA; ³Arcus Biosciences, Biology, Hayward CA, USA; ⁴Arcus Biosciences, Drug Metabolism and Pharmacokinetics, Hayward CA, USA

Background: AXL receptor tyrosine kinase (AXL) is a transmembrane protein which is overexpressed in a variety of cancers and has been implicated in the development of resistance to chemotherapy and immunotherapy. Higher expression generally correlates with worse patient prognosis. Extracellular activation of AXL by growth arrest specific protein 6 (GAS6) facilitates AXL dimerization and autophosphorylation, which subsequently initiates two main signaling cascades, RAS-RAF-MEK-ERK and PI3K-AKT, both of which promote cancer cell proliferation and survival. Here we present the characterization of novel, potent, and selective AXL inhibitors which show promise in the field of small-molecule cancer therapeutics.

Materials and Methods: The potency of compounds inhibiting kinase activity of AXL and other kinases was determined by detecting phosphorylated substrate using homogeneous time-resolved fluorescence (HTRF).

Intracellular target engagement was determined by monitoring displacement of a competitive fluorescent tracer using an AXL NanoBRET™ intracellular kinase assay. To further assess the inhibitory effects of compounds on intracellular AXL kinase activity, AXL autophosphorylation induced SH2 domain translocation was measured in cells using an enzyme fragment complementation technology (EFC) assay. PK/PD and anti-tumor effects of selected AXL inhibitors were evaluated in murine models.

Results: These novel compounds are highly potent, reversible, and selective inhibitors of AXL. They exhibit high potency in both biochemical and cell-based assays in addition to exhibiting good selectivity against closely-related kinases (MER and TYRO3) and other kinases involved in downstream signaling such as PI3K. In general, these molecules do not show significant inhibition of the major CYP450 isoforms or the hERG potassium channel. Initial studies in animal models indicate a favorable pharmacokinetic profile and anti-tumor efficacy.

Conclusions: AXL inhibition is a promising therapeutic mechanism for impairing the growth and metastasis of chemotherapy and immunotherapy-resistant tumors. Highly potent and selective AXL inhibitors have been designed, some of which display profiles superior to those of less-selective molecules currently advancing through clinical development.

Conflict of interest

Ownership: All authors are employees of Arcus Biosciences and may hold equity in the company.

144 Extended 8b inhibition of CDK 6 inhibits TWIST 1 expression and induces therapeutic senescence in KRASG13D mutant colon cancer

Poster

A. Qayum¹. ¹CSIR-IIIM, Cancer Pharmacology Division, Jammu, India

KRAS mutant colon cancer patients resistant to EGFR-inhibitors are frequently resistant to other therapies, such as immune checkpoint inhibitors, and individuals succumb to their disease. New drugs that control tumor growth and favorably modulate the immune environment are therefore needed. We report that the small molecule 8b has potent activity against KRAS^{G13D} resistant colon cancer cell lines through modulation of CDK6/TWIST1 identified as a target. 8b inhibition resulted in reduced proliferation, frequent formation of polyploidization (senescence) and activation of the CDK6-TWIST1 pathway. In murine model, 8b induced a potent regression response in tumor cells *in vivo* with increased IFN γ producing CD8⁺ T-cells and reduced Treg frequency. 8b was more selective in targeting mutant cells compared to normal cells and its inhibition had minimal toxicity *in vivo* expanded human tumor-infiltrating lymphocytes (TILs), proliferating TILs suggesting a potential therapeutic index for anti-cancer therapy. Furthermore, the activity of 8b was validated in multiple KRAS cancer cell lines. Thus, 8b inhibition may overcome drug resistance in KRAS^{G13D}, modulate the immune environment and target vulnerability in different cancer lineages.

No conflict of interest.

145 High-Resolution Limited Proteolysis (HR-LiP): A novel approach for target validation and lead compound optimization

Poster

Y. Feng¹, N. Beaton², J. Adhikari³, R. Bruderer², R. Tomlinson³, I. Cornella-Taracido³, L. Reiter². ¹Biognosys AG, Business Development, Schlieren, Switzerland; ²Biognosys AG, Research & Development, Schlieren, Switzerland; ³Cedilla Therapeutics, Proteomics and Chemical Biology, Cambridge, USA

Background: A central focus of preclinical drug discovery is the thorough characterization of lead compounds. This is a key step that helps ensure that drug candidates are worthy of clinical testing. In addition to phenotypic characterization, quantitative profiling of drug-protein interactions is a major hurdle during preclinical lead optimization.

Traditionally, the gold standard technique informing structure-based drug design has been x-ray crystallography, despite the fact that under crystallization conditions protein conformation is frozen and aspects of protein structural transitions are neglected by this approach. More recently, hydrogen-deuterium exchange (HDX) has emerged as an alternative tool to profile ligand-protein interactions. While correlation of HDX-profiles with functional readouts provides valuable insights into structure-activity relations (SAR), the method itself can be laborious with extensive optimization required to generate high quality data.

To address some of these shortcomings, we developed a high-throughput approach based on limited proteolysis (LiP) and next-generation quantitative mass spectrometry that enables the dissection of drug-protein interactions at peptide-level resolution.

Methods: To simulate the complex protein mixture obtained from cell lysis, purified recombinant proteins were spiked into a cell lysate background. Next, the mixtures were incubated with the compounds of interest at increasing concentrations. The samples were subjected to limited digestion with proteinase K and subsequently processed to peptides with trypsin for LC-DIA-MS analysis.

Results: High-Resolution Limited Proteolysis (HR-LiP) was established using calmodulin and its robust interactions with Ca²⁺ ions and CAMKII peptide as a model system. From here, we expanded the technique to small molecule-protein interactions of established, druggable protein targets spanning several protein classes.

Herein we demonstrate that using HR-LiP we are able to identify binding sites of various compound classes on their target proteins including well characterized small molecules such as the BRD4 inhibitor JQ1. HR-LiP data are in good accordance with orthogonal HDX-MS, NMR and X-ray studies.

Conclusions: We demonstrate that HR-LiP can be used to dissect small molecule-protein binding characteristics with a resolution of 5–10 amino acids. Quantitative properties of the binding events are accurately recapitulated in dosage series and can therefore be deployed to rank and compare different compounds and compound classes. The ability to deal with complex backgrounds and unpurified proteins enables its application on difficult-to-purify or unstable proteins, and potentially multi-protein complexes. We envision the application of HR-LiP as a routine approach for target validation and lead optimization in small molecule drug discovery pipelines.

Conflict of interest:

Corporate-sponsored Research: Yuehan Feng, Nigel Beaton, Roland Bruderer and Lukas Reiter are employee of Biognosys AG. Jagat Adhikari, Ron Tomlinson and Ivan Cornella-Taracido are employee of Cedilla Therapeutics.

146 Transition state analogue of MTAP extends lifespan of APCMin/+ mice

Poster

R. Firestone¹, V. Schramm². ¹Icahn School of Medicine at Mount Sinai, Medicine, New York, USA; ²Albert Einstein College of Medicine, Biochemistry, Bronx, USA

Methylthio-DADMe-Immucillin-A (MTDIA) is an 86 pM transition state analogue of human 5 ϕ -methylthioadenosine phosphorylase (MTAP). 5 ϕ -Methylthioadenosine (MTA) is formed in polyamine synthesis and is recycled by MTAP to S-adenosyl-L-methionine (SAM) via salvage pathways. MTDIA treatment causes accumulation of MTA, an inhibitor of human head and neck (FaDu) and lung (H359, A549) cancers in immunocompromised mouse models. We investigated the efficacy of oral MTDIA as an anti-cancer therapeutic for intestinal adenomas in immunocompetent APC^{Min/+} mice, a murine model of human Familial Adenomatous Polyposis. APC^{Min/+} mouse lifespan nearly doubled when treated with an optimal daily oral dose of 20 mg/kg/day MTDIA. Oral MTDIA reduced tumor burden and markedly improved anemia. Metabolomic analysis of treated mice showed no changes in polyamine, methionine, SAM or ATP levels when compared with control mice but indicated a >4-fold increase in levels of MTA, the MTAP substrate. *In vitro* experiments generated an MTDIA-resistant FaDu cell line in culture. Genomic analysis of resistant cells showing 4-fold gene amplification of the methionine adenosyl transferase (MAT2A) locus. We hypothesize that MTDIA exerts its anti-cancer effects by increasing cellular concentrations of MTA, inhibiting PRMT5-mediated histone methylation and intron splicing to slow cancer cell growth. Oral dosing of MTDIA may provide a monotherapy for delaying the onset and progression of colorectal cancers in Familial Adenomatous Polyposis. MTDIA causes a chemical knock-out of MTAP and may therefore also have efficacy in combination with inhibitors of MAT2A or PRMT5, known synthetic-lethal interactions in cancer cell lines.

No conflict of interest.

POSTER SESSION

Drug Resistance and Modifiers

147 Repotrectinib increases KRAS-G12C inhibitor effectiveness via simultaneous inhibition of SRC, FAK, and JAK2

Poster

B. Murray¹, W. Deng¹, D. Zhai¹, N.V. Lee¹, L. Rodon¹. ¹Turning Point Therapeutics, Cancer Biology & Translational Research, San Diego, USA

Background: The KRAS^{G12C} gain-of-function mutation occurs in 13% of lung, 3% of colorectal, and 2% of other cancers. KRAS-G12C inhibitors

AMG510 and MRTX849 have clinical activity in patients harboring a KRAS^{G12C} mutation, however, the durability of response is attenuated by the onset of multiple resistance mechanisms. Feedback-mediated activation of upstream receptor tyrosine kinases (RTK) in concert with the co-activation of the PI3K/AKT signaling pathway is proposed to bypass MAPK pathway dependence. SRC/FAK signaling promotes tumor cell survival by activation of the PI3K/AKT survival pathway. In addition, oncogenic KRAS induces secretion of various cytokines and growth factors by tumor cells leading to a tumor promoting microenvironment. Tumor cell cytokine secretion is driven, in part, through JAK2/STAT3 signaling. Therefore, combination of KRAS-G12C inhibitors with agents that simultaneously inhibit SRC, FAK, and JAK2 could suppress drug resistance as well as attenuate oncogenic stromal remodeling.

Material and methods: *In vitro* and *in vivo* models of KRAS^{G12C} cancer are used to evaluate KRAS-G12C inhibitor combinations with repotrectinib, a next generation ROS1/TRK/ALK inhibitor with SRC/FAK/JAK2 inhibitory potencies at clinically relevant exposures.

Results: The combination of repotrectinib and AMG510 potentially inhibits activation of SRC, FAK, STAT3, AKT, and ERK in KRAS^{G12C} non-small cell lung cancer (NSCLC) cells and a xenograft tumor model at clinically relevant exposures. Repotrectinib/AMG510 suppresses more KRAS signaling nodes than AMG510 combinations with dasatinib, defactinib, or ruxolitinib and therefore affects a broader signaling network. Repotrectinib/AMG510 synergistically decreases KRAS^{G12C} NSCLC cell viability and induces apoptosis more robustly relative to either single agent treatments or AMG510 combinations with inhibitors that have a subset of repotrectinib activities. A rapid adaptive RTK feedback reactivation occurs in response to AMG510 which is suppressed by repotrectinib. Tumor cell cytokine secretion is suppressed by repotrectinib implicating tumor extrinsic effects. In the H358 KRAS^{G12C} xenograft tumor model, repotrectinib has single agent activity and enhances AMG510 efficacy in combination. Significant combination activity is observed in the KRAS-G12C inhibitor resistant LU11693 PDX tumor model. In a survival study using the H2122 xenograft tumor model, repotrectinib significantly prolongs survival for both moderate (10 mg/kg) and high dose (30 mg/kg) AMG510 treatment groups.

Conclusions: In preclinical studies, simultaneous inhibition of SRC/FAK/JAK2 by repotrectinib has a range of effects that synergize with KRAS-G12C inhibitor pharmacology and suppress mechanisms of resistance. Further investigation for the potential to increase the duration of response for KRAS-G12C inhibitor therapies is warranted.

Conflict of interest:

Ownership: All of the authors are employees of Turning Point Therapeutics.

148

Poster

Discovery proteomics detects expression trends associated with resistance to the most commonly used chemotherapies in esophageal adenocarcinoma

S. Mittal¹, J. Abdo², D. Agrawal³. ¹St. Joseph's Hospital and Medical Center, Norton Thoracic Institute, Phoenix, USA; ²Stella Diagnostics- LLC, Research and Development, New York, USA; ³Western University of Health Sciences, Translational Research, Pomona, USA

Background: The rate of incidence of esophageal adenocarcinoma (EAC) is increasing faster than any cancer in the United States, and the survival rates have remained very low for decades, even in the current era of molecular medicine. Despite a dozen chemotherapeutic treatment options currently used for EAC, durable patient responses to anticancer therapies are hard to achieve in these cohorts. Indeed, a study in 2014 found no survival advantage for EAC patients treated with chemotherapy. A large-scale mass spectrometric experiment was designed to detect proteomic expression patterns that may contribute to the robust chemoresistance observed in EAC tumors.

Materials and Methods: Formalin fixed paraffin embedded (FFPE) tissue was cut at 10 microns with one 5µm section stained with H&E. Twenty EAC tumors and 20 normal esophageal samples were analyzed in this study. The serially sectioned unstained slides were microdissected with the guidance of a board-certified pathologist. Dissected cells were heated with proprietary buffers to break formalin cross-links, trypsinized, and reduced with DTT. All samples were analyzed by reverse-phase high-pressure liquid chromatography electrospray ionization tandem mass spectrometry (RP-HPLC-ESI-MS/MS) using a 6600 TripleTOF spectrometer. Overexpression was confirmed in a selected biomarker via immunofluorescence. Gene knockdown of the marker and subsequent cytotoxicity and proliferation (MTT) assays were completed using OE-33 cell lines.

Results: The expression trends of seven markers that are associated with resistance to cisplatin were detected ($P < 0.0001$). Two markers, which were downregulated significantly when comparing EAC tissue to normal

squamous epithelium, are associated with decreased sensitivity to taxanes ($P < 0.0001$). The upregulation of two other markers, which overexpression is associated with increased resistance to 5-fluorouracil, were also discovered ($P < 0.0001$). The expression pattern of a selected marker was confirmed with immunofluorescence, and knockdown of the associated gene yielded increased cytotoxicity and decreased proliferation in OE-33 esophageal cancer cells.

Conclusions: The three most common classes of drugs used for EAC are platinum-based (95%), anthracyclines (63%), and taxanes (37%). Here we have discovered a network of consistently downregulated or overexpressed biomarkers that may contribute to broad resistance against these chemotherapies during the course of treatment for EAC. These findings demonstrate a clinical need for actionable molecular diagnostics and new targeted therapy options for EAC patients. Additional studies are required to confirm these markers as major players in the low efficacy of chemotherapy regimens against solid tumors of the esophagus.

Conflict of interest:

Ownership: Stella Diagnostics, LLC.

149

Poster

Secondary resistance to the PI3K inhibitor copanlisib in marginal zone lymphoma

A. Arribas¹, S. Napoli¹, L. Cascione¹, E. Gaudio¹, R. Bordone-Pittau², M. Barreca³, G. Sartori¹, T. Chiara¹, F. Spriano¹, A. Rinaldi¹, A. Stathis⁴, G. Stussi⁵, D. Rossi⁴, Z. Emanuele⁴, F. Bertoni¹. ¹Faculty of Biomedical Sciences- USI, Institute of Oncology Research, Bellinzona, Switzerland; ²Oncology Institute of Southern Switzerland, Ematologia - Laboratori di ematologia EOLAB, Bellinzona, Switzerland; ³University of Palermo, Department of Biological- Chemical and Pharmaceutical Sciences and Technologies, Palermo, Italy; ⁴Faculty of Biomedical Sciences- USI, Oncology Institute of Southern Switzerland, Bellinzona, Switzerland; ⁵Oncology Institute of Southern Switzerland, Ematologia - Unità leucemie IOSI, Bellinzona, Switzerland

Background: PI3K kinase has a prominent role in the B-cell receptor signaling. Copanlisib, a pan-PI3K inhibitor with predominant selectivity to PI3K α and PI3K δ , is Food and Drug Administration (FDA) approved for the treatment of patients with relapsed or refractory follicular lymphoma, and it is currently under clinical development in other indolent lymphomas including marginal zone lymphoma (MZL). However some patients might eventually relapse because of acquired resistance and so a better understanding of resistance mechanisms is needed. Thus we generated MZL cell lines resistant to copanlisib which could help to design improved therapies.

Materials and Methods: Cells from VL51 line were treated with no drug (parental, PAR) or high concentrations of copanlisib (IC90) until acquisition of resistance (RES). Sensitivity to vincristine ruled out multi-drug resistance and MTT assay after 3-weeks of drug-free culture confirmed stable resistance. Transcriptome profiling (RNA-Seq) and immunophenotypic analysis were performed in PAR and RES cells.

Results: RES models from VL51 cell line exhibited over 50-fold times higher IC50 s than PAR counterparts. The mechanism observed here might drive resistance to others downstream B-cell receptor inhibitors since sensitivity to other PI3K inhibitors such as duvelisib (50-fold) and idelalisib (5-fold), to the BTK inhibitor ibrutinib (15-fold) was decreased in RES. Transcriptome analyses of RES revealed overexpression of negative regulators of apoptosis (CD44, JUN), cytokine signaling (IL1A, IL1B, CXCR4), NFkB (LTA, TNF), MAPK (RASGRP4, RASGRP2) and JAK-STAT (STAT3, JAK3) signaling pathways; while genes involved in cell adhesion (ITGA4, ITGB1), antigen presentation (HLAs) and IFN response (PARP12, GBP6) were repressed in RES. Accordingly to the elevated expression of anti-apoptotic signaling genes, RES cells were resistant to the BCL2-inhibitor venetoclax, either as a single as in combination with copanlisib. Paired with transcript expression, RES exhibited increased surface expression of CXCR4 and repression of CD49d, CD20 and CD81 by flow-cytometry. Finally, combination of copanlisib with a CXCR4 inhibitor overcome resistance.

Conclusions: We have developed and characterized a preclinical model of secondary resistance to the PI3K inhibitor copanlisib in splenic marginal zone lymphoma. We have also identified novel potential targets, including IL1 and CXCR4, that are worth of further investigations. The current work provides new insights into the mechanisms of resistance to copanlisib and can lead to novel therapeutic approaches to overcome the resistance.

No conflict of interest.

150

Poster

Glucocorticoid receptor antagonism overcomes resistance to BRAF inhibition in BRAFV600E-mutated metastatic melanomaE. Obrador¹, J.M. Estrela¹, R. Salvador¹, P. Marchio¹, S.L. Valles¹, R. Lopez-Blanch¹, M. Benlloch², J. Alcacer³, C.L. Perez⁴, J.A. Pellicer¹.¹University of Valencia, Physiology, 46010 Valencia, Spain; ²San Vicente Martir Catholic University, Health & Functional Valorization, 46001 Valencia, Spain; ³Quiron Hospital, Pathology Laboratory, 46010 Valencia, Spain; ⁴Institute of Basic and Preclinical Sciences Victoria de Giron, Biochemistry, 3102146 La Habana, Cuba

Clinical applications of glucocorticoids (GC) in Oncology are dependent on their pro-apoptotic action to treat lymphoproliferative cancers, and to alleviate side effects induced by chemotherapy and/or radiotherapy. However, the mechanism(s) by which GC may also promote tumor progression remains unclear. GC receptor (GR) knockdown decreases the antioxidant protection of highly metastatic B16-F10 melanoma cells. We hypothesize that a GR antagonist (RU486, mifepristone) could increase the efficacy of BRAF-related therapy in BRAF^{V600E}-mutated metastatic melanoma. *In vivo* formed spontaneous skin tumors were reinoculated into nude mice to expand the metastases of different human BRAF^{V600E} melanoma cells. The GR content of melanoma cell lines was measured by [³H]-labeled ligand binding assay. Nuclear Nrf2 and its transcription activity was investigated by RT-PCR, western blotting, and by measuring Nrf2- and redox state-related enzyme activities and metabolites. GR knockdown was achieved using lentivirus, and GR overexpression by transfection with the NR3C1 plasmid. shRNA-induced selective Bcl-xL, Mcl-1, AKT1 or NF-κB/p65 depletion was used to test the efficacy of vemurafenib (VMF) and RU486 against BRAF^{V600E}-mutated metastatic melanoma. During early progression of skin melanoma metastases, RU486 and VMF induced a drastic metastases regression. However, treatment at an advanced stage of growth demonstrated the development of resistance to RU486 and VMF. This resistance was mechanistically linked to overexpression of specific proteins of the Bcl-2 family (Bcl-xL and Mcl-1 in our experimental models). We found that melanoma resistance is decreased if AKT and NF-κB signaling pathways are blocked. Our results highlight mechanisms by which metastatic melanoma cells adapt to survive.

No conflict of interest.

151

Poster

Role of miR-21 in chemotherapeutic drug resistance of oral squamous cell carcinomaN. Chatterjee¹, S. Roy¹, A. Das¹. ¹CNCI, RBTM, Kolkata, India

Background: Head and neck carcinoma spreads malignancies tumors arising from the epithelium or squamous covering the upper aerodigestive tract including oral that metastasize to other organs. The oral squamous cell carcinoma primarily addressing Head and neck carcinoma cancer that could affect the majority of older people with approximately 650,000 new cases per year. The consumption of alcohol and tobacco might be the prime cause of OSCC risk. But the recurrence or relapse of the malignancies is the major obstacle of the convention chemotherapeutic drug like paclitaxel or carboplatin. We know the circulating miRNAs is noted as the potential biomarkers of OSCC but their role in drug resistance is yet to reveal. In the present study, an attempt made to find the expression of miR-21 in serum/whole blood of relapse OSCC (rOSCC) and newly identified OSCC (nOSCC) (N = 40). The expression of miR-21 was evaluated in relation to different demographical and clinicopathological features aiming to identify correlation with relapse and their cancer clinical stages (perineural invasion and N-stage).

Material and Methods: The relative expression level of miR-21 was determined by quantitative real-time RT-PCR (qRT-PCR) in the sera of rOSCC, nOSCC patients (n = 20/each group) with respective healthy subjects as a control. Association between the expression of miR-21 and rOSCC/nOSCC clinical stages was identified with Immunofluorescence/IHC of relapse stages and analyzed demographical parameters.

Results: The results obtained by chi-square revealed a significant increase in the expression level of miR-21 in rOSCC/nOSCC. The study also revealed the positive correlation between higher miR-21 expression and tobacco consumers. The over expression of α-SMA also identified in relapse cases of advanced stages in Immunofluorescence/IHC. The statistical test, ANOVA has also indicated a positive correlation between up-regulation of miR-21 in the clinical stages of the relapse cases.

Outcome: The present study indicated higher expression of circulating miR-21 in the serum of OSCC (relapsed/newly identified), this study also revealed the positive correlation between miR-21 expression in rOSCC/nOSCC patients. Other findings suggested a significant increase

(p = 0.0001) in the expression of miR-21 of rOSCC in clinical staging (I-IV) of metastasis. We also examined the hazard ratio for disease free survival in relation to clinical and histological characteristics. Only nodal spread, perineural invasion, and high stage were associated with reduced disease-free survival. More studies are needed to validate it as potential diagnostic and prognostic biomarker for relapsed and resistance for development therapy.

No conflict of interest.

152

Poster

c-Met activation leads to the establishment of a TGFβ-receptor regulatory network required for bladder cancer invasionP. Eichhorn¹. ¹Curtin University, School of Pharmacy and Biomedical Sciences, Perth, Australia

Background: Treatment of muscle-invasive bladder cancer remains a major clinical challenge. Aberrant HGF/c-MET upregulation and activation is frequently observed in bladder cancer correlating with cancer progression and invasion. However, the precise mechanisms underlying HGF/c-MET mediated invasion in bladder cancer remains unknown.

Material and Methods: To gain an understanding in the role of HGF induced invasion we compared changes in cell plasticity with early transcriptomics following HGF treatment in bladder cancer cell lines.

Results: As part of a negative feedback loop SMAD7 binds to the E3 ligase SMURF2 targeting the TGFβ receptor for degradation. Under these conditions SMAD7 acts as a SMURF2 agonist by disrupting the intramolecular interactions within SMURF2. We demonstrate that HGF stimulates TGFβ signalling by inducing c-SRC-mediated phosphorylation of SMURF2 at two tyrosine residues impeding SMAD7 binding and enhancing SMURF2 C2-HECT domain interaction, resulting in SMURF2 inhibition and TGFβ receptor stabilization. Interestingly we demonstrate that this phosphorylation on SMURF2 acts as a bi-modal switch transitioning the cells from a MAPK dependent pro-proliferative state to a TGFβ dependent invasive state. This upregulation of the TGFβ pathway by HGF leads to TGFβ-mediated Epithelial-Mesenchymal Transition (EMT), invasion, and metastasis. Furthermore, analysis of patient derived samples indicates a clear correlation with HGF pathway activation and TGFβ induction leading to invasion. Using orthotopic mouse models we show that inhibition of TGFβ signalling completely prevents HGF induced bladder cancer invasion. Furthermore, we make a rationale for the use of combinatorial TGFβ receptor kinase and MEK inhibitors in the treatment of high-grade non-muscle-invasive bladder cancers or early stage muscle invasive bladder cancers.

Conclusions: Our study reveals a functional requirement for TGFβ signalling in HGF/c-MET-mediated bladder cancer invasion and metastasis. In addition our findings suggest that combined treatment with TGFβ receptor and MAPK inhibitors is warranted in early stage bladder cancers.

No conflict of interest.

153

Poster

Chitinase-like proteins as candidate markers for tamoxifen responsivenessN. Babyshkina^{1,2}, T. Dronova^{1,2}, N. Fedulova¹, S. Patalyak¹, J. Kzyshkowska^{2,3}, N. Cherdyntseva^{1,2}. ¹Cancer Research Institute-Tomsk National Research Medical Center, Department of Molecular Oncology and Immunology, Tomsk, Russian Federation; ²National Research Tomsk State University, Department of Translational Cellular and Molecular Biomedicine, Tomsk, Russian Federation; ³Institute of Transfusion Medicine and Immunology, Medical Faculty Mannheim University of Heidelberg, Mannheim, Germany

Background: The interplay between the tumor cells and regulatory microenvironment proteins such as chitinase-like proteins YKL-39, YKL-40, SI-CLP and stabilin-1 may play a critical role in the disease progression and response to treatment. The aim of this study was to examine the expression levels of the *CHI3L2*, *CHI3L1*, *CHID1*, *STAB1* gene coding chitinase-like proteins in relation to tamoxifen treatment in hormone-receptor positive breast cancer patients; and the relationship between these levels and expression of Akt1-associated genes.

Material and methods: We performed gene expression analysis by qRT-PCR on two cohorts of fresh frozen breast cancer samples derived from 64 patients who either developed distant metastasis or recurrence during the adjuvant tamoxifen therapy (tamoxifen resistance group – TR) or had responsive to tamoxifen treatment (tamoxifen sensitive group – TS). The primary outcome was progression-free survival.

Results: *CHI3L2*, *CHID1* and *STAB1* gene expression levels were higher in TS patients (10.54 ± 3.48 ; 9.19 ± 4.57 and 3.95 ± 1.59 , respectively) compared with the TR group (4.37 ± 3.38 ; 0.51 ± 0.14 and 0.29 ± 0.14 , respectively) with borderline statistical significance. A significant positive correlation in tamoxifen sensitive group between *STAB1* and *PTEN* mRNA was found ($r = 0.51$; $p = 0.0003$). We showed statistically significant correlation between mRNA expression of all investigated Akt1-associated genes (*ESR1*, *Akt1* and *PTEN*) and the *CHID1* transcriptional activity ($r = 0.282$, $p = 0.031$; $r = 0.296$, $p = 0.025$, and $r = 0.274$, $p = 0.031$; respectively). A high expression level of both *CHID1* and *Akt1* genes was associated with low survival rates in breast cancer patients (log-rank $p = 0.031$ and log-rank $p = 0.044$; respectively).

Conclusion: Our preliminary findings suggest that chitinase-like proteins may be involved in the tamoxifen resistance/sensitivity via Akt1-dependent signaling.

The study was supported by the Russian Scientific Foundation, grant #19-75-30016

No conflict of interest.

POSTER SESSION

Drug Screening

154

Poster

Potential lung cancer therapy using plant derived cholesterol structural analogs

D. Perez¹, A. Torres¹, M. Milian¹, Y. Inostroza¹, Y. Delgado¹. ¹San Juan Bautista School of Medicine, Biochemistry and Pharmacology, Caguas, Puerto Rico

The acquired multidrug resistance syndrome (MDRS) is one of the leading causes for the failure of chemotherapy in lung cancer. Recently plant-derived triterpenoids (eg, cholesterol-structural analogs) have showed a wide spectrum of pharmacological activities. In addition, in different studies, anticancer agents have been combined to cholesterol moieties to improve their cellular uptake and target specificity. Herein, we investigated the cytotoxic activity of various triterpenoids cholesterol analogs: oleanolic acid (OleA), ursolic acid (UrA), betulinic acid (BeA), asiatic acid (AsA), lupeol (Lupe), stigmasterol (Stg) and β -sitosterol (β -Sito) on non-small lung adenocarcinoma cells (A549) and normal lung cells (MRC5). From our studies, the IC50 for most of these cholesterol-analogs were in the low μ M range after 24 h of incubation. β -Sito and Stg did not show any significant cytotoxic pattern in this μ M range. In addition BeA and OleA showed the highest therapeutic indexes comparing the cytotoxic effect in A549 vs MRC5 cells. Metabolic activity assays were performed to determine the mechanism of action of these natural compounds. Caspases activity and cell membrane integrity assays were performed and all the cytotoxic triterpenoids induced no activation of caspase-3, and high membrane permeabilization. Gene expression assays of MDRS-related genes (EGF, VEGF, Pgp, Bcl-2, P53, NDRG1, GLIPR1) demonstrated the down regulation of some of these genes after the incubation with these triterpenoids. These results demonstrated that even slight structural changes in these cholesterol analogs can influence the cytotoxic response and cellular mechanistic pathways. Complete results will be presented. This study opens promising perspectives for further research on the role of phytochemical triterpenoids, which ultimately will contribute to a more rational application in cancer therapy.

No conflict of interest.

POSTER SESSION

Epigenetic Modulators

(HDAC Bromodomain modulators, EZH2)

155

Poster

Clinical significance of c-MYC/EZH-2 expression and Merlin loss

A.M. Arslan¹, S. Paydas², D. Gümrüdü³, E. Bağır³, C. Mirili⁴. ¹Baykan Public Hospital, Internal Medicine, Siirt, Turkey; ²Cukurova University Faculty of Medicine, Medical Oncology, Adana, Turkey; ³Cukurova University Faculty of Medicine, Medical Pathology, Adana, Turkey; ⁴Atatürk University Faculty of Medicine, Medical Oncology, Erzurum, Turkey

Aim: Malignant mesothelioma (MM) is an aggressive tumor originating from pleural, peritoneal or perikardiyal cavities. Although the most powerful prognostic factors are stage and histologic subtypes there is need to find prognostic and/or predictive factors for targeted treatment. The aim of this study is to explore the association between known prognostic factors and also prognostic significance of EZH-2, c-MYC and Merlin in MM.

Patients and methods: Sixty seven patients with MM followed by Çukurova University Faculty of Medicine Dept of Oncology were evaluated retrospectively. Demographic properties of the 67 patients including asbest exposure, smoker history, tumor localization, histopathologic type, treatment modalities, ECOG performance status and disease stage were evaluated. EZH-2, c-MYC and Merlin expressions were evaluated by immunohistochemistry (IHC) Expression and/or loss of EZH-2, c-MYC and Merlin were compared with demographic/clinical findings and survival times. IBM SPSS version 20.0 was used for statistical analyses. Cut off level for XH-2 was 30%. c-MYC and Merlin were evaluated according to staining intensity as weak (1-19%), moderate (20-59%), strong (60-100%).

Findings: Female/male ratio was 38/29, mean age was 60.3 ± 10.5 . The majority of the cases had epitheloid type MM (54 cases), 11 had biphasic and 2 had sarcomatoid type. Median overall survival was longer in women, in early stage disease, in non-smokers, in good performance status and in cases with epitheloid type MM.

Merlin loss was not found to be associated with overall survival (OS) and progression free survival (PFS). Strong EZH-2 expression with 30% cut off level was found to be associated with shorter overall survival. Strong c-MYC expression was found to be associated with shorter overall survival. Interestingly double expression for EZH-2 and c-MYC was found to be associated with shortest survival while double negative cases had longest survival. Histologic subtype, stage, ECOG performance status and EZH-2 were found to be prognostic in multivariate analysis.

Conclusion: EZH-2, c-MYC and Merlin expressions were detected by IHC in biopsy specimens. EZH-2 and c-MYC expressions were found to be associated with shorter PFS and OS times. However our results must be validated with further studies. It is well known that EZH-2 inhibitors and also c-MYC inhibitors have been found to be successful in some types of tumors. We can propose that inhibition of EZH-2 and/or c-MYC may be an important therapeutic alternative in cases with MM.

No conflict of interest.

156

Poster

The role of enhancer RNAs in glioblastoma multiforme

B. Akobundu¹, J. Zepecki², E. Fajardo³, A. Fiser³, S. Toms⁴, N. Tapinos⁵.

¹Brown University, Molecular Pharmacology & Physiology and Biotechnology, Providence, USA; ²Brown University, Pathobiology, Providence, USA; ³Albert Einstein College of Medicine, Systems and Computational Biology, Bronx, USA; ⁴Brown University/Rhode Island Hospital, Neurosurgery, Providence, USA; ⁵Brown University/Rhode Island Hospital/Laboratory of Cancer Epigenetics and Plasticity, Neurosurgery, Providence, USA

Background: Glioblastoma Multiforme (GBM) represents the most aggressive type of human brain cancer with dismal prognosis. Studies have revealed the presence of self-propagating cancer stem cells which exhibit increased phenotypic plasticity under the influence of the tumor microenvironment. Common therapies for GBM include surgical resection, radiation and adjuvant chemotherapy. Despite these therapeutic efforts, GBM has a 5-year survival of about 5%. Although DNA (genetic) variations account for 30–50% of the abnormalities identified in GBM and other cancers, epigenetic abnormalities such as histone modifications and non-coding RNA species account for the remaining drivers of cancer. A decade ago, a new class of non-coding RNA termed enhancer RNA (eRNA) was discovered. It is accepted that the combinatorial binding of RNA Pol II and the histone mark H3K27Ac at specific enhancer regions mark active enhancers that can produce eRNAs. Multiple articles have demonstrated the presence and role of eRNAs in breast cancer, prostate cancer and macrophages; the main role being the regulation of gene transcription through stabilization of enhancer-promoter looping. However, the functional role of eRNAs in the maintenance of the glioma stem cell fate and the contribution of eRNAs to the reversible phenotypic transition of glioma stem cells are not known. We hypothesize that eRNAs are expressed in glioma stem cells and may modulate the activity of neighboring and stemness essential genes as well as regulate genome organization.

Materials and Methods: We used Chromatin Immunoprecipitation Sequencing (ChIP-Seq) for RNA Pol II and H3K27Ac to identify the presence of eRNAs in patient-derived glioma stem cells. Next, we validated the expression levels of eRNAs in the stem cells as well as patient-derived glioma tissue samples. We further correlated expression of the eRNAs to patient survival to determine their clinical significance. We inhibited one of

the clinically relevant eRNAs in order to understand its functional implication for glioma stemness using two different RNA interference approaches: Antisense Locked Nucleic Acid (LNA) Gapmer and short hairpin RNA (shRNA) lenti-viral vectors.

Results: Our ChIP-seq data showed that there are (15) stem-cell specific eRNAs among our stem cell samples. Further analysis showed that (5) of these eRNAs have significant implications for patient survival. Of the (5) candidates, one was successfully inhibited and appears to affect the expression of both the corresponding gene and other genes that are important for cell stemness and development.

Conclusions: Taken together, our work so far implicates eRNAs as novel epigenetic regulators of human glioma stem cells. Moreover, manipulation of these RNAs can be ideal target for designing tailored RNA therapeutics for human glioblastoma.

No conflict of interest.

157

Poster

DNA methyltransferases drive gastric cancer growth and present a therapy target for gastric cancer

A. Huber¹, C. Dijkstra¹, M. Ernst¹, M. Eissmann¹. ¹Olivia Newton-John Cancer Research Institute, Cancer and Inflammation, Melbourne, Australia

Background: Gastric cancer (GC) remains the third leading cause of cancer-related death worldwide. While inflammation is a well-established driver of gastric tumorigenesis, only a small subset of GC patients responds to immunotherapy. The understanding of the tumour microenvironment, which suppresses anti-tumour immune responses, is a field of great interest. One proposed mechanism of immune escape is silencing tumour-antigen expression by DNA methylation, and thereby avoiding immune recognition. DNA methyltransferases (DNMTs) are the enzymes responsible for DNA methylation and hence, for the epigenetic silencing of gene expression of tumour-antigens and other immune-related molecules. DNMTs are often overexpressed in solid tumours. Epigenetic drugs inhibiting these DNMTs have shown anti-tumour effects in combination with immune checkpoint inhibitors by re-activating the expression of tumour antigens, amongst others. Here we are studying the role of DNMTs in GC mouse models and the possibility of combining DNMT inhibitors with immunotherapy for the treatment of GC.

Material and Methods: This project utilises various mouse models of GC. The Gp130^{Y757F/Y757F} (gp130^{FF}) mutant mouse model develops spontaneous inflammation-driven gastric adenomas. We established a gp130^{FF} Dnmt3a-overexpressing gastric cancer mouse model (gp130^{FF}, A33^{Dnmt3a}) where Dnmt3a overexpression occurs in gastric tumours. In a second mouse model, mutant *Kras*, *Pi3kca* and *Tp53* expression results in highly advanced invasive gastric carcinoma formation (KPT model). We successfully established gastric cancer organoids of one of these triple mutant tumours (KPT organoids) which can be injected subcutaneously into wild type mice and result in allograft tumour formation.

Results: DNMT3A overexpression was detected in human GC specimen and associated with bad overall survival of patients. Gastric adenomas of our gp130^{FF}, A33^{Dnmt3a} mouse model have a 10-fold elevated Dnmt3a expression. Importantly, tumour-specific Dnmt3a overexpression significantly increased gastric tumour burden. In the KPT model, we have identified DNMT3A as being highly expressed in the invasive front of tumours, their liver metastases as well as in the allograft tumours established by the KPT organoids. In this model of advanced gastric cancer, treatment with the DNMT inhibitor decitabine significantly decreased tumour growth and we are currently investigating the efficacy of decitabine in combination with anti-PD-1 immunotherapy.

Conclusion: Taken together, we provide evidence for a driver function of Dnmt3a in gastric tumorigenesis and gastric tumour growth. In addition, we demonstrate the vulnerability of an aggressive gastric carcinoma model to DNMT inhibition and hence its non-oncogene addiction to DNMTs. Therefore, our findings encourage further studies to investigate the potential of DNMT inhibitors for the treatment of GC.

No conflict of interest.

158

Poster

Epigenetic regulation of epithelial-to-mesenchymal transition as a captain of journey of cancer from lung to brain

Y.M. Lee¹, S.H. Kim², M.S. Kim³, Y.Z. Kim¹. ¹Sungkyunkwan University Samsung Changwon Hospital, Neurosurgery, Changwon, South Korea; ²Sungkyunkwan University Samsung Changwon Hospital, Medical Oncology, Changwon, South Korea; ³DGIST, New Biology, Daegu, South Korea

Background: There have been many studies for epithelial-to-mesenchymal transition (EMT) of the cancer, especially focused on the important transcriptional factors. Recently epigenetic mechanisms, including histone modification have been comprehensively studied for establishing the role on the prohibiting metastasis of cancer cell. The objective of presenting study is to investigate the epigenetic role of histone lysine methylation/demethylation on the regulating expression of the transcriptional factors of EMT in lung cancer and brain metastasis.

Material and Methods: The paired samples of NSCLC and brain metastasis were analyzed in 23 individual patients. Both samples were obtained by surgical resection or biopsy of the lung and brain. The paraffin-fixed formalin embedded (FFPE) samples was obtained at the pathological archives in our institute. The medical record (age, gender, performance status, interval of metastasis, site of extracranial metastasis, survival after diagnosis of NSCLC, and survival after diagnosis of brain metastasis) was reviewed retrospectively. In both samples of NSCLC and brain metastasis, immunohistochemical staining was performed for epithelial markers, mesenchymal markers, transcriptional factors of EMT factors, histone lysine methyltransferase, and histone lysine demethylase.

Results: The epithelial markers such as E-cadherin (24.6% vs 12.6%, p = 0.037), Desmoplakin (15.6% vs 2.3%, p = 0.007), α -catenin (41.3% vs 28.3%, p = 0.042), and β -catenin (38.6% vs 16.9%, p = 0.029) were significantly decreased in brain metastasis samples compared with NSCLC sample. The mesenchymal markers such as N-cadherin (20.6% vs 43.2%, p = 0.028), Vimentin (15.3% vs 51.6%, p = 0.004), and Fibronectin (7.6% vs 39.4%, p = 0.002) were significantly increased in brain metastasis samples compared with NSCLC sample. The immunoreactivity of transcriptional factors such as Slug (15.6% vs 42.6%, p = 0.005), Twist (23.6% vs 45.9%, p = 0.010) and ZEB1 (15.0% vs 55.9%, p = 0.002) was also increased in brain metastasis samples compared with NSCLC sample. Epigenetic inducers such as MLL4 (H3K4 methyltransferase) and UTX (H3K36 demethylase) were statistically increased and epigenetic repressor such as EZH2 (H3K27 methyltransferase) was statistically decreased in brain metastasis samples compared with NSCLC sample. The expression of UTX-ZEB1 (R2 linear = 1.204) and MLL4-Slug (R2 linear = 0.987) was increased in direct proportion and EZH2-Twist (R2 linear = -2.723) was decreased in reverse proportion.

Conclusion. This study suggested that MLL4 and UTX should epigenetically induce the expression of EMT transcriptional factor such as Slug and ZEB1 respectively, and EZH2 should epigenetically reduce the expression of EMT transcription factor such as Twist in the process of NSCLC metastasis to the brain.

No conflict of interest.

POSTER SESSION

Molecular Targeted Agents

159

Poster

Antitumor activity of tipifarnib and PI3K pathway inhibitors in HRAS-associated head and neck squamous cell carcinoma

F. Burrows¹, M. Shivani¹, Z. Wang², S. Chan¹, M. Gilardi², S. Gutkind². ¹Kura Oncology, Translational Research, San Diego, USA; ²University of California- San Diego, Department of Pharmacology, San Diego, USA

HRAS is an important driver oncogene in head and neck squamous cell carcinoma (HNSCC) and other squamous cell carcinomas. HRAS mutations are found in 4–10% of HNSCC cases and appear to represent a unique subset associated with low TP53 mutation rates, co-mutated caspase 8 and a characteristic methylation pattern. RAS proteins undergo several post-translational modifications that facilitate their attachment to membranes, including the addition of a farnesyl isoprenoid moiety by the enzyme farnesyltransferase (FT), prompting the development of FT inhibitors (FTIs) for the treatment of RAS-driven cancers. Tipifarnib is a potent and selective FTI that has demonstrated compelling antitumor activity in a heavily pretreated cohort of recurrent/metastatic HNSCC with HRAS mutations. Based on these data, a pivotal study (NCT03719690) evaluating the efficacy of tipifarnib in HRAS mutant HNSCC (AIM-HN) is currently ongoing.

HRAS is the predominant RAS isoform in squamous epithelial cells and it is commonly overexpressed in squamous cell carcinomas. In TCGA PanCancer Atlas, approximately 30% of HNSCC cases have elevated HRAS gene expression, raising the possibility that some HRAS wild-type (WT) HNSCCs may also display some dependence on the oncoprotein. The PI3K-AKT-mTOR pathway is another prominent driver in HNSCC, with TCGA reporting a combined mutation/amplification rate of 29% and a remarkable negative correlation between HRAS and PIK3CA expression (p = 2.5e-32), suggesting cooperativity between the two. In this study we

explored the activity of tipifarnib in cellular models and six HRAS-mutant and twelve HRAS WT HNSCC patient-derived xenograft models alone and in combination with clinical stage inhibitors of PI3K- α (alpelisib), AKT (uprosertib) and mTORC1/2 (sapanisertib).

In both HNSCC lines and a congenic panel of transformed squamous epithelial cells, HRAS and PIK3CA mutations conferred resistance to inhibitors of the alternative pathway but the combination treatment was usually effective. Tipifarnib induced stasis or regression in several HRAS WT-overexpressing models, and in cases where the FTI was only moderately active, robust inhibition of tumor growth was observed in the majority of animals treated with the combination of tipifarnib and alpelisib. Similar activity was noted with combinations of tipifarnib and uprosertib or sapanisertib. Regressions with the FTI-PI3K- α inhibitor doublet were observed both in tumors that were WT or with PIK3CA mutations or amplification and in HRAS mutants that carried or lacked PIK3CA mutations, suggesting concomitant blockade of both targets may have broad and potent anti-tumor activity in HNSCC. Additional biomarkers associated with sensitivity or resistance and alterations in gene expression (by RNAseq) and oncogenic signaling following treatment either as a monotherapy or in combinations will be reported.

No conflict of interest.

160

Poster

Tilvestamab, a novel clinical stage humanized anti-AXL function blocking antibody

M. Blö¹, L. Hodneland Nilsson¹, A. Jackson¹, A. Boniecka¹, J.E. Toombs², L. Ahmed¹, P.M. Mydel³, H.P. Marti⁴, R.A. Brekken^{2,5}, H. Gabra¹, J.B. Lorens^{1,5,6}, D.R. Micklem¹, G. Gausdal¹. ¹BerGenBio ASA, BerGenBio, Bergen, Norway; ²University of Texas Southwestern Medical Center, Department of Surgery, Dallas, USA; ³University of Bergen, Department of Clinical Science, Bergen, Norway; ⁴University of Bergen, Department of Clinical Medicine, Bergen, Norway; ⁵Center of Biomarkers CCBIO, University of Bergen, Bergen, Norway; ⁶Department of Biomedicine, University of Bergen, Bergen, Norway

The AXL receptor tyrosine kinase is expressed in several hematological and solid malignancies, including acute myeloid leukemia, triple-negative breast cancer, non-small-cell lung cancer, renal cell carcinoma and pancreatic cancer. In patients, elevated levels of AXL expression in tumors is correlated with aggressive, disseminated disease and poor overall survival. AXL is important in epithelial to mesenchymal plasticity, metastasis, immune evasion and resistance to chemo- immune- and targeted therapeutics. AXL is also a key regulator of innate immune responses, serves to dampen inflammatory processes and is often expressed on pro-tumorigenic tumor infiltrating macrophages and dendritic cells. Therefore, blocking AXL function represents a promising therapeutic approach for aggressive cancer.

Here we report the development of a novel function blocking, humanized anti-AXL antibody, tilvestamab. Tilvestamab has high affinity for the extracellular IG1 domain of AXL and inhibits binding of the AXL ligand GAS6. Tilvestamab blocks GAS6-mediated AXL receptor activation and mediates receptor internalization and degradation. In cancer cells, tilvestamab reduces cell migration and invasion. Further, tilvestamab showed efficacy in a panel of mouse xenograft models. In a non-human primate dose-ranging toxicokinetic study with chronic weekly administration for 26 weeks, tilvestamab was well tolerated during dosing phase, with no abnormal necropsy findings on termination, and with predictable dose-proportional plasma pharmacokinetics, up to the highest studied dose of 25 mg/kg. Tilvestamab is currently being evaluated in a Phase I clinical study (BGB149-101; NCT03795142) in healthy volunteers to evaluate safety, tolerability and pharmacokinetics.

Conflict of interest.

Ownership: J.B. Lorens and D. Micklem has ownership interest (including patents) in BerGenBio. Corporate-sponsored Research: R.A. Brekken reports receiving a commercial research grant from BerGenBio.

161

Poster

Identification of potent small molecule allosteric inhibitors of SHP2

K. Hearn¹, V. Berdini², G. Chessari³, T.G. Davies⁴, J.E.H. Day³, C. Hamlett³, S. Hiscock³, V. Martins⁵, S. Muench¹, Y. Nakatsuru⁶, H. Ochiwa⁶, A. Price⁴, S. Rich¹, A. Shah⁵, Y. Shibata⁷, T. Shimamura⁸, T. Smyth¹, N.G. Wallis¹, N.E. Wilsher⁵, C.N. Johnson³. ¹Astex Pharmaceuticals- Cambridge- United Kingdom, Biology, Cambridge, United Kingdom; ²Astex Pharmaceuticals- Cambridge- United Kingdom, Computational Chemistry, Cambridge, United Kingdom; ³Astex Pharmaceuticals- Cambridge- United Kingdom, Chemistry,

Cambridge, United Kingdom; ⁴Astex Pharmaceuticals- Cambridge- United Kingdom, Molecular Sciences, Cambridge, United Kingdom; ⁵Astex Pharmaceuticals- Cambridge- United Kingdom, Dmpk, Cambridge, United Kingdom; ⁶Taiho Pharmaceutical Co.- Ltd- Tsukuba- Japan, Biology, Tsukuba, Japan; ⁷Taiho Pharmaceutical Co.- Ltd- Tsukuba- Japan, Dmpk, Tsukuba, Japan; ⁸Taiho Pharmaceutical Co.- Ltd- Tsukuba- Japan, Chemistry, Tsukuba, Japan

Background: SHP2 is a ubiquitously expressed protein tyrosine phosphatase required for signalling downstream of receptor tyrosine kinases (RTKs) and plays a role in regulating many cellular processes. Genetic knockdown and pharmacological inhibition of SHP2 inhibits proliferation of RTK-driven cancer cell lines and suppresses RAS/MAPK signalling. As SHP2 is a master regulator of RTK signalling and RTK deregulation often leads to a wide range of cancers, SHP2 inhibitors are therefore a promising therapeutic approach and several compounds are being tested in the clinic. Using our fragment-based screening approach, PyramidTM, we identified fragment hits binding to the tunnel region between the phosphatase domain and the C-SH2 domain of SHP2. Here we describe the optimisation of these mM fragment hits into potent SHP2 antagonists with in vitro and in vivo antitumor activity.

Materials and methods: SHP2 catalytic activity was monitored using the DiFMUP-based fluorescence enzyme assay. The anti-proliferative and MAPK pathway inhibition was characterised in RTK-driven human cancer cell lines using viability assays, ELISA, meso scale discovery (MSD) and western blotting to monitor the modulation of markers such as pERK and pRSK. The pharmacodynamic and anti-tumour activity was characterised in an EGFR-driven subcutaneous HCC827 xenograft model in vivo.

Results: Fragment hits with mM binding affinity were optimised by Fragment Based Drug Design to compounds that potently inhibit SHP2 enzyme activity with IC₅₀ values in the low nM range. Improved potency translated into a pathfinder compound which inhibited proliferation of RTK-driven cell lines with no effect in negative control BRAF-mutant cells. Further cellular characterisation showed potent inhibition of the MAPK pathway with IC₅₀s of 110nM and 43nM in pERK ELISA and pRSK MSD assays respectively as well as modulation of these markers by western blotting. In addition, pharmacodynamic and efficacy studies were conducted in mice bearing HCC827 xenografts. In line with our in vitro data, we observed MAPK pathway modulation in tumour tissue with decreases in pERK and pRSK 2 hours after oral dosing which was sustained at 6 hours. The compound treatment was well tolerated following daily oral dosing for 14 days, resulting in significant anti-tumour activity at a dose of 50 mg/kg.

Conclusions: Weak fragment hits were optimised to potent small molecule inhibitors of SHP2 with in vitro and in vivo activity in RTK-driven models. These have potential for further optimisation into clinical candidates.

No conflict of interest.

162

Poster

Combined inhibition of SHP2 and ERK enhances anti-tumour effects in preclinical models

T. Smyth¹, J. Brothwood¹, L. Fazal¹, K. Hearn¹, C. Hindley¹, C. Johnson¹, M. Jones¹, N. Kandola¹, J. Lyons¹, V. Martins¹, K. Miyadera², S. Muench¹, J. Munck¹, Y. Nakatsuru², H. Ochiwa², H. Saini¹, A. Shah¹, S. Wagner¹, N. Wilsher¹, N. Wallis¹. ¹Astex Pharmaceuticals, Discovery Research, Cambridge, United Kingdom; ²Taiho Pharmaceuticals, Discovery and Preclinical Research, Tsukuba, Japan

Background: MAPK signalling is frequently dysregulated in cancer. The pathway can be targeted by inhibition of different nodes and is tightly regulated by feedback mechanisms. Resistance to single-agent therapies frequently occurs through several different mechanisms including upregulation of receptor tyrosine kinases (RTKs), therefore, combination therapies are of interest. The Src homology region 2 (SH2)-containing protein tyrosine phosphatase 2 (SHP2) is a key regulator of MAPK pathway downstream of RTKs and upstream of RAS, whilst ERK acts at the bottom of the pathway phosphorylating multiple substrates. We investigated the potential of targeting the MAPK pathway through a combination of SHP2 and ERK inhibition in preclinical models, representing a number of different indications and genetic backgrounds.

Materials and methods: The ERK inhibitor, ASTX029, currently in a Phase I-II clinical trial (NCT03520075), and an advanced SHP2 inhibitor from our internal program were used. The effects of SHP2 and ERK inhibitors, as single-agents and in combination, on cell viability were investigated in a panel of 491 cell lines from 18 cancer indications. The panel comprised 97 KRAS-mutant cell lines cultured in 3D and 394 KRAS WT cell lines with various genetic backgrounds, cultured in 2D. IC₅₀ and maximum % inhibition

values were used to determine response rates. Effects of the combination treatment and synergy patterns were assessed using the SynergyFinder R package. *In vivo* anti-tumour effects were investigated using the MIA PaCa-2 xenograft model.

Results: Across this broad panel, 58% and 36% of the cell lines exhibited sensitivity towards single-agent ERK and SHP2 inhibitors, respectively. Many cell lines showed sensitivity to both inhibitors as expected. When treated with the combination, 32% of the cell lines that had been resistant to the single-agents became sensitive, increasing the overall responding proportion of cell lines to 76%. In addition, the response of many single-agent-sensitive cell lines was increased when treated with the combination.

We further tested the SHP2-ERK inhibitor combination *in vivo* in a MIA PaCa-2 (KRAS^{G12C}) xenograft model. Each single-agent treatment led to significant but transient stasis of tumor growth. In contrast, combined treatment resulted in significant tumor regression. Durable inhibition of MAPK signalling and an increase in cleaved PARP were also observed in the combination-treated tumors.

Conclusions: Combining SHP2 and ERK inhibitors enhanced inhibition of cell growth over single-agent therapies in a range of cell lines with similar effects observed in an *in vivo* xenograft model. These data suggest that this combined targeting of the MAPK pathway could be effective in several different tumor types and warrants further investigation in the clinic.

Conflict of interest:

Other Substantive Relationships: TS, JB, LF, KH, CH, CJ, MJ, NK, JL, VM, SM, JM, HS, AH, SW, NWi and NWA are employees of Astex Pharmaceuticals. OH, KM and YN are employees of Taiho Pharmaceuticals.

163

Poster

PDK1 inhibitor SNS-510 shows synergy with targeted cancer therapies in solid tumor and hematologic cancer models

P. Taverna¹, S. Hansen², J.A. Fox¹. ¹Sunesis Pharmaceuticals, Sunesis Pharmaceuticals, South San Francisco, USA; ²Carmot Therapeutics, Carmot Therapeutics, Berkeley, USA

Background: Phosphatidylinositol (PI) dependent kinase 1, PDK1, is a master kinase that activates other kinases important in cell growth and survival including members of the AKT, PKC, RSK and SGK families. PDK1 can interact with its substrates through both PI-dependent or PI-independent (PIF-mediated) mechanisms. SNS-510 is a potent, orally bioavailable inhibitor of active and inactive conformations of PDK1 and binds deep in the adaptive pocket. This interaction inhibits PI3K activity and perturbs the hydrophobic PIF-pocket, thereby affecting both PI-dependent and -independent pathways (Hansen Mol Cancer Ther 2015).

Methods and Results: SNS-510 was evaluated for anti-proliferative activity vs molecular features in the OncoPanel system of 300 genomically profiled cancer cell lines (Taverna Mol Cancer Ther 2019). SNS-510 showed broad activity in both solid tumor and hematologic cancer lines. Cell lines with deletions of CDKN2A/B were particularly sensitive to SNS-510. Of note, SNS-510 caused G1/S arrest in ≥100 cancer cell lines. Since PDK1 high expression has been associated with disease progression and resistance to treatment in multiple solid and hematological cancers, we investigated the combination of SNS-510 with other anticancer pathway inhibitors (i) in cancer cell lines of different origin. Each compound was assayed over a concentration range selected by single agent IC50 s (SNS-510 range 10 μM-1 nM) and proliferation was measured by standard techniques after 3-day incubation. Combination activity was evaluated by Bliss score methodology. Synergy was apparent at various concentration combinations of SNS-510 with CDK4/6i ribociclib and palbociclib in the ER+ breast cancer cell lines MCF7 (CDKN2b del, PI3Kca mut) and EFM19 (CDKN2A del, PI3Kca mut), with the BCL2i venetoclax in both the anaplastic large cell lymphoma SR (CDKN2a del) and the DLBCL-GCB SU-DHL-4 (TP53 mut) cell lines, and with the K-Ras G12C AMG-510 in the K-Ras mutated Calu-1 (lung) and Mia-PaCa-2 (pancreas) cell lines. Combination with the BTKi ibrutinib or the PI3Kdelta inhibitor umbralisib in these 2 lymphoma models did not produce strong synergy, perhaps due to partially overlapping mechanism of action.

Conclusion: SNS-510 is a potent PDK1 inhibitor with *in vitro* activity as a single agent and in combination with other anticancer agents. The observed synergies support a potential role of PDK1 inhibition to reverse resistance and/or improve activity of CDK4/6i in breast cancer, BCL2i in lymphoma and K-Rasi in G12C mutated cancers. Each combination will be further characterized in xenografts/PDXs studies.

Conflict of interest:

Other Substantive Relationships: P. Taverna and J.A. Fox are employed by Sunesis Pharmaceuticals.

164

Poster

Clinical pharmacokinetics of adavosertib in the presence or absence of PD-L1 inhibitor durvalumab in patients with refractory solid tumors

M.K. Miah¹, E. R Imedio², L. Ottesen², S. Kumar², G. Mugundu¹.

¹AstraZeneca, Clinical & Quantitative Pharmacology, Waltham, USA;

²AstraZeneca, Late Clinical Development, Cambridge, United Kingdom

Background: Adavosertib (AZD1775; AD), a highly selective WEE1 inhibitor, is mainly metabolized by CYP3A4 and FMO3. AD is a time-dependent inhibitor of CYP3A4 and weak reversible inhibitor of CYP2C8, –2C9 and –2C19. Toxicity in the initial cohort of AD and durvalumab (DB; PD-L1 inhibitor) in a Phase I study (NCT02617277) led to hypothesis that immune-mediated increase in cytokine levels and consequent suppression of CYP expression may alter AD exposure. We evaluated the impact of DB on AD pharmacokinetics (PK); safety and tolerability data were presented at ASCO 2019.

Methods: Patients were treated with various doses of AD (BID 125–175 mg, schedule B; QD 200–300 mg, schedule D; N = 5–11) with 1500 mg of DB after lead-in AD monotherapy. Schedules A and C were excluded from this analysis, because a single dose level (125 mg) of AD was evaluated. DB was administered on day 1 and AD on days 15–17 and 22–24 BID or on days 15–19 and 22–26 QD in a 28-day cycle. PK samples were collected on days 5 (lead-in), 17 (BID) or 19 (QD); interleukin 6 (IL-6) and IL-10 were measured Q2W. Power model analysis was performed with R (v3.5.1).

Results: Steady-state AUC_{0–10h} (nM·h) was similar at 125 mg (4284 ± 895 vs 4550 ± 706), 150 mg (4644 ± 1570 vs 5130 ± 2730) or 175 mg (7742 ± 2537 vs 6974 ± 3049) BID dose. Identical results were observed in PK parameters in the QD schedule, despite higher IL-6 levels. AD exposure appeared greater than dose proportional irrespective of DB; power model estimates for AUC vs dose in the presence and absence of DB were β = 1.48 (90% CI 0.181–2.78) and β = 1.70 (90% CI 0.501–2.90), respectively.

Conclusion: Although this was not a formal drug–drug interaction study, similar AD exposure in the presence or absence of DB suggests lack of significant interaction between these drugs, thus no dose adjustment is anticipated.

Conflict of interest:

Ownership: M.K. Miah, L. Ottesen, S. Kumar, and G. Mugundu are current employee at AstraZeneca and hold stocks in the company. Esteban RI was former employee at AstraZeneca and used to hold stocks in the company. Corporate-sponsored Research: This research was sponsored by AstraZeneca.

166

Poster

A novel allosteric inhibitor of phosphoglycerate mutase 1 suppresses growth and metastasis of non-small cell lung cancer

Y. Shen¹, Q. Liang¹, M.Y. Luo¹, H.Z. Chen², L. Zhou³. ¹Shanghai Jiao Tong University School of Medicine, Department of Pharmacology and Chemical Biology, Shanghai, China; ²Shanghai University of Traditional Chinese Medicine, Institute of Interdisciplinary Integrative Biomedical Research, Shanghai, China; ³Fudan University, Department of Medicinal Chemistry, Shanghai, China

Phosphoglycerate mutase 1 (PGAM1) plays a pivotal role in cancer metabolism and tumor progression via its metabolic activity and interaction with other proteins like α-smooth muscle actin (ACTA2). Allosteric regulation is considered as an innovative strategy to discover a highly selective and potent inhibitor targeting PGAM1. Here, we identified a novel PGAM1 allosteric inhibitor, HKB99, via structure-based optimization. HKB99 acted to allosterically block conformational change of PGAM1 during catalytic process and PGAM1-ACTA2 interaction. HKB99 suppressed tumor growth and metastasis, and overcame erlotinib resistance in non-small cell lung cancer (NSCLC). Mechanistically, HKB99 enhanced the oxidative stress and altered multiple signaling pathways including the activation of JNK/c-Jun, suppression of AKT and ERK. Collectively, the study highlights the potential of PGAM1 as a therapeutic target in NSCLC, and reveals a distinct mechanism that HKB99 inhibits both metabolic activity and non-metabolic function of PGAM1 by allosteric regulation.

No conflict of interest.

167

Poster

hTERT and IGF1R protein expression as possible biomarkers and molecular targets in cervical cancer

P. Moreno-Acosta¹, O. Gamboa¹, M. Molano², J. Acosta³, S. Carrillo¹, A. Romero Rojas¹, N. Magne⁴,
Research Group in Radiobiology Clinical Molecular and Cellular. ¹Instituto Nacional de Cancerología, Bogotá- D.C., Bogotá D.C., Colombia;
²Microbiology and Infection Diseases- The Royal Women's Hospital, Victoria, Melbourne, Australia; ³Pathology Group- National University of Colombia, Bogotá- D.C., Bogotá- D.C., Colombia; ⁴Department of Radiation Oncology- Institut de cancérologie de la Loire-Lucien Neuwirth, Saint-Priest en Jarez, Saint-Priest en Jarez, France

Background: The expression of the hTERT protein was studied in chronic cervicitis, intraepithelial neoplasms, and invasive cervical cancer in different studies. An increase in hTERT expression as cervical disease progresses was evidenced. This increase in hTERT expression may be due to the action of high-risk HPVs. IGF1R was previously described as a predictive biomarker of tumor aggressiveness in cervical cancer, through hypoxia-mediated phenomenon. The increasing expression reported between pre-neoplastic and neoplastic tissues suggested that IGF1R might play an early and key role in invasive cancer development. For several years our team research has studied the modulation of genes and proteins such as IGF1R, hTERT (status methylation and protein expression) among other and the presence of HPV in cervical cancer and response to treatment. The results of our studies showed that response to treatment, gene expression and protein expression in the presence of high-risk HPV and variants of HPV-16 were linked. Through these studies we contributed to the identification of predictive and prognostic biomarkers. The aim of the present study was to retrospectively report the detection of hTERT protein expression, IGF1R protein expression and HPV genotype in patients with cervical cancer and assess the relationship of hTERT protein expression with clinicopathological characteristics (age, size tumoral, stage) including response to treatment and IGF1R protein expression.

Material and methods: Type specific HPV infection was detected by using GP5+/GP6+PCR-RLB and hTERT and IGF1R protein expression was detected by immunohistochemistry in twenty one patients with invasive squamous cell carcinoma of the cervix.

Results: HPV-16 was the type more frequent followed by HPV-58 and HPV-56. hTERT protein expression was found in both cytoplasm and nucleus with equal frequency (90.4%) and IGF1R protein expression was detected in 85.7%. Our results regarding the clinicopathological characteristics analyzed, including response to treatment did not show any association with the expression of the hTERT protein, however was observed an association with IGF1R protein expression (Fisher's exact test $p = 0.041$).

Conclusions: One of the important findings in this study was the subcellular localization of hTERT and relationship between hTERT and IGF1R protein expression, therefore both hTERT and IGF1R protein expression could be used in the future as biomarkers and molecular targets in the development of new diagnostic and treatment strategies for cervical cancer, however, these findings need to be confirmed through further studies with a larger sample size.

No conflict of interest.

168

Poster

Inhibition of farnesyl transferase by tipifarnib leads to cell growth inhibition in HRAS-mutated human rhabdomyosarcoma

P. Obasaju¹, K. Pollard¹, A. Allen¹, J. Wang¹, L. Kessler², C.A. Pratilas¹.
¹The Sidney Kimmel Comprehensive Cancer Center at Johns Hopkins University School of Medicine, Division of Pediatric Oncology, Baltimore, USA; ²Kura Oncology, Kura Oncology, San Diego, USA

Rhabdomyosarcoma (RMS) is the most common soft tissue sarcoma in children and adolescents. A subset of RMS express PAX3-FOXO1 or PAX7-FOXO1 characteristic translocations, thought to be oncogenic drivers. Among the fusion-negative subset of RMS, a substantial proportion express oncogenic mutations in RAS proteins or other elements of RAS signaling pathways. Activating RAS mutations are disproportionately seen in patients with high-risk RMS, and attempts to augment combination chemotherapy have not resulted in improvement in overall survival in this poor prognosis group. Given the common finding of dysregulated RAS signaling, targeting RAS represents an attractive therapeutic approach. RAS family members require posttranslational modification for plasma membrane localization and subsequent downstream signaling. One therapeutic strategy, therefore, includes disruption of RAS protein prenylation, and

thereby its membrane localization, via inhibition of farnesyl transferase (FTase). NRAS and KRAS may utilize geranylgeranyltransferase prenylation as a bypass when FTase is inhibited, but HRAS is uniquely dependent on FTase, and therefore, tumor cells with HRAS mutations may be preferentially sensitive to the effects of farnesyltransferase inhibition (FTI). We therefore tested human RMS cell lines harboring mutations in HRAS, KRAS or NRAS, and those wild type (WT) for H- K- and N-RAS, and found that only tumor cells with oncogenic HRAS mutations demonstrate growth inhibition in two-dimensional and three-dimensional assays when treated with tipifarnib. Using immunofluorescence assays, HRAS plasma membrane localization is decreased in response to tipifarnib in HRAS-mutated RMS cell lines. We observed a reduction in phosphorylated MEK and ERK in HRAS mutated cell lines indicating effective RAS signaling inhibition. Activity of the PI3K-mTOR pathway element RPS6 is inhibited by tipifarnib in cell lines that demonstrate an antiproliferative response to the compound. Cell cycle progression is halted in the presence of tipifarnib in HRAS mutated cell lines. *In vivo* exposure to tipifarnib in HRAS-mutated RMS xenografts results in tumor growth inhibition. Therapeutic strategies targeting RAS protein prenylation may therefore provide an effective approach as an alternative to traditional chemotherapy, while improving outcomes and decreasing toxicities. Based on these data, a genomically-selected clinical trial using tipifarnib to treat pediatric patients with HRAS-mutated tumors, including RMS, would be of interest.

No conflict of interest.

169

Poster

Engineered hydrogels to elucidate contributions of matrix mechanics to esophageal adenocarcinoma and identify matrix-activated therapeutic targets

R. Cruz-Acuña¹, C. Loebel², T. Karakasheva³, J. Gabre¹, J. Burdick², A. Rustgi¹. ¹Columbia University Medical Center, Herbert Irving Comprehensive Cancer Center, New York, USA; ²University of Pennsylvania, Department of Bioengineering, Philadelphia, USA; ³Children's Hospital of Philadelphia, Division of Gastroenterology-Hepatology and Nutrition, Philadelphia, USA

Background: *In vitro* (2D) studies have revealed a stiff extracellular matrix (ECM) in association with esophageal adenocarcinoma (EAC) progression, including features of reduced drug delivery and resistance to therapy. However, these studies are limited by the lack of ability to model 3D intercellular interactions and a physiologically relevant tumor microenvironment. This underscores the need for 3D culture models that better recapitulate the human tumor microenvironment.

Methods: We have engineered a visible light-mediated stiffening hydrogel platform that supports the development of patient-derived Barrett's esophagus (BE) organoids and EAC organoids. This synthetic biomaterial platform allows temporal control over hydrogel stiffness to better recapitulate the mechanically dynamic microenvironment, and may help identify therapeutic targets in matrix stiffening-exposed EAC organoids.

Results: Our preliminary studies demonstrate that BE and EAC organoids growth and viability can be controlled by synthetic ECM biomechanical properties. This demonstrates the significance of understanding the contributions of ECM properties to EAC progression, which is inherently limited in biologically-derived materials (e.g. MatrigelTM). Furthermore, our data show that the synthetic ECM allows precise control over hydrogel stiffness as a function of visible light exposure time, and that matrix stiffening produces changes in EAC organoid growth and phenotypical characteristics while demonstrating no reduction in cell viability. Future studies involve identifying matrix-activated therapeutic targets by assessing changes in expression of tumor-associated genes (e.g. TP53, EGFR) and mediators of mechanotransduction (e.g. ROCK, YAP1) as a function of matrix stiffening, and identifying differentially expressed genes using high-throughput transcriptome sequencing between stiffened hydrogel-encapsulated BE and EAC organoid conditions.

Conclusions: Our work is significant because it establishes a biomaterial platform that overcomes the limitations of current 3D organoid culture methods (MatrigelTM) to elucidate the role of the tumor microenvironment in EAC tumorigenesis and to identify disease-relevant therapeutic targets. Successful completion of this work will also provide an opportunity to establish the engineered biomaterial as a platform to potentially elucidate the mechanisms of, and therapy targets for, other human cancers in the context of changes in the mechanics of tumor microenvironment.

Funding: CEET T32-ES019851, NCI P01-CA098101, NCI 5U54CA163004.

No conflict of interest.

170

Poster

Potent anti-tumor activity of AUR102, a selective covalent inhibitor of CDK7

L.K. Satyam¹, R. Poddutoori², S. Thiyagarajan¹, S. Mukherjee³, L.N. Kaza¹, K. Charamanna⁴, S. Marappan⁵, D. Samiulla⁶, N.K. Tiwar⁶, T. Devaraja², A. Aravind⁷, A.A. Dhudashya⁶, R. Boohar⁸, G. Dagainakatte⁷, T. Antony⁵, S. Chelur⁴, K. Nellore¹, S. Gir⁶, M. Ramachandra⁹, S. Samajdar². ¹Aurigene Discovery Technologies Limited, Cell and Molecular Biology, Bangalore, India; ²Aurigene Discovery Technologies Limited, Medicinal Chemistry, Bangalore, India; ³Aurigene Discovery Technologies Limited, Computational Chemistry, Bangalore, India; ⁴Aurigene Discovery Technologies Limited, Toxicology, Bangalore, India; ⁵Aurigene Discovery Technologies Limited, Biochemistry, Bangalore, India; ⁶Aurigene Discovery Technologies Limited, Drug Metabolism and Pharmacokinetics, Bangalore, India; ⁷Aurigene Discovery Technologies Limited, Pharmacology, Bangalore, India; ⁸Exelixis-Inc., External Innovation Director, Alameda, USA; ⁹Aurigene Discovery Technologies Limited, Chief Executive Officer, Bangalore, India

Background: AUR102 is a potent, selective, and orally bioavailable covalent inhibitor of cyclin-dependent kinase 7 (CDK7), which is an important regulator of the cellular transcriptional and cell cycle machinery. In view of the critical dependency on transcription for the maintenance of oncogenic state, pharmacological modulation of CDK7 kinase activity is considered as an approach to treat cancer. Here we report the detailed characterization of AUR102 in cancer cell lines and xenograft models.

Methods: Anti-proliferative activity of AUR102 was determined in a large panel of cell lines derived from multiple solid and haematological cancer indications. Dose-response curves were generated in selected cell lines derived from breast cancer, prostate cancer and lymphoma as a single agent and in combination with the standards of care. Synergy due to the combination treatment was estimated using the Chou-Talalay method. Cellular target occupancy was determined using a biotin-tagged CDK7 inhibitor. Impact of compound treatment on expression of genes in PBMCs was analysed by NanoString. In vivo anti-tumor activity was evaluated in xenograft models of breast cancer, leukemia, and lymphoma upon oral administration.

Results: AUR102 exhibited potent anti-proliferative activity in a large panel of cell lines with induction of cell death in cell lines derived from multiple cancer types. The observed anti-proliferative activity correlated with cellular CDK7 target engagement and decreased P-Ser5 RNAPII levels. In vitro combination studies showed synergy with fulvestrant in a ER+ breast cancer cell line (MCF-7), with docetaxel in a prostate cancer cell line (DU-145), and venetoclax in a mantle cell lymphoma cell line (Z-138). Oral dosing with AUR102 resulted in dose-dependent anti-tumor activity including complete tumor regression in DLBCL (OCI-LY10), AML (MV4-11) and TNBC (HCC70) xenograft models. Inhibition of tumor growth was accompanied by complete target engagement as demonstrated in a parallel PK-PD study. NanoString pan-cancer panel analysis of ex vivo human whole blood treated with AUR102 indicated that several pathways and key cancer driver and immune-response genes were impacted significantly by AUR102 treatment, supporting the use of this method as a pharmacodynamic readout in the clinic.

Conclusion: AUR102 exhibits potent anti-tumor activity in vitro and in vivo models. Findings presented here support further evaluation of AUR102 in the clinic for the treatment of cancer both as a single agent and in combination with approved anticancer agents.

No conflict of interest.

171

Poster

SCLC subtype-enriched biomarkers define positioning of Aurora B inhibitor combination with venetoclax

C. Della Corte¹, C. Gay¹, J. Urošević², U. Polanska², L. Ajpacaja¹, P. Wijnhoven², J. Wang¹, E. Coker³, G. Fabbri⁴, P. Jaaks³, M. Jerome⁴, J. Cosaert², M. Garnett³, R. Cardnell¹, J.E. Pease², J. Travers², L.A. Byers¹. ¹MD Anderson Cancer Center, Department of Thoracic Medical Oncology, Houston, USA; ²AstraZeneca, Oncology R&D, Cambridge, United Kingdom; ³Wellcome Trust Sanger Institute, Genomics of Drug Sensitivity in Cancer, Cambridge, United Kingdom; ⁴AstraZeneca, Oncology R&D, Waltham, USA

Background: Definition of subtypes in SCLC has provided a robust platform to guide molecularly specified monotherapy regimens in this disease. However, the aggressive nature of SCLC frequently limits the durability of monotherapies and requires development of combinations. We sought to use emerging subtype-specific resistance (BCL-2) and sensitivity (MYC) markers for the Aurora Kinase B inhibitor AZD2811 to guide rational positioning of novel combinations with an AZD2811 backbone.

Method: Using a SCLC cell panel combination screen coupled to basal proteomic and transcriptomic analysis, we identified cell lines where these markers defined combination activity, in terms of synergy and combination max effect, with the selective BCL2 antagonist venetoclax. We used five xenograft models with a range of sensitivities to validate these findings in vivo, with clinically relevant dosing regimens. We then screened this combination across seven PDX models representing both BCL2^{HI} ASCL1/POU2F3 and BCL2^{LO} NEUROD1 subtypes, and performed semi-quantitative pharmacodynamic analysis in four of the PDX models to assess combination biomarkers.

Results: Combination activity with AZD2811 and venetoclax was driven in the ASCL1 BCL2^{HI}/MYC^{LO} subtype by Aurora sensitivity and BCL-2 expression with a 2-fold increase in the average Bliss matrix synergy score in AZD2811 sensitive vs resistant cell lines. In the BCL2^{HI}/MYC^{HI} POU2F3 cell lines, venetoclax synergised in all instances with AZD2811 irrespective of single agent Aurora inhibitor sensitivity. Using the NCI-H69 (ASCL1), NCI-H82/NCI-H446 (NEUROD1) and NCI-H1048/NCI-H211 (POU2F3) models and a nanoparticle formulation of AZD2811(NP), we confirmed that the AZD2811+venetoclax combination was most effective in the POU2F3 models with combinations achieving regression, and with stasis (80% growth inhibition) in the ASCL1 model. As predicted by the cell-based screen, we found no combination benefit in the BCL2^{LO}/MYC^{HI} NEUROD1 models, despite monotherapy AZD2811NP activity. Combination activity was also independent of expression of other key pro-survival factors, such as BCLX_L and MCL1. These findings were validated in a panel of PDX models where all ASCL1 models showed combination activity, and 2/4 were driven to regression, again with no combination activity in the NEUROD1 subtype models. This selective combination activity was underpinned by 2-fold increase in apoptotic marker induction in sensitive models.

Conclusions: We have previously shown in AML that induction of pro-apoptotic BH3 domain proteins and depletion of pro-survival MCL1 underpin AZD2811 combination activity with BCL-2 antagonism, independently of TP53 status. Here, we support this mechanism in a solid tumor type with universal loss of TP53 in a biomarker selected population, and thus define a subtype-specific strategy to develop novel combinations in SCLC.

Conflict of interest:

Corporate-sponsored Research: Drs Byers, Gay and Cardnell are recipients of research grants from AstraZeneca.

Other Substantive Relationships: Authors from AstraZeneca are employees and shareholders of AstraZeneca.

172

Poster

Regorafenib targets YAP1 to inhibit epithelial-mesenchymal transition and cancer metastasis of cholangiocarcinoma

Y.C. Chang¹, M.H. Chen², M. Hsiao³. ¹National Yang-Ming University, Department of Biomedical Imaging and Radiological Sciences, Taipei, Taiwan; ²Taipei Veterans General Hospital, Department of Oncology, Taipei, Taiwan; ³Academia Sinica, Genomics Research Center, Taipei, Taiwan

Background: Cholangiocarcinoma (CCA) is a rare cancer type that formed by the transformation of bile duct epithelial cells. Its survival rate is low and there is no clear standard treatment strategies in clinical terms. Although regorafenib has been announced as a secondary treatment option for patients with CCA. However, the detailed molecular mechanism is still unknown.

Material and methods: In this study, we established the transcriptome databases in CCA cells using microarray chips. We merged all probes that had significant changes after treatment with regorafenib in two CCA malignant cells, and analyzed their common signatures.

Results: Our profiles predicted that YAP1 is the one of the most significant transcription factors inhibited by regorafenib. Moreover, we also observed that genes related to epithelial-mesenchymal transition (EMT) were regulated by YAP1, including E-cadherin and SNAI2. We screened the YAP1 activity, phosphorylation status, and expression levels of YAP1 downstream target genes and found a positive correlation with the migration/invasion ability of CCA cells. In the clinical part, we processed immunohistochemical staining and found that patients with high YAP1 and EMT expression had worse survival than patients with low YAP1 and EMT expression. The translocation state, phosphorylation status of YAP1 have been determined in our patients' specimens. After univariate/multivariate analysis, we provided evidence that YAP1 and its downstream genes can be used as independent prognostic factors in CCA. We further recruited the YAP-1 inhibitor verteporfin and validated that verteporfin treatment has reversed these phenotypes. In addition, we performed tumorigenicity and lung foci formation through CCA cells in vivo model, and our results revealed that verteporfin can significantly suppress these symptoms. Most importantly, regorafenib and verteporfin exhibited synergistic effects against CCA cells.

Conclusions: Our findings indicate that the combination of YAP1 inhibitors verteporfin and regorafenib can reverse the CCA metastatic

phenotype and EMT *in vitro* and *in vivo*. These findings provide a novel therapeutic strategy for CCA.

No conflict of interest.

173

Poster

Preclinical therapeutic synergy of MEK1/2 and IGF1R inhibition in RAS-driven rhabdomyosarcoma

M. Yohe¹, X. Wan¹, J. Roth², K. Isanogle³, C. Robinson³, X. Liu⁴, J. Chen⁴, M. Hall², S. Difilippantonio³, J. Khan⁵. ¹NCI/CCR, Pediatric Oncology Branch, Bethesda- MD, USA; ²NCATS, Early Translation Branch, Rockville- MD, USA; ³FNLCR, Laboratory Animal Science Program, Frederick- MD, USA; ⁴NCI/CCR, Collaborative Protein Technology Resource, Bethesda- MD, USA; ⁵NCI/CCR, Genetics Branch, Bethesda- MD, USA

Background: Several pediatric solid tumors, such as rhabdomyosarcoma (RMS) and neuroblastoma (NB) are driven by alterations in the RAS/MAP kinase pathway and are partially responsive to MEK inhibition. Overexpression of the IGF1R as well as its ligands has been observed in multiple malignancies, including pediatric sarcomas and NB. Preclinical and clinical studies have suggested that IGF1R is itself an important target in these diseases. Previous studies revealed preclinical efficacy of the MEK1/2 inhibitor, trametinib, and an inhibitor of IGF1R, BMS75807, in cell line xenograft models of RAS-mutated RMS; however, clinical translation of this combination was limited by toxicity. Here, we sought to identify a combination of a MEK1/2 inhibitor and IGF1R inhibitor that would be better tolerated.

Methods: We studied the combinatorial effects of the MEK1/2 inhibitor trametinib, and the IGF1R monoclonal antibody ganitumab using proliferation and apoptosis assays in a panel of RAS-mutated RMS cell lines. The molecular mechanism of the observed synergy was determined using conventional and capillary immunoassays. The efficacy and tolerability of the combination was assessed using a panel of RAS-mutated cell-line and patient-derived RMS xenograft models.

Results: Treatment with trametinib and ganitumab resulted in synergistic cellular growth inhibition in all cell lines tested and significant inhibition of tumor growth in five out of six models of RMS. The combination did not induce body weight loss, thrombocytopenia, or neutropenia in tumor-bearing SCID beige mice. Mechanistically, ganitumab treatment prevented the AKT phosphorylation that is induced by MEK inhibition alone. The therapeutic response to the combination correlated with the degree to which intra-tumoral AKT phosphorylation was inhibited.

Conclusions: We demonstrate that combined trametinib and ganitumab treatment shows therapeutic synergy across a wide panel of RAS-mutated RMS preclinical models. These data support testing this combination in a phase I/II clinical trial for pediatric patients with relapsed or refractory RAS-mutated RMS.

No conflict of interest.

174

Poster

Dissecting the landscape of CAF-mediated drug resistance mechanisms in ALK-rearranged NSCLC

Q. Hu^{1,2}, L.L. Remsing Rix¹, X. Li¹, E.A. Welsh³, B. Fang⁴, S. Yun^{1,5}, J. Kroeger⁶, H.R. Lawrence^{1,5}, A. Marusyk^{7,8}, J.M. Koomen^{4,9,10}, E.B. Haura¹¹, U. Rix¹. ¹H. Lee Moffitt Cancer Center and Research Institute, Department of Drug Discovery, Tampa, USA; ²University of South Florida, Cancer Biology PhD Program, Tampa, USA; ³H. Lee Moffitt Cancer Center and Research Institute, Biomedical Informatics Core, Tampa, USA; ⁴H. Lee Moffitt Cancer Center and Research Institute, Proteomics and Metabolomics Core, Tampa, USA; ⁵H. Lee Moffitt Cancer Center and Research Institute, Chemical Biology Core, Tampa, USA; ⁶H. Lee Moffitt Cancer Center and Research Institute, Flow Cytometry Core, Tampa, USA; ⁷H. Lee Moffitt Cancer Center and Research Institute, Department of Cancer Physiology, Tampa, USA; ⁸University of South Florida, Department of Molecular Medicine, Tampa, USA; ⁹H. Lee Moffitt Cancer Center and Research Institute, Department of Molecular Oncology, Tampa, USA; ¹⁰University of South Florida, Department of Chemistry, Tampa, USA; ¹¹H. Lee Moffitt Cancer Center and Research Institute, Department of Thoracic Oncology, Tampa, USA

Background: Cancer-associated fibroblasts (CAFs) are predominant stromal cells associated with cancer development and drug resistance. Due to the complexity of the crosstalk between CAFs and cancer cells, the underlying mechanism often remains elusive. Here, we aim to elucidate the complex, bidirectional signaling network that governs CAF-mediated

resistance to targeted drugs in *EML4-ALK*-rearranged non-small-cell lung cancer (NSCLC) cells.

Materials and methods: Cell viability of *EML4-ALK*+ NSCLC cells in co-culture, trans-well culture, or in the presence of CAF conditioned medium (CM) was monitored by live-cell imaging and CellTiter-Glo assay. Signaling changes in *EML4-ALK*+ NSCLC cells in the presence/absence of CAF CM were characterized by immunoblotting. Gene expression profiles of NSCLC cells and CAFs were determined using Affymatrix microarrays. CAF secreted factors were identified using secretome proteomics and cytokine arrays. Signaling effects of CAF CM on *EML4-ALK*+ NSCLC cells were determined using RTK and phosphokinome arrays.

Results: CAFs conferred resistance to ALK inhibitors in several different *EML4-ALK*+ NSCLC cell lines. However, co-culture of cancer cells with CAFs conferred yet more resistance than CAF CM treatment or trans-well cultures, indicating that cell-cell interactions between NSCLC cells and CAFs contribute to drug resistance. Signaling changes suggested that the HGF-MET pathway is only partially responsible for CM-mediated drug resistance, which agrees with the detection of HGF in the CAF secretome and transcriptome. However, MET inhibition by crizotinib or capmatinib did not completely rescue drug sensitivity.

Conclusions: We aim to determine the complexity of mechanisms underlying CAF-mediated drug resistance in *EML4-ALK* rearranged NSCLC. In line with previous reports, we have found HGF secreted from CAFs to activate MET signaling in LC cells, which contributes to drug resistance. However, our data indicate that there exist multiple mechanisms involving additional secreted proteins and cell-cell interactions. Co-culture-based proteomics is expected to comprehensively decipher the bidirectional and drug-adaptive crosstalk between CAFs and *EML4-ALK*+ NSCLC cells, add to our understanding of tumor microenvironment signaling and identify therapeutic vulnerabilities.

No conflict of interest.

175

Poster

Enhanced tumor suppression by conditionally replicating adenovirus in multidrug-resistant human ovarian carcinoma

S. Ali¹, D. Lei¹, T. Muhammad², A.A. Khan². ¹Beijing Institute of Technology, College of Life Science, Beijing, China; ²Beijing University of Technology, College of Life Sciences and Bio-Engineering, Beijing, China.

Background: Breast and ovarian cancers are among the most common and deadly gynecologic malignancies. Today, interest in the non-cytotoxic drug development is at an all-time high, albeit platinum-based combination chemotherapy is still the standard of care for ovarian cancer. However, the treatment of advanced malignancies is restricted due to chemotherapy resistance, which in most cases is acquired. Therefore, identifying novel anti-cancer strategies for gynecological cancers is imperative. We have developed a highly tumor-targeting oncolytic adenovirus by controlling its replication via tumor-specific promoter, survivin. Hitherto, we have tested the anti-tumor potency of this genetically engineered oncolytic virus against breast and lung cancers and found it very toxic and tumor-targeting. In the present study, we continued our investigation of using survivin responsive conditionally replicating adenovirus (CRAd) to chemotherapy-resistant cancers of different origins.

Methods: We employed three ovarian cancer cells including A2780, A2780/R, and SKOV-3. The anti-proliferative effect of the treatment on ovarian cancer cells was assessed *in vitro* via MTT and colony formation assays, while CRAd's anti-metastatic potential was analyzed through transwell assay. Mouse xenograft models were developed to assess CRAd's anti-tumor potency *in vivo*. The studies involving animals were approved by the relevant ethical committee of the institute.

Results: We show through western blotting that the CAR gene is overexpressed both in cisplatin-treated and chemotherapy-resistant cancer cells. Compared to sensitive cells, resistant cells showed higher adenoviral transduction in the X-gal staining assay, which might be due to the difference in CAR expression. Cisplatin monotherapy significantly decreases the viability of chemo-sensitive ovarian cancer cells, and its co-treatment with CRAd synergistically inhibited cancer cell survival. Protein level expressions of epithelial to mesenchymal transition (EMT) markers revealed that in all cancer cells, CRAd treatment increases the expression of E-cadherin, while Vimentin and N-cadherin levels were reduced. CRAd's monotherapy significantly increases the animal's survival. Results of CRAd monotherapy experiments establish our hypothesis that CRAd alone could be a drug of choice for chemotherapy-resistant cancers.

Conclusion: These insights may prove to be a timely opportunity for the application of CRAd in recurrent drug-resistant tumors and demand further investigation.

No conflict of interest.

176

Poster

Inhibition of serum response factor as a new strategy to overcome resistance to enzalutamide in prostate cancer

W. Watson¹, C. Gonzalez², N. Russell², H. Azam², E. Corey³, C. Morrissey³, W. Gallagher², M. Prencipe². ¹UCD Conway Institute, UCD School of Medicine, Dublin, Ireland; ²UCD Conway Institute, UCD School of Biomolecular and Biomedical Science, Dublin 4, Ireland; ³University of Washington, Department of Urology, Seattle, USA

Background: Castrate-resistant prostate cancer (CRPC) is challenging to treat with the Androgen Receptor (AR) still the main target and key player of resistance. Understanding the mechanisms of AR interaction with co-factors will identify new therapeutics not susceptible to AR resistance mechanisms. We identified Serum Response Factor (SRF) as a lead target in an *in vitro* model of CRPC and showed that SRF expression in tissues of CRPC patients was associated with shorter survival. Here we tested SRF-inhibition *in vitro* and *in vivo* to assess SRF as a potential target in CRPC.

Materials and methods: SRF was inhibited with the small-molecule inhibitor CCG1423. *In vitro* studies were performed in an isogenic model of CRPC: LNCaP parental (sensitive to androgen ablation) and LNCaP Abl (resistant). A patient-derived xenograft (PDX) was used for *in vivo* experiments.

Results: MTT assays showed that CCG1423 decreases cell viability in both parental and Abl cell lines. However, while parental cells show lower IC50 values in response to Enzalutamide compared to CCG1423 (7.75 ± 3.3 vs. 13.41 ± 2.51, respectively), the Abl cells, a model for castrate-resistance, were more responsive to CCG1423 than Enzalutamide, with IC50 values of 9.97 ± 2.19 vs. 24.27 ± 2.28, respectively. Combination with Enzalutamide showed decreased Enzalutamide IC50 values with increasing concentrations of CCG1423.

To confirm these data *in vivo*, an Enzalutamide-resistant PDX line was used. Mice were treated with vehicle, CCG1423 (0.15 mg/Kg), Enzalutamide (50 mg/kg) or combination for 6 weeks. No significant difference in tumor volume was observed post-treatments, possibly due to the low dose of CCG1423 used. However, immunohistochemistry analysis of AR in PDX tissues, showed that nuclear expression of AR protein post CCG1423, singly or in combination with Enzalutamide, was significantly decreased ($p < 0.01$ singly and $p < 0.05$ for the combination), indicating that treatment with CCG1423 affects AR nuclear localisation and therefore its activation as a transcription factor.

Next, SRF expression was assessed in a TMA of CRPC metastases to study the relationship between SRF expression and response to Enzalutamide in patients. Kaplan Meier curves showed that high SRF expression was associated with shorter response to Enzalutamide, in both visceral ($n = 23$, HR 4.26, logrank 7.15, $p = 0.007$) and bone metastases ($n = 21$, HR 5.81, logrank 8.29, $p = 0.004$). High expression of SRF in visceral metastases was also associated with shorter time to develop CRPC ($n = 37$, HR 2.38, logrank 5.53, $p = 0.019$).

Conclusion: Here we showed that SRF expression is elevated in Enzalutamide-resistant patients and that its inhibition can be used in combination with Enzalutamide to overcome resistance to this drug. Our study supports the rationale of using alternative ways to target AR by inhibiting co-regulators and co-factors such as SRF.

No conflict of interest.

177

Poster

A pivotal study in human prostate cancer tissues and cell lines to measure the expression levels of eukaryotic Elongation Factor 1A proteins and the effect of a nucleic acid-based GT75 aptamer

B. Scaggianti¹, B. Dapas¹, A. Bosutti¹, F. Giudici², R. Bussani², C. Bottin², G. Grassi¹, F. Zanconati². ¹University of Trieste, Department of Life Sciences, Trieste, Italy; ²University of Trieste, Department of Department of Medical- Surgical and Health Sciences, Trieste, Italy

Background: Two major isoforms of the eukaryotic Elongation Factor 1A are recognised: the eEF1A1, ubiquitously expressed, and the eEF1A2 presents in adult heart and skeletal muscle, in nervous system and in some other specialized cells. Both proteins are implicated in the development and progression of human cancers with different role. In prostate cancer, overexpression of eEF1A2 has been proposed to be involved in the onset of the tumour and it was related to a worse outcome. However, the expression level of both proteins in prostate cancer tissue is not well known. We explore the expression level of the two proteins and mRNAs in formalin-fixed paraffin-embedded tissues derived from prostate cancer patients. Moreover, we investigated the effect of the nucleic acid-based GT75 aptamer, targeting eEF1A protein, in human prostate cancer cell lines.

Materials and methods: Formalin-fixed, paraffin-embedded samples of hyperplasia ($n = 10$), of Gleason 4–6 ($n = 10$) and of Gleason 7–8 ($n = 10$) were analysed. Protein level of eEF1A1 and eEF1A2 was determined by an IHC method previously described; the mRNA levels were quantified by ddPCR with probes. The tumorigenic PC-3 and the non-tumorigenic PZHPV-7 cell lines were transfected with the GT75 aptamer or CT75 control, the cell growth was evaluated by MTS assay; the expression level of the proteins in cell culture was determined by an immunofluorescent assay. The results were statistically examined by Anova, Mann-Whitney and Fisher tests.

Results: The expression level of the proteins in tissues was a score 0, 1, 2, 3. With respect to Gleason 4–6, eEF1A1 protein was found to increase in samples with Gleason 7–8 ($p = 0.001$); whereas a decrease in eEF1A2 levels was found in cancer samples with respect to hyperplasia (Gleason 4–6, $p < 0.001$; Gleason 7–8 $p = 0.005$). No significant difference among the groups were found in mRNA levels for both proteins. In cancer PC-3 cells, the transfection of the GT75 aptamer led to 40% of cell growth inhibition with respect to CT75 oligonucleotide control. In agreement, a 60% decrease in eEF1A1 protein level was measured, but only a 20% reduction in eEF1A2. Interestingly, no effects were found in the non-tumorigenic PZHPV-7 cells.

Conclusion: eEF1A1 protein could be an interesting molecular target for the control of cell proliferation in more aggressive prostate cancer forms.

No conflict of interest.

178

Poster

Development of casein kinase 2 related oral cancer prevention targets by genomic database analysis

C. Koenigsberg¹, F. Ondrey². ¹University of Minnesota, Medical School, Minneapolis, USA; ²University of Minnesota, Department of Otolaryngology, Minneapolis, USA

Background: Casein kinase 2 is a serine/threonine kinase involved in cell-cycle control, and a myriad of processes associated with cancer progression. CK-2 overexpression is demonstrated in multiple cancer types, including head and neck cancer. CK-2 and related genes may represent possible targets or biomarkers for oral carcinogenesis prevention.

Material and methods: We interrogated an Affymetrix microarray dataset for CK2 expression and expression of related genes in 41 cancer specimens compared with 13 normal, using Welch's t-test and $p < 0.05$ as a level of stringency.

Results: We found upregulation of casein kinase 2 (CK2) subunits as well as various phosphorylation targets in head and neck squamous cell carcinoma when compared with mucosal control specimens. CK2 alpha 1 subunit demonstrates upregulation in one of two expressed sequence tags analyzed ($p = 0.027$, 0.58). CK2 beta polypeptide demonstrates upregulation in head and neck cancer ($p = 6.5 \times 10^{-4}$). Multiple targets of CK2 also demonstrate increased expression in head and neck cancer. Lactate dehydrogenase (LDHA) demonstrates upregulation ($p = 5 \times 10^{-3}$). Pyruvate kinase also demonstrates increased expression in cancer ($p = 3 \times 10^{-3}$). Facilitated glucose transporter 1 (GLUT1) also demonstrates upregulation in cancer ($p = 3.7 \times 10^{-3}$, 9.1×10^{-4}). Hypoxia-inducible factor 1 (HIF-1) demonstrates upregulation in cancer ($p = 8.95 \times 10^{-8}$) while HIF-1 inhibitor demonstrates downregulation in head and neck cancer ($p = 0.005$, 0.001). Interestingly, growth suppressor PTEN demonstrates upregulation in two of the four examined ESTs ($p = 0.02$, 0.014, 0.35, 0.28). Growth promoter AKT demonstrates upregulation in head and neck cancer ($p = 0.002$). AKT acts to increase cellular metabolic activity by stabilizing beta catenin. Beta catenin, however does not demonstrate differential expression in head and neck cancer ($p = 0.23$).

Conclusions: Differential expression of casein kinase 2-associated pathway genes, including CK-2 alpha and beta subunits, LDHA, HIF-1, GLUT1, and AKT, represent potential targets for head and neck cancer chemoprevention agents. We conclude that existing genetic databases have hypothesis generating capacity for target identification in chemoprevention and treatment clinical trials.

No conflict of interest.

179

Poster

Combination PI3K and NOS targeted therapy for metaplastic breast cancer

T. Reddy¹, R. Rosato¹, L. Guzman¹, W. Qian¹, J. Zhou¹, H. Piwnica-Worms², S. Moulder³, J. Chang¹. ¹Houston Methodist Research Institute, Cancer Center, Houston, USA; ²The University of Texas MD Anderson Cancer Center, Cancer Biology, Houston, USA; ³The University of Texas MD Anderson Cancer Center, Breast Oncology, Houston, USA

Background: Metaplastic breast cancer (MBC) is a highly chemoresistant cancer, accounting for <1% of all breast cancers. Most MBCs typically display a triple-negative breast cancer (TNBC) phenotype, yet MBC exhibits a worse prognosis than TNBC and a dismal survival rate. The current mainstay of treatment include surgery and systemic chemotherapy, despite its chemofactory nature. A common molecular alteration in MBC is hyperactivation of the phosphoinositide 3-kinase (PI3K) pathway. We published that MBC displays a gain-of-function oncogenic mutation in ribosomal protein L39 (RPL39), which is responsible for treatment resistance, stem cell self-renewal, and lung metastasis. The mechanistic function of RPL39 is mediated through inducible nitric oxide synthase (iNOS)-mediated nitric oxide production. In addition, we demonstrated that inhibiting the NOS pathway using pan-NOS inhibitor NG-methyl-L-arginine acetate (L-NMMA) represents a highly effective therapeutic option for MBC patients. Alpelisib, an FDA-approved, isoform-specific PI3K inhibitor, is currently used with antiestrogen therapy, to treat hormone receptor (HR)-positive, *PIK3CA*-mutated breast cancer patients. Therefore, we hypothesize that the combinatorial approach of inhibiting the two major pathways implicated in MBC, namely PI3K and NOS pathways, would lead to significant tumor regression.

Materials and Methods: MBC cell lines (Hs578t and BT549) and MBC patient-derived xenograft (PDX) models were used in our preliminary studies. Flow cytometry, immunoblotting, bulk RNA-sequencing, gene set enrichment analysis (GSEA), and pathway-focused RT-PCR was performed.

Results: Flow cytometry to detect Annexin V+/DAPI+ cells showed increased cell death in MBC cell lines treated with L-NMMA+alpelisib combination therapy in comparison to monotherapy. Immunoblotting of samples from single (L-NMMA or alpelisib) or combination treated cell lines and PDXs showed increased PARP degradation and cleaved caspase 3/9 with combination treatment. *In vivo* data using PDX models showed that combination therapy was most effective at reducing tumor volume in comparison to monotherapy. Preliminary bulk-RNA sequencing analysis of tumors collected from PDX BCM-4664 treated with vehicle control, monotherapy of L-NMMA or alpelisib, and combination therapy was performed. GSEA found that E2F and Hedgehog signaling pathways were the top two enriched pathways in BCM-4664 tumors treated with combination therapy. Pathway-focused RT-PCR of MBC PDXs confirmed GSEA results and showed significant gene expression alterations involving E2F signaling and cell cycle regulation.

Conclusion: Our results support the concept that L-NMMA and alpelisib combination therapy has therapeutic potential in the treatment of MBC, which may enable rapid translational into clinical trials, and impact the exceeding poor prognosis of women with MBC.

No conflict of interest.

Methods: Pts in dose escalation received daily oral SY-5609 in consecutive 28-day cycles. Safety, including cycle-1 dose-limiting toxicities (DLTs), was evaluated. Serial plasma PK, and PD in PBMCs were obtained on days 1 and 15 in cycle 1. PD responses were measured as changes in normalized *POLR2A* mRNA expression relative to baseline.

Results: As of May 22, 2020, data were available on 5 pts (2 ovarian/fallopian; 1 CRC; 1 endometrial; 1 breast cancer; with Rb pathway abnormalities in 2/5) enrolled into the first two completed single-agent dosing cohorts at 1 mg/day (n = 1) and 3 mg/day (n = 4). Four were female, median age was 73 (range 53–76). The median treatment duration was 56 days (range 14–65+). The most common AEs (≥ 2 pts) were nausea, constipation, diarrhea, and fatigue. The majority of AEs were low grade and reversible with no DLTs. At 3 mg, the SY-5609 plasma Cmax on days 1 and 15 occurred at 2–4 h. The half-life on day 15 ranged from 14.7 to 23.9 hours. The ratios of Cmax (ng/mL) and AUC 0–8 h (ng/mL·hr) on day 15 to day 1 were 1.33 ± 0.55 and 2.29 ± 0.83 , respectively, suggesting increased SY-5609 plasma exposure at two weeks. On days 1 and 15, maximum *POLR2A* expression occurred at 4–8 h and SY-5609 dose-dependent changes in average *POLR2A* expression were observed. The magnitude of *POLR2A* expression changes increased from day 1 to 15 consistent with the increased SY-5609 plasma exposure.

Conclusions: SY-5609 is a highly selective and potent oral inhibitor of CDK7 in phase 1 development. The increase in plasma exposures of SY-5609 from day 1 to 15 with daily dosing is consistent with the PK half-life and steady-state PK. The dose-dependent changes in *POLR2A* expression are consistent with data from preclinical *in vivo* models and provide initial evidence of biological activity that was observed in association with TGI in these models. Current safety data supports continued dose escalation, which is ongoing, including in the SY-5609/fulvestrant combination. Updated data will be presented.

Conflict of interest:

Advisory Board: DR: reports an advisory role for: AstraZeneca, Mersana, Ipsen, Tesaro, Deciphera, Genentech, Bayer, Foundation Medicine.

KP: reports an advisory role for: Bayer, ArQule, Basilea.

Corporate-sponsored Research: BB: reports research funding paid to institution only from: Kena Oncology, Inc., Bicycle Therapeutics., Boehringer Ingelheim Pharmaceuticals Inc. Syros Pharmaceuticals, Inc.

DR: reports research funding paid to institution only from: Syros Pharmaceuticals, Inovvent Biologics, ArQule, Inc., Hookipa Biotech, Genentech, Aravive, Harpoon Therapeutics, Lycera, Tesaro, Karyopharm, AstraZeneca, Deciphera, Five Prime Therapeutics, Roche, Merck, Mersana. MS: reports research funding paid to institution only: Alexo, Alpine, Amgen, Apexian, Asana, Ascentage, Astellas, Astra-Zeneca, Beigene, Bolt Biotherapeutics, Bristol-Myers Squibb, Celgene, Compugen, Coordination, Constellation, CytomX, Effector Therapeutics, Exelixis, Formation Biologics, Forty Seven, Genmab, Ikena, Inovvent Biologics, InhibRx, Incyte, Ipsen, Jounce Therapeutics, KLUS Pharma, Lexicon, LOXO, Lilly, Livzon, MacroGenics, Merck, Mersana, Northern Biologics, Novocure, Odonate Therapeutics, Pfizer, QED, Regeneron, Shattuck Labs, Symphogen, Syros, Tempest Therapeutics, Tesaro, TaiRx.

EH: reports research funding paid to institution only from: Seattle Genetics, Puma, AstraZeneca, Hutchinson MediPharma, OncoMed, MedImmune, StemCentrx, Genentech/Roche, Curis, Verastem, Zymeworks, Syndax, Lycera, Rgenix, Novartis, Mersana, Millenium, TapImmune, Lilly, BerGenBio, Medivation, Pfizer, Tesaro, Boehringer Ingelheim, Eisai, H3 Biomedicine, Radius Health, Acerta, Takeda, MacroGenics, Abbvie, Immunomedics, FujiFilm, Effector, Merus, Nucana, Regeneron, Leap Therapeutics, Taiho Pharmaceutical, EMD Serono, Daiichi Sankyo, ArQule, Syros, Clovis, Cytomx, InventisBio, Deciphera, Unum Therapeutics, Sermonix Pharmaceuticals, Sutro, Aravive, Zenith Epigenetics, Arvinas, Torque, Harpoon, Fochon, Black Diamond, Orinove, Molecular Templates, Silverback Therapeutics, Compugen, G1Therapeutics, Karyopharm Therapeutics and Torque Therapeutics.

KP: reports research funding paid to institution only from: Abbvie, Amgen, MabSpace Biosciences, Daiichi Sankyo, Jounce Therapeutics, Anheart, Mirati, Syros Pharmaceuticals, Merck, 3D Medicines, OncoMed, Linnaeus, Sanofi, ARMO Biosciences, Calithera Biosciences, Bayer, MedImmune, Regeneron, Incyte, Peloton Therapeutics, ADC Therapeutics, EMD Serono, F-Star, Tempest Therapeutics, ArQule, Mersana.

Other Substantive Relationships: Syros Pharmaceuticals Employee and Stockholder (GH, NK, QK-F, LZ, HJ, CM, MJK, DAR).

Syros Pharmaceutical Consultant (WZ).

EH: reports consulting fees paid to institution only from: Pfizer, Genentech/Roche, Lilly, Puma Biotechnology, Daiichi Sankyo, Mersana Therapeutics, Boehringer Ingelheim, AstraZeneca, Novartis, Silverback Therapeutics, Black Diamond and NanoString.

DR: reports travel accommodations and expenses paid by: Karyopharma Therapeutics, Agenus, Tesaro, Merck, Roche.

POSTER SESSION

New Drugs

180

Poster

Early evidence of dose-dependent pharmacodynamic activity following treatment with SY-5609, a highly selective and potent oral CDK7 inhibitor, in patients with advanced solid tumors

K. Papadopoulos¹, M. Sharma², E. Hamilton³, D. Richardson⁴, B. Bashir⁵, G. Hodgson⁶, N. Ke⁶, Q. Kang-Fortner⁶, L. Zhou⁶, W. Zamboni⁶, H. Jolin⁶, C. Madigan⁶, M. Kelly⁶, D. Roth⁶. ¹South Texas Accelerated Research Therapeutics, Oncology, San Antonio, USA; ²South Texas Accelerated Research Therapeutics, Oncology, Grand Rapids, USA; ³Sarah Cannon Research Institute/Tennessee Oncology, Oncology, Nashville, USA; ⁴Stephenson Cancer Center- OK/Sarah Cannon Research Institute/TN, Oncology, Oklahoma, USA; ⁵Thomas Jefferson University Hospital, Oncology, Philadelphia, USA; ⁶Syros Pharmaceuticals, Clinical Development, Cambridge, USA

Background: SY-5609 is an oral, noncovalent, highly selective, and potent inhibitor of CDK7, a key regulator of two fundamental processes important in cancer: transcription and cell cycle control. Preclinical *in vivo* studies identified a pharmacodynamic (PD) gene expression marker, *POLR2A* mRNA, associated with SY-5609 dose-dependent tumor growth inhibition (TGI). A phase 1 single-agent dose-escalation study of SY-5609 initiated in January 2020 in patients (pts) with advanced breast, colorectal, lung or ovarian cancer, or solid tumors with Rb pathway abnormalities. Dose escalation of SY-5609 in combination with fulvestrant in hormone receptor positive (HR+) breast cancer pts after CDK4/6 inhibitor treatment failure began in June 2020. We report early results from the initial pts with a focus on tolerability, safety, pharmacokinetics (PK) and PD.

181

Poster

The preclinical characterization of the N-terminal domain androgen receptor inhibitor, EPI-7386, for the treatment of prostate cancer

N.H. Hong¹, R. Le Moigne¹, P. Pearson¹, V. Lauriault¹, C.A. Banuelos², N.R. Mawji², T. Tam², J. Wang², P. Virsik¹, R.J. Andersen³, M.D. Sadar², H.J. Zhou¹, A. Cesano¹. ¹ESSA Pharmaceuticals, South San Francisco office, South San Francisco, USA; ²BC Cancer Agency, Department of Genome Science Centre, Vancouver, Canada; ³University of British Columbia, Department of Chemistry, Vancouver, Canada

Background: Androgen receptor (AR) signaling remains an important driver even in late stage prostate cancer. While current anti-androgen therapies targeting the ligand binding domain (LBD) are effective, resistance to these therapies ultimately develops and new methods of inhibiting the AR pathway are needed. ESSA's compounds selectively target the N-terminal domain (NTD), a region of the AR which is essential for AR transactivation. EPI-7386 is a potent and metabolically stable AR NTD inhibitor which has been selected for clinical evaluation based on its biological effects, pharmaceutical characteristics, preclinical efficacy, and toxicology profile as described below.

Material and methods: Target engagement was measured by classic Cellular Thermal Shift Assay (CETSA). The potency and selectivity of EPI-7386 was determined in cellular models expressing different forms of AR using reporter and cell viability assays. Both Nanostring and RNAseq was used to explore the activity of EPI-7386 on AR signaling and its transcriptomic signature. The pre-clinical toxicology profile was assessed both in *in vitro* and in rat and dog studies.

Results: EPI-7386 effectively inhibited AR transcriptional activity with IC₅₀ of 421 nM in a LNCaP reporter assays. Target engagement of EPI-7386 on full-length AR (AR-FL) was confirmed in LNCaP cells by CETSA. Transcriptomic analysis of LNCaP cells demonstrated that EPI-7386 suppresses AR-associated gene expression similar to enzalutamide but with a few notable differences, suggesting more robust and thorough inhibition of the AR pathway with combination treatment. Indeed, the combination of EPI-7386 with LBD inhibitors resulted in broader and deeper inhibition of AR-associated transcriptional activity in both LNCaP and VCaP cells. In addition, EPI-7386 showed superior activity to enzalutamide in AR-V7 driven LNCaP95 cells by inhibiting both AR-FL and AR-V7 regulated genes. Furthermore, significant inhibition of tumor growth was observed with EPI-7386 treatment in LBD resistant animal models in which enzalutamide showed no activity. IND-enabling studies in rats and dogs showed good tolerability at an exposure several fold higher than efficacious dose required in animal xenograft models. PK simulations predicted that tolerated and active doses can be achieved during the phase 1 dose escalation.

Conclusion: EPI-7386 is an AR NTD inhibitor with a favorable safety and ADME profile and has the capacity to overcome resistance to current anti-androgen therapies by uniquely inhibiting AR-mediated signaling. The agent also has the potential for providing clinical benefit in combination with current anti-androgens in earlier line patients. The Phase I dose escalation first in human clinical trial of EPI-7386 (NCT04421222) is currently enrolling.

Conflict of interest:

Ownership: Hong, Le Moigne, Virsik, Zhou, Cesano = ESSA Pharmaceuticals.
Advisory Board: Sadar, Andersen = ESSA Pharmaceuticals.
Corporate-sponsored Research: Sadar, Andersen = ESSA Pharmaceuticals.
Other Substantive Relationships: Pearson, Lauriault = consultants for ESSA Pharmaceuticals.

182

Poster

Dose derivation of oral anticancer agents: Tolerability in late phase registration trials

C. McCabe¹, E. Bryson¹, R.D. Harvey². ¹Winship Cancer Institute, Pharmacy, Atlanta, USA; ²Winship Cancer Institute, Emory University School of Medicine, Atlanta, USA

Background: Trial designs of anticancer agents have become more seamless with earlier efficacy readouts in an effort to bring therapies to patients rapidly. Dose and schedule derivation in first-in-human (FIH) trials within an accelerated development paradigm carries even greater importance now because fewer patients may be treated in subsequent trials compared to historical approvals. Additionally, adherence and patterns of agent use post-approval may be driven by dose tolerability. To understand this further, we assessed new oral molecular entities in oncology approved since 2010 and rates of dose reductions, interruptions and discontinuations due to adverse drug events (ADEs).

Materials and methods: Agents were identified and characterized by review of publicly available FDA databases. Clinical trial dosing and safety data was collected for each drug for the initial approved indication at www.accessdata.fda.gov/scripts/cder/daf/, and rates of dose reductions, interruptions and discontinuations due to ADEs were determined. Time of approval, indication (hematologic vs solid tumor cancer), and molecular specificity were recorded. If available materials did not contain an ADE dose- or regimen-related discrete endpoint, agents were excluded from analysis.

Table 1. Dosing and safety data of recently approved oncology drugs.

| | Approved between 2010–2015 | Approved between 2016–2020 |
|--|------------------------------------|-------------------------------|
| Dose Reduction Rate (%) | N = 24 32, 2 – 90 | N = 35 24, 2 – 96 |
| Median, range | | |
| Dose Interruption Rate (%) | 44, 6 – 90 | 57, 13 – 97 |
| Median, range | | |
| Discontinuation due to ADEs (%) | 9, 2 – 34 | 11, 5 – 35 |
| Median, range | | |
| Dose Reduction Rate (%) | Hematology Approvals | Solid Tumor Approvals |
| Median, range | N = 15 | N = 44 |
| | 19, 2 – 96 | 32, 2 – 90 |
| Dose Interruption Rate (%) | 56, 11 – 96 | 48, 4 – 90 |
| Median, range | | |
| Discontinuation due to ADEs (%) | 9, 2 – 35 | 10, 3 – 34 |
| Median, range | | |
| | Molecularly Targeted Agents | Non-Targeted Agents |
| | N = 25 | N = 34 |
| Dose Reduction Rate (%) | 24, 3 – 66 | 36, 2 – 96 |
| Median, range | | |
| Dose Interruption Rate (%) | 45, 4 – 25 | 61, 11 – 96 |
| Median, range | | |
| Discontinuation due to ADEs (%) | 9, 3 – 35 | 11, 2 – 35 |
| Median, range | | |

Results: In total, 59 drugs were included for review. For each agent, the overall median rates of dose reductions (n = 54), interruptions (n = 42) and discontinuations due to ADEs (n = 57) were 28%, 55%, and 10%, respectively. Comparisons in toxicity were made based on approval date (before and after 2015), indication (solid vs hematologic malignancy), and molecular target (genetically targeted versus not). The rates were comparable for dose reduction, dose interruptions and discontinuations due to ADEs between drugs in the comparison cohorts (Table 1).

Conclusion: No clear differences were observed in data between indications or approval dates, a trend toward improved tolerability was seen with agents that are more targeted. Further exploration and methods to optimize dose are warranted.

No conflict of interest.

183

Poster

Preferences of US adults with Ph+ALL for first-line treatment with TKI-chemotherapy combinations: A discrete choice experiment

A. Ashaye¹, C. Thomas², M. Dalal¹, V. Kota³, N. Krucien², M. Sae-Hau⁴, M. Barnhart⁴, E. Weiss⁵, S. Campbell⁶, K. Marsh². ¹Takeda Pharmaceuticals International Co., Global Evidence & Outcomes - Oncology, Cambridge, USA; ²Evidera, Patient-Centered Research, London, United Kingdom; ³Georgia Cancer Center- Augusta University, Hematology and Oncology, Augusta, USA; ⁴Leukemia & Lymphoma Society, Access Initiatives & Evaluation, New York, USA; ⁵Leukemia & Lymphoma Society, Education- Services- & Health Research, New York, USA; ⁶Takeda Pharmaceuticals International Co., Patient Advocacy & Engagement - Oncology, Cambridge, USA

Background: Since the 2000s, rates of remission and overall survival (OS) in patients with Philadelphia chromosome positive acute lymphoblastic leukaemia (Ph+ALL) have improved thanks to combination therapy with tyrosine kinase inhibitors (TKIs) and conventional chemotherapy. The aim of this study was to elicit relative preferences for risks and benefits of first-line treatment with TKI-chemotherapy combinations in adult Ph+ALL patients.

Material and Methods: Between February and April 2020, adult patients in the US with self-reported Ph+ALL completed an online discrete choice experiment (DCE) comprising 12 experimental and 2 internal validity choice tasks. Each task asked participants to choose between 2 hypothetical

treatments comprising different levels of benefits and risks. The DCE was pilot tested and refined through interviews with 5 patients to ensure that the attributes and levels were understood. Attributes and levels in the final DCE included OS (30–90 months in 5-month increments), duration of remission (15–75 months in 5-month increments), risk of a major cardiovascular (CV) event (0%, 25%, 50%), and risk of myelosuppression (0%, 50%, 100%). Preferences for attributes were analysed using a linearly coded multinomial logit model and are expressed as marginal utilities.

Results: The DCE was completed by 201 patients. Mean age was 44.8 ± 12.9 years, 67% had at least a college education. At completion of the DCE, 17% had ≥2 relapses, 58% were diagnosed >12 months previously, and 67% were in remission. The most common current treatments were dasatinib (24%) and imatinib (18%). Internal validity was high: 94% of participants had high health numeracy, 84% had high health literacy, 78% passed the choice stability test, 88% passed the choice dominance test, 98% never selected the same option, 96% did not display dominated decision-making, and 96% had an adequate response time. When selecting a preferred treatment, patients placed the most weight on a 1-month increase in OS (0.032 [0.021–0.042]) and a 1-month increase in duration of remission (0.017 [0.012–0.023]) and less weight on reducing the risk of a major CV event by 1% (0.011 [0.008–0.013]) and reducing the risk of myelosuppression by 1% (0.009 [0.008–0.010]). Participants would be willing to tolerate an increase in the risk of a major CV event of 2.9% (1.78–4.02) for 1 additional month of OS and 1.59% (0.95%–2.24%) for an additional 1 month in remission.

Conclusions: This study identified the weights that patients attach to treatment characteristics when choosing between TKI-chemotherapy combinations. This insight can inform shared decision-making between patients and their healthcare providers. Further research will focus on understanding variation in preferences between patients.

Conflict of interest:

Ownership: A.Ashaye, M. Dalal, S. Campbell are employees of Takeda Pharmaceuticals with restricted stock ownership.

Advisory Board: N/A.

Board of Directors: N/A.

Corporate-sponsored Research: M. Barnhart, M. Sae-Hau, and E. Weiss, are employees of LLS, a patient advocacy organization which was funded for this research study. C. Thomas, N. Krucien, and K. Marsh are employees of Evidera, an HEOR consulting company which was funded for this research study.

Other Substantive Relationships: V. Kota received consulting fees for serving as a clinical expert on this research study.

184

Poster

Development of KSQ-4279 as a first-in-class USP1 inhibitor for the treatment of BRCA-deficient cancers

L. Cadzow¹, J. Brennen², P. Sullivan³, H. Liu⁴, S. Shenker⁵, M. McGuire³, P. Grasberger³, K. Sinkevicius¹, N. Hafeez³, G. Histen³, E. Chipumuro³, J. Hixon³, E. Krall³, S. Cogan⁶, J. Wilt⁷, M. Schlabach⁸, F. Stegmeier⁹, A. Olaharski¹⁰, A. Wylie¹. ¹KSQ Therapeutics, Pharmacology, Cambridge, USA; ²KSQ Therapeutics, Chemistry, Cambridge, USA; ³KSQ Therapeutics, Discovery Biology, Cambridge, USA; ⁴KSQ Therapeutics, Drug Metabolism and Pharmacokinetics, Cambridge, USA; ⁵KSQ Therapeutics, Computational Biology, Cambridge, USA; ⁶KSQ Therapeutics, Project Management, Cambridge, USA; ⁷KSQ Therapeutics, Small Molecule CMC, Cambridge, USA; ⁸KSQ Therapeutics, Target Discovery, Cambridge, USA; ⁹KSQ Therapeutics, Research, Cambridge, USA; ¹⁰KSQ Therapeutics, Toxicology, Cambridge, USA

Background: Drugs targeting poly (ADP-ribose) polymerase (PARP) have provided significant clinical benefit for cancer patients with tumors harboring mutations in BRCA1/2 or other homologous recombination deficiencies (HRD). Despite their success, not all patients respond to PARP inhibitors, and those that do benefit often develop resistance.

Material and methods: To address these challenges, we applied our proprietary CRISPRomics[®] technology to over 700 cancer cell lines, a subset of which contained mutations in either BRCA1/2 or other genes involved in DNA repair. The genetic dependencies that were selective for this subset of cell lines were then ranked for their suitability for therapeutic targeting.

Results: One of the top ranked targets was the deubiquitinating enzyme USP1. USP1 has established roles in DNA damage repair processes including Translesion Synthesis and the Fanconi Anemia pathway. We developed a series of potent small molecule inhibitors that are highly selective for USP1 relative to other family members. These inhibitors were active in cells, leading to the accumulation of mono-ubiquitinated substrates of USP1 and demonstrating selective activity in cell lines with BRCA mutations or other HRD alterations. Evaluation of our lead compound, KSQ-4279, in both ovarian-derived and triple-negative breast cancer (TNBC)-derived tumor

xenograft models, demonstrated dose-dependent tumor growth inhibition. In xenograft models with only partial sensitivity to PARP inhibitors, the combination of KSQ-4279 with a PARP inhibitor led to significantly greater and more durable tumor regressions than either agent alone. KSQ-4279 has favorable *in vitro* ADME properties and pharmacokinetic profile across multiple non-clinical species. Preliminary safety data indicates that KSQ-4279 is well tolerated as a single agent and in combination with PARP inhibitors, with no evidence of dose limiting heme-related toxicities.

Conclusions: Our data supports the clinical evaluation of KSQ-4279 as a potential first-in-class USP1 inhibitor in patients with tumors harboring BRCA1/2 or other HRD mutations, both as a single agent and in combination with PARP inhibitors.

Conflict of interest:

Ownership: Employee and stockholder of KSQ Therapeutics.

185

Poster

Antibody blockade resets Chi3L1-induced glioma stem cell phenotypic transitions and reduces glioblastoma tumor burden

C. Guetta-Terrier¹, B. Akosmam², J.S. Chen¹, S. Kamle², E. Fajardo³, A. Fiser³, S. Toms⁴, C. Lee², J. Elias⁵, N. Tapinos⁶. ¹Brown University/Rhode Island Hospital, Laboratory of Cancer Epigenetics and Plasticity, Providence, USA; ²Brown University, Department of Molecular Microbiology and Immunology, Providence, USA; ³Albert Einstein College of Medicine, Department of Systems and Computational Biology, Bronx, USA; ⁴Brown University, Department of Neurosurgery, Providence, USA; ⁵Brown University, Department of Molecular Microbiology and Immunology & Department of Internal Medicine- Warren Alpert Medical School of Brown University, Providence, USA; ⁶Brown University/Rhode Island Hospital, Laboratory of Cancer Epigenetics and Plasticity & Department of Neurosurgery, Providence, USA

Background: Glioblastoma (GBM) is one of the most aggressive human tumors. Current treatment of GBM includes surgical resection followed by radiation in the vicinity of the resection cavity and administration of temozolomide. Even with this multi-therapeutic approach, tumor recurrence is inevitable. In recent years it became evident that the “aggressiveness” of glioblastomas is mainly due to the presence of a population of cancer stem cells (GSCs) within the tumor mass, which exhibit high migratory potential, resistance to chemotherapy and radiation and the ability to form secondary tumors. In addition, GSCs exhibit remarkable plasticity, the ability to transition between immature and differentiated stages and to reversibly express various phenotypic markers, depending on the tumor microenvironment. Due to these challenging biological features, GSCs have been the target of extensive research.

Chi3L1 (Chitinase 3-like 1) is a secreted glycoprotein normally expressed by numerous cell types including neutrophils, endothelial cells, epithelial cells and macrophages. In addition, it has been shown that Chi3L1 is highly expressed in numerous types of cancer such as breast, colon, lung, ovary, prostate and GBM. RNA-seq on patient-derived GBMs and TCGA database analysis, showed that Chi3L1 is one of the highest expressed genes in GBM and is associated with therapy resistance and low survival of patients.

Materials and methods: Patient derived GSCs were cultured *in vitro* and treated with or without human recombinant Chi3L1 (rec-Chi3L1). We performed multiplex gene expression analysis of a set of Chi3L1-treated GSCs and a set of non-Chi3L1 treated GSCs, ATAC-seq as well as flow cytometry experiments to determine the role of Chi3L1. To determine the *in vivo* efficacy of anti-Chi3L1 antibody as localized treatment for glioblastoma, we generated orthotopic xenograft glioblastoma in immunocompromised mice using patient derived GSCs.

Results: Here, we show that exposure of GSCs to Chi3L1 induces marked phenotypic and transcriptomic change from CD133+/SOX2+ pro-neural to CD44+/CHI3L1+ mesenchymal phenotype. Chi3L1 induces chromatin remodeling in GSCs and regulates accessibility of ZNF281, CTCFL, SOX9, and the OCT4-SOX2-TCF3-NANOG transcription factor complex that drive the CHI3L1-mediated mesenchymal “switch” and maintain GSC identity. To demonstrate the potential of Chi3L1 as therapeutic target for human glioblastoma, we developed a humanized monoclonal antibody against CHI3L1 (blocking antibody). *In vivo* sustained local treatment of human glioblastoma xenografts with the anti-Chi3L1 antibody results in inhibition of glioblastoma growth by more than 60%.

Conclusions: Our work implicates Chi3L1 as modulator of GSC mesenchymal phenotypic transitions and demonstrates pre-clinical efficacy of our anti-Chi3L1 antibody to reduce phenotypic plasticity and tumor burden.

No conflict of interest.

186

Poster

Optimal therapeutic positioning of a selective bi-steric inhibitor of mTORC1 in genetically defined cancers

J. Jiang¹, Y.C. Yang¹, C.J. Schulze¹, J.W. Evans¹, Z.C. Wang¹, B.J. Lee¹, T.J. Choy¹, D.F. Reyes¹, R.P. Zhao¹, J.Y. Tao², H. Du³, T. Ozawa⁴, D.P. Wildes¹, D.R. Raleigh⁴, Z.P. Wang¹, S.P. Monga², D.J. Kwiatkowski³, W.A. Weiss⁴, J.A. Smith¹, M. Singh¹. ¹Revolution Medicines, Research and Development, Redwood City, USA; ²University of Pittsburgh & University of Pittsburgh Medical Center, Department of Pathology & Pittsburgh Liver Research Center, Pittsburgh, USA; ³Brigham & Women's Hospital, Division of Pulmonary & Critical Care Medicine, Boston, USA; ⁴University of California- San Francisco, UCSF Helen Diller Family Comprehensive Cancer Center, San Francisco, USA

Hyperactivation of the PI3K/mTOR pathway occurs frequently in human cancer, via mutation or deletion of different components. We have developed a class of selective mTORC1 inhibitors, termed 'bi-steric', which comprise a rapamycin-like core moiety covalently linked to an mTOR active-site inhibitor. Bi-steric mTORC1 inhibitors exhibit potent and selective (>10-fold) inhibition of mTORC1 over mTORC2, durably suppress S6K and 4EBP1 phosphorylation, and induce growth suppression and apoptosis in multiple cancer cell lines. These inhibitors provide the mTORC1 selectivity of rapalogs and potentially inhibit translation initiation by the 4EBP1-eIF4E axis while sparing mTORC2.

To examine the potential of mTORC1 inhibition as a monotherapy, we focused on tumors in which PI3K/mTOR pathway aberrations are primary drivers. The bi-steric mTORC1 inhibitor RM-006 exhibited anti-tumor activity in preclinical models of genetically-defined tumor types including PTEN-deficient glioblastoma multiforme, TSC1/2-deficient bladder cancer, and hepatocellular cancer harboring mTOR-activating β -catenin mutations and, unlike rapalogs, decreased both p4EBP1 and pS6 levels in tumors.

We next explored mTORC1 inhibition as a combination therapy in RAS mutant cancers. First-in-class covalent inhibitors of KRAS^{G12C} (OFF) have demonstrated promising anti-tumor activity in cancer patients with KRAS^{G12C} mutations. Drug-anchored CRISPR screens and combination experiments have identified mTOR signaling as a key mediator that limits therapeutic response to KRAS^{G12C} inhibition. We observed a significant combinatorial activity of a bi-steric mTORC1 inhibitor and covalent KRAS^{G12C} inhibitors in preclinical models of KRAS^{G12C} STK11^{deficient} NSCLC, where activation of mTORC1 signaling is also an oncogenic driver. Combinatorial effects were observed *in vitro* and *in vivo*, including delayed on-treatment resistance. The combination effects observed were consistent with downstream modulation of RAS and mTOR pathways in these models.

The bi-steric mTORC1-selective inhibitor RMC-5552 is currently in IND-enabling studies and due to enter clinical trials in early 2021. Our results support the deployment of a genetic biomarker-based approach to position this investigational mTORC1 inhibitor in the clinic to identify and benefit cancer patients with high unmet medical need.

Conflict of interest:

Corporate-sponsored Research: Dr. Monga and Dr. Kwiatkowski are recipients of Corporate Research Grant from Revolution Medicines.

187

Poster

The clinical candidate, ASTX029, is a novel, dual mechanism ERK1/2 inhibitor and has potent activity in MAPK-activated cancer cell lines and in vivo tumor models

J. Munck¹, V. Berdini², A. Courtin¹, C. East³, T. Heightman⁴, C. Hindley¹, J. Kucia-Tran³, J. Lyons¹, V. Martins⁵, S. Muench³, C. Murray², D. Norton⁴, M. O'Reilly⁶, M. Reader⁴, D. Rees⁴, S. Rich³, N. Thompson³, N. Wilshe⁵, A. Woolford⁴, N. Wallis³. ¹Astex Pharmaceuticals, Translational Biology, Cambridge, United Kingdom; ²Astex Pharmaceuticals, Computational Chemistry, Cambridge, United Kingdom; ³Astex Pharmaceuticals, Biology, Cambridge, United Kingdom; ⁴Astex Pharmaceuticals, Chemistry, Cambridge, United Kingdom; ⁵Astex Pharmaceuticals, Dmpk, Cambridge, United Kingdom; ⁶Astex Pharmaceuticals, Molecular Sciences, Cambridge, United Kingdom

Background: The MAPK signaling pathway is commonly upregulated in human cancers due to oncogenic mutations of upstream components such as BRAF or KRAS. Targeting of the MAPK pathway has been clinically validated, with agents targeting BRAF and MEK approved. As the final node in the MAPK pathway, ERK is also an attractive therapeutic target for the treatment of MAPK-activated cancers. We have previously described the discovery of a chemical series targeting ERK using fragment-based drug design. ASTX029 is a highly potent and selective ERK inhibitor from this

series, which is now being tested in a Phase 1/2 clinical trial (NCT03520075). Here, we describe the activity of ASTX029 in a number of MAPK-activated cell-based and in vivo models.

Materials and Methods: Anti-proliferative effects and modulation of the MAPK pathway were studied in a range of cell lines using viability assays, Meso Scale Discovery assays, ELISA and Western Blotting. *In vivo*, subcutaneous mouse xenograft models were used to measure pharmacodynamic effects and anti-tumor activity.

Results: ASTX029 is a potent inhibitor of ERK discovered using fragment-based drug design (IC₅₀ 2.7 nM vs ERK2) with excellent selectivity across a panel of 465 kinases. As described previously for compounds in this series, ASTX029 is a dual mechanism inhibitor with a distinctive ERK binding mode, inhibiting both the catalytic activity of ERK and its phosphorylation by MEK (despite not directly inhibiting MEK activity). ASTX029 potently inhibited the *in vitro* proliferation of a wide range of MAPK-activated cell lines, derived from multiple tumor types including melanoma, colorectal and lung. The phosphorylation of the ERK substrate, RSK, was inhibited in a dose-dependent manner in A375 (BRAF-mutant melanoma) and HCT116 (KRAS-mutant colorectal) cells treated with ASTX029 with IC₅₀ values of 3.3 nM and 4 nM, respectively. In addition, ASTX029 treatment resulted in a decrease in phospho-ERK levels in these cells. ASTX029 was shown to have good oral bioavailability. Once daily dosing resulted in dose-dependent tumor growth inhibition and regressions in a number of MAPK-activated tumor xenograft models including Colo205 (BRAF-mutant colorectal), A375 (BRAF-mutant melanoma) and Calu-6 (KRAS-mutant lung). Consistent with the *in vitro* observations, inhibition of both the ERK catalytic activity and the phosphorylation of ERK itself was also observed in xenograft tissue along with an induction of apoptosis.

Discussion: The ERK inhibitor, ASTX029 has potent activity against MAPK-activated tumor models and is now being tested in a Phase 1/2 clinical trial. These data highlight the therapeutic potential of the compound for the treatment of MAPK-activated cancers and support its further investigation in the clinic.

No conflict of interest.

188

Poster

PT-112, a first-in-class pyrophosphate-platinum conjugate, selectively targets highly glycolytic tumor cells

R. Soler¹, T. Ames², J. Marco-Brualla¹, R. Moreno-Loshuertos¹, M. Price², J. Jimeno^{1,2}, A. Anel¹. ¹University of Zaragoza/Aragón Health Research Institute, Biochemistry and Molecular and Cell Biology, Zaragoza, Spain; ²Phosplatin Therapeutics, Research & Development, New York, USA

Background: PT-112 is a novel pyrophosphate-platinum conjugate, with clinical activity in advanced, pre-treated solid tumors including lung cancers, thymoma and castration resistant prostate cancer (CRPC). The molecular model of PT-112 cancer target disruption is not centered on DNA-binding, and results in robust immunogenic cell death (ICD) induction, as demonstrated in *in vitro* and *in vivo* models. In prior work, we have established a cellular model with an extreme glycolytic phenotype (L929dt cells) vs. its parental OXPHOS-competent cell line (L929 cells), together with mitochondrial cybrids that reproduce both phenotypes (L929^{dt} and dt^{L929} cells, respectively). Here we deploy this model system to investigate the relationship of tumor metabolism to PT-112 sensitivity.

Materials and methods: Effects of PT-112 or of cisplatin control on tumor cell growth were studied using MTT reduction assay, and effects on cell death by simultaneous staining with Annexin-V-FITC and 7-AAD and flow cytometry; mitochondrial ROS production using mitoSox labeling and flow cytometry; autophagy induction using the cyto-ID assay and immunoblot analysis of the LC3B-I/LC3B-II ratio and p62 expression; Rab5 prenylation status and HIF-1 α expression by immunoblot. PT-112 concentrations are pharmacologically relevant in animal models.

Results: Glycolytic tumor cells presenting mutations in mtDNA (L929dt and L929^{dt} cybrid cells) are especially sensitive to cell death induced by PT-112, while cells with an intact OXPHOS pathway (L929 and dt^{L929} cybrid cells) are less so. Cells exposed to cisplatin control do not show such differential sensitivity. The type of cell death induced by PT-112 does not follow the classical apoptotic pathway. Although caspase-3 activation is observed at the same time as cell death, the general caspase inhibitor Z-VAD-fmk does not inhibit PT-112-induced cell death, alone or in combination with the necroptosis inhibitor necrostatin-1. PT-112 induces a marked mitochondrial reactive oxygen species (ROS) accumulation in the most sensitive, glycolytic cells, together with mitochondria hyperpolarization, and induces the initiation of autophagy in all cell lines tested, although p62 degradation was not observed. Finally, the expression of HIF-1 α is higher in glycolytic cells especially sensitive to PT-112 than in cells with an intact OXPHOS pathway. Initial validation of these data in human cancer cells is ongoing.

Conclusion: In our model system, cells with mitochondrial dysfunction were more sensitive to PT-112, likely explained by differences in energy metabolism and/or ROS generation. PT-112's initiation of autophagy is consistent with its robust induction of ICD, as ICD is known to require autophagy. PT-112's selectivity to glycolytic cells may mean high expression of HIF-1 α could be a marker of sensitivity and have clinical applications.

Conflict of interest:

Ownership: Dr. Ames, Mr. Price and Dr. Jimeno all have ownership interests in Phosplatin Therapeutics, which holds the global rights to all uses of PT-112 in oncology.

Board of Directors: Mr. Price serves on the Board of Directors of Phosplatin Therapeutics.

Corporate-sponsored Research: This work was sponsored by Phosplatin Therapeutics.

Other Substantive Relationships: Phosplatin Therapeutics pays Dr. Ames, Mr. Price, and Dr. Jimeno as part of consulting or employment relationships.

189

Poster

The antitumor role of glatiramer acetate and fingolimod in neural tumor cell lines

K. Doello¹, C. Mesas², G. Perazzoli², R. García-Fumero³, F. Quiñero², R. Ortiz². ¹Service of Medical Oncology, Virgen de las Nieves Hospital, Granada, Spain; ²Institute of Biopathology and Regenerative Medicine, Center of Biomedical Research- University of Granada, Granada, Spain; ³Service of Pharmacy, Virgen de las Nieves Hospital, Granada, Spain

Background: glatiramer acetate (GA) and fingolimod (FG) are two disease course modifying drugs used in multiple sclerosis. Both drugs act at the level of cellular receptors related to adhesion to the extracellular matrix. GA is a peptide consisting of glutamic acid, lysine, alanine, and tyrosine that mimics a ligand of the myelin basic protein. FG is a modulator of sphingosine receptors. Both drugs, therefore, act at the level of the relationship that the cellular component presents with the myelin of the central nervous system. The objective of the present work is to study the antitumor role that these compounds can have, both as cytotoxic and at the level of cell migration in neural tumor cell lines.

Material and methods: cells from A172 (glioblastoma, p53 wild type), LN229 (glioblastoma, p53 mutated), SF268 (anaplastic glioma, p53 mutated) and SK-N-SH (neuroblastoma, p53 wild type) cell lines were cultured in 48-well plates for 72 hours with different concentrations of GA (250, 500, 750, 1000, 2500 and 5000 μ M) and FG (1, 5, 10, 25, 50, 75, 100, 125, 150 and 200 μ M) in order to obtain Inhibitory Concentration 50 (IC50) values. Likewise, cell migration studies were carried out with the wound healing assay in SF268 cell line. In order to characterize these cell lines, methylation studies of the MGMT promoter were carried out with the bisulfite technique and RT-PCR in order to determine the expression of P-glycoprotein (PG). Also, cell morphology studies were performed by light microscopy.

Results: the IC50 values for the GA were: 2667 μ M in A172, 1927.65 μ M in SF268, 2188.76 μ M in LN229 and 2757.44 μ M in SK-N-SH. In the case of FG, the results obtained were: 20.26 μ M in A172, 16.55 μ M in SF268, 23.61 in LN229 and 29.26 in SK-N-SH. The cytotoxicity is greater in the case of FG respect to GA. In the case of cell migration at 72 hours, GA was observed to inhibit it by 28% at a dose of 500 μ M while FG, 12% at a dose of 10 μ M. In this case, GA has a greater capacity to inhibit tumor cell migration, even at subcytotoxic doses. Molecular characterization of the cell lines revealed that lines A172 and LN229 show methylation of the MGMT promoter while SF268 and SK-N-SH do not. The only line that expressed PG was SF268. In the light microscopy images, cell changes compatible with anoikis were observed in the case of FG.

Conclusions: GA and FG showed significant antitumor activity in studied cell lines, with greater cytotoxicity in the case of FG and greater cell migration inhibition in the case of GA. The antitumor power of GA appears to be related to mutated p53 cell lines that have been shown to be the most sensitive. In the case of FG, the most sensitive cell line is the one that presents expression of PG, which could be related to the fact that FG is a powerful inhibitor of PG. Cell death caused by FG could be caused by anoikis according to studies.

No conflict of interest.

191

Poster

New antibody therapeutics targeting connexin hemichannels in treatment of osteosarcoma and breast cancer bone metastasis

J. Jiang¹, M. Riquelme¹, Z. An², N. Zhang², W. Xiong², Y. Zhang³, C. Wang³. ¹University of Texas Health Science Center at San Antonio, Biochemistry and Structural Biology, San Antonio, USA; ²University of Texas Health Science Center at Houston, Texas Therapeutics Institute- Brown

Foundation Institute of Molecular Medicine, Houston, USA; ³AlaMab Therapeutics Inc., AlaMab Therapeutics Inc., San Antonio, USA

Background: The growth and migration of tumor cells is largely influenced by their microenvironment, and bone is the primary site for osteosarcoma and a preferred site for cancer metastasis. Connexin 43 (Cx43) hemichannels are highly expressed in osteocytes, the most abundant bone cell type, and have been shown to permit small molecules, such as ATP, to be released into the extracellular environment.

Materials and Methods: We have shown that functional hemichannels associated with ATP release suppress tumor growth in the bone, suggesting that activation of Cx43 hemichannels could be an effective therapeutic strategy in treating bone-associated tumors. We have developed a humanized monoclonal antibody, ALMB-0168, that specifically binds to the extracellular domain of Cx43 and activates the Cx43 hemichannels in osteocytes, but not gap junctions.

Results: ALMB-0168 enhanced the activation of Cx43 hemichannels both in cultured osteocytes and in mouse osteocytes in situ and promoted the release of ATP. Moreover, conditioned media collected from ALMB-0168-treated osteocytes reduced osteocyte and breast cancer cell migration in vitro. A weekly injection of ALMB-0168 reduced bone cancer growth in WT mice, but not in Cx43 knockout mice. The administration of ALMB-0168 significantly increased levels of cytotoxic lymphocytes (CD3+/CD8+) and helper lymphocytes (CD3+/CD4+) isolated from the tumor and draining lymph nodes. ALMB-0168 also increased the survival rate and reduced tumor spreading. Furthermore, a series of pharmacology, toxicology, tissue cross-reactivity (TCR), and hemolytic assessment studies demonstrated the safety of ALMB-0168. Pharmacokinetic (PK) and toxicokinetic (TK) studies following single and repeated IV administration were conducted in C57BL/6 mice and in cynomolgus monkeys with no noticeable differences in PK and TK parameters observed in either species. The ALMB-0168 drug substance and drug product have been formulated and manufactured under good manufacturing practice (cGMP) conditions. Animal protocols were approved by the University of Texas Health Science Center, San Antonio Institutional Animal Care and Use Committee.

Conclusions: These results suggest that ALMB-0168 suppressed the growth and spread of osteosarcoma and breast cancer bone metastases. ALMB-0168 is a first in class antibody therapeutic for the treatment of osteosarcoma and bone metastases. Approval for commencement of a Phase 1 clinical trial in patients is pending.

Conflict of interest:

Ownership: AlaMab Therapeutics Inc.

Advisory Board: AlaMab Therapeutics Inc.

Board of Directors: AlaMab Therapeutics Inc.

Corporate-sponsored Research: AlaMab Therapeutics Inc.

192

Poster

LiP-Quant, an automated chemoproteomic approach to identify drug targets in complex proteomes

Y. Feng¹, N. Beaton², I. Piazza³, R. Bruderer², P. Picotti³, L. Reiter².

¹Biognosys AG, Business Development, Schlieren, Switzerland; ²Biognosys AG, Research & Development, Schlieren, Switzerland; ³ETH Zurich, Institute of Molecular Systems Biology, Zurich, Switzerland

Background: Target identification is a critical step in elucidating the mechanism of action (MoA) for bioactive compounds. For phenotypic drug discovery pipelines, current unbiased, label-free chemoproteomics-based methods rely predominantly on the modulation of target thermal stability upon drug binding. We developed an automated drug target deconvolution workflow combining limited proteolysis with mass spectrometry (LiP-Quant) that exploits protein structural alterations, as well as steric effects driven by drug binding. A major advantage of LiP-Quant is its unique focus on the detection of signature peptides that discern ligand binding, peptides that are generated by a limited digestion and identified by proteomic analysis. Here we demonstrate the performance of LiP-Quant using two well-characterized kinase inhibitors (KIs), Selumetinib (SE) and Staurosporine (ST), as well as two natural product-derived phosphatase inhibitors (PIs) Calyculin A and Fostriecin in human cell lysate. Furthermore, LiP-Quant can be deployed to estimate in-lysate EC50 value of compound binding.

Methods: Mechanically sheared HeLa cell lysate was incubated with compound at multiple concentrations. Next, a limited digest was performed using proteinase K. Finally, the limited digests were processed to peptides with trypsin for mass spectrometry analysis.

Results: Herein, we demonstrate the ability of our LiP-Quant approach to identify unique peptides generated by the binding of either a highly specific (selumetinib) or broad specificity (staurosporine) KI in human cell line lysate. While > 20 kinases met the qualifying LiP-score cutoff for staurosporine, the direct targets MEK1 and MEK2 were clearly identified as main hits in the

unbiased ranking by LiP scores. Both cases represent a highly specific enrichment given that we quantified > 100,000 peptides in each of the experiments. These findings confirm our approach's ability to identify genuine drug targets regardless of drug specificity in a complex biological matrix.

To characterize the specificity of LiP-Quant, we treated lysate with two separate protein PIs. According to literature calyculin A targets protein phosphatase 1 and 2 (PP1A and PP2A) and fostriecin also targets PP2A, in addition to protein phosphatase 4 (PP4C) but does not bind PP1A. Robust phosphatase identification was achieved for both calyculin A and fostriecin treatment. Importantly, with LiP-Quant, we could recapitulate the known relative affinities of the PIs towards their respective targets.

Conclusions: Collectively, this data demonstrate that LiP-Quant can be used to effectively identify protein drug targets and characterize the binding properties in complex proteomes, without compound modification or labeling, and regardless of the specificity of the compound. These capabilities make LiP-Quant a powerful target deconvolution and identification strategy.

Conflict of interest:

Advisory Board: Paola Picotti is a member of the scientific advisory board at Biognosys AG.

Corporate-sponsored Research: Yuehan Feng, Nigel Beaton, Roland Bruderer and Lukas Reiter are employee of Biognosys AG.

193

Poster

OP-1250: A potent orally available complete antagonist of estrogen receptor-mediated signaling that shrinks wild type and mutant breast tumors

L. Hodges-Gallagher¹, R. Sun¹, D. Myles¹, P. Klein¹, J.A. Zujewski¹, C. Harmon¹, P. Kushner¹. ¹Olema Pharmaceuticals, Molecular Biology, San Francisco, USA

Background: Antiestrogens are widely used for the treatment of estrogen receptor positive (ER+) breast cancer; however, some antiestrogens, such as tamoxifen, may exhibit agonist estrogen-like effects in a gene- and cell type-specific manner. Our goal was to develop a next generation antiestrogen that is both orally available and potentially blocks all agonist signaling mediated by ERalpha by targeting both activation functions of the ER (AF1 and AF2). SERMs (selective estrogen receptor modulators) block estrogen-responsive AF2 signaling, but still allow agonist signaling via AF1 stimulated by other pro-proliferative signaling pathways in uterine cells and that become hyperactive during breast cancer tumorigenesis and resistance. The injectable drug fulvestrant (Faslodex[®]) is a complete antagonist of both AF1 and AF2 of the ER and lacks agonist activity in uterine cells, but is not orally bioavailable and incompletely saturates the receptor in patient tumors. Here we describe the preclinical development of OP-1250, a complete ER antagonist with good oral bioavailability and favorable pharmacokinetics, a combination that may particularly benefit ER+ resistant tumors in which the receptor acquires activating mutations that confer estrogen-independent agonist activity.

Materials and Methods: We have developed a set of novel and sensitive cell culture assays that distinguish between complete estrogen receptor antagonists and SERMs in breast and uterine cells. In addition, RNA-seq was used to evaluate changes in the expression of genes associated with cell proliferation. Guided by these assays, we identified OP-1250, an orally available complete antagonist with activity in multiple xenograft models expressing wild type and Y537S mutant ER.

Results: OP-1250 completely blocked AF1 signaling of both wild type and mutant ER, degraded the receptor, blocked estrogen-stimulated proliferation in breast cells, and shrank breast tumors expressing wild type and mutant ER in xenograft models. In contrast, several investigational drugs designed to degrade the ER performed more similarly to SERMs in our assays: they were agonists of AF1, induced the expression of pro-proliferative genes and, consequently, were unable to completely inhibit E2-stimulated breast cell proliferation.

Conclusions: OP-1250 is a potent, novel ER antagonist with best in class potential. OP-1250 is orally available in all tested species, completely antagonizes both AF1 and AF2 of the ER, degrades the receptor, and shrinks breast tumors expressing both wild type and mutant receptor. A Phase 1/2 dose escalation and expansion study in patients with ER-positive, HER2-negative metastatic or advanced breast cancer previously treated with an endocrine therapy will be initiated this year.

Conflict of interest:

Ownership: Cyrus Harmon, Peter Kushner.
Advisory Board: Pamela Klein.

194

Poster

A phase Ib/II trial of high dose ascorbic acid (AA) + paclitaxel protein bound (PP) + cisplatin (C) + gemcitabine (G) with digital spatial profiling (DSP) in patients (pts) with metastatic pancreatic cancer (MPC)

D.D. Von Hoff¹, G. Jameson². ¹TGen/Scottsdale Clinical Research Institute, MMD, Scottsdale, USA; ²HonorHealth, Research Institute, Scottsdale, USA

Background: Increasing evidence suggests that high concentration of AA (vitamin C) can decrease the growth of aggressive tumors, including Ras-mutant tumors. Based on the unmet medical need in MPC, its high frequency of Ras mutations, and prior work combining PP + C + G with MPC (response rate of 70.5%, median survival 16.4 mos), we are exploring the addition of AA to that regimen. Pre and post-treatment biopsies for biomarkers and DSP are also being performed.

Materials/Methods: This pilot trial utilizes a 3 + 3 design for dose escalation of AA. Eligibility criteria include stage IV MPC, ECOG 0–1, and measurable disease. Excluded are pts with a G6PD deficiency, renal oxalate stones, or need of capillary blood glucose monitoring as AA causes false low readings.

Doses are PP 125 mg/m², G 1000 mg/m², C 25 mg/m² on days 1 & 8 of a 21-day cycle. AA infusions are given on days 1, 3, 8, 10, 15, and 17 of a 21-day cycle. Dose levels of AA are 25, 37.5 and 56.25 gm/m².

Results: As of 6/2020, 6 pts were treated in the cohort of AA 25gm/m², 4 pts at AA 37.5gm/m², and 2 pts at 56.25 gm/m². A brisk tumor response of at least partial remission has been observed in 8 of 11 pts who have had at least 1 restaging scan.

There has been 1 study related serious adverse event, in a pt who developed colitis with neutropenia and thrombocytopenia. The pt fully recovered has continued treatment with a dose reduction. Pts who experienced a response to study treatment continued treatment with a good performance status and reported a decrease in tumor related symptoms including abdominal pain, nausea and vomiting. Peak plasma AA levels in all pts in the first 2 dose levels were < 20 mM. However, both pts in the 56.25 gm/m² cohort, achieved desired peak AA level (28.87 mM and 24.0 mM respectively). The cohort of AA 56.25 gm/m² is being expanded.

To gain insight into the cellular and molecular basis for this therapeutic response to date, we performed NanoString GeoMx[™] (DSP) on paired pre- and post-treatment biopsy specimens from 6 pts. Regions of interest on 200 µm in diameter were selected from freshly sectioned FFPE blocks for enrichment in tumor cells, immune cells, or fibroblasts (based on expression of cytokeratin, CD45, and αSMA). This analysis has allowed us to identify therapy induced changes in protein and mRNA within distinct cellular compartments from limited tissues specimens. These changes, which are being further verified, will be presented in detail at the meeting.

Conclusions: This combination appears clinically promising with additional leads generated using DSP.

Supported by SU2C, Cancer Research UK, Lustgarten Foundation & Destroy Pancreatic Cancer.

Conflict of interest:

Corporate Sponsored research: BMS, Honoraria from speaker's bureau.

195

Poster

Small molecule PTP4A3 phosphatase inhibitors targeting acute myeloid leukemia

J. Lazo¹, N. Tasker², E. Rastelli², P. Wipf², E. Sharlow¹. ¹University of Virginia, Pharmacology, Charlottesville, USA; ²University of Pittsburgh, Chemistry, Pittsburgh, USA

Background: The protein tyrosine phosphatase PTP4A3 (Phosphatase of Regenerating Liver-3, PRL-3), which is overexpressed in multiple cancers, including in Acute Myeloid Leukemia (AML), is associated with an overall survival disadvantage. New chemotherapeutic agents are needed to treat AML and the pharmacological targeting of PTP4A3 phosphatase represents a new therapeutic strategy.

Material and methods: We recently synthesized and characterized the novel PTP4A3 small molecule inhibitor, JMS-053 (7-imino-2-phenylthieno [3,2-c]pyridine-4,6-dione), which is a reversible, allosteric, and cell active PTP4A3 inhibitor with an *in vitro* IC₅₀ for PTP4A3 of 30 nM. JMS-053 displayed no significant *in vitro* inhibition of 21 other protein phosphatases and 49 kinases at 1 µM, suggesting considerable specificity towards PTP4A3. We have now synthesized second-generation analogs, including structures designed to stimulate intracellular target phosphatase degradation.

Results: Several analogs, namely EJ-866-75 (7-iminomorpholinoethoxyphenyl thienopyridinedione), EJ-866-81 (chlorophenyl-iminothienopyridinedione) and NRT-870-59 (7-iminomethylphenylthienopyridinedione), retained potent *in vitro* PTP4A3 enzymatic inhibitory activity with IC₅₀

values ranging from 36 to 98 nM. Compounds designed to stimulate intracellular PTP4A3 degradation, namely EJ-887–35 (2-adamantanyliminodioxotetrahydrothienopyridinyl phenoxyacetamidobisethoxyethyl acetamide) and EJ-876–35 (2-adamantanyliminodioxo tetrahydrothienopyridinylphenoxy-butylacetamide), exhibited *in vitro* IC₅₀ values of 107 and 640 nM, respectively. JMS-053 inhibited the growth of Kasumi cells with an IC₅₀ of 19 µM, which was similar to that seen with EJ-866-81 and EJ-887-35. The chemodegrader EJ-876-35 had a cellular IC₅₀ of 4.3 µM while EJ-866-75 and NRT-870-59 had IC₅₀ values >50 µM. JMS-053 and EJ-866-81 inhibited the growth of C1398, MOLT4, R54;11 and MV-4-11 cells with IC₅₀ values ranging from 4–14 µM.

Conclusions: These results support the further investigation of the iminodioxypyridone chemotype as potential cell active PTP4A3 phosphatase inhibitors directed against AML.

Conflict of interest:

Ownership: The authors have assigned the intellectual property regarding these compounds to the University of Virginia and University of Pittsburgh. Drs. Lazo, Sharlow and Wipf are co-founders of KeViRx, which has an agreement with the University of Virginia and the University of Pittsburgh to evaluate these compounds further with an option to license them.

Advisory Board: Peter Wipf is the Chair of the Scientific Advisory Board of KeViRx.

Board of Directors: Elizabeth Sharlow is the CEO of KeViRx.

John Lazo is the CSO of KeViRx.

Other Substantive Relationships: The authors have assigned the intellectual property regarding these compounds to the University of Virginia and University of Pittsburgh. Drs. Lazo, Sharlow and Wipf are co-founders of KeViRx, which has an agreement with the University of Virginia and the University of Pittsburgh to evaluate these compounds further with an option to license them.

196

Poster

Dissection of cancer therapy combinations in RTK driven tumors using zotatifin (eFT226), a potent and selective eIF4A inhibitor

A. Gerson-Gurwitz¹, V.K. Goel¹, N.P. Young¹, B. Eam¹, C.R. Stumpf¹, M. Barrera¹, E. Sung¹, J. Staunton¹, J. Chen¹, S. Fish¹, G.G. Chiang¹, P.A. Thompson¹. ¹eFFECTOR Therapeutics, Cancer Biology, San Diego, USA

Background: Oncoprotein expression is controlled at the level of mRNA translation and is regulated by the eukaryotic translation initiation factor 4F (eIF4F) complex. eIF4A, a component of eIF4F, catalyzes the unwinding of secondary structure in the 5'-untranslated region (5'-UTR) of mRNA facilitating ribosome scanning and translation initiation. Alterations in receptor tyrosine kinases (RTKs) lead to activation of the RAS/MAPK and PI3K/mTOR signaling pathways, enhance eIF4A activity, and promote the translation of select oncogenes that are required for tumor cell proliferation and survival. Zotatifin (eFT226) is a selective eIF4A inhibitor that increases the affinity between eIF4A and sequence specific polypurine motifs in the 5'-UTR of zotatifin target genes, such as FGFR1/2 and HER2. Here we show that activation of eIF4A through RTK alterations along with downregulation of RTK protein expression by zotatifin creates a pathway dependency that drives selectivity to zotatifin treatment. Since many RTKs act as resistance mechanisms to current cancer therapies, regulation of RTKs by zotatifin also provides an effective drug combination strategy.

Methods: *In vitro* antitumor activity was assessed as single agents or in combination by proliferation and apoptosis assays. Regulation of protein expression was analyzed by western blot analysis. 5'-UTR dependency was evaluated using cell-based reporter assays. Athymic nude or NOD/SCID mice were implanted with subcutaneous xenograft models of FGFR1/2 or HER2 driven tumors and treated with zotatifin administered Q4D IV.

Results: Zotatifin inhibits the translation of FGFR1/2 and HER2 through the formation of a sequence dependent ternary complex with eIF4A1 and 5'-UTR mRNA polypurine motifs. In tumor cell lines driven by alterations in FGFR1/2 or HER2 and mTOR-dependent activation of eIF4A, downregulation of RTK expression by zotatifin results in decreased MAPK and AKT signaling, potent inhibition of cell proliferation and an induction of apoptosis. These same models tested *in vivo* demonstrate significant *in vivo* single agent activity. Using our mechanistic understanding of zotatifin targets and signaling pathways, combination strategies targeted vertical inhibition of the PI3K/mTOR/eIF4F pathway. Combination of zotatifin with HER2, PI3K, AKT or mTOR inhibitors was beneficial across RTK driven cancer models.

Conclusions: Downregulation of RTK expression by zotatifin coupled with RTK activation of eIF4A through mTOR signaling offers a unique pathway dependency for selective activity of zotatifin in cancers driven by RTK alterations. In addition, benefits achieved through vertical pathway inhibition, by combining zotatifin with PI3K/mTOR targeted agents, demonstrate the

clinical potential of rationally designed combination strategies. A clinical trial in patients with solid tumor malignancies has been initiated.

Conflict of interest:

Other Substantive Relationships: Share holders at eFFECTOR Therapeutics.

197

Poster

Marine bioprospecting: Investigating new bioactive compounds with antineoplastic potential in glioblastoma

I.V. Gomes E Silva¹, M.H. Campos Baeta Neves¹, K. Lani Silva², R. Ciuvalschi Maia², R. Coutinho¹, A. Ribeiro Soares¹, G. Pinto de Faria Lopes¹. ¹Instituto de Estudos do Mar Almirante Paulo Moreira, Marine Biotechnology, Arraial do Cabo, Brazil; ²Instituto Nacional de Câncer, Coordenação de Pesquisa, Rio de Janeiro, Brazil

Background: Glioblastoma is the most malignant brain tumor of the central nervous system, with a high rate of proliferation and invasive growth, which limits its treatment. Cyanobacteria are photoautotrophic prokaryote organisms, recognized as major producers of secondary metabolites with unique structural characteristics, presenting anti-inflammatory and antitumor activities. The aim of this study was to evaluate the antitumoral effect of extracts from different species of marine cyanobacteria in human glioblastoma cells.

Material and methods: Samples of the cyanobacteria *Oscillatoria sp.*, *Phormidium sp.*, *Lyngbya sp.* and *Aphanothece sp.* were collected in hypersaline systems located in the Lagoa de Araruama, Rio de Janeiro (RJ), and Arraial do Cabo, RJ. The samples were extracted in ethyl acetate (AcOEt): methanol (1: 1), rotary evaporated and kept at -20°C until antineoplastic tests. After reconstitution in dimethyl sulfoxide, increasing concentrations were used in MTT assay with cancer cell lines, T98G and U251 (glioblastoma) for 72 h. For the cytostatic effect, the cells were cultured with their respective IC₅₀, after 72 h it was analyzed by flow cytometry as well as DNA fragmentation. For chemical basic profile, thin layer chromatography was performed, using Hexane: CH₂Cl₂ 1.5:8.5 and AcOEt 100% elutions and revealed by Dragendorff, KMnO₄, FeCl₃, EtOH 5% H₂SO₄ and Ninhydrin.

Results: The extracts from *Oscillatoria sp.*, *Phormidium sp.* and *Lyngbya sp.* demonstrated IC₅₀ = 51.91; 197.5 and 299.2 µg/ml in the U251 cells, respectively. In the T98G cells the extracts from *Oscillatoria sp.* and *Phormidium sp.* demonstrated IC₅₀ = 124.9 and 261.8 µg/ml, respectively. *Aphanothece sp.* extracts did not have cytotoxic effect. Extracts from *Oscillatoria sp.*, *Phormidium sp.* and *Lyngbya sp.* demonstrated significant S and G2/M arrest. The chemical analysis exhibited that all samples was positive for the presence of phenols, sterols and aromatic polycarboxylic acids chemical classes. The extract of *Oscillatoria sp.* showed the presence of amino acids and alkaloids; *Phormidium sp.* extracts also showed the presence of alkaloids, showing a great chemical diversity.

Conclusions: The secondary metabolites of the marine's cyanobacteria *Oscillatoria sp.* and *Phormidium sp.* presents bioactive compounds such as amino acids and alkaloids that may be conferring a greater antitumor effect *in vitro* that could be a source of marine biopharmaceutical in the future.

No conflict of interest.

POSTER SESSION

New Therapies in Immuno-Oncology

198

Poster

LncRNA H19/miR-486-5p/miR-17-5p: A novel immunoregulatory loop regulating TNBC cellular recognition by cytotoxic T lymphocytes and natural killer cells

A. Elkhoul¹, R. Youness², M. Gad¹. ¹Faculty of Pharmacy and Biotechnology- German University in Cairo, Biochemistry Department, Cairo, Egypt; ²Faculty of Pharmacy and Biotechnology- German University in Cairo, Pharmaceutical Biology Department, Cairo, Egypt

Background: Cytotoxic T lymphocytes (CTLs) and Natural Killer cells (NKs) are the most dominant players in the TNBC-immune surveillance. CTLs and NKs express an array of activating receptors on their surface such as NKG2D and CD226 receptors. These receptors specifically bind to unique activating ligands exclusively present on cancer cells such as MICA, MICB and CD155. Yet, shedding of such activating ligands is one of the immune-escape tactics cancer cells usually bravely exhibit. Thus inducing the expression of such activating ligands is a promising strategy to re-sensitizing TNBC cells to be eradicated by CTLs and NKs. Recently, our research group has extensively

employed several non-coding RNAs (ncRNAs) in modulating the tumor microenvironment and oncogenic profile of TNBC. Therefore, the aim of this study is to unravel the impact of ncRNAs and their interplay on immunogenic profile of TNBC at the immune-synapse with CTLs and NKs.

Methods: Breast biopsies were collected from 25 BC patients. Several computational prediction analysis was performed. MDA-MB-231 and MCF7 cells were cultured. TNBC cells were transfected with miR-486-5p, miR-17-5p and H19 lncRNA oligonucleotides. Total RNA was extracted and quantified by qRT-PCR.

Results: MICA/B were found to be down-regulated in MDA-MB-231 compared to MCF-7 cells. Yet it was not expressed on normal BC tissues. *In-silico* analysis was performed where miR-486-5p, miR-17-5p and H19 lncRNA were predicted to target MICA/B and CD155. miR-486-5p and miR-17-5p were found to be markedly down-regulated in BC patients, while lncRNA H19 was found to be up-regulated. Ectopic expression of either miR-486-5p or miR-17-5p induced MICA/B expression levels. Moving to CD155 expression, it was found to be paradoxically altered by miR-486-5p and miR-17-5p. This finding grabbed our attention to consider another factor missing in this loop having the upper hand. Knocking down of H19 solved the puzzle where it induced CD155 expression on TNBC cells.

Conclusion: This study crystallizes lncRNA H19, miR-486-5p and miR-17-5p as novel immunomodulatory ncRNAs in TNBC patients with promising effects on CTLs and NKs cytotoxic ability to eradicate TNBC.

No conflict of interest.

199

Poster

Quantification of myeloid cell repolarization and their interplay with the tumor in 3D with image-based analysis

G. Gouvea¹, N. Beztinna¹, B. Visser¹, E. Spanjaard¹, K. Yan¹, L. Price¹, L. Daszkiewicz¹. ¹Ocello B.V., Leiden, Netherlands

Background: The myeloid cell compartment plays an important role in anti-tumor immune responses and represents a heterogeneous population with both cancer-promoting and cancer-restraining actions. Unleashing the full potential of cancer immunotherapies requires an understanding of the cellular mechanisms that govern these opposite actions. Building on our established platform for measuring the effects of immune-modulators on the infiltration and killing of tumor organoids we further increased the biological relevance of this assay by incorporating the myeloid cell compartment. This complex co-culture of myeloid cells, T cells and tumor cells results in a better representation of the complete tumor microenvironment (TME). This assay is well suitable to test cancer immunotherapies that target multiple cell types involved in anti-tumor immune responses and to understand in general the suppressive tumor environment.

Material and Methods: Different myeloid populations were generated in 3D from monocytes derived from healthy donor PBMCs. Polarized M1 and M2 macrophages, DCs and undifferentiated monocytes were then co-cultured with either tumor conditioned media or spheroids derived from different cancer cell lines or colon rectal cancer organoids, growing in protein hydrogel. In addition, purified CD8⁺ T cells were also incorporated in these cultures. The cellular interactions were visualized using high-content microscopy and in-house developed OMinerTM software was trained on a set of features that enabled discrimination between different myeloid cell populations in 3D.

Results: 3D imaging and phenotypic analysis was used to classify different myeloid cell populations. This classification was confirmed functionally by profiling of released cytokines. In addition, our analysis demonstrated repolarisation of M2 type macrophages into M1 type macrophages upon treatment with CSF1r inhibitor or STING agonist. This repolarisation was confirmed with an increased similarity score towards M1 macrophages upon treatment. We also used this approach to reveal the different effects of tumor cells and their immunosuppressive microenvironment on the myeloid cell phenotypes. Moreover, triple co-cultures with T cells showed the suppressive effect of tumor associated myeloid cells on the proliferation and function of these T cells.

Conclusions: The assay presented here enables visualization and quantification of effects of immunotherapies on myeloid cells using 3D phenotypic analysis. This co-culture system provides means to elucidate the bi-directional interplay between tumor and immune cells, allowing for analysis of functional reprogramming of the suppressive population towards a M1 phenotype induced by drug candidates. This advanced platform for testing cancer immunotherapies also combines the complexity of the TME with the robustness of a high throughput screening platform.

Conflict of interest:

Ownership: Leo Price.

200

Poster

Emergence of novel long-acting mono- and bi-specific IL-2/IL-13 superkines as potent immune modulators

F. Merchant¹, M. To², R. Merchant². ¹Medicenna Therapeutics, Clinical, Toronto, Canada; ²Medicenna Therapeutics, Pre-Clinical, Toronto, Canada

Background: Use of IL-2 (Proleukin[®]) remains limited due to a short half-life, toxicity, and preferential activation of Tregs driven by a high affinity for IL2R α over IL2R β . To bypass these limitations, we further engineered MDNA109, an IL-2 superkine, to generate MDNA11 by (1) addition of mutations to abrogate IL2R α binding and (2) fusion with albumin to extend half-life. We also leveraged the versatility of our superkine platforms to engineer long-acting bispecific constructs to simultaneously activate IL-2 signaling (i.e. pro-inflammatory) and suppress IL-4/IL-13 function (i.e. anti-inflammatory) and/or enable accumulation in tumors.

Materials and Methods: *In vitro* and *in vivo* studies included IL-2 signaling in human PBMCs, BLI/Octet binding analyses, PK studies in mice, and efficacy studies in syngeneic tumor models with or without immune checkpoint inhibitors (ICIs). A dose ranging finding study in cynomolgus monkeys (NHP) was performed to characterize the safety and PK/PD profiles of MDNA11.

Results: MDNA11 and bispecific constructs displayed enhanced STAT5 signaling in human NK and resting CD8 T cells with diminished Treg activity compared to IL-2. In spite of qwk dosing for two weeks, MDNA11 monotherapy or in combination with ICI demonstrated potent efficacy in a CT26 tumor model, resulting in long-term tumor regression and strong memory response. MDNA11 also inhibited growth of B16F10 melanomas with durable increase in tumor infiltrating CD8 T and NK cells. Preliminary studies with bispecific constructs demonstrated therapeutic responses in both CT26 and B16F10 tumor models. In NHP, MDNA11 induced durable proliferation and expansion of NK and CD8 T cells with limited effects on Tregs. Repeat dose of MDNA11 did not trigger cytokine storm, anti-drug antibody response nor eosinophilia (associated with vascular leak syndrome; VLS). Histopathological evaluation confirmed an absence of pulmonary edema, a major IL-2 induced toxicity.

Conclusions: MDNA11 is a long-acting IL-2 superkine with superior potency at activation of naïve CD8 T cells and NK cells, and diminished activity on Tregs. MDNA11 potently inhibited growth of tumors and induced durable regression and strong memory response. Novel bispecific constructs also demonstrated efficacy in these *in vivo* tumor models. In NHP, MDNA11 induced durable proliferation and expansion of immune effector cells without adverse side effects. These data demonstrate the potency of MDNA11 and underscore the versatility of our superkine platforms to the design of multi-functional therapeutics for immuno-oncological indications.

Conflict of interest:

Ownership: Fahar Merchant, Nina Merchant.

Board of Directors: Fahar Merchant, Nina Merchant.

201

Poster

A phase I/II study of JX-594 oncolytic virus in combination with immune checkpoint inhibition in refractory colorectal cancer

C. Monge¹, C. Xie², G. Brar¹, E. Akoth¹, S. Webb³, D. Mabry², B. Redd⁴, E. Levy⁴, B. Wood⁴, T. Greden². ¹National Cancer Institute, Gastrointestinal Malignancies Branch, Bethesda, USA; ²National Cancer Institute, Gastrointestinal Malignancies Branch, Bethesda, USA; ³National Cancer Institute, Gastrointestinal Malignancies, Bethesda, USA; ⁴National Cancer Institute, Radiology and Imaging Sciences, Bethesda, USA

Background: Immune-based approaches in colorectal cancer have been unsuccessful with the exception of immune checkpoint inhibition in micro-satellite unstable disease. This may relate to advanced colorectal cancer being less immunogenic than other tumors, as evidenced by the lack of infiltrating lymphocytes. JX-594 (Pexa-Vec[®]) is a thymidine kinase gene-inactivated oncolytic vaccinia virus engineered for the expression of transgenes encoding human granulocyte-macrophage colony-stimulating factor and β -galactosidase. JX-594 has direct oncolytic activity and mediates tumor cell death via the induction of innate and adaptive immune responses. This study aims to enhance the anti-tumor immunity induced by JX-594 oncolytic viral therapy by administering the vaccine with immune checkpoint inhibition; the combination of tremelimumab (CTLA-4 antibody) and durvalumab (PD-L1 antibody). The primary objective was to establish the safety and tolerability of the treatment and the secondary objective to explore progression free survival.

Methods: JX-594 was administered IV every 2 weeks for 4 doses, the first dose was administered on Day minus 12, followed by administration on Days 2, 16 and 30. The study had two arms; arm A received durvalumab 1500 mg IV on Day 1 of 28-day cycles; arm B received tremelimumab 300 mg IV on

C1D1 only, in addition to the treatment administered to arm A. Eligibility included recurrent, metastatic, histologically confirmed adenocarcinoma of the colon, after progression on oxaliplatin and irinotecan containing, fluorouracil-based, chemotherapeutic regimens. Patients with known KRAS wild type tumor must have progressed on cetuximab or panitumumab based therapy. All tumors were documented to be micro-satellite stable.

Results: 30 patients enrolled, 15 on arm A and 15 on arm B; the median age was 55 years (range 28–76 years). Upon enrollment onto protocol 39% of patients had metastasis to the liver; followed by pulmonary metastasis seen in 13%. The median number of cycles until disease progression in both arms was 1.7 months (range 1 to 10 months) with a median PFS in Arm A of 2.3 months (range 1.3 to 9.6 months) and Arm B of 1.7 months (range 0.4 to 5.5 months). A statistically significant difference in PFS between arms A and B was not found. There were no deaths on study. The most common grade 3–4 toxicities included decreased lymphocyte count (40%), fever (23%) and anemia (17%).

Conclusions: Combined JX-594 and immune checkpoint inhibition treatment with durvalumab and tremelimumab is feasible and safe in refractory CRC. A durable response was evidenced in some patients; further studies are needed to identify the subgroup that may benefit from this treatment.

No conflict of interest.

202

Poster

TAS1553, a novel class of RNR inhibitor, has robust antitumor activity in murine syngeneic tumor models as a single agent and in combination with anti-PD-1 checkpoint inhibitor

H. Fukushima¹, T. Sayaka¹, Y. Wakako¹, H. Takuya¹, U. Hiroyuki¹, F. Satoshi¹, M. Hiromi¹, Y. Keisuke¹, S. Takamasa¹, I. Kenjiro¹, M. Seiji¹, M. Kazutaka¹, U. Teruhiro¹, S. Takeshi¹. ¹Taiho Pharmaceutical Co.-Ltd., Discovery and Preclinical Research Div., Tsukuba, Japan

Background: Deoxyribonucleoside triphosphates (dNTPs) are the building blocks of DNA and are essential for cancer cell growth and survival. Ribonucleotide reductase (RNR) regulates a rate-limiting step in the supply of dNTP, which suggests RNR as a promising therapeutic target of cancer. TAS1553 is a novel class of RNR inhibitor that abrogates protein-protein interactions between RNR subunits; this compound has shown promising antitumor activity in preclinical models for both solid tumors and hematological malignancies.

Gemcitabine (GEM) reportedly promotes tumor immunity in addition to its direct cytotoxic activity and has a significant antitumor efficacy in combination with immune checkpoint inhibitors such as anti-PD-1 antibody. In addition to its ability to inhibit DNA synthesis, GEM also has an inhibitory effect against RNR enzyme activity.

Here, we evaluated the effect of TAS1553 on the expression of immune-oncology related markers and the antitumor activity of TAS1553 in murine syngeneic tumor models when used as a single agent and in combination with an anti-PD-1 checkpoint inhibitor.

Materials and methods: The antitumor efficacy was evaluated in both athymic nude mice and immunocompetent mice bearing EMT6 (murine mammary carcinoma) or MC38 (murine colon adenocarcinoma) cells. Global immunity in the tumors was analyzed using flow cytometry and qPCR.

Results: TAS1553 exerted a robust antitumor activity against EMT6 and MC38 tumors in syngeneic mouse models. Furthermore, the antitumor efficacy of TAS1553 in immunocompetent mice was greater than that in immunodeficient mice (77% vs. 42% TGI at 100 mg/kg in the EMT6 model), suggesting that TAS1553 affected a functional immune system. We additionally found that TAS1553 monotherapy significantly increased the number of CD8⁺ T-cells and the expression of interferon gamma in tumors, followed by increased expressions of perforin and granzyme B. Interestingly, TAS1553 promoted the infiltration of not only immune-enhancing factors, but also immunosuppressive factors such as PD-1 and PD-L1 in the tumors. Next, we investigated the antitumor activity of TAS1553 in combination with anti-PD-1 therapy and demonstrated that TAS1553 combined with an anti-PD-1 antibody enhanced the antitumor efficacy of the anti-PD-1 antibody, with complete responses observed in 4 of the 10 mice in the MC38 model.

Conclusions: TAS1553 exerted robust antitumor activities in murine syngeneic tumor models when used as a single agent through an immunological mechanism. Furthermore, TAS1553 significantly enhanced the antitumor efficacy of anti-PD-1 antibody by providing a more suitable tumor microenvironment for anti-PD-1 treatment. These findings indicate that a combination therapy consisting of TAS1553 and anti-PD-1 might be a new promising therapeutic option for cancer patients.

No conflict of interest.

203

Poster

A FliC armed oncolytic tanapoxvirus causes regression of colorectal cancer xenografts in immuno-competent models

S.I. Kana¹, M. Monaco¹, S. Kohler¹, R. Eversole¹, K. Essani¹. ¹Laboratory of Virology, Department of Biological Sciences, Western Michigan University, Kalamazoo, USA

Background: Colorectal cancer is the third most common neoplasm in the world and the third leading cause of cancer related deaths in the USA. Oncolytic virotherapy has emerged as a potential treatment modality for colorectal carcinoma. We have previously shown that a tanapoxvirus recombinant armed with FliC, TPV/Δ2L/Δ66R/fliC, resulted in significant reduction of HCT116 tumors in athymic mice (Conrad SJ, El-Aswad M, Kurban E, et al. Oncolytic tanapoxvirus expressing FliC causes regression of human colorectal cancer xenografts in nude mice. J Exp Clin Cancer Res. 2015;34(1):19. Published 2015 Feb 19. doi:10.1186/s13046-015-0131-z). The current study was conducted to evaluate the immuno-oncolytic efficiency of this virus in immuno-competent models.

Materials and methods: Colorectal tumors were induced by subcutaneous injection of HCT 116 cells on both the left and right flanks of inbred BALB/c nude mice. We then made the mice immuno-competent by injecting 3*10⁶ splenocytes/mouse intraperitoneally from inbred BALB/c immuno-competent mice. Each of the mice received an intratumoral injection of either 5*10⁶ TPV/Δ66R/Δ2L/fliC in DPBS or just DPBS.

Result: A single intratumoral injection of the virus resulted in significant and robust regression of tumor volume (P < 0.01) and resulted in almost complete reduction of 80% of the injected tumors. The regression of a second non-injected tumor, contralateral to the injected ones, could also be observed, albeit the reduction was not significant. We aim to conduct future studies to evaluate the systemic efficacy of this virus.

Conclusion: Our results indicate that the recombinant TPV/Δ2L/Δ66R/fliC could be a potential candidate for the treatment of colorectal cancers in humans and should be explored further for the complete realization of its potential.

No conflict of interest.

POSTER SESSION

Preclinical Models

204

Poster

Correlation of molecular profiles with response to targeted drugs in pancreatic cancer models

D. Behrens¹, R. Lawlor², C. Heeschen³, B. Buettner¹, J. Siveke⁴, J. Hoffmann¹. ¹EPO - Experimental Pharmacology & Oncology Berlin-Buch GmbH, Experimental Pharmacology, Berlin, Germany; ²ARC-NET-University of Verona, Policlinico G.B. Rossi, Verona, Italy; ³QMUL- Barts Cancer Institute, Centre for Stem Cells in Cancer & Ageing, London, United Kingdom; ⁴DKFZ University Hospital Essen, West German Cancer Center, Essen, Germany

Background: Pancreatic cancer (PC) remains a lethal disease with only 3–8% of patients surviving 5 years after diagnosis of the tumor (WHO, 2018). Within the EU project “CAM-PaC” a comprehensive panel of twenty patient-derived PC xenografts (PDX) was established and characterized for morphology, genetic profile and sensitivity to standard of care. Additionally, responders to the targeted MEK inhibitor Trametinib were identified and analyzed for correlation with the genetic profile.

Methods: Pancreatic tumor samples were collected either during surgery or generated from circulating tumorigenic cancer stem cells, isolated from the peripheral blood using VAR2CSA-coated magnetic beads. Both were transplanted subcutaneously into NOD/SCID/IL2γ^{-/-} mice and after engraftment further propagated in NMRI:nu/nu mice. The PDX were morphologically and molecularly characterized by histopathology and with NGS panel sequencing, based on pathway aggregated genes that were identified by the International Cancer Consortium (described by Bailey et al., Nature 531, 2016). Standard drugs (Gemcitabine, Abraxane, 5FU, Oxaliplatin) were applied at clinically relevant doses and schedules. Trametinib was given daily as monotherapy.

Results: All PDX correlated with the histopathological and molecular characteristics of original patient tumours. The most efficacious drug was Abraxane with 80% response rate (stable disease, partial regression).

Gemcitabine reached a response rate of 35% and the combination of 5-FU and Oxaliplatin 45%.

The MEK kinase inhibitor Trametinib was tested in 16 PDX models, where 5 identified as responders with a biologically relevant tumor growth inhibition of > 50%. However only 1 out of the tested 16 PDX models showed tumor regression and more than > 80% tumor growth inhibition in comparison to the control (T/C). KRAS mutations have been identified as one driver mutation in pancreatic cancer, however we did not find a correlation between the MAP-Kinase pathway inhibitor sensitivity and KRAS mutations in our PDX.

Conclusion: The newly established pancreatic cancer PDX panel reflect the patient disease. Histology, inherent heterogenic growth, and frequently acquired treatment resistance are in correlation with the clinical situation. We are currently analyzing the molecular data to determine better response markers, offering a more personalized treatment of pancreatic cancer patients.

No conflict of interest.

205

Poster

'In vitro clinical trials' platform for drug testing in patient-derived ex vivo 3D cultured human tumor tissues

N. Beztsinna¹, F. Grillet², A. Jariani², J. Overkamp¹, D. van der Meer², L. Daszkiewicz¹, K. Yan¹, W. Vader², L. Price¹. ¹Ocellio BV, Ocellio, Leiden, Netherlands; ²VitroScan BV, VitroScan, Leiden, Netherlands

Introduction: Despite the widespread utilization of animal models in pre-clinical drug research these do not fully represent the complexity of human cancer, which leads to significant failure rates for anticancer drugs in clinical development. In recent years, 3D organotypic cell culture models, such as organoids, have emerged to help bridge the gap between conventional *in vitro* models and patients. However, organoids are clonal and lack tumor associated cells, such as fibroblasts, T cells (TIL) and other immune cells which both modulate the responses to drugs and are themselves important drug targets.

Here we present an innovative 'in vitro clinical trials' (IVCT) platform - a high throughput short-term 3D *ex vivo* tumor culture combined with high content image-based analysis. Patients' tumor tissue from resections, biopsy, pleural fluid or ascites is tested *ex vivo* such that tumor heterogeneity and resident immune cells are preserved.

This paper reports a detailed quantification of tumors' sensitivity to standard of care and novel (immune) drugs and drug combinations, tested on patient-derived ovarian, breast and non-small-cell lung cancer (NSCLC) tumor tissue.

Methods: Tumor tissue was obtained from ongoing multi-center clinical trials in the Netherlands and commercial tissue providers. Freshly isolated tumor cells from ovarian, breast cancer and NSCLC patients were embedded in a protein-rich hydrogel and exposed to panels of drugs (and combinations) at different concentrations. The automated high content imaging analysis platform, Ominer(TM), measured the effect of the drugs on biologically relevant morphological features, such as tumor cell killing, growth arrest, invasion and immune cell proliferation, and subsequently quantified the tumors sensitivity to the drugs.

Results: We present results of drug sensitivity testing in patient-derived primary tumoroids of fresh ascites, pleural fluids and solid tumor. Patient-specific drug sensitivity was identified for a broad range of drugs including standard of care (e.g. platinum, paclitaxel, gemcitabine), targeted therapies (e.g. PARP inhibitors), and activity of immunomodulatory drugs (e.g. Nivolumab, Ipilimumab, Pembrolizumab and STING agonists). Accurate and reproducible response evaluation demonstrates the feasibility of high-throughput drug screening on patient primary material within the IVCT platform.

Conclusion: The presented IVCT platform successfully combines *ex vivo* drug testing using patients' tumor tissue with preserved tumor microenvironment and advanced 3D image analysis. IVCT represents a rapid, reliable and biologically relevant approach to test various candidate compounds (e.g. antibodies, antibody-drug conjugates and small molecules) for various cancer types. IVCT aims to significantly improve pre-clinical evaluation of drugs and potentiate their future performance in clinical trials.

Conflict of interest:

Ownership: Leo Price is a founder and stock holder of Ocellio BV. Other Substantive Relationships: N. Beztsinna, J. Overkamp, L. Daszkiewicz, K. Yan, L. Price are full-time employees of Ocellio BV. F. Grillet, D. van der Meer, W. Vader are full time employees of VitroScan BV.

206

Poster

Assessing the impact of cGAS-STING pathway activation on adoptive cell therapy using a patient-derived 3D ex vivo tumor organoid model

M. Pabon¹, T. Pastoor¹, J. Ehrhart¹, J. Krehling¹, S. Altio¹. ¹Nilogen Oncosystems, Research and Development, Tampa, USA

Introduction: Adoptive cell therapy (ACT) with *ex vivo* expanded tumor infiltrating lymphocytes (TILs) has been of growing interest in the treatment of solid tumors. It is critical to develop effective combination therapies to overcome intrinsic immune escape mechanisms limiting the efficacy of ACT in individual tumors. Stimulation of the cyclic GMP-AMP synthase-stimulator of interferon genes (cGAS-STING) pathway results in the expression of pro-inflammatory genes which can result in activation of multiple immune cells promoting innate immunity in addition to senescence of cancer cells. Here we analyzed the efficacy of cGAS-STING pathway activation alone and in combination with a PD-1 inhibitor nivolumab on activation and infiltration of TILs in the 3D tumor organoids.

Materials and Methods: All human tumor samples were obtained with proper patient consent and IRB approval. Fresh patient tumor tissue of various histologic types was processed to generate uniform sized live 3D tumor organoids measuring 150 µm in size. Treatment groups included STING agonists, ADU-S100 and 23'-cGAMP, alone or in combination with nivolumab. Culture supernatants were collected for multiplex analysis of cytokine release in media. Additionally, flow cytometry was used to assess the activation profile of resident immune cells as well as TILs in combination with high-content confocal imaging to determine extent of tumor cell death and TIL penetration in the intact tumor extracellular matrix.

Results: In this study we documented how activation of STING pathway alone and in combination with PD1 blockade affects TME and TIL activation in solid tumors. Flow cytometric analysis of immune cell populations isolated from 3D tumor organoids demonstrated treatment mediated activation of TILs which coincided with marked changes in pro-and anti-inflammatory cytokine profiles determined from multiplex analysis. Furthermore, this data was correlated with quantitative confocal analysis of tumor cell killing within tumor organoids.

Conclusion: These results demonstrate that the 3D *ex vivo* tumor organoid model is an effective system to assess the efficacy of ACT and to develop novel therapeutic combinations. Furthermore, implementation of this platform in the clinical studies may also allow determining the most effective combinatorial cellular therapy strategies for individual patients.

No conflict of interest.

207

Poster

Benchmarking syngeneic tumor models to explore immuno-pathogenesis and anti-PD1 mechanism of action

A.X. An¹, Y. Jin¹, B. Mao¹, D. Ouyang¹, H. Li¹. ¹Crown Bioscience Inc., Scientific Research & Innovation, San Diego, USA

Background. Syngeneic *in vivo* models are commonly used for proof of concept (POC) and mechanistic exploration of immune-oncology (IO) therapies, e.g. immune-checkpoint inhibitors (ICIs). Each model responds differently to a given ICI, which is believed to be dependent on the unique intrinsic tumor immunity of each model, as well as unique mechanisms of actions (MOA) for a specific ICI, in each tumor. However, our knowledge on these mechanisms remain limited due to large experiment variations and lack of comprehensive benchmark of these models, preventing optimal model utilization.

Material and methods: The present study systematically investigated a panel of syngeneic models, including MC38, Hepa1-6, EMT-6, CT26, etc., to benchmark their baseline dynamic immunophenotypes (tumor-infiltrate leukocytes, or TILs) by flow cytometry, the anti-PD-1 antibody pharmacology and the associated TIL-pharmacodynamics by flow.

Results: Our data clearly demonstrated that all the parametric values of these models are different from each other, implicating distinctive intrinsic tumor immunity, as well as treatment MOAs. In general, different lineages of T cell- and macrophage-TILs seem to exhibit dominant roles in tumor immunology and observed anti-PD1 treatment efficacy. Among the tumors responsive to ICI, a balance between the roles of TIL-CD4⁺-effectors/CD8⁺-CTLs and TIL-M₂-macrophages in Hepa1-6 seem to play critical role in the tumor growth inhibition with or without anti-PD1-treatment, whereas a balance between TIL-T_{reg} and -CD8⁺ CTLs in MC38 tumor seemed to be more critical. In contrast, TIL-M₂-macrophages and -T-cells also seems to be responsible for the partial tumor inhibition in EMT-6 and CT-26 syngeneic tumors.

Conclusions: Benchmarking the baseline dynamic immunophenotype of syngeneic model will not only help to select optimal models to evaluate a

given IO-pharmacology, but also can potentially translate into understanding of patient disease mechanisms and strategizing IO-therapies in the clinics.

Conflict of interest:

Corporate-sponsored Research: Crown Bioscience Inc.

POSTER SESSION

Tumour Immunology and Inflammation

208

Poster

Targeting oncogenic signalling pathways to modulate the lung cancer immune microenvironment

F. Van Maldegem¹, E. Mugarza¹, M. Molina-Arcas¹, K. Valand¹, S. Rana¹, M. Cole¹, P. Romero-Clavijo¹, J. Boumelha¹, C. Moore¹, J. Downward¹.

¹The Francis Crick Institute, Oncogene Biology Laboratory, London, United Kingdom

Fourteen percent of lung adenocarcinomas harbour a KRAS-G12C mutation as their main driver mutation. Recently, novel KRAS-G12C covalent inhibitors were reported to yield very promising early results in clinical trials. However, as with many monotherapies targeting oncogenic pathways, rapid onset of resistance is expected to occur, and combination strategies are needed. Recent research has shown that there may be synergism between KRAS inhibition and immunotherapy. Furthermore, we have evidence that KRAS signalling can modulate the expression of numerous immunomodulating molecules.

To further investigate the role of oncogenic KRAS in immune suppression, we have extensively characterised the immune composition of the tumour microenvironment, with the use of flow cytometry, RNAseq, and Imaging Mass Cytometry (IMC), in mouse models of KRAS-G12C mutant lung cancer. IMC allows for the simultaneous visualisation of more than 35 markers in tissue sections, thereby giving unprecedented insight into the complex tumour microenvironment.

We found that KRAS-mutant tumours very strongly regulate their immune cell composition, by attracting myeloid cells while excluding effector cells. Subsequent inhibition of oncogenic signalling using the KRAS-G12C inhibitor MRTX1257, led to profound changes in immune activation state and composition within the tumours. Tumour cell intrinsic changes in expression of chemokines and cytokines, antigen presentation and interferon pathway activation, altogether relieve immune suppression mechanisms.

In conclusion, there will be an excellent opportunity to exploit the liberation of the anti-tumour immune response upon KRAS-G12C inhibition in lung cancer.

No conflict of interest.

209

Poster

Interleukin 33: A new target against gastrointestinal cancer?

M. Eissmann¹, C. Dijkstra¹, M. Ernst¹. ¹Olivia Newton-John Cancer Research Institute and La Trobe University- School of Cancer Medicine, Cancer and Inflammation, Heidelberg, Australia

Cytokine-mediated inflammation is a driver of gastric and colonic tumorigenesis. IL1-family cytokine Interleukin 33 (IL33) regulates inflammatory responses and antibodies targeting IL33 or its receptor ST2 are in clinical trials against various inflammatory and allergy diseases. Only recently, a role of IL33 in cancer started to emerge. Depending on the cancer stage or type IL33 can provoke either pro- or anti-tumoral responses.

To evaluate the potential of targeting IL33 signalling to abrogate gastric and colonic cancer growth, we employ *gp130^{Y757F/Y757F}* (FF) gastric cancer mice and the 6xAOM sporadic colon cancer models as well subcutaneously engrafted MC38 colon cancer models. IL33 signalling inhibition was achieved via genetic deficiency (ST2^{-/-}), while recombinant IL33 was administered to hyper activate the IL33-signalling pathway.

We found, that IL33 cytokine and ST2 receptor are overexpressed in human gastric cancers and high ST2 expression predicts poor survival for gastric cancer patients. In accordance, IL33 and ST2 are highly elevated in our FF mouse tumors. Deficiency of IL33 signalling (ST2^{-/-}) diminishes gastric tumour growth, and is associated with a decrease in tumour-adjacent pro-tumoral mast cells and tumour-infiltrating macrophages (TAM) as well as reduced angiogenesis. Furthermore, ST2-deficiency potentiates the anti-tumor effects of oxaliplatin chemotherapy in the FF mouse model.

In the colon cancer setting, ST2-deficiency lead to increased tumour burden in 6xAOM sporadic colorectal cancer. Reciprocal bone marrow chimera indicated that the radio-resistant non-hematopoietic compartment contributes to the increased tumour growth. Indeed, we found ST2 expression in the mesenchymal cells. Loss of IL-33 signalling in the non-hematopoietic radio-resistant compartment coincided with a strong reduction of an IFN γ gene expression signature. Importantly, IL-33 cytokine administration reduced colon cancer allograft growth associated with tumour-infiltrating IFN γ -positive T cells.

Our data demonstrates the opposing roles of IL33 signalling in the growth of gastric and colonic cancers and identifies cellular mediators of these divergent tumor responses. Further studies are warranted to stratify IL33-signalling sensitive GI cancers and to verify the potential of anti-IL33/ST2 antibodies against gastric cancer and activating IL33 cytokine administration in colon cancers as novel therapy strategies.

No conflict of interest.

210

Poster

CD8⁺ T tumour-infiltrating lymphocytes lacking CD5 cell surface expression exhibited increased levels of activation and exhaustion

F. Alotaibi¹, R. Figueredo², M. Vincent², W.P. Min³, J. Koropatnick¹.

¹University of Western Ontario, Microbiology and Immunology, London,

Canada; ²University of Western Ontario, Oncology, London, Canada;

³University of Western Ontario, Pathology and Laboratory Medicine, London, Canada

Background: CD5, a member of the scavenger receptor cysteine-rich superfamily, is a marker for T cells and subset of B cells (B1a). CD5 associates with T-cell and B-cell receptors and increased CD5 is an indication of B cell activation. An inverse correlation between CD5 expression and anti-tumour immunity in CD8⁺ T cells has been reported in several human studies. Tumour-infiltrating lymphocytes (TILs) isolated from lung cancer patients have been reported to exhibit different anti-tumour activity based on CD5 expression: CD5 levels were negatively correlated with anti-tumour activity. Increased tumour-mediated activation-induced death, which increases as T cells are activated, has been reported in T cells with undetectable CD5 levels compared to CD5^{high} T cells, suggesting that CD5 could impair activation of anti-tumour T cells. Herein, CD5 levels in T cell subsets was determined in different organs in mice bearing syngeneic breast tumour homographs, and the relationship between CD5 and T cell activation and exhaustion was assessed.

Methods: CD5 levels were assessed in T cells in peripheral organs and tumours from mice harbouring triple-negative mouse 4T1 breast tumour homographs. T cell activation and exhaustion were assessed using CD69 and PD-1 antibodies in association with CD5 levels by flow cytometry.

Results: We report that CD5 levels on T cells were higher in CD4⁺ T cells than CD8⁺ T cells in 4T1 tumour-bearing mice and that high CD5 levels on CD4⁺ T cells were maintained in peripheral organs (spleen and lymph nodes) and in blood. However, the fraction of both CD4⁺ and CD8⁺ T cells recruited to tumours had reduced CD5 compared to CD4⁺ and CD8⁺ T cells in peripheral organs. In addition, CD5^{high}CD4⁺ T cells and CD5^{high}CD8⁺ T cells from peripheral organs exhibited higher levels of activation and associated exhaustion compared to CD5^{low}CD4⁺ T cell and CD5^{low}CD8⁺ T cell from peripheral organs. Interestingly, CD8⁺ T cells among tumour-infiltrating lymphocytes (TILs) and lacking CD5 were activated to a higher level, with concomitantly increased exhaustion markers, than CD8⁺CD5⁺ T cell TILs.

Conclusion: Differential CD5 levels exist among T cells in tumours and lymphoid organs. Those differential levels can be associated with different levels of T cell activation and exhaustion, suggesting that CD5 may be a therapeutic target for immunotherapeutic activation in cancer therapy.

Supported by a Catalyst grant from the London Regional Cancer Program.

No conflict of interest.

211

Poster

Epidermal growth factor receptor influences the antigen presentation pathway in pancreatic cancer

S. Knoche¹, J. Solheim¹. ¹University of Nebraska Medical Center, Eppley Institute for Research in Cancer and Allied Diseases, Omaha, USA

Background: Pancreatic cancer is one the deadliest neoplasms, with a poor 5-year survival rate of 10%. The ability of pancreatic cancer cells to evade the immune system hinders an anti-tumor response and contributes to the poor five-year survival rate. In some cases, the down regulation of major histocompatibility complex (MHC) class I cell-surface expression assists in immune evasion by preventing endogenous tumor antigen from being

presented to cytotoxic T cells. The objective of the current study is to evaluate the role epidermal growth factor receptor (EGFR) plays in the regulation of MHC class I expression by pancreatic cancer cells.

Methods: Pancreatic cancer cell lines were treated with epidermal growth factor (EGF) to activate EGFR or with the small molecule drug erlotinib to inhibit EGFR. Post treatment, cells were further analyzed by immunoprecipitation, western blot analysis, or flow cytometry at various time points. Mechanistic studies in pancreatic cancer cells utilized siRNA followed by western blot analysis or flow cytometry.

Results: Pancreatic cancer cell lines (BxPC-3, T3M4, S2-013, Panc-1) were found to decrease MHC class I expression after EGFR activation by EGF. In contrast, when EGFR was inhibited by erlotinib, MHC class I expression was found to increase by greater than 2.5-fold on pancreatic cancer cells. Mechanistic studies were done to evaluate the role of src homology 2 phosphatase (SHP2) in EGFR's regulation of MHC class I. Following SHP2 knockdown, a slight increase in MHC class I expression was observed, suggesting SHP2 does play a partial role. The MAP kinase signaling pathway is being evaluated to see if it also contributes to MHC class I regulation. Interestingly, EGFR was found to co-immunoprecipitate with MHC class I, suggesting that it may also directly affect MHC class I expression.

Conclusions: Activating EGFR by EGF negatively regulates MHC class I expression on pancreatic cancer cells, while, in contrast, EGFR inhibition increases MHC class I on pancreatic cancer cells. SHP2 was discovered to play a partial mechanistic role in the regulation of MHC class I. In addition, EGFR was found to co-immunoprecipitate with MHC class I, implying that EGFR may directly influence MHC class I turnover and/or localization. By defining a role for activated EGFR in reducing MHC class I expression and revealing that EGFR inhibitors can boost MHC class I expression on cancer cells, this could facilitate the adoption of new, more effective therapeutic tactics that combine the use of EGFR inhibitors with immunotherapies to augment patients' immune systems to effectively target and kill cancer cells.

No conflict of interest.

212

Poster

Fostriecin potentiates genome instability and anti-tumor immunity in ovarian cancer

R. Raja¹, C. Wu¹, K. Butler², M. Curtis³. ¹Mayo Clinic, Department of Immunology, Scottsdale, USA; ²Mayo Clinic, College of Medicine and Science & Division of Gynecology, Scottsdale, USA; ³Mayo Clinic, Department of Immunology & Division of Gynecology, Scottsdale, USA

Background: Increased immune infiltration in ovarian tumors has been linked to improved patient outcome. Nonetheless, responses to checkpoint blockade therapies have been disappointing in ovarian cancer patients. This has been attributed to the low mutational burden present in ovarian tumors. However, many tumor antigens have been identified in ovarian cancer, which underscores the critical need to identify new treatment strategies that will trigger anti-tumor immunity in ovarian cancer. Recent studies have revealed that defects in DNA damage repair (DDR) pathways can contribute to improved responses to immune-directed therapies. We previously discovered that CT45 expression sensitizes ovarian cancer cells to chemotherapy via its interaction with the protein phosphatase 4 (PP4) complex. PP4 is known to play a key role in DDR pathways; however, its potential effects on anti-tumor immunity remain unknown.

Materials and Methods: Using fostriecin, a commercially available inhibitor of PP4, we studied the effect of fostriecin on chemosensitivity using cell cycle analysis and cell viability assays. To study the effect of fostriecin on DNA damage, we performed comet assays and measured micronuclei along with FANCD2 foci formation. Furthermore, using western blot, qPCR, and T cell activation assays, we assessed the role of fostriecin in promoting an inflammatory response. We tested the efficacy of combining fostriecin with carboplatin and PD-1 inhibition in a syngeneic mouse model of ovarian cancer.

Results: Our results show that fostriecin treatment combined with carboplatin leads to increased carboplatin sensitivity, DNA damage, and micronuclei formation. Using a panel of ovarian cancer cells, we show that fostriecin treatment triggers an anti-tumor immune response via STAT1 activation resulting in increased expression of pro-inflammatory cytokines. Furthermore, in a syngeneic mouse ID8 ovarian cancer cell line, we demonstrate that combination treatment of fostriecin and carboplatin significantly increased CD8 T cell activation over carboplatin treatment alone.

Conclusions: Our work has identified a role for PP4 inhibition in promoting anti-tumor immunity. These findings form the groundwork for the rationale design of a clinical trial combining PP4 inhibitors with chemo-immunotherapy as a new approach in ovarian cancer treatment.

No conflict of interest.

213

Poster

Restricted STAT3 inhibition among tumour infiltrating immune cells restricts colorectal tumour growth

M. Alorro¹, M. Eissmann¹, F. Masson², M. Ernst¹. ¹Olivia Newton-John Cancer Research Institute, Cancer and Inflammation, Melbourne, Australia; ²National Institute for Health and Medical Research INSERM, Centre of Physiopathology, Toulouse-Purpan, France

Despite advances in therapies, colorectal cancer accounts for 862,000 patient deaths annually, highlighting the need to identify novel therapeutic targets and approaches to control this disease. The Signal Transducer and Activator of Transcription 3 (STAT3) is a transcription factor found to be overexpressed in multiple cancers, and is often associated with poorer patient survival. The aberrant tumour intrinsic activity of STAT3 has been implicated in pro-tumoural proliferation, survival, and progression. While the tumour intrinsic STAT3 signalling is well described, its influence among tumour microenvironment (TME) infiltrating cells is less explored. Consequently, this project aims to determine the role of STAT3 signalling in the TME and to assess its potential as an anti-cancer therapeutic target.

To address these aims we utilised the *CAGsrTA;Stat3.1348* and *RosaCRE^{ERT2};STAT3^{fl/fl}* genetic models to induce short hairpin mediated *Stat3* reduction or *Stat3*-gene deletion respectively, along with the STAT3 targeting small molecule inhibitor BBI-608. These STAT3 abrogating approaches were then tested in mouse models of colorectal cancer.

The genetic and pharmacological STAT3-inhibition resulted in robust anti-tumour effects. Both ubiquitous STAT3 inhibition (affecting all the cells in the TME), and selective STAT3 reduction (only among TME infiltrating cells) restricted MC38 colon cancer growth *in vivo*. This effect however, was not enhanced by the checkpoint inhibitor anti-PD-1 therapy. Furthermore, TME immune landscape changes, particularly in myeloid cell abundance, were associated with the pro-tumoural effect of STAT3 in the TME.

Taken together this work rationalises the use of STAT3 as a novel anti-cancer therapeutic target. We demonstrated that STAT3-targeting is applicable for MSS and MSI colon cancer subtypes, and cautions for its use in combination with anti-PD-1 therapy. Furthermore, our data highlights a role for utilising TME immune cell composition as a biomarker to support patient stratification for STAT3 inhibition sensitivity.

No conflict of interest.

214

Poster

Regulation of MDSCs in the urothelial carcinoma of bladder: Relevant role of YAP1

P. Sadhukhan¹, M.T. Ugur¹, A. Ooki¹, M. Hoque^{1,2,3}. ¹Johns Hopkins University, Department of Otolaryngology, Baltimore, USA; ²Johns Hopkins University, Department of Urology, Baltimore, USA; ³Johns Hopkins University, Department of Oncology, Baltimore, USA

Background: Highly coordinated multifactorial intrinsic activity of immune system plays a critical role in the initiation and progression of almost all types of human malignancies. We have recently reported that both the YAP1 and COX2/PGE2 signaling pathways accelerate urothelial cancer stem cells (UCSCs) expansion in a mutually exclusive manner and the activation of these pathways hamper the efficacy of systemic chemotherapy. Due to prolonged administration of chemotherapeutic drugs, immunosuppression is manifested by changing the infiltration of immune cells and their differentiation in the tumor microenvironment (TME). Several reports have suggested that cancer stem cells (CSCs) can evade immune attack and enrichment of myeloid-derived suppressor cells (MDSCs) in the TME.

Materials and Methods: TCGA database was utilized to identify the major oncogenic pathway activated in tumors with high level of MDSCs population and other associated correlation between different signaling molecules. Subsequently, stable YAP1 knockdown/overexpressed clones were prepared using bladder cancer cell lines from mice (MB-49) and human (BFTC 905, T24, BFTC909 and UMUC3). Cell derived xenografts were prepared in C57Bl/6 mice and different immune regulatory parameters were quantified using FACS and RT PCR analysis. Human primary bladder cancer samples were also used to investigate for any correlation among YAP1 and different chemokines expression in tumor samples.

Results: We have found that expression of YAP1 may contribute to the immune suppressive cold TME in the UCB. Subcutaneous transplantation of YAP1sh tumor cells in wild type immunocompetent mice exhibited growth inhibition of the urothelial tumor. Our data indicate that YAP1 inhibition attenuated tumor trafficking of MDSCs, leading to high CD8/CD4 and CD8/MDSC ratio. Furthermore, immune associated cytokines (TNF- α , IL-6, TGF- β) and chemokines (CXCL2, CXCL3, CXCL5) were also reduced in YAP1-attenuated cell lines and xenografted tumors. Additionally, downregulation of YAP1 signaling results increased expression of MHC class I and CD80

molecules that are required for sustained T cell activation. Furthermore, inhibition of YAP1 results in increased cytotoxic efficiency of CD8+ T cells and improved immune sensitivity by the upregulation of PD-L1.

Conclusions: Further studies are ongoing to understand YAP1 signaling in the UCB tumor microenvironment and to determine whether inhibition of YAP1 enhanced checkpoint inhibitors efficacy in UCB. Overall, this study indicates that YAP1 is a critical signaling intermediate in regulating the infiltration of MDSCs in the TME and endogenous immune response.

No conflict of interest.

215

Poster

Visualization and quantification of anti-tumor immune responses in 3D cultures

G. Goverse¹, N. Beztsinna¹, B. Visser¹, E. Spanjaard¹, K. Yan¹, L. Price¹, L. Daszkiewicz¹. ¹Ocello B.V., Leiden, Netherlands

Introduction: Reaching the full potential of cancer immunotherapies and maintaining durable clinical benefits requires understanding of cellular mechanisms that govern anti-tumor immune responses. However, these treatment modalities have very diverse mechanisms of action, which are not fully understood and the progress in this direction is hampered by a lack of appropriate pre-clinical testing models that are both clinically relevant and suitable for routine screening of drug candidates. To address this issue, we developed an in vitro platform that combines complexity of the tumor microenvironment with robustness of a high-throughput automated set-up. Within this assay immune cells are co-cultured with cancer cells in a 3D setting which recapitulates the tumor micro-environment and its complex cellular interactions. Image based analysis is applied to read out effects of drug candidates on active migration of immune cells towards tumoroids, infiltration of immune cells into the tumoroids and their killing. These clinically relevant endpoints allow for a better understanding of the immune-modulatory profile of different immunotherapies.

Material and Methods: 3D tumor cultures were generated from cancer cell lines (e.g. breast, prostate) and colorectal cancer organoids (from HUB Organoid Technology) and seeded using liquid handlers in 384 well plates. Different immune cells, such as PBMCs, T cells or macrophages were added to the 3D culture and their infiltration into tumoroids and subsequent killing upon treatment with different immune-modulators (e.g. superantigens, activating antibodies, T cell engagers, CSF1R inhibitor or STING agonist) was visualized using high-content microscopy. Quantification of immune cell effects was achieved with morphometric analysis with OMiner™ software.

Results: Upon treatment with immune-modulators we detected different levels of immune cell infiltration and killing of tumoroids and organoids, which also could be suppressed by signals from the tumor microenvironment. Image-based analysis enabled the discrimination of immune-tumor cell interactions in 3D cultures and dissection of spatially resolved information, not accessible by monolayer cultures or biochemical assays. The 3D environment, both for the cell culture and image analysis allows for obtaining very rich data in models that closely reflect human physiology.

Conclusion: Our image-based platform described here allows the analysis of immunotherapy effects on different cell types that engage in a more physiologically relevant spatial setting than when culturing them in traditional 2D cultures. Visualization and quantification of these tumor-

immune cell interactions offer a powerful tool for cancer immunotherapy drug developers to understand the mechanism of action of their treatments and ultimately translating to a better clinical performance.

Conflict of interest:

Ownership: Leo Price.

216

Poster

Positive association between macrophage infiltration and PD-L1 expression in the tumor microenvironment

M. Cumberbatch¹, L. Memeo², M. Bhagat¹, C. Womack¹, W.H. Kim³.

¹TriStar technology Group- LLC, Immuno-oncology, Washington DC, USA;

²The Mediterranean Institute of Oncology, Oncology, Catania, Italy; ³Seoul National University College of Medicine, Pathology, Seoul, South Korea

Background: Expression of PD-L1 in macrophages has been correlated with improved overall survival in NSCLC patients treated with immunotherapy (Liu Y et al, Clin Cancer Res 2020). Furthermore, high macrophage PD-L1 is associated with elevated tumor PD-L1 and CD8+ T cell infiltration in this tumor indication, characteristic of immune hot tumors. Here, we have explored whether a similar relationship is evident between PD-L1 and macrophage infiltration across other tumor types.

Materials & Methods: We utilized a multi-tumor tissue microarray (TMA) comprising 360 donor patient FFPE tumor samples, each donor case represented in duplicate with 1 core (1 mm) taken from invasive margin (IM) and 1 from tumour centre (TC), selected by a pathologist. Serial sections were stained by single-plex immunohistochemistry (IHC) for CD68 (PG-M1) and PD-L1 (22C3). Macrophage infiltration was assessed by digital image analysis (CellProfiler™), and PD-L1 was scored by a pathologist to deliver standard Tumor Proportion Score (TPS) and Combined Positivity Score (CPS).

Results: We found that 16/29 different tumor types (approx. 12 cases/tumor type) represented in this TMA displayed a TPS ≥1% in one or more patient cases, and 25/29 tumor types exhibited a CPS of ≥1. The contribution of immune cell PD-L1 positivity to the overall PD-L1 expression pattern in the tumor microenvironment was highlighted by the observation that CPS was significantly greater than TPS for 15/29 tumor types (including NSCLC, SCLC, CRC, small bowel, TNBC, esophageal, gastric, bladder, cervical, ovarian, endometrial). Furthermore, a significant (p < 0.05) trend towards elevated macrophage infiltration (1.9-fold increase) was observed for tumors with higher immune cell PD-L1 expression, in particular those where CPS was significantly greater than TPS.

Conclusions: Although it is recognised that analyses performed on TMAs may misrepresent biomarker expression in whole tissue sections due to tumor heterogeneity, this analysis approach permits direct comparisons of immune profiles in PD-L1+ and PD-L1- tumor microenvironments across multiple tumor types simultaneously. We conclude that macrophage infiltration is positively associated with PD-L1 expression, in particular with CPS; a score that combines tumor and immune cell PD-L1 expression, CPS is being recommended increasingly across tumor types to select patients for PD-1/PD-L1 axis immunotherapy.

No conflict of interest.

Author index

A

Aaronson S., S5 (97LBA)
 Abdo J., S40 (148)
 Abdul-Karim R., S11 (20)
 Abdul Sater H., S10 (7)
 Abdusamad M., S8 (4)
 Abe Y., S14 (28)
 Ab O., S15 (30)
 Abou Alaiwi S., S7 (1)
 Abuhammad S., S7 (1)
 Achrol A.S., S6 (99LBA)
 Acosta J., S46 (167)
 Ada C., S16 (32)
 Adamopoulos C., S5 (97LBA)
 Adebayo A., S26 (103)
 Adelani I., S26 (103)
 Adesina G., S26 (103)
 Adhikari J., S39 (145)
 Agatsuma T., S14 (28)
 Aghi M.K., S6 (99LBA)
 Agrawal D., S40 (148)
 Aguirre A., S8 (4)
 Ahmed A., S34 (130)
 Ahmed L., S44 (160)
 Ahmed T., S5 (97LBA)
 Ahrens-fath I., S5 (98LBA)
 Ahuja N., S12 (22)
 Ait-Mohand S., S24 (56)
 Ajpacaja L., S47 (171)
 Akobundu B., S42 (156)
 Akosmam B., S52 (185)
 Akoth E., S57 (201)
 Akyerli C.B., S32 (124)
 Alahari S., S29 (111)
 Alcacer J., S41 (150)
 Alcaro S., S35 (133)
 Al-Hasani H., S27 (105)
 Ali S., S48 (175)
 Allen A., S24 (58), S46 (168)
 Allen E., S2 (5LBA)
 Almubarak M., S11 (21)
 Alorro M., S61 (213)
 Alotaibi F., S60 (210)
 Altel T., S38 (142)
 Altiock S., S59 (206)
 Ambler R., S10 (9)

Ames T., S53 (188)
 An A.X., S15 (29), S59 (207)
 Andersen R.J., S51 (181)
 Andric Z., S5 (96LBA)
 Anel A., S53 (188)
 Annis A., S5 (96LBA)
 Antony T., S47 (170)
 An Z., S54 (191)
 Apolo A., S10 (7)
 Aravind A., S47 (170)
 Arribas A., S40 (149)
 Arribas A.J., S17 (36)
 Arslan A.M., S42 (155)
 Asfaw A., S8 (4)
 Ashaye A., S51 (183)
 Asuelime G., S33 (125)
 Au J., S16 (32)
 Aust S., S32 (123)
 Averbuch S., S2 (5LBA)
 Azad A., S11 (20)
 Azad N., S12 (22)
 Azambuja J.H., S19 (44)
 Azam H., S49 (176)
 Azizkhan-Clifford J., S37 (138)

B

Babyshkina N., S41 (153)
 Baca S., S7 (1)
 Bachmann F., S25 (101)
 Baek S., S30 (116)
 Bağır E., S42 (155)
 Baiev I., S21 (49)
 Bai R., S35 (133)
 Baird R., S19 (43)
 Baker L., S11 (20)
 Balayan J., S16 (33)
 Bandini M., S21 (48)
 Bankiewicz K., S6 (99LBA)
 Bannen L., S16 (33)
 Banuelos C.A., S51 (181)
 Barcellos-Hoff M., S14 (27)
 Barkund S., S22 (50)
 Barnhart M., S51 (183)
 Barragan F., S23 (55)
 Barraja P., S35 (133)

Barreca M., S17 (36), S35 (133), S40 (149)
 Barrera M., S56 (196)
 Barve M., S1 (3LBA), S2 (4LBA)
 Bashir B., S50 (180)
 Bauer R.J., S19 (44)
 Bauer T.M., S3 (7LBA)
 Baumeister H., S5 (98LBA)
 Baylin S., S12 (22)
 Bazhenova L., S1 (1LBA), S1 (3LBA)
 Beaton N., S39 (145), S54 (192)
 Beatty J., S16 (32)
 Behrens D., S58 (204)
 Bélissant Benesty O., S24 (56)
 Belvin M., S15 (30)
 Bendell J., S8 (5), S11 (20)
 Benedetti F., S11 (21)
 Benlloch M., S41 (150)
 Berdini V., S44 (161), S53 (187)
 Bertagnolli M., S9 (6)
 Bertoni F., S17 (36), S35 (133), S40 (149)
 Besnik B., S1 (2LBA)
 Bexon M., S6 (99LBA)
 Beztsinna N., S57 (199), S59 (205), S62 (215)
 Bhagat M., S62 (216)
 Bhattacharya A., S20 (45)
 Bhatt A.N., S36 (134)
 Bhatta S., S30 (115)
 Bhushan K., S7 (2)
 Bilguvar K., S32 (124)
 Bilusic M., S10 (7)
 Biswas D., S18 (41)
 Black P., S21 (48)
 Blake D., S7 (2)
 Blay J.Y., S32 (123)
 Blezinger P., S27 (106)
 Blø M., S44 (160)
 Bohlander S., S30 (115)
 Bollag G., S2 (5LBA)
 Boniecka A., S44 (160)
 Booher R., S47 (170)
 Bordone-Pittau R., S40 (149)
 Bosutti A., S49 (177)
 Bottin C., S49 (177)
 Boule S., S15 (30)

Boult J., S25 (101)
 Boumelha J., S60 (208)
 Boumhela J., S20 (47)
 Brahmer J., S8 (5)
 Brandish P., S20 (45)
 Brar G., S57 (201)
 Brekken R.A., S44 (160)
 Brem S., S6 (99LBA)
 Brennen J., S52 (184)
 Brenner A., S6 (99LBA)
 Briganti A., S21 (48)
 Briggs M., S20 (46)
 Bristow C.A., S22 (51)
 Brothwood J., S44 (162)
 Brousseau M., S1 (2LBA)
 Brown T., S12 (22)
 Bruderer R., S39 (145), S54 (192)
 Bryson E., S51 (182)
 Buchanan S., S5 (97LBA)
 Buettner B., S58 (204)
 Burdick J., S46 (169)
 Burger M., S8 (4)
 Burkard M.E., S11 (21)
 Burrows F., S43 (159)
 Bussani R., S49 (177)
 Butler K., S61 (212)
 Butowski N., S6 (99LBA)
 Byers L.A., S47 (171)

C

Cadzow L., S7 (3), S52 (184)
 Cahill D., S14 (26)
 Caldas C., S19 (43)
 Caldeira J., S27 (106)
 Calder P., S16 (34)
 Caldwell C., S5 (96LBA)
 Callari M., S19 (43)
 Call S.G., S3 (6LBA)
 Campbell S., S51 (183)
 Campos Baeta Neves M.H., S56 (197)
 Can O., S32 (124)
 Capasso A., S8 (5)
 Capizzi L., S26 (102)
 Caplin M., S32 (123)
 Cardnell R., S47 (171)
 Carreiro S., S20 (46)
 Carrillo S., S46 (167)
 Cascione L., S40 (149)
 Caswell D., S20 (47)
 Cattaruzza F., S10 (8)
 Cazzaniga M.E., S26 (102)
 Cerami E., S18 (40)
 Cercek A., S12 (22)
 Ceric T., S5 (96LBA)
 Cerrito M.G., S26 (102)
 Cesano A., S51 (181)
 Chang J., S49 (179)
 Chang Y.C., S47 (172)
 Chan M.H., S34 (131)
 Chan S., S43 (159)
 Chao R.C., S1 (3LBA), S2 (4LBA)
 Charamanna K., S47 (170)
 Chatterjee N., S41 (151)

Chaudhari P., S38 (141)
 Chauhan A., S36 (134)
 Chelur S., S47 (170)
 Chen A., S10 (7)
 Cheng G., S13 (25)
 Cheng M., S25 (100)
 Chen H.Z., S45 (166)
 Chen J., S48 (173), S56 (196)
 Chen J.S., S52 (185)
 Chen M.H., S47 (172)
 Chen X., S5 (97LBA)
 Chen Y., S38 (143)
 Cherdyntseva N., S41 (153)
 Cherniack A., S8 (4)
 Chessari G., S44 (161)
 Chhagan S., S12 (24)
 Chiang G.G., S56 (196)
 Chiao J., S7 (2)
 Chiappori A.A., S12 (24)
 Chiara T., S40 (149)
 Chipumuro E., S7 (3), S52 (184)
 Chittivelu S., S8 (5)
 Cho B.C., S1 (1LBA)
 Choi P., S7 (1)
 Chong C., S16 (33)
 Chowdhary S., S6 (99LBA)
 Chowdhury N.R., S12 (24)
 Choy G., S11 (21)
 Choy T.J., S53 (186)
 Christensen J.G., S1 (3LBA), S2 (4LBA)
 Ciccone D., S20 (46)
 Cipolletta D., S12 (24)
 Ciuvalechi Maia R., S56 (197)
 Coello M., S6 (99LBA)
 Cogan S., S52 (184)
 Coker E., S47 (171)
 Colechia M., S21 (48)
 Cole M., S60 (208)
 Collis A., S20 (46)
 Cordes L., S10 (7)
 Corey E., S49 (176)
 Cornejo M., S23 (55)
 Cornelius C., S1 (3LBA)
 Cornella-Taracido I., S39 (145)
 Corr B., S12 (23)
 Cosaert J., S47 (171)
 Costa S., S28 (108)
 Coughlin C.A., S28 (110)
 Courtin A., S53 (187)
 Coutinho R., S56 (197)
 Croce S., S32 (123)
 Cruz-Acuña R., S46 (169)
 Cullum R., S32 (122)
 Cumberbatch M., S62 (216)
 Cunningham T.A., S28 (110)
 Curtin N., S36 (136), S37 (137)
 Curtis M., S61 (212)

D

Daemen A., S22 (50)
 Daginakatte G., S47 (170)
 Dalal M., S51 (183)
 Dalgai S., S21 (49)

D'Amico A., S28 (108)
 Daniele J., S22 (51)
 Daniel H., S9 (6)
 Dapas B., S49 (177)
 Darini C., S23 (54)
 Daris M., S33 (125)
 Das A., S41 (151)
 Das S., S27 (105)
 Daszkiewicz L., S57 (199), S59 (205), S62 (215)
 Davicioni E., S21 (48)
 David A., S32 (122)
 Davies T.G., S44 (161)
 Davis M., S28 (109)
 Day J.E.H., S44 (161)
 De Braud F., S12 (24)
 de Carne S., S18 (41)
 de Carné Trécesson S., S20 (47)
 Dees E., S9 (6)
 Dees E.C., S11 (21)
 Deguchi T., S14 (28)
 de Jonge M.J.A., S12 (24)
 de Jong J.J., S21 (48)
 Dekker H., S19 (42)
 Dela Cruz F., S16 (34)
 delaFouchardiere C., S32 (123)
 Delasos L., S15 (31)
 Del Conte G., S5 (98LBA)
 Delgado Y., S42 (154)
 Della Corte C., S47 (171)
 DeMattei J., S12 (23)
 Deng W., S39 (147)
 Derynck M., S10 (8)
 de Stanchina E., S15 (31)
 Devaraja T., S47 (170)
 Dhudashiya A.A., S47 (170)
 Diamond J., S12 (23)
 Dickson B., S13 (25)
 Difilippantonio S., S48 (173)
 Dijkstra C., S43 (157), S60 (209)
 Dixit R., S27 (105)
 Djan I., S35 (132)
 Doello K., S54 (189)
 Doench J., S7 (1)
 Do K.T., S7 (2)
 Domingues B., S23 (53)
 Dong S., S29 (111)
 Downward J., S10 (9), S18 (41), S20 (47), S60 (208)
 Driscoll H., S28 (108)
 Dronova T., S41 (153)
 Dua R., S8 (5)
 Du H., S53 (186)
 Dumulon-Perreault V., S24 (56)
 Dwivedi V., S32 (122)

E

Eam B., S56 (196)
 East C., S53 (187)
 East P., S18 (41), S20 (47)
 Eckhardt S.G., S8 (5), S12 (23)
 Edokwe C., S26 (103)
 Ehrhart J., S59 (206)

Eichhorn P., S41 (152)
 Eissmann M., S43 (157), S60 (209),
 S61 (213)
 El-Awady R., S38 (142)
 Elias J., S52 (185)
 Elie B., S23 (55)
 El Khoueiry A., S12 (22)
 El-Khoueiry A., S11 (21)
 Elkhoully A., S56 (198)
 Ellingson B.M., S6 (99LBA)
 El Shemerly M., S25 (101)
 Emanuele Z., S40 (149)
 Erickson S., S18 (37)
 Ernst M., S43 (157), S60 (209), S61 (213)
 Ersen-Danyeli A., S32 (124)
 Espiritu L., S11 (21)
 Essani K., S58 (203)
 Estrela J.M., S41 (150)
 Etheridge A., S9 (6)
 Evans J.W., S53 (186)
 Evans K., S18 (37)
 Eversole R., S58 (203)

F

Fabbri G., S47 (171)
 Fairfield H., S28 (108)
 Fajardo E., S42 (156), S52 (185)
 Falank C., S28 (108)
 Fang B., S48 (174)
 Fan S., S25 (100)
 Farrell M., S28 (108)
 Fazal L., S44 (162)
 Federico L., S22 (51)
 Fedulova N., S41 (153)
 Feng N., S22 (51)
 Feng Y., S39 (145), S54 (192)
 Ferraldeschi R., S28 (109)
 Ferrari D., S5 (96LBA)
 Ferrari N., S28 (109)
 Feun L.G., S2 (5LBA)
 Fiebig H.H., S27 (105)
 Fiedler W., S5 (98LBA)
 Figueredo R., S60 (210)
 Fijuth J., S35 (132)
 Firestone R., S39 (146)
 Fiser A., S42 (156), S52 (185)
 Fish S., S56 (196)
 Floquet A., S32 (123)
 Floudas C., S10 (7)
 Floyd J.R., S6 (99LBA)
 Foley C.N., S38 (143)
 Fournier J., S16 (32)
 Fox J.A., S45 (163)
 Freedman M., S7 (1)
 Frej K., S7 (2)
 Friedman L.S., S22 (50)
 Fukushima H., S58 (202)
 Fu S., S3 (6LBA)

G

Gabra H., S44 (160)
 Gabre J., S46 (169)

Gabrelow G., S33 (125)
 Gad M., S56 (198)
 Gallagher W., S49 (176)
 Gallina A., S21 (48)
 Gamboa O., S46 (167)
 Gan H., S11 (20)
 Gao M., S19 (43)
 Gao S., S20 (45)
 García-Fumero R., S54 (189)
 Garnett M., S47 (171)
 Garralda E., S5 (98LBA)
 Gatti-Mays M., S10 (7)
 Gaudio E., S35 (133), S40 (149)
 Gausdal G., S44 (160)
 Gay C., S47 (171)
 Gelbard M., S7 (1)
 Gerlach D., S22 (51)
 Gerlevik U., S32 (124)
 Gerona-Navarro G., S23 (55)
 Gerritse S., S19 (42)
 Gerson-Gurwitz A., S56 (196)
 Gewinner C., S28 (109)
 Ghaddar N., S23 (54)
 Ghosh T., S32 (122)
 Giannatempo P., S21 (48)
 Gibb E.A., S21 (48)
 Gibbs B.K., S17 (35)
 Gietema J., S32 (123)
 Gilardi M., S43 (159)
 Ginn E., S16 (32)
 Girard N., S32 (123)
 Giri S., S47 (170)
 Giudici F., S49 (177)
 Gladstone E., S15 (31)
 Glazer R., S20 (45)
 Gmachl M., S22 (51)
 Goel V.K., S56 (196)
 Golub T., S8 (4)
 Gomes E Silva I.V., S56 (197)
 Gonçalves A., S12 (24)
 Gonzalez C., S49 (176)
 Goon L., S16 (33)
 Gordon G., S12 (23)
 Gordon M., S8 (5)
 Gouda M., S3 (6LBA)
 Gounder M.M., S3 (7LBA)
 Goverse G., S57 (199),
 S62 (215)
 Goyal L., S21 (49)
 Grange R., S38 (143)
 Grasberger P., S7 (3), S52 (184)
 Grassi G., S49 (177)
 Grassilli E., S26 (102)
 Grell P., S12 (24)
 Greten T., S57 (201)
 Grillet F., S59 (205)
 Grilley Olson J., S35 (132)
 Guarino M., S11 (21)
 Guérin B., S24 (56)
 Guetta-Terrier C., S52 (185)
 Guidry J., S29 (111)
 Gulley J., S10 (7)
 Gümürdülü D., S42 (155)
 Gupta S., S38 (141)
 Gutkind S., S43 (159)

Guzman E., S29 (112)
 Guzman L., S49 (179)

H

Habel B., S5 (98LBA)
 Haeno H., S31 (120)
 Hafeez N., S7 (3), S52 (184)
 Hager G., S30 (116)
 Hahn W., S7 (1), S8 (4)
 Halanych K., S32 (122)
 Hall M., S48 (173)
 Hamburger A., S33 (125)
 Hamel E., S35 (133)
 Hamilton E., S50 (180)
 Hamlett C., S44 (161)
 Hammond M., S10 (8)
 Hancock D., S18 (41)
 Han S., S6 (99LBA)
 Hansen S., S45 (163)
 Han X., S29 (114)
 Harman J., S29 (111)
 Harmon C., S55 (193)
 Harvey R.D., S51 (182)
 Hasegawa J., S14 (28)
 Hassett M., S18 (40)
 Hattori C., S14 (28)
 Haura E.B., S48 (174)
 Hay M., S13 (25)
 Hearn K., S44 (161), S44 (162)
 He D.X., S15 (29)
 Heeschen C., S58 (204)
 Heffernan T.P., S22 (51)
 Heightman T., S53 (187)
 Heim A., S12 (23)
 Heist R., S1 (1LBA)
 Heist R.S., S1 (3LBA)
 He L., S34 (129)
 Henkensiefken A., S10 (8)
 Herskovits A., S23 (55)
 Hicks S., S15 (30)
 Higuchi F., S14 (26)
 Hill C., S20 (46)
 Hinck A.P., S19 (44)
 Hinck C.S., S19 (44)
 Hindley C., S44 (162), S53 (187)
 Hiromi M., S58 (202)
 Hiroyuki U., S58 (202)
 Hiscock S., S44 (161)
 Histen G., S7 (3), S52 (184)
 Hixon J., S52 (184)
 Hodges-Gallagher L., S55 (193)
 Hodgson G., S50 (180)
 Hodneland Nilsson L., S44 (160)
 Hoffmann J., S58 (204)
 Hofmann M., S22 (51)
 Ho J.J.D., S28 (110)
 Hong A., S8 (4)
 Hong C.R., S13 (25)
 Hong D., S1 (1LBA), S3 (7LBA)
 Hong D.S., S3 (6LBA)
 Hong N.H., S51 (181)
 Hong Y., S3 (7LBA)
 Hoque M., S61 (214)
 Houghton P.J., S18 (37)

Howard M., S9 (6)
 Howarth R., S37 (137)
 Hsiao M., S34 (131), S47 (172)
 Hsu J., S16 (33)
 Huang H., S3 (6LBA)
 Huang J., S22 (51)
 Huber A., S43 (157)
 Hu J., S25 (100)
 Hunter F., S30 (115)
 Hu Q., S48 (174)
 Hurtado F.K., S12 (24)
 Hwang J., S7 (1)

I

Ianari A., S1 (2LBA)
 Ibáñez G., S16 (34)
 Idbaih A., S32 (123)
 Imedio E. R., S45 (164)
 Innocenti F., S9 (6)
 Inokuchi K., S2 (5LBA)
 Inostroza Y., S42 (154)
 Irving B., S10 (8)
 Isanogle K., S48 (173)
 Ito T., S5 (97LBA)
 Izumi N., S14 (28)

J

Jaaks P., S47 (171)
 Jackson A., S44 (160)
 Jakopovic M., S5 (96LBA)
 Jameson G., S55 (194)
 Jamieson S., S13 (25), S30 (115)
 Janku F., S2 (5LBA), S11 (20)
 Jänne P.A., S1 (3LBA)
 Jariani A., S59 (205)
 Jenab-Wolcott J., S11 (21)
 Jennings L., S17 (36)
 Jérémie K., S8 (4)
 Jerome M., S47 (171)
 Jerusalem G., S12 (24)
 Jiang C., S9 (6)
 Jiang J., S53 (186), S54 (191)
 Jimeno J., S53 (188)
 Jing C., S15 (30)
 Jin J., S5 (97LBA)
 Jin L., S16 (32), S38 (143)
 Jin Y., S59 (207)
 Joerger M., S12 (24)
 Johnson C., S44 (162)
 Johnson C.N., S44 (161)
 Johnson E., S16 (33)
 Johnson M.L., S1 (3LBA), S2 (4LBA)
 Jolin H., S50 (180)
 Jones M., S44 (162)
 Jones P., S12 (22)
 Jueliger S., S28 (109)
 Jun L., S29 (114)
 Junming Z., S1 (1LBA)

K

Kadwad V., S38 (141)
 Kageyama S.I., S36 (135)

Kagihara J., S12 (23)
 Kaila N., S20 (46)
 Kalekar R., S8 (4)
 Kamb A., S33 (125)
 Kamle S., S52 (185)
 Kana S.I., S58 (203)
 Kandola N., S44 (162)
 Kang-Fortner Q., S50 (180)
 Kannan K., S36 (135)
 Kapiteijn H., S32 (123)
 Karacan S., S32 (124)
 Karakasheva T., S46 (169)
 Karoulia Z., S5 (97LBA)
 Karp D., S3 (6LBA)
 Karzai F., S10 (7)
 Kashima Y., S36 (135)
 Kasper S., S12 (24)
 Kato K., S3 (7LBA)
 Kaufmann D., S32 (122)
 Kavanaugh M., S15 (30)
 Kaza L.N., S47 (170)
 Kazutaka M., S58 (202)
 Kebenko M., S5 (98LBA)
 Keisuke Y., S58 (202)
 Kellenberger L., S25 (101)
 Kelley R.K., S21 (49)
 Kelly G., S18 (41)
 Kelly M., S50 (180)
 Kelly W., S9 (6)
 Ke N., S50 (180)
 Kenjiro I., S58 (202)
 Kesari S., S6 (99LBA)
 Kessler L., S46 (168)
 Khade B., S38 (141)
 Khan A.A., S48 (175)
 Khan J., S48 (173)
 Kheoh T., S1 (3LBA), S2 (4LBA)
 Khodos I., S15 (31)
 Kim H., S31 (118)
 Kim M.S., S43 (158)
 Kim S., S30 (116)
 Kim S.H., S43 (158)
 Kim S.T., S31 (118)
 Kim W.H., S62 (216)
 Kim Y.M., S29 (113)
 Kim Y.Z., S43 (158)
 Kindler H., S9 (6)
 Kizilbash S.H., S11 (21)
 Klein P., S55 (193)
 Klinghammer K.F., S5 (98LBA)
 Knerr E., S32 (122)
 Knoche S., S34 (128), S60 (211)
 Kobayashi S. S., S31 (120)
 Koczywas M., S8 (5)
 Koenigsberg C., S49 (178)
 Kohler S., S58 (203)
 Koomen J.M., S48 (174)
 Koromilas A., S23 (54)
 Koropatnick J., S60 (210)
 Koski C., S10 (8)
 Kota V., S51 (183)
 Krall E., S52 (184)
 Kraut N., S22 (51)
 Krehling J., S59 (206)
 Krieger J.R., S28 (110)

Krishnamoorthy J., S23 (54)
 Kroeger J., S48 (174)
 Kroetz D., S9 (6)
 Krucien N., S51 (183)
 Kucia-Tran J., S53 (187)
 Kugener G., S8 (4)
 Kumari P., S18 (40)
 Kumar P., S3 (7LBA)
 Kumar S., S45 (164)
 Kung A., S16 (34)
 Kurmasheva R.T., S18 (37)
 Kushner P., S55 (193)
 Kwiatkowski D.J., S53 (186)
 Kzhyskowska J., S41 (153)

L

Labots M., S19 (42)
 Ladanyi M., S15 (31)
 Lamb P., S16 (33)
 Lane H., S25 (101)
 Lange Z., S10 (8)
 Lang M., S17 (35)
 Lani Silva K., S56 (197)
 Larson A., S34 (128)
 Larsson O., S23 (54)
 Lauriault V., S51 (181)
 Lavitrano M., S26 (102)
 Lawlor R., S58 (204)
 Lawrence H.R., S48 (174)
 Lawson K., S16 (32)
 Lazari V., S20 (46)
 Lazo J., S55 (195)
 Leaf H., S37 (140)
 Leal T.A., S1 (3LBA), S2 (4LBA), S12 (24)
 Lee B.J., S53 (186)
 Lee C., S14 (26), S52 (185)
 Lee J., S1 (1LBA)
 Lee J.M., S10 (7)
 Lee N.V., S39 (147)
 Lee S., S28 (110)
 Lee T.W., S30 (115)
 Lee V., S12 (22)
 Lee Y.M., S43 (158)
 Lehutová D., S19 (42)
 Lei D., S48 (175)
 Leland S.M., S15 (31)
 Leleti M., S16 (32)
 Leleti M.R., S38 (143)
 Le Moigne R., S51 (181)
 Lenz H., S12 (22)
 Le Quesne J., S23 (54)
 Lerner R.E., S11 (21)
 Leveque J., S11 (20)
 Levi M., S20 (45)
 Levy E., S57 (201)
 Lewis B., S26 (104)
 Le X., S1 (1LBA)
 Leyton V.J., S25 (59)
 Liang Q., S45 (166)
 Licitra L., S32 (123)
 Lieu C., S12 (23)
 Liew L., S13 (25)
 Li H., S59 (207)
 Li H.Q., S31 (119)

Li H.Q.X., S15 (29)
 Li J., S7 (1)
 Lilly E., S12 (22)
 Lin C.C., S12 (24)
 Lin D., S9 (6)
 Lindsay J., S18 (40)
 Linehan W.M., S17 (35)
 Linney I., S20 (46)
 Lipert B., S30 (115)
 Li R., S5 (97LBA)
 Liu B., S15 (30)
 Liu H., S52 (184)
 Liu J., S5 (97LBA)
 Liu X., S48 (173)
 Liu Y., S15 (30)
 Li X., S48 (174)
 Lock R.B., S18 (37)
 Loebel C., S46 (169)
 Loh C., S20 (46)
 Lopes J. M., S23 (53)
 Lopez-Bertoni H., S33 (126), S33 (127)
 Lopez-Blanch R., S41 (150)
 Lorens J.B., S44 (160)
 Lorenzana G., S16 (33)
 LoRusso P., S3 (7LBA)
 Lucas J., S15 (30)
 Lucas L., S32 (122)
 Ludwig N., S19 (44)
 Lui A.J.W., S15 (31)
 Lu J., S20 (45)
 Luo D., S11 (20)
 Luo M.Y., S45 (166)
 Luria A., S11 (21)
 Lyons J., S28 (109), S44 (162), S53 (187)

M

Mabry D., S57 (201)
 Macchini M., S5 (98LBA)
 Machado A., S22 (51)
 Madan R., S10 (7)
 Madigan C., S50 (180)
 Maejima T., S14 (28)
 Magne N., S46 (167)
 Makinoshima H., S31 (120)
 Ma L., S11 (20)
 Maliyan A., S16 (32)
 Mangel L., S35 (132)
 Mao B., S31 (119), S59 (207)
 Ma P.C., S11 (21)
 Marandino L., S21 (48)
 Marappan S., S47 (170)
 Marchbank K., S37 (137)
 Marchio P., S41 (150)
 Marco-Brualla J., S53 (188)
 Marina N., S11 (20)
 Markham J., S32 (122)
 Marsh K., S51 (183)
 Marszalek J.R., S22 (51)
 Marte J., S10 (7)
 Marti H.P., S44 (160)
 Martin A., S33 (125)
 Martins V., S44 (161), S44 (162), S53 (187)

Marusyk A., S48 (174)
 Masciari S., S8 (5)
 Masina R., S19 (43)
 Masson F., S61 (213)
 Mattar M.S., S15 (31)
 Mauguen A., S16 (34)
 Mawji N.R., S51 (181)
 Mazor T., S18 (40)
 McCabe C., S51 (182)
 McCarren P., S1 (2LBA)
 McCoach C., S8 (5)
 McConnell D.B., S22 (51)
 McElvain M., S33 (125)
 McGuire M., S7 (3), S52 (184)
 McKinney D., S1 (2LBA)
 McMillan B., S1 (2LBA)
 McSheehy P., S25 (101)
 Meeus P., S32 (123)
 Melamed L., S14 (26)
 Meleza C., S16 (32)
 Memeo L., S62 (216)
 Meng X., S37 (139)
 Meniawy T., S11 (20)
 Merchant F., S6 (99LBA), S57 (200)
 Merchant N., S6 (99LBA)
 Merchant R., S57 (200)
 Meric-Bernstam F., S3 (6LBA)
 Mesas C., S54 (189)
 Metaferia N., S7 (1)
 Metibemu O., S26 (103)
 Miah M.K., S45 (164)
 Michael N., S29 (114)
 Micklem D.R., S44 (160)
 Miguel-Gordo M., S17 (36)
 Miles D., S38 (143)
 Miles T., S12 (22)
 Milian M., S42 (154)
 Milla M., S11 (20)
 Miller J., S14 (26)
 Milot M.C., S24 (56)
 Min W.P., S60 (210)
 Mirili C., S42 (155)
 Mittal S., S40 (148)
 Miyadera K., S44 (162)
 Mock J.Y., S33 (125)
 Mody K., S11 (21)
 Mohan P., S29 (113)
 Mohanty B., S38 (141)
 Molano M., S46 (167)
 Molina-Arcas M., S20 (47), S60 (208)
 Monaco M., S58 (203)
 Monga S.P., S53 (186)
 Monge C., S57 (201)
 Montalbano A., S35 (133)
 Montorsi F., S21 (48)
 Mooney J., S11 (20)
 Moore C., S20 (47), S60 (208)
 Moore J., S14 (27)
 Moreno-Acosta P., S46 (167)
 Moreno-Loshuertos R., S53 (188)
 Morfouace M., S32 (123)
 Morita T. Y., S31 (120)
 Moroco J., S1 (2LBA)
 Morris E., S12 (24)
 Morrissey C., S49 (176)

Moulder S., S49 (179)
 Muench S., S44 (161), S44 (162), S53 (187)
 Mugarza E., S60 (208)
 Mugarza-Strobl E., S20 (47)
 Mugundu G., S45 (164)
 Muhammad T., S48 (175)
 Mukherjee S., S47 (170)
 Mulvaney K., S1 (2LBA)
 Munck J., S28 (109), S44 (162), S53 (187)
 Mu P., S22 (52)
 Murphy C., S28 (108)
 Murray B., S39 (147)
 Murray C., S53 (187)
 Musch A., S27 (105)
 Musetti S., S37 (140)
 Mydel P.M., S44 (160)
 Myles D., S55 (193)

N

Nagasaka M., S8 (5)
 Nagashima H., S14 (26)
 Naing A., S3 (6LBA)
 Nakada T., S14 (28)
 Nakatsuru Y., S44 (161), S44 (162)
 Nampe D., S33 (125)
 Nancy D., S8 (4)
 Napoli S., S40 (149)
 Nazeer A., S10 (8)
 Ndengu A., S16 (34)
 Necchi A., S21 (48)
 Neggers J., S8 (4)
 Negri K., S33 (125)
 Nellore K., S47 (170)
 Neumann S. Piperno, S32 (123)
 Ng K., S8 (5)
 Ngo Q., S24 (57)
 Nguyen L., S16 (33)
 Nguyen T., S29 (111)
 Nie C., S15 (29)
 Nikolin B., S35 (132)
 Nishiya Y., S14 (28)
 Niu H., S36 (135)
 Nogueira M., S7 (1)
 Norton D., S53 (187)

O

Obasaju P., S46 (168)
 Obrador E., S41 (150)
 O'Brien S., S17 (36)
 Ochiwa H., S44 (161), S44 (162)
 Ochsenreiter S., S5 (98LBA)
 Odintsov I., S15 (31)
 O'donohue T., S16 (34)
 Ohashi A., S31 (120), S36 (135)
 Oh J., S33 (125)
 O'Keefe M., S1 (2LBA)
 Okpechi S., S29 (111)
 Olaharski A., S52 (184)
 Olson P., S1 (3LBA)
 Omar H., S38 (142)

Ondrey F., S49 (178)
 Ooki A., S61 (214)
 O'Reilly M., S53 (187)
 Ortiz R., S54 (189)
 Osada A., S35 (132)
 Oseha O., S26 (103)
 O'Sullivan Coyne G., S10 (7)
 Otero J., S12 (24)
 Ottesen L., S45 (164)
 Ou S.H., S8 (5)
 Ou S.H.I., S1 (3LBA), S2 (4LBA)
 Ouyang D., S15 (29), S59 (207)
 Ovalle A., S18 (40)
 Overkamp J., S59 (205)
 Owzar K., S9 (6)
 Ozawa T., S53 (186)
 Ozduman K., S32 (124)

P

Pabon M., S59 (206)
 Pacheco J., S8 (5), S12 (23)
 Pacheco J.M., S1 (3LBA)
 Pamir M.N., S32 (124)
 Panda D., S38 (141)
 Pant S., S3 (6LBA)
 Paoletta B., S8 (4)
 Papadopoulos K., S50 (180)
 Papadopoulos K.P., S1 (3LBA), S2 (4LBA)
 Pappworth I., S37 (137)
 Paprcka S.L., S38 (143)
 Parikh A.R., S2 (5LBA)
 Parkinson R., S12 (22)
 Pastoor T., S59 (206)
 Patalyak S., S41 (153)
 Patel J., S9 (6)
 Patel P., S3 (7LBA)
 Patti J., S27 (106)
 Paydaş S., S42 (155)
 Pearson P., S51 (181)
 Pease J.E., S47 (171)
 Pedot G., S24 (57)
 Peille A.L., S27 (105)
 Pei W., S29 (114)
 Pellicer J.A., S41 (150)
 Perazzoli G., S54 (189)
 Perez C.L., S41 (150)
 Perez D., S42 (154)
 Perrine M., S27 (106)
 Petronczki M., S22 (51)
 Piazza I., S54 (192)
 Picotti P., S54 (192)
 Piha-Paul S., S3 (6LBA)
 Pijnenburg D., S24 (58)
 Pinto de Faria Lopes G., S56 (197)
 Piovesan D., S16 (32)
 Piscopio A., S12 (23)
 Pitts T., S29 (112)
 Piwnica-Worms H., S49 (179)
 Plessinger D., S15 (31)
 Poddutoori R., S47 (170)
 Polanska U., S47 (171)
 Pollard K., S24 (58), S46 (168)

Ponce Aix S., S5 (96LBA)
 Ponz-Sarvise M., S1 (1LBA)
 Poojari R., S38 (141)
 Popper H., S23 (54)
 Pópulo H., S23 (53)
 Poulikakos P., S5 (97LBA)
 Powers J., S16 (32)
 Powers J.P., S38 (143)
 Pratilas C., S24 (58)
 Pratilas C.A., S46 (168)
 Prencipe M., S49 (176)
 Prendergast L., S36 (136)
 Price A., S44 (161)
 Price L., S57 (199), S59 (205), S62 (215)
 Price M., S53 (188)
 Print C., S30 (115)
 Prokunina L., S30 (116)
 Pruitt-Thompson S., S7 (2)
 Pujana M.A., S14 (27)

Q

Qayum A., S39 (144)
 Qian W., S31 (119), S49 (179)
 Qing W., S25 (100)
 Quiñero F., S54 (189)
 Quintanilha J., S9 (6)

R

Rafferty S., S14 (26)
 Raggi D., S21 (48)
 Rahal R., S7 (3)
 Raimondi M.V., S35 (133)
 Rajan A., S10 (7)
 Raja R., S61 (212)
 Raleigh D.R., S53 (186)
 Ramachandra M., S47 (170)
 Ramadan W., S38 (142)
 Ramharter J., S22 (51)
 Rami V., S12 (22)
 Ramlau R., S5 (96LBA)
 Ranaghan M., S1 (2LBA)
 Rana S., S60 (208)
 Rancic M., S5 (96LBA)
 Randazzo D., S6 (99LBA)
 Rangan V., S15 (30)
 Ranjit S., S20 (45)
 Rastelli E., S55 (195)
 Ratain M., S9 (6)
 Ray-Coquard I., S32 (123)
 Reader M., S53 (187)
 Reagan M., S28 (108)
 Redd B., S57 (201)
 Reddy T., S49 (179)
 Redman J., S10 (7)
 Rees D., S53 (187)
 Reichert T.E., S19 (44)
 Reiter L., S39 (145), S54 (192)
 Remsing Rix L.L., S48 (174)
 Ren Y., S25 (100)
 Reyes D.F., S53 (186)
 Ribeiro Soares A., S56 (197)
 Richard P., S24 (56)

Richardson D., S50 (180)
 Richardson J., S15 (30)
 Rich S., S44 (161), S53 (187)
 Ricketts C.J., S17 (35)
 Riely G.J., S1 (3LBA)
 Riese D., S32 (122)
 Riess J., S8 (5)
 Rinaldi A., S40 (149)
 Rioux-Chevalier A., S25 (59)
 Riquelme M., S54 (191)
 Rix U., S48 (174)
 Roberts S., S16 (34)
 Robinson C., S48 (173)
 Robinson S., S25 (101)
 Rodon J., S3 (6LBA)
 Rodon L., S39 (147)
 Rodriguez F., S24 (58)
 Rodriguez Y., S23 (55)
 Rojas A., S27 (106)
 Rolling C., S5 (98LBA)
 Romero-Clavijo P., S60 (208)
 Romero Rojas A., S46 (167)
 Rosales N., S16 (34)
 Rosato R., S49 (179)
 Rosen B., S16 (32)
 Rossi D., S40 (149)
 Rothberg M., S8 (4)
 Roth D., S50 (180)
 Roth J., S48 (173)
 Rousseau É., S24 (56)
 Roy S., S41 (151)
 Rudek M., S19 (42)
 Rudolph D., S22 (51)
 Rugo H., S9 (6)
 Russell N., S49 (176)
 Rustgi A., S46 (169)
 Rybkin I.I., S1 (3LBA), S2 (4LBA)

S

Sabari J.K., S1 (3LBA)
 Sachsenmeier K., S20 (47)
 Sadar M.D., S51 (181)
 Sadhukhan P., S61 (214)
 Sae-Hau M., S51 (183)
 Saha S., S15 (30), S37 (137)
 Saini H., S44 (162)
 Salameh A., S27 (106)
 Saluja D., S30 (117)
 Salvador R., S41 (150)
 Samajdar S., S47 (170)
 Samiulla D., S47 (170)
 Sampaio C., S23 (53)
 Sampson J., S6 (99LBA)
 Sandberg M., S33 (125)
 Sankar N., S11 (21)
 Saratov V., S24 (57)
 Sartori G., S40 (149)
 Satija Y.K., S30 (117)
 Satoshi F., S58 (202)
 Satyam L.K., S47 (170)
 Sauquet I. Guix, S14 (27)
 Savarese F., S22 (51)
 Sayaka T., S58 (202)

Scaggiante B., S49 (177)
 Scagliotti A., S26 (102)
 Schäfer B., S24 (57)
 Schatz J.H., S28 (110)
 Scheffold C., S16 (33)
 Schellenberger V., S10 (8)
 Schlabach M., S7 (3), S52 (184)
 Schleyer S., S15 (30)
 Schlom J., S10 (7)
 Schmidt L.S., S17 (35)
 Schneider B., S9 (6)
 Schramm V., S39 (146)
 Schulze C.J., S53 (186)
 Schwartz G.K., S3 (7LBA)
 Seckl M., S32 (123)
 Seiji M., S58 (202)
 Seiler R., S21 (48)
 Sellers W., S1 (2LBA), S5 (97LBA)
 Sen S., S1 (1LBA), S11 (20)
 Seo J.H., S7 (1)
 Severson P., S2 (5LBA)
 Sezerman O.U., S32 (124)
 Shah A., S44 (161), S44 (162)
 Shapiro G.I., S7 (2)
 Sharlow E., S55 (195)
 Sharma M., S50 (180)
 Shay C., S34 (129)
 Shen F., S9 (6)
 Sheng G., S31 (119)
 Shen J., S15 (30)
 Shenker S., S7 (3), S52 (184)
 Shen Y., S45 (166)
 Sherman E.J., S2 (5LBA)
 Shibata Y., S44 (161)
 Shibutani T., S14 (28)
 Shi D., S25 (100)
 Shimamura T., S44 (161)
 Shivani M., S43 (159)
 Shroff R.T., S21 (49)
 Sibley A., S9 (6)
 Siddiquee A., S16 (34)
 Siegel E., S18 (40)
 Sims M., S28 (109)
 Singh M., S53 (186)
 Singh R., S1 (2LBA)
 Singleton D., S30 (115)
 Sinkevicius K., S7 (3), S52 (184)
 Siraj F., S30 (117)
 Sisso E.M., S15 (31)
 Sisso W.J., S15 (31)
 Siveke J., S58 (204)
 Sivick Gauthier K., S16 (32)
 Skipper T., S8 (4)
 Smit E., S5 (96LBA)
 Smith H., S36 (136)
 Smith J.A., S53 (186)
 Smith M.A., S18 (37)
 Smith P., S20 (47)
 Smyth T., S28 (109), S44 (161), S44 (162)
 Soares P., S23 (53)
 Soler R., S53 (188)
 Solheim J., S34 (128), S60 (211)
 Somwar R., S15 (31)
 Sourbier C., S17 (35)
 Spanjaard E., S57 (199), S62 (215)

Spanò V., S35 (133)
 Spira A., S8 (5)
 Spira A.I., S1 (3LBA)
 Spriano F., S17 (36), S40 (149)
 Srivastava R., S38 (141)
 Stanetic M., S5 (96LBA)
 Stathis A., S40 (149)
 Staunton J., S56 (196)
 Stegmaier K., S8 (4)
 Stegmeier F., S7 (3), S52 (184)
 Steuer C., S8 (5)
 Stevovic A., S32 (123)
 Strathdee C., S7 (1)
 Strauss J., S10 (7)
 Stumpf C.R., S56 (196)
 Stussi G., S40 (149)
 Subbiah V., S3 (6LBA)
 Subramanian M., S14 (26)
 Sullivan P., S7 (3), S52 (184)
 Sung E., S56 (196)
 Sun R., S55 (193)
 Suryawanshi D., S38 (141)
 Su W., S25 (100)
 Suzuki A., S31 (120)
 Swanton C., S18 (41)
 Swift M., S37 (138)

T

Takamasa S., S58 (202)
 Takeda D., S7 (1)
 Takeshi S., S58 (202)
 Takuya H., S58 (202)
 Tam T., S51 (181)
 Tan D.S., S12 (24)
 Tang R., S25 (100)
 Tang S., S7 (1)
 Tan T., S11 (20)
 Tao B., S3 (7LBA)
 Tao J.Y., S53 (186)
 Tapinos N., S42 (156), S52 (185)
 Tarcic G., S2 (5LBA)
 Tasker N., S55 (195)
 Tateishi K., S14 (26)
 Taverna P., S45 (163)
 Teng Y., S34 (129)
 ter Heine R., S19 (42)
 Teruhiro U., S58 (202)
 Thiyagarajan S., S47 (170)
 Thomas A., S10 (7)
 Thomas C., S51 (183)
 Thomas C.J., S17 (35)
 Thomas O., S17 (36)
 Thompson N., S53 (187)
 Thompson P.A., S56 (196)
 Tihan T., S32 (124)
 Tiwari N.K., S47 (170)
 Tobin E., S7 (3)
 Tokatlian T., S33 (125)
 To M., S57 (200)
 Tomar T., S24 (58)
 Tomlinson R., S39 (145)
 Toms S., S42 (156), S52 (185)
 Toombs J.E., S44 (160)
 Topisirovic I., S23 (54)

Torres A., S42 (154)
 Toscan C., S18 (37)
 Trapani F., S22 (51)
 Travers J., S47 (171)
 Treilleux I., S32 (123)
 Tsai F., S2 (5LBA)
 Tsai P., S30 (115)
 Tscherniak A., S8 (4)
 Tsimberidou A.M., S3 (6LBA)
 Tummino P., S20 (46)

U

Uboha N., S21 (49)
 Uboveja A., S30 (117)
 Udyavar A., S16 (32)
 Ueberheide B., S5 (97LBA)
 Ugurlu M.T., S61 (214)
 Ulahannan S., S8 (5)
 Ulanska M., S5 (96LBA)
 Ulgen E., S32 (124)
 Urošević J., S47 (171)
 Ursulovic T., S35 (132)

V

Vader W., S59 (205)
 Valand K., S60 (208)
 Valles S.L., S41 (150)
 van den Hombergh E., S19 (42)
 van der Meer D., S59 (205)
 van Erp N., S19 (42)
 Van Hoef V., S23 (54)
 Van Maldegem F., S60 (208)
 Varticovski L., S30 (116)
 Vazquez F., S8 (4)
 Velastegui K., S1 (3LBA), S2 (4LBA)
 Vellano C.P., S22 (51)
 Verheul H., S12 (22), S19 (42)
 Vincent M., S60 (210)
 Virsik P., S51 (181)
 Visser B., S57 (199), S62 (215)
 Viswanathan S., S7 (1)
 Vocke C., S17 (35)
 Vogelbaum M., S6 (99LBA)
 Vojnic M., S15 (31)
 Von Hoff D.D., S55 (194)
 Von Karstedt S., S10 (9)
 Vrionis F., S6 (99LBA)
 Vuaroqueaux V., S27 (105)
 Vukovic V., S5 (96LBA)

W

Waddell I., S20 (46)
 Wagner S., S44 (162)
 Waits D., S32 (122)
 Waizenegger I., S22 (51)
 Wakako Y., S58 (202)
 Wakimoto H., S14 (26)
 Walling J., S2 (5LBA)
 Wallis N., S44 (162), S53 (187)
 Wallis N.G., S44 (161)
 Walters M., S16 (32)

Walters M.J., S38 (143)
 Wang C., S25 (100), S54 (191)
 Wang F., S34 (129)
 Wang H., S5 (97LBA)
 Wang J., S9 (6), S11 (20), S24 (58),
 S37 (139), S46 (168), S47 (171),
 S51 (181)
 Wang L., S5 (97LBA), S25 (100)
 Wang S., S23 (54)
 Wang X., S8 (5), S33 (125)
 Wang Z., S8 (5), S43 (159)
 Wang Z.C., S53 (186)
 Wang Z.P., S53 (186)
 Wan X., S48 (173)
 Ward G., S28 (109)
 Watanabe A., S14 (28)
 Watson W., S49 (176)
 Webb S., S57 (201)
 Wei D., S17 (35)
 Weiss E., S51 (183)
 Weiss J., S2 (4LBA)
 Weiss W.A., S53 (186)
 Welsh E.A., S48 (174)
 Whiteside T.L., S19 (44)
 Wieteska L., S19 (44)
 Wijnhoven P., S47 (171)
 Wildes D.P., S53 (186)
 Williams E., S32 (122)
 Wilsher N., S44 (162), S53 (187)
 Wilsher N.E., S44 (161)
 Wilson K., S17 (35), S23 (55)
 Wilson W., S13 (25), S30 (115)
 Wilt J., S52 (184)
 Winkler J., S12 (23)
 Wipf P., S55 (195)
 Wolf J., S12 (24)
 Womack C., S62 (216)
 Wong W., S13 (25)
 Wood B., S57 (201)
 Woods J., S32 (122)
 Woodvine B., S23 (54)

Woolford A., S53 (187)
 Wright A., S29 (112)
 Wu C., S61 (212)
 Wu S., S16 (33)
 Wu X., S5 (97LBA)
 Wylie A., S7 (3), S52 (184)

X

Xiang H., S20 (45)
 Xie C., S57 (201)
 Xie G., S31 (121)
 Xie L., S5 (97LBA)
 Xiong W., S54 (191)
 Xiong Y., S5 (97LBA)
 Xuan D., S1 (1LBA)
 Xu H., S33 (125)
 Xu W., S16 (33)
 Xu X., S31 (119), S31 (121)
 Xu Y., S29 (114)

Y

Yakicier C., S32 (124)
 Yakubu O., S26 (103)
 Yamato M., S14 (28)
 Yang A., S8 (4)
 Yang X., S5 (97LBA)
 Yang Y.C., S53 (186)
 Yan K., S57 (199), S59 (205), S62 (215)
 Yao Z., S24 (58)
 Yerneni S.S., S19 (44)
 Yohe M., S48 (173)
 Yong H., S30 (115)
 Youness R., S56 (198)
 Young N.P., S56 (196)
 Young S., S16 (32)
 Young S.W., S38 (143)
 Yousefi H., S29 (111)
 Yuan H., S20 (45)

Yu J., S18 (40), S25 (100),
 S36 (135)
 Yuksel S.K., S32 (124)
 Yun S., S48 (174)
 Yu P., S16 (33)
 Yu W., S15 (30)

Z

Zabek M., S6 (99LBA)
 Zaher D., S38 (142)
 Zahurak M., S12 (22)
 Zamboni W., S50 (180)
 Zanconati F., S49 (177)
 Zaric B., S5 (96LBA)
 Zehra B., S34 (130)
 Zepecki J., S42 (156)
 Zhai D., S39 (147)
 Zhang C., S2 (5LBA)
 Zhang G., S23 (55)
 Zhang K., S21 (49)
 Zhang N., S54 (191)
 Zhang W., S25 (100)
 Zhang X., S7 (1), S11 (21)
 Zhang Y., S54 (191)
 Zhao R.P., S53 (186)
 Zhao S., S16 (32)
 Zhao X., S38 (143)
 Zhao Y., S27 (107)
 Zheleva D., S7 (2)
 Zheng L., S15 (29)
 Zhou H., S22 (50)
 Zhou H.J., S51 (181)
 Zhou J., S49 (179)
 Zhou L., S45 (166), S50 (180)
 Zhu Y., S37 (139)
 Zimmerman Z., S1 (1LBA)
 Zujewski J.A., S55 (193)
 Żurawski B., S35 (132)
 Zurlo A., S5 (98LBA)